DOCTORAL THESIS

PREPARATION AND CHARACTERIZATION OF ANTIGEN LOADED CHITOSAN NANOPARTICLES FOR IMMUNIZATION

Maruthi Prasanna

Doctoral Program in Nanomedicine and Pharmaceutical Innovation
International Doctoral School

SANTIAGO DE COMPOSTELA

2020

USC
UNIVERSIDADE
DE SANTIAGO
DE COMPOSTELA

TESIS DE DOCTORADO

PREPARACIÓN Y CARACTERIZACIÓN DE NANOPARTÍCULAS DE QUITOSANO CARGADAS DE ANTÍGENO PARA INMUNIZACIÓN

Maruthi Prasanna

Programa de Doctorado en Nanomedicina e Innovación Farmacéutica

Escuela de Doctorado Internacional

SANTIAGO DE COMPOSTELA

2020

USC
UNIVERSIDADE
DE SANTIAGO
DE COMPOSTELA

AUTHORIZATION OF THE THESIS SUPERVISORS

Prof. Noemi Csaba, Professor at the Department of Pharmacology, Pharmacy and Pharmaceutical Technology in the University of Santiago de Compostela, Spain

Dr. Cyrille Grandjean, Chargé de Recherche at CNRS – Unité Fonctionnalité et Ingénierie des Protéines (UFIP), UMR 6286, Université de Nantes, France / Assistant Researcher at French National Centre for Scientific Research (CNRS), UFIP, UMR 6286, University of Nantes, France

REPORT:

That the experimental dissertation entitled: "**Preparation and characterization of antigen loaded chitosan nanoparticles for immunization**" presented by **Maruthi Prasanna** was conducted under their supervision at the Department of Pharmacology, Pharmacy and Pharmaceutical Technology at the University of Santiago de Compostela and at the Faculty of Sciences and Techniques, Unit of Functionality and Proteins Engineering, UMR CNRS 6286 at the University of Nantes, France. Being completed, they authorize its presentation, evaluation by the assigned jury members, considering that it meets the requirements demanded in article 34 of the Regulation of Doctoral Studies of the USC, and that as supervisors of this thesis they do not incur in the abstention causes established by the law 40/2015.

And for the record, they issue and sign the present certificate in Santiago de Compostela and Nantes, June 4th 2020.

Prof. Noemi Csaba

Dr. Cyrille Grandjean

USC
UNIVERSIDADE
DE SANTIAGO
DE COMPOSTELA

AUTORIZACIÓN DEL DIRECTOR/ TUTOR DE LA TESIS

Prof. Noemí Csaba, profesora del Departamento de Farmacología, Farmacia y Tecnología Farmacéutica de la Universidad de Santiago de Compostela, España

Dr. Cyrille Grandjean, Chargé de Recherche en CNRS / Investigador en el Centro Nacional Francés de Investigación Científica (CNRS), UFIP, UMR 6286, Universidad de Nantes, Francia

INFORMA:

Que la disertación experimental titulada: **"Preparación y caracterización de nanopartículas de quitosano cargadas de antígeno para inmunización"** presentada por **Maruthi Prasanna** se realizó bajo su supervisión en el Departamento de Farmacología, Farmacia y Tecnología Farmacéutica de la Universidad de Santiago de Compostela y en la Facultad de Ciencias y Técnicas, Unidad de Funcionalidad e Ingeniería de Proteínas, UMR CNRS 6286 en la Universidad de Nantes, Francia. Una vez completado, autorizan su presentación, evaluación por parte de los miembros del jurado asignados, considerando que cumple con los requisitos exigidos en el artículo 34 del Reglamento de Estudios Doctorales de la USC, y que como supervisores de esta tesis no incurren en las causas de abstención establecido por la ley 40/2015.

Y para que conste, emiten y firman el presente certificado en Santiago de Compostela y Nantes, el 4 de junio de 2020.

Prof. Noemi Csaba

Dr. Cyrille Grandjean

USC
UNIVERSIDADE
DE SANTIAGO
DE COMPOSTELA

PhD CANDIDATE STATEMENT

Preparation and characterization of antigen loaded chitosan nanoparticles for immunization

Mr. Maruthi Prasanna

I submit my Doctoral thesis, following the procedure according to the Regulation, stating that:

1) This thesis gathers the results corresponding to my work.
2) When necessary, explicit mention is given to the collaborations the work may have had.
3) The present document is the final version submitted for its defense and coincide with the document sent in electronic format.
4) I confirm that this thesis does not incur in any plagiarism of any other authors or documents submitted by me for obtaining other degrees.

At Santiago de Compostela, on June 4th 2020

Sgd. Maruthi Prasanna

USC
UNIVERSIDADE
DE SANTIAGO
DE COMPOSTELA

DECLARACIÓN DEL AUTOR DE LA TESIS

Preparación y caracterización de nanopartículas de quitosano cargadas de antígeno para inmunización

Mr. Maruthi Prasanna

Presento mi tesis, siguiendo el procedimiento adecuado al Reglamento, y declaro que:

1) La tesis abarca los resultados de la elaboración de mi trabajo.
2) En su caso, en la tesis se hace referencia a las colaboraciones que tuvo este trabajo.
3) La tesis es la versión definitiva presentada para su defensa y coincide con la version enviada en formato electrónico.
4) Confirmo que la tesis no incurre en ningún tipo de plagio de otros autores ni de trabajos presentados por mí para la obtención de otros títulos.

En Santiago de Compostels, a 4 de junio de 2020

Sgd. Maruthi Prasanna

USC
UNIVERSIDADE
DE SANTIAGO
DE COMPOSTELA

CONFLICT OF INTEREST

I hereby declare that there is no conflict of interest with the topics or materials discussed in this thesis.

Mr. Maruthi Prasanna

USC
UNIVERSIDADE
DE SANTIAGO
DE COMPOSTELA

To my Family and Friends

USC
UNIVERSIDADE
DE SANTIAGO
DE COMPOSTELA

‘Let noble thoughts come to us from all sides’

....Rig Veda

USC
UNIVERSIDADE
DE SANTIAGO
DE COMPOSTELA

Acknowledgements

My deepest gratitude goes to my supervisors; Dr. Noemi Csaba, Dr. Cyrille Grandjean and Dr. Emilie Camberlein. Noemi's patient guidance, encouragement and advice has been beyond enough to see me through this amazing but challenging journey. The great efforts you put at improving this manuscript humbles me and I will forever be grateful.

Cyrille was more than a supervisor and he provided me almost everything I need for scientific research by guiding me how to efficiently address many issues logically. I do not have words to express my gratitude towards him.

To my co-supervisor Dr. Emilie Camberlein, thanks for providing technical expertise and valuable suggestions. I have been extremely fortunate as a researcher to learn the work of bacterial cultures and protein expression from you.

I would like to extend my special thanks to Dr. Marcos Garcia. I am deeply indebted to him for assistance, guidance, and constructive advices he provided during the meetings.

I would like to thank Prof. Maria Jose for constantly inspiring us with her energy and the talks. The suggestions you gave during the seminars and the congress are always valuable.

I would like to show my greatest gratitude towards Dr. Ruben Varela for introducing me to the science of immunology and Cristina Calvino for initially helping me with the dendritic cell experiments.

I would like to thank our collaborators from Lille: Dr. Francois Trottein and Daphnee Soulard for their help in animal experimentation.

I would like to express my thanks to all the members of the Nanoscopy for Nanomedicine lab, especially to the Dr. Lorenzo Albertazzi and Dr. Silvia Pujals for kindly hosting me in their laboratory in Barcelona, Spain. I also thank Maria Arista Romero for helping me with my experiments during my stay.

I would like to thank members of follow-up thesis committee Prof. Jeremy Brown and Dr. Marcos Garcia for their time and insightful advices.

I would like to thank Sindhu for helping me with the statistical analysis and proofreading of the thesis. Thanks, Sandra for helping me with the Spanish translations. Thanks, Tamara for helping me with the documents required for the thesis.

To my beloved Nanochachos: José, Tamara, Sakthi, Shubaash, Sara, German, Edi, Mireya, Sergio, Ana, Irene, Belén, Cecilia, Catarina, Fernando, Lena, Mati, Sofia, Carmen, Lungile, Nataliya, Niu, Howl, Sonia, Surasa, Andrea, Vanessa, Bhanu, Iago, Franchesco and Desi. To my Hermanos, Carla and Diego, whom I always annoy. Thanks, Diego for helping me with the experiments whenever needed. My labmates Sandra, Sheila, Chema, Hector, Saeedeh, Paul and Howl were a wonderful company. You guys were incredible. I can never forget the coffee breaks, lab dinners, the movies we watched and the sports we played together. Altogether, you guys made my stay at lab a total bliss. Thanks Howl and Lu, you guys received me on the first day and help me get familiar with the university. Thank you, Belen and Sonia for being very nice to me. Thanks, Sofia and Carla for your wonderful company. Thank you, Belen, Rafa and Balbi for providing the technical support during this journey of PhD. Puri helped me in solving the issues related to the administration and university registration process, thanks a lot.

I would like to thank the other members of CiMUS: Sulay, Anxo, Vanessa and Lucia. They helped me and provided me the guidance to work with the common facilities at CiMUS. Thankyou Carmen for helping me with the necessary documentation from the CiMUS.

Furthermore, I would like to mention people from research teams at the University of Nantes: Johann, Amelie, Annie, Fabienne, Charles and Fabrice. Also, I would like to thank my other friends from UFIP Iyanar, Mahesh, Aline, Lidiya, Typhaine, Christophe, Yuonnick, Benoit and Ennis for your wonderful company. The Friday evening movie time, the food parties, the chess games and the coffee breaks are the best moments that I had there. Thank you all for those memories.

I sincerely acknowledge the Erasmus mundus, European doctorate in nanomedicine and pharmaceutical innovation (NanoFar) Fellowship for the financial assistance during my PhD. I would like to thank Prof. Frank Boury, Marion and related NanoFar members for their commitment towards this European doctorate program.

Special thanks to Jose for his wonderful company to play badminton and table tennis. You thought me first Spanish song “no es mi culpa” and the memories of the time we spent at your farm will always remain special.

I would like to thank my Indian friends at Santiago: Bhanu, Sunil, Shubaash and Sakthi. For the amazing company and lot of fun that we had together. The evening chats and the food exchange parties with them relieved my home sick. The after-work hours we spent cooking, playing sports and watching movies will always be remembered.

I would like to thank my friends Sindhu, Vijay and Narendra for always being there for me. Thank you very much Sindhu for the unconditional support and encouragement. Thank you, Vijay for constantly boosting my confidence.

It would not be complete without mentioning my parents and my brother. I cannot forget the hardship that my parents took to make me what I am today, specially my mom. My greatest strength, my brother, always acted as a backbone and supported me in every decision I took. My gratitude towards my uncles and sisters who helped me during my education, I would not be what I am today without you all.

USC
UNIVERSIDADE
DE SANTIAGO
DE COMPOSTELA

Table of Contents

USC
UNIVERSIDADE
DE SANTIAGO
DE COMPOSTELA

Abstract/Resumen

USC
UNIVERSIDADE
DE SANTIAGO
DE COMPOSTELA

Abstract

Existing pneumococcal vaccines are based on capsular polysaccharides from selected serotypes and provide no complete protection against pneumonia, and the major concern is serotype replacement. Current preventive strategies involve the development of vaccines based on common pneumococcal proteins. When used independently or as a carrier in glycoconjugate vaccines, protein antigens could induce serotype independent protection. While pneumococcal protein-based glycoconjugates have demonstrated their immunogenicity and ability to activate humoral immune response, their combination with nanotechnological approaches can improve protein stability, provide adjuvancy and enhance immune response. In this line, we investigated glycoconjugate-loaded nanoparticles as next-generation pneumococcal vaccines.

In this study, we have developed a semisynthetic glycoconjugate (GC) by covalently linking the pneumococcal surface adhesin A (PsaA) with a synthetic mimic of the capsular polysaccharide from *Streptococcus pneumoniae* serotype 14 (Pn14TS). The required PsaA was obtained from rDNA technology and Pn14TS was chemically synthesized. The prepared GC had high yield, high purity and long-term storage stability after freeze drying. Further characterization was performed by circular dichroism, which showed that the protein maintained its secondary structural confirmation throughout the conjugation process. Preliminary immunization studies in mice have shown that the GC was able to induce IgG antibodies against both of its protein and tetrasaccharide components.

Next, we explored chitosan nanoparticles (CNPs) as carriers for the GC. The GC-CNPs were prepared using a simple ionic gelation method, resulting in nanoparticles with 150 nm size and zeta potential of 30 mV. The GC-CNPs showed 70% encapsulation efficiency, colloidal stability in simulated nasal mucosal fluid for 24h and were able to control the antigen release more than 24h. In addition, the GC-CNPs could be freeze dried and reconstituted without altering their properties. These nanoparticles displayed low levels of toxicity and were successfully internalized by dendritic cells. In addition, they were able to induce the upregulation of co-stimulatory markers and T cell activation.

Finally, the immunization studies in the mice reveal that, on S.C immunization the GC-CNPs displayed a 100-fold and 10-fold higher anti-PsaA IgG and anti-CP (capsular polysaccharide) IgG response respectively over the mice immunized with GC. In summary, the study demonstrates that chitosan nanoparticles can enhance the immunogenicity of semisynthetic glycoconjugate antigen.

USC
UNIVERSIDADE
DE SANTIAGO
DE COMPOSTELA

Resumen

Las vacunas actuales frente el neumococo están constituidas por polisacárido capsular de serotipos específicos, lo que no ofrece una protección completa contra la neumonía, siendo el problema principal la falta de cobertura serotípica. Las estrategias profilácticas actuales comprenden el desarrollo de vacunas basadas en proteínas neumocócicas comunes. Estos antígenos proteicos, empleados tanto de manera independiente o como vehículo en vacunas glicoconjugadas podrían dar lugar a una protección independiente del serotipo. Aunque los glicoconjugados constituidos por proteínas neumocócicas han demostrado ser inmunogénicos y capaces de iniciar una respuesta inmune humoral, su uso dentro de una perspectiva nanotecnológica puede contribuir a mejorar la estabilidad proteica, proporcionar adyuvancia e incrementar su respuesta inmune. En esta línea, hemos investigado el desarrollo de nanopartículas glicoconjugadas como la siguiente generación de vacunas neumocócicas.

En este estudio, se desarrolló un glicoconjugado semisintético (GC) uniendo covalentemente la adhesina A de la superficie del neumococo (PsaA) con un imitador sintético del polisacárido capsular del serotipo 14 del *Streptococcus pneumoniae* (Pn14TS). El PsaA se obtuvo a través de la tecnología de ADN recombinante y el Pn14TS fue sintetizado químicamente. El GC resultante presentó un alto rendimiento, alta pureza y buena estabilidad durante su almacenamiento a largo plazo tras un proceso de liofilización. Su caracterización adicional mediante técnicas de dicroísmo circular demostró que la proteína mantuvo la conformación de su estructura secundaria durante todo el proceso de conjugación. Los estudios preliminares de inmunización en ratones demostraron que el GC fue capaz de inducir anticuerpos IgG contra sus componentes tanto proteicos como tetrasacáridos.

Posteriormente, estudiamos el uso de las nanopartículas de quitosano (CNP) como sistemas transportadores del GC. Estas GC-CNP se prepararon mediante un método de gelificación iónica simple, dando como resultado nanopartículas de 150 nm de tamaño y con un potencial zeta de 30 mV. Las GC-CNP presentaron una eficiencia de encapsulación del 70%, estabilidad coloidal en fluido simulado de mucosa nasal durante 24h y fueron capaces de controlar la liberación de antígeno durante más de 24h. Además, las GC-CNP pudieron liofilizarse y reconstituirse sin que conllevara un cambio en sus propiedades. Las nanopartículas mostraron bajos niveles de toxicidad y una internalización exitosa por las células dendríticas. Además, las nanopartículas fueron capaces de inducir una regulación positiva de marcadores coestimuladores y la activación de células T.

Finalmente, estudios de inmunización en ratones revelaron que, tras su inmunización subcutánea, las GC-CNP mostraron una respuesta 100 y 10 veces mayor de niveles de IgG anti-PsaA y anti-CP (polisacárido capsular), respectivamente, en comparación los ratones inmunizados con GC. En resumen, el estudio demuestra que las nanopartículas de quitosano pueden mejorar la inmunogenicidad del antígeno glicoconjugado semisintético.

USC
UNIVERSIDADE
DE SANTIAGO
DE COMPOSTELA

Resumen in extenso

USC
UNIVERSIDADE
DE SANTIAGO
DE COMPOSTELA

Resumen en español

Introducción

La neumonía constituye la causa principal de muerte entre las enfermedades infecciosas, siendo el *Streptococcus pneumoniae* responsable de la mayoría de las neumonías adquiridas. Este patógeno es, además, causante de meningitis bacteriana, sepsis y otitis media, causas de morbilidad y mortalidad tanto en niños como en adultos. El Instituto de Medición y Evaluación de la Salud (IHME) estima que las infecciones debidas a *S. pneumoniae* son responsables de 1,2 millones de muertes al año [1,2]. Se han identificado alrededor de 96 serotipos distintos de *S. pneumoniae* a partir de los polisacáridos que componen la superficie de la cápsula de la bacteria [3]. Las vacunas antineumocócicas disponibles se basan en polisacáridos capsulares de un serotipo específico, sin embargo, estos polisacáridos varían para cada serotipo neumocócico.

Actualmente, se utilizan dos tipos de vacunas antineumocócicas: una vacuna de polisacárido neumocócico 23-valente (PPV23) con una mezcla de polisacáridos de diferentes serotipos neumocócicos; y vacunas conjugadas neumocócicas (PCV-7, 10, 13), con polisacáridos antigénicos conjugados con proteínas transportadoras, capaces de generar una respuesta inmune potente. Aunque la introducción de estas vacunas conjugadas ha reducido la carga global de neumonía, las vacunas disponibles protegen solo contra las infecciones causadas por un número limitado de serotipos. Hoy en día, las vacunas comercializadas cubren hasta el 75-90% de las cepas prevalentes en niños [4]. Sin embargo, las infecciones por los serotipos no incluidos en las vacunas han aumentado, produciéndose un reemplazo de cepas virulentas [5]. Es necesario llevar a cabo una búsqueda de candidatos a vacunas con capacidad de abordar estos problemas de cobertura y reemplazo.

Una estrategia eficiente para mejorar la cobertura y la inmunogenicidad consiste en la incorporación de proteínas neumocócicas universales, que estén presentes en todos los serotipos. PsaA es una proteína de 37 kDa altamente conservada, presente en los 96 serotipos de *S. pneumoniae* [6], y es miembro de la familia de transportadores ABC dependientes de ATP. Además, la PsaA es una proteína de superficie que juega un papel importante en la adhesión y colonización de *S. pneumoniae* [7,8], lo que la convierte en candidata ideal para la vacunación [9,10]. La PsaA se unió covalentemente a un tetrasacárido sintético de polisacárido capsular Pn14TS, obteniéndose un glicoconjugado (Pn14TS-mPsaA /GC) [11]. El Pn14TS es el tetrasacárido más pequeño aislado del polisacárido capsular del serotipo 14 de *S. pneumoniae*, capaz de provocar una respuesta opsonofagocítica [12].

El principal obstáculo en el desarrollo de una vacuna eficaz y exitosa es el diseño de un sistema de liberación de antígenos. La búsqueda de vacunas más seguras ha aumentado la demanda de aquellas constituidas por subunidades de componentes bacterianos o virales purificados. Sin embargo, la mayoría de estos componentes son débilmente inmunogénicos [13,14]. Por este motivo se incorporan o se administran conjuntamente con adyuvantes para desencadenar la respuesta inmune. Las células dendríticas (DCs) son las principales células presentadoras de antígeno que desempeñan un papel vital en el desarrollo de la inmunidad humoral mediada por células [15,16]. Como células presentadoras de antígeno profesionales (APC), las DCs actúan como la conexión entre el sistema inmune innato y adaptativo [15,17]. Al tener la capacidad de procesar los antígenos capturados, las DCs pueden estimular eficazmente las células T.

En los últimos años se ha estudiado el uso de polímeros biocompatibles y biodegradables como adyuvantes y sistemas de liberación de antígenos. Polímeros como el quitosano,

alginato, protamina, dextrano, ácido hialurónico o ácido poliláctico-co-glicólico (PLGA) se han investigado en busca del desarrollo de vacunas basadas en proteínas/péptidos [18] o ADN[19]. Entre ellos, el quitosano continúa mostrando un gran potencial. Es un polímero natural biocompatible, biodegradable y mucoadhesivo, considerado como un excelente biomaterial para el diseño de sistemas de liberación de antígenos [20]. Es un adyuvante potencial para la administración mucosa, debido a sus propiedades mucoadhesivas y su capacidad para abrir uniones estrechas, promoviendo el transporte paracelular de antígenos [21,22]. Su naturaleza catiónica promueve su interacción con las células epiteliales, aumentando el tiempo de residencia. Como adyuvante inmune, se sabe que el quitosano mejora la inmunidad humoral y celular [23]. Estas propiedades hacen del quitosano un candidato ideal para el desarrollo de nanopartículas para la administración de vacunas.

El uso de nanopartículas como sistema de liberación ofrece varias ventajas debido a sus características fisicoquímicas: tamaño de partícula, carga superficial y propiedades inmunoestimuladoras [24,25]. La preparación de nanopartículas de quitosano (CNP) implica un método de gelificación iónico simple y sin solventes. Además, permiten formar un depósito en el sitio de administración, controlando la liberación del antígeno [26,27]. A pesar de estos aspectos positivos, algunas limitaciones como una rápida liberación inicial y una reducida estabilidad en medios biológicos constituyen un desafío para su aplicabilidad como sistema de liberación de fármacos [28].

En la presente tesis hemos investigado las nanopartículas basadas en quitosano como un posible vehículo para la administración de vacunas [18]. En este estudio, el glicoconjugado se encapsuló en las CNP (GC-CNP) y se realizó la caracterización. Se llevó a cabo un estudio comparativo sobre la inmunogenicidad del GC y las GC-CNP para identificar la importancia de

la nanoencapsulación para incrementar la inmunogenicidad de los glicoconjugados. En resumen, esta tesis demuestra el uso potencial de los sistemas de nanopartículas para administrar vacunas glicoconjugadas de manera efectiva.

Objetivo 1: Preparación y caracterización del glicoconjugado semisintético.

La expresión de PsaA se realizó mediante la tecnología de ADN recombinante en E. Coli. La PsaA es una proteína de 37 kDa constituida por 309 residuos de aminoácidos. Esta proteína completa presenta un péptido señal en el extremo N-terminal de la región transmembrana. La presencia de esta secuencia líder reduce significativamente la expresión de dicha proteína[29]. Para evitar esta limitación, se produjo un PsaA maduro (mPsaA o PsaA 21-309) que no presentaba esta secuencia peptídica terminal. Se aisló el plásmido pET11a que albergaba el gen PsaA junto con una secuencia de polihistidina (HHHHHH) y una proteasa TEV (ENLYFQS) en su extremo N-terminal y se replicó en *E. coli* BL21 (DE3) mediante el método de choque térmico. Esta secuencia adicional de polihistidina se introdujo con el fin de facilitar la purificación de la proteína. Aunque se puede realizar su expresión y purificación en ausencia de esta cola [29], si se emplea, es necesario llevar a cabo su eliminación posterior para garantizar la ausencia de interferencia con la respuesta inmune. La proteasa TEV interviene en el enlace peptídico Q-S, dejando en su lugar un residuo de serina. Este residuo de serina, que asimismo se produce naturalmente en esta posición, lo que significa que la mPsaA nativa se recupera después de la digestión con la proteasa TEV. La expresión de mPsaA se confirmó mediante SDS-PAGE observándose la banda correspondiente a la proteína con el peso molecular esperado (**Figura 1, Carril 2**). La cola de histidina del HtTEV-mPsaA se eliminó usando la proteasa AcTEV ™ y la mPsaA resultante se purificó usando cromatografía de afinidad para eliminar la etiqueta de histidina.

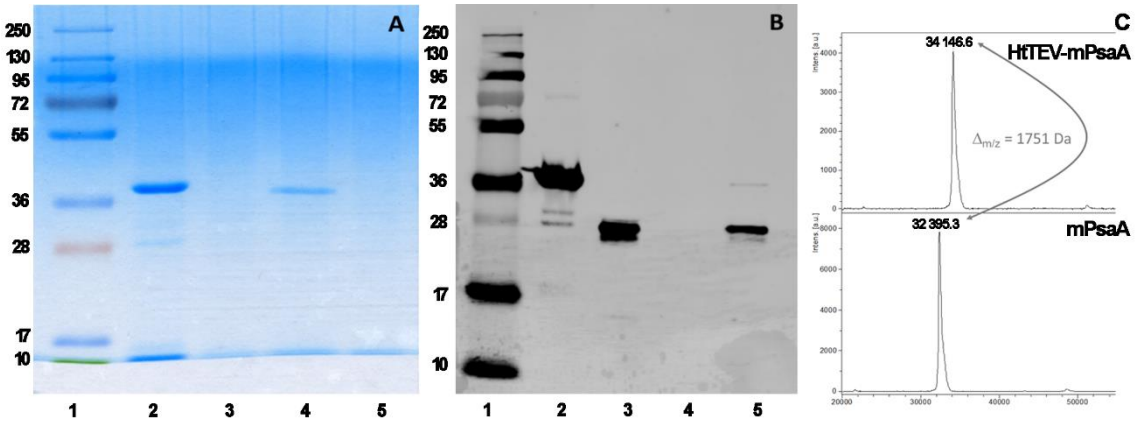

Figura 1: Caracterización de mPsaA. Análisis de la eliminación de la etiqueta de histidina de HtTEV-mPsaA por SDS-PAGE (A) y por Western blot (B). Carril 1: marcador de proteína; Carril 2: HtTEV-mPsaA; Carril 3: proteasa AcTEV ™ utilizada; Carril 4: mPsaA purificada después de la eliminación de la etiqueta de polihistidina; Carril 5: eluido después de la purificación de proteína mPsaA en perlas de NiNTA; Espectros MALDI-TOF-MS de PsaA antes y después de la eliminación de la etiqueta de histidina (C).

Los resultados experimentales obtenidos a partir del Western blot mediante el empleo de anticuerpos anti-histidina confirmaron la identidad y pureza de HtTEV-mPsaA y la eliminación del residuo de polihistidina. Mediante cromatografía de afinidad se observó que la muestra correspondiente a la fracción no unida presentó una banda ligeramente por debajo de la HtTEV-mPsaA SDS-PAGE, tras ser revelada mediante azul Coomassie, y ausente en el análisis de Western blot (**Figura 1A y B, Carril 4**). También se pueden observar en el eluido, tanto una primera banda correspondiente a la proteasa HtTEV como una segunda banda de HtTEV-mPsaA sin escindir, con muy baja intensidad, tras la purificación en perlas de NiNTA (**Figura 1, Carril 5B**). La identidad de ambas formas de PsaA fue confirmada mediante MALDI-TOF (**Figura 1C**). El peso molecular de las dos proteínas difiere en 1751 unidades de masa, lo que corresponde a la cola y al residuo terminal de metionina. El peso molecular de mPsaA equivalente a una molécula de PsaA que se obtuvo fue de 32.395 Da. La síntesis del tetrasacárido antigénico Pn14TS se realizó previamente en el grupo de Ingeniería Molecular y Glicobiología de la Universidad de Nantes, Francia.

El mPsaA se conjugó con Pn14TS mediante una reacción de acoplamiento tiol/maleimida. Con este objetivo, los grupos amino libres de las lisinas expuestas en la superficie de la proteína se derivatizaron por tratamiento con reactivo SATA-NHS (relación 120M). El exceso del reactivo fue eliminado mediante diálisis. Posteriormente, el vehículo modificado se conjugó con Pn14TS-mal en una relación 1:16M en presencia de exceso de hidrocloruro de hidroxilamina con el fin de generar grupos reactivos tiol in situ. El conjugado PsaA-Pn14TS resultante se purificó por filtración en gel, se liofilizó y almacenó a -80 °C. De manera similar, se preparó un conjugado BSA-Pn14TS como control para evaluar la importancia de PsaA como un elemento portador. El análisis de la composición química de los glicoconjugados por el método fenol-sulfúrico y el ensayo de Bradford revelaron que las relaciones molares de azúcar/proteína de los dos conjugados fueron de 5.4/1. El análisis de dicroísmo circular (CD) del conjugado mPsaA-Pn14TS y sus intermedios en comparación con mPsaA reveló que no hay cambios en la estructura secundaria de la proteína. El PsaA exhibió picos negativos a 208 nm y 222 nm en todas las etapas de conjugación y liofilización, lo que demuestra un plegado de proteína similar y con un número significativo de hélices alfa y láminas beta de acuerdo con la estructura mPsaA determinada [6]. Se observó un patrón de plegado similar tras la superposición de los espectros de DC de HtTEV-PsaA, mPsaA y mPsaA-Pn14TS, confirmando la estabilidad en la proteína durante el proceso de conjugación (**Figura 2**).

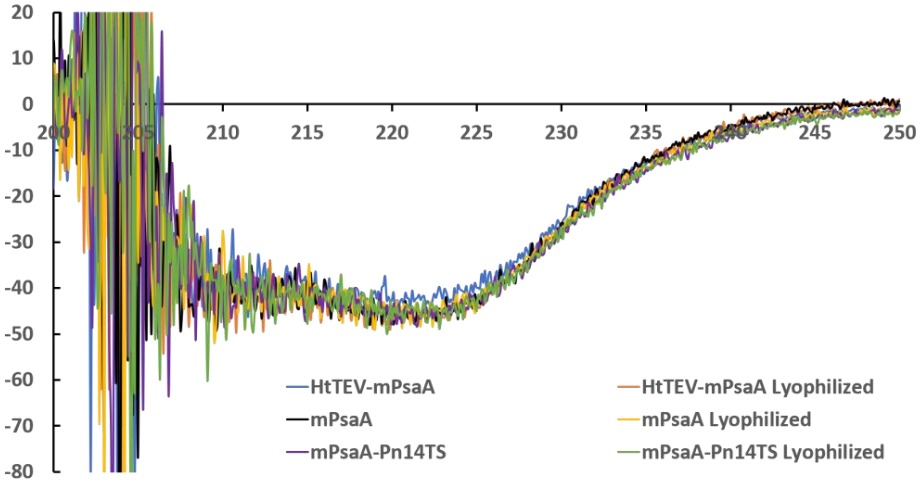

Figura 2: La superposición de los espectros CD de la proteína en las diferentes etapas de purificación, conjugación y liofilización.

La conservación de mPsaA y mPsaA-Pn14TS se realizó mediante almacenamiento a -80 °C después de su liofilización y también en glicerol al 40%. En ambos casos el mPsaA ha mantenido su estructura secundaria incluso después de un almacenamiento de 12 meses a -80 °C. La eficacia de inmunización del conjugado mPsaA-Pn14TS con α-GalCer como adyuvante se examinó en ratones, comparándose mPsaA y un conjugado modelo de BSA-Pn14TS. Se demostró que los conjugados mPsaA-Pn14TS (GC) fueron capaces de inducir una respuesta de IgG contra la proteína y el tetrasacárido.

Objetivo 2: Preparación y caracterización de nanopartículas de quitosano cargadas con GC

Se prepararon nanopartículas de quitosano (CNP) cargadas con GC mediante un procedimiento de gelificación iónica simple. Su dispersión en medio acuoso reveló un diámetro medio de 142 ± 18 nm y un potencial zeta de 27 ± 3 mV. Se demostró que el PDI de las GC-CNP era inferior a 0.2, indicando homogeneidad de las nanopartículas. La representación esquemática de la formación de las CNP se muestra en la **figura 3**.

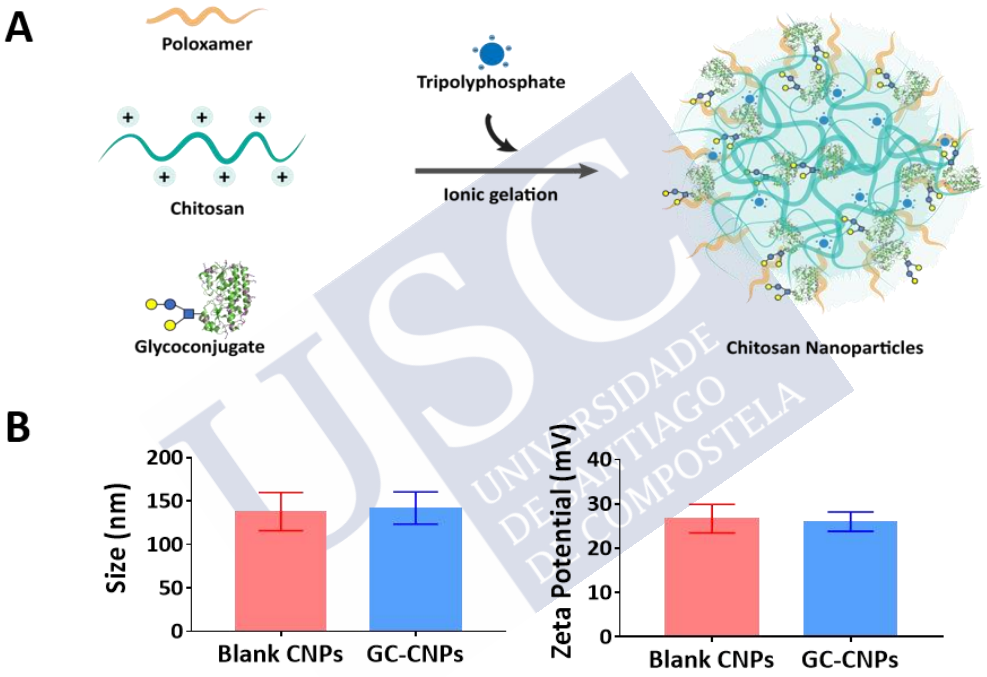

Figura 3: Preparación de nanopartículas de quitosano; (A) Representación esquemática de la preparación de nanopartículas de quitosano por el método de gelificación iónica; (B) Tamaño de partícula y potencial zeta de CNP blancas y GC-CNP.

La eficiencia de encapsulación (E.E.) de GC en las CNP fue del 70 ± 3% tras incorporar 35 µg de GC por miligramo de NP. La formulación contenía aproximadamente 6.000 GC por partícula, medido mediante análisis de seguimiento de nanopartículas (NTA) (~ 1.9 x 10^{10} partículas por mg de GC-CNP). Las nanopartículas se liofilizaron utilizando 5% de trehalosa, las CNP fueron fácilmente redispersables en agua sin alterar el tamaño de las partículas.

Como se puede observar en la **figura 4B**, los resultados de la microscopía electrónica de barrido muestran una distribución de tamaño estrecha tanto en CNP blancas como en GC-CNP. Las micrografías SEM demuestran una morfología casi esférica de las CNP sin signos de agregación. La distribución del tamaño de las partículas se representa gráficamente como se muestra en la **figura 4C.** Los tamaños medios de partículas fueron de 147 ± 19 nm y 145 ± 28 nm para las nanopartículas blancas y GC-CNP respectivamente. No se observaron diferencias significativas en el patrón de distribución de las NP, a pesar de que las GC-CNP presentaban un número ligeramente mayor de partículas en un rango de tamaño por debajo de 100 nm.

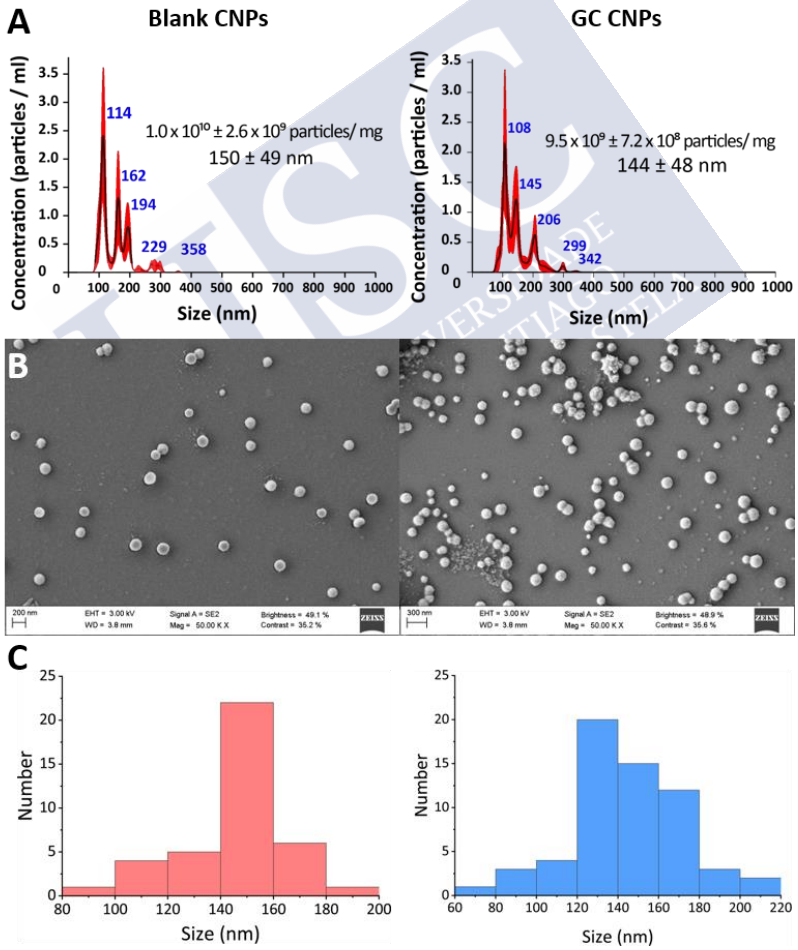

Figura 4: Determinación del tamaño de partícula por análisis de seguimiento de nanopartículas (NTA) y microscopía electrónica de barrido de emisión de campo (FESEM) de las CNP blancas y GC-CNP; A) La figura representa la distribución del tamaño de partícula y la concentración de nanopartículas blancas y GC-CNP determinadas por NTA; B) La morfología de CNPs blancas y GC-CNPs determinada por FESEM muestra que las CNPs presentaron forma esférica; C) La distribución del tamaño de partícula a partir de las imágenes FESEM.

Los resultados obtenidos de la interacción de las nanopartículas de quitosano con mucina en fluido nasal simulado (SNF) se muestran en las **figuras 5A y 5B**, indicando un aumento en la estabilidad de las nanopartículas en este medio en presencia de mucina. Los tamaños de partícula en SNF con 0.1% de mucina fue de alrededor de 320 nm a t = 0, el doble del tamaño medio observado cuando las NP se dispersan en agua.

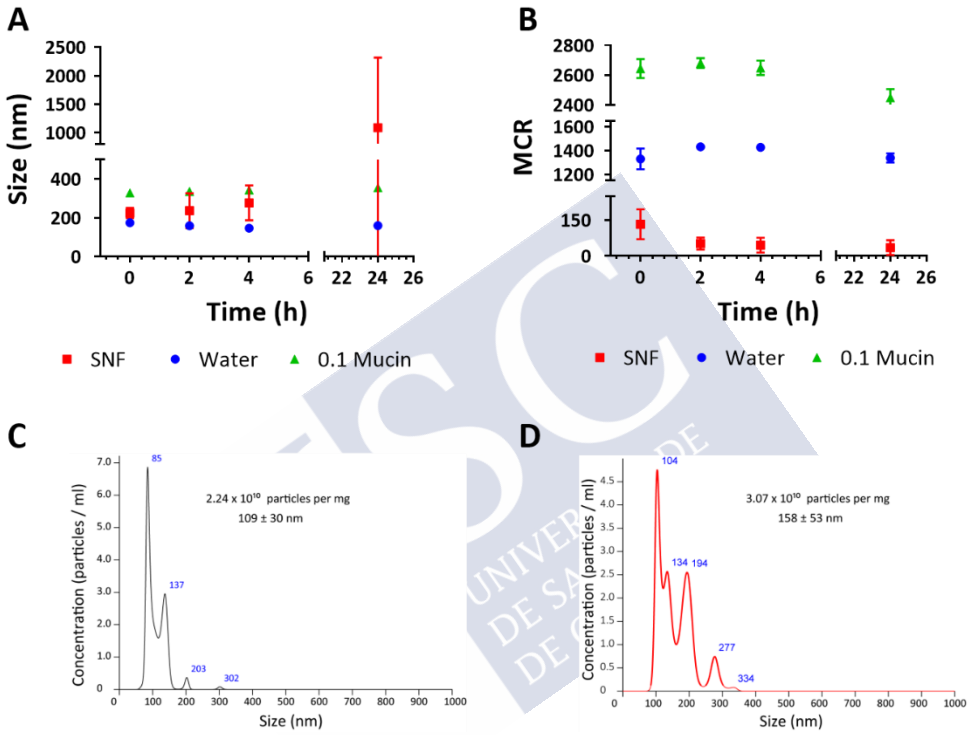

Figura 5: Estabilidad coloidal de GC-CNP en medio mucoso. Caracterización del tamaño de partícula (A) y tasa de recuento medio (MCR) (B) de las GC-CNP medidas a diferentes intervalos de tiempo durante 24 horas; distribución del tamaño de partícula medido por NTA para comparar la estabilidad de GC-CNP en agua (C) y tras su incubación en RPMI con 10% de FCS (D).

Las nanopartículas fueron estables durante un período de 24h, conservando su tamaño y numero de partículas en 0.1% de mucina en SNF. Frente a estas observaciones, en el caso de las nanopartículas incubadas en SNF, el tamaño de partícula aumentó con el tiempo y el número de las mismas se redujo drásticamente. La razón del aumento inicial en el tamaño de las nanopartículas con 0.1% de mucina en SNF, a pesar de que fueron estables a partir de entonces, podría deberse a la propiedad mucoadhesiva de las nanopartículas de quitosano.

Los datos obtenidos por NTA confirman que las GC-CNP no presentaron agregación en medios R10 a concentraciones inferiores a 500 µg/mL **(Figura 5C y 5D).**

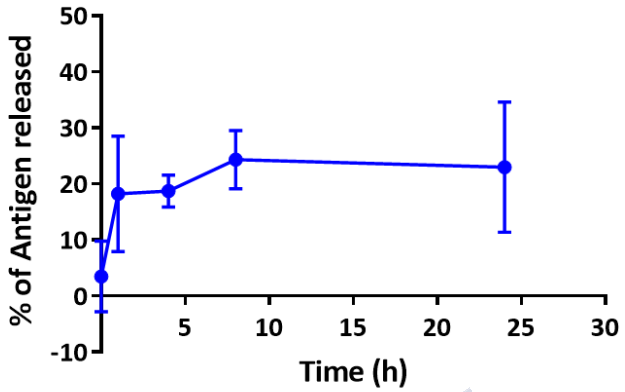

Figura 6: Porcentaje de antígeno liberado después de incubar las GC-CNP en SNF durante un período de 24 h (N = 3)

La cantidad de GC liberada a diferentes intervalos de tiempo de las GC-CNP se cuantificó frente al sobrenadante de las CNP blancas. Aproximadamente el 18% del antígeno se liberó después de 1 h de incubación en SNF. Sin embargo, a partir de ese punto no hubo un aumento significativo en el porcentaje del antígeno liberado. Como se puede observar en la **figura 6**, tras 24h, el porcentaje de antígeno liberado fue del 24 ± 9%. Esto podría deberse a una fuerte asociación del GC con las CNP. Una liberación inicial rápida podría corresponder al GC no encapsulado o al GC que se adsorbe en la superficie de las CNP.

Objetivo 3: Eficiencia in vivo e in vitro de las nanopartículas cargadas con glicoconjugado

Interacción de GC-CNP con células dendríticas.

En primer lugar, se estudió la compatibilidad de las GC-CNP con las células dendríticas, mediante el ensayo 7-AAD. El 7-AAD es un colorante de ADN fluorescente con capacidad de atravesar la membrana plasmática de células apoptóticas o muertas. La mortalidad de las DCs, dependiente de la dosis, se muestra en la **Figura 7A**. Las GC-CNP mostraron niveles de

supervivencia superiores al 90%, en un rango de concentración de 25 a 100 µg/mL. Tanto las CNP blancas como las GC-CNP tenían un perfil similar de citocompatibilidad y se consideraron menos tóxicas para las DCs a concentraciones inferiores a 100 µg/mL. De manera similar, para estudiar la influencia de la concentración de GC-CNP en la actividad metabólica y/o la supervivencia de células dendríticas inmaduras (iDCs), se realizó un ensayo MTS. Como se observa en la **Figura 7B**, las GC-CNP mostraron la reducción de la actividad metabólica de las iDCs, de manera dependiente de la dosis. Los resultados sugieren que las GC-CNP se encontraban en rango no tóxico aceptable a una concentración de 25 a 100 µg/mL.

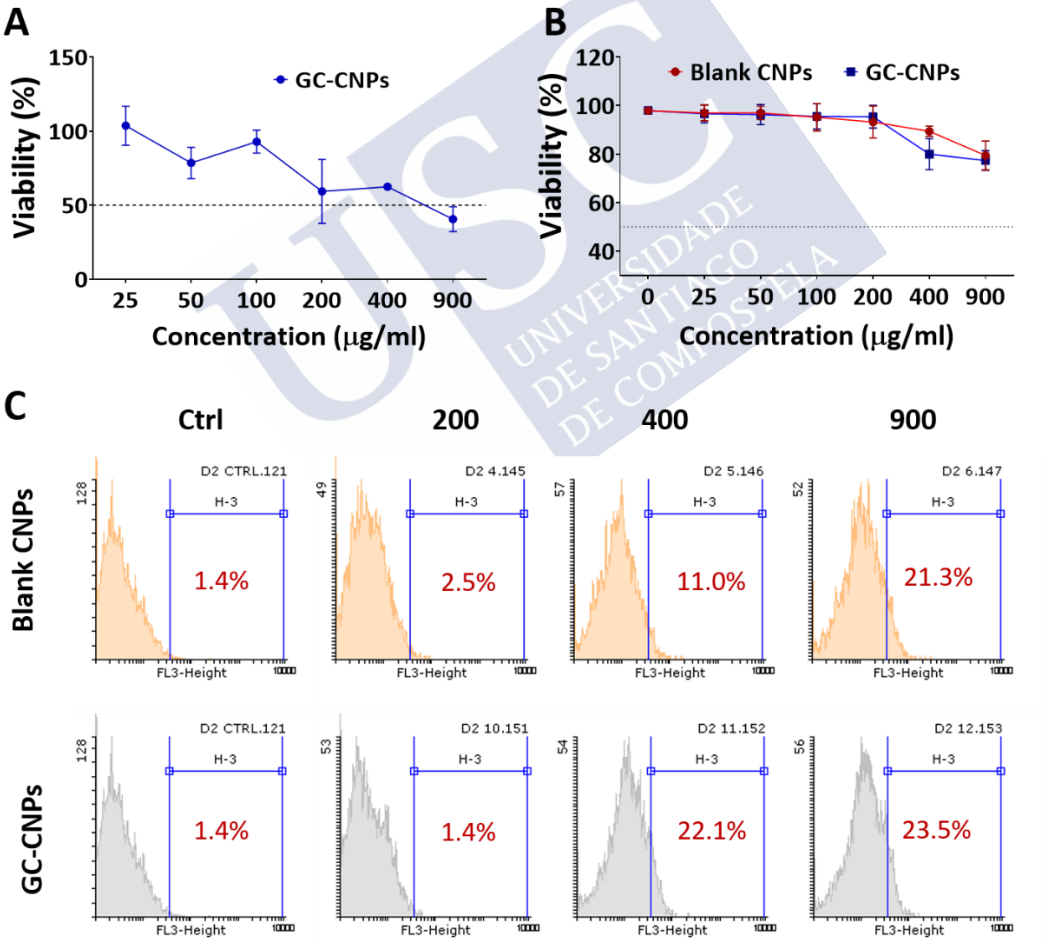

Figura 7: Citotoxicidad de nanopartículas de quitosano (CNP) en células dendríticas inmaduras (iDCs). A) ensayo de tinción MTS; B) Se realizó un ensayo de 7-AAD tanto para GC-CNP (líneas azules) como para CNP blancas (líneas rojas) y C) Histogramas representativos obtenidos del análisis de citometría de flujo después de la tinción con 7-AAD. Los resultados se presentan como media ± desviación estándar (DE) de 4 donantes.

Además, se estudió la interacción de las GC-CNP con las DCs (**Figura 8A)**. El patrón de internalización de las GC-CNP (50 µg/mL) en las DCs a 37 °C aumenta al incrementarse el tiempo de incubación. Sin embargo, no se observa mucha diferencia entre la internalización de las GC-CNP a las 2h y 4h tras su incubación a 37 °C. Por otra parte, las DCs incubadas a 4 °C como control no mostraron una internalización significativa de las GC-CNP incluso después de 4h, mostrando una internalización específica de nanopartículas dependientes de energía a 37 °C.

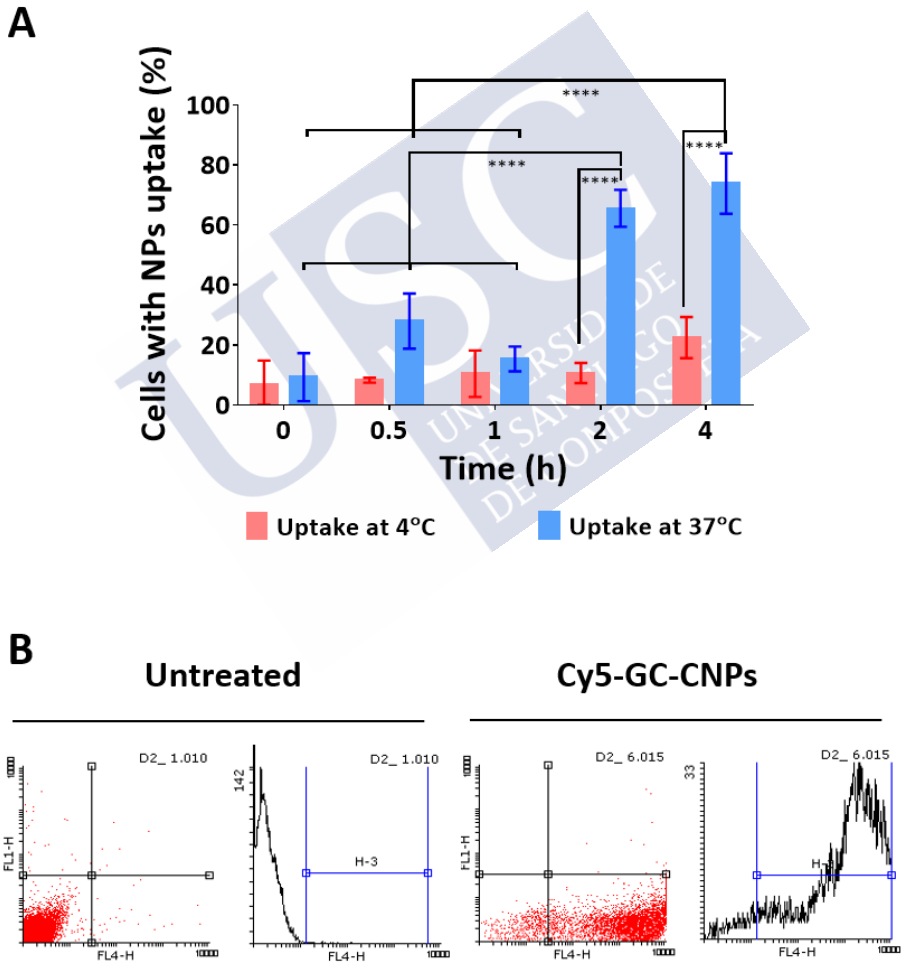

Figura 8: Internalización de las Cy5-GC-CNP en MoDCs. Como se muestra en (A), se analizó la absorción dependiente del tiempo para GC-CNP marcadas con Cy5 (50 µg/mL) a 4 °C y 37 °C utilizando citometría de flujo. Las imágenes que se muestran en (B) muestran la comparación de las DCs no tratadas con las DCs tratadas con Cy5-GC-CNP (50 µg/mL para 2h a 37 °C). Los resultados se presentan como media ± D.E. de 3 donantes. La diferencia estadística entre los grupos es *, P <0.05; **, P <0,01; ***, P <0,001; ****, P <0,0001.

Se llevó a cabo un estudio de la expresión de marcadores coestimuladores para conocer el papel de las GC-CNP en la maduración de las DCs. Como se muestra en la **Figura 9**, las iDCs tratadas con CNP blancas y GC-CNP mostraron una expresión mayor de marcadores CD80, CD83 y CD86, aunque esta regulación positiva no fue estadísticamente significativa, probablemente debido a la variabilidad observada entre los diferentes donantes. Las DCs tratadas con CNP blancas y GC-CNP mostraron un perfil similar de expresión de marcadores de activación, y la regulación positiva siempre fue mayor en el caso de las células tratadas con GC-CNP. Aunque los resultados no son estadísticamente significativos, esto indica que la presencia de GC en las CNP potencia la estimulación de CD80, CD83 y CD86 por parte de las DCs. Por otra parte, se observa una clara regulación al alza de todas las moléculas coestimuladoras cuando las iDCs se trataron con LPS e INF-γ (**Figura 9**, columnas violetas).

El papel de los diferentes componentes de las CNP en la estimulación de linfocitos periféricos y monocitos se determinó mediante la cuantificación de la síntesis de TNF-α por estos tipos de células. Staphylococcus Enterotoxin-B (SEB) se usó como control positivo para la estimulación de linfocitos T, mientras que el lipopolisacárido bacteriano (LPS) se usó como control positivo para la estimulación de monocitos. Cuando las PBMCs se trataron con las CNP o sus componentes, no se observó una activación significativa de los linfocitos T (medidos como células positivas para TNF-α) para ningún tratamiento en particular.

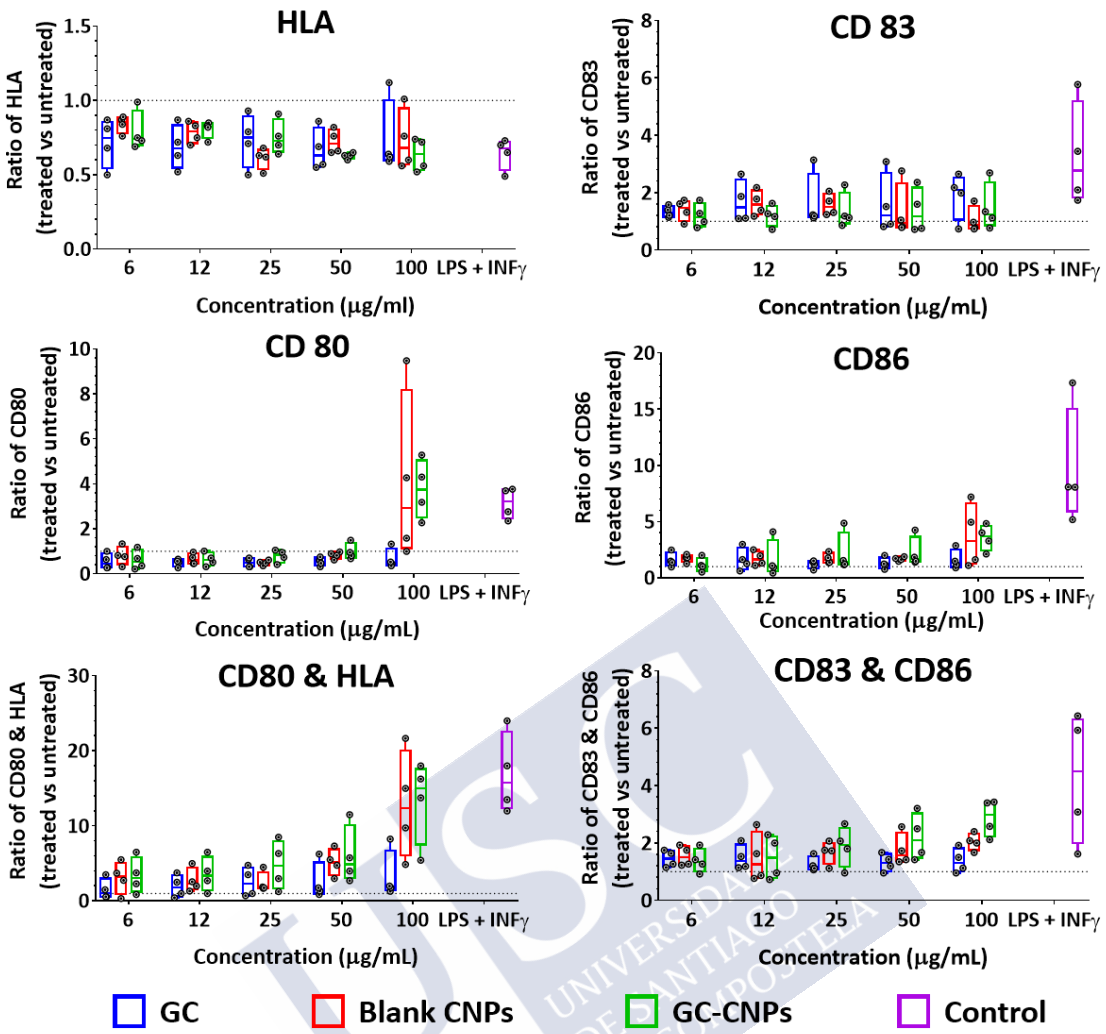

Figura 9: Las GC-CNP inducen la activación y maduración de MoDCs. La expresión de las moléculas coestimuladoras como HLA, CD86, CD88 y CD83 en la superficie de CD1a + MoDCs se determinó por citometría de flujo 48 h después de la estimulación con 50 µg/mL CNP blancas o GC-CNP. Las barras en los diferentes colores indican GC (azul), CNP blancas (rojo), GC-CNP (verde) y el control con tratamiento LPS + INF-γ (púrpura). Los datos representan la media ± desviación estándar de los resultados obtenidos de los 4 donantes. No se observó significancia estadística entre los grupos.

Sin embargo, se observa un resultado diferente en el caso de los monocitos periféricos. El tratamiento con CNP blancas estimula la producción de TNF-α por monocitos en comparación con las iDCs no tratadas, pero en menor medida en comparación con los PBMCs tratadas con GC-CNP. Las iDCs incubadas con GC-CNP sintetizan más TNF- α en comparación con sus componentes antigénicos individuales (Pn14TS y mPsaA; **Figura 10**, monocitos). Sin embargo, se puede observar que el GC solo induce la secreción de TNF- α por los monocitos a un nivel similar al observado con LPS.

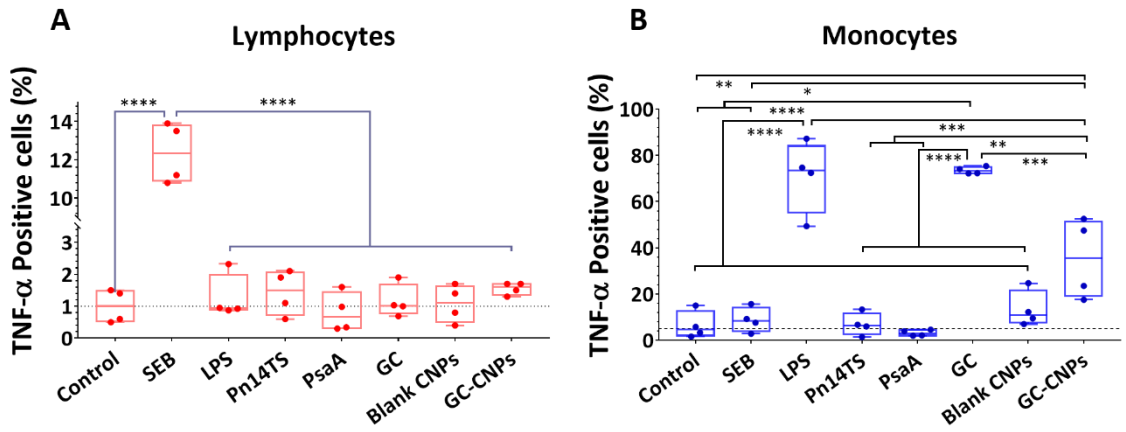

Figura 10: Los gráficos indican el porcentaje de células positivas para TNF-α después del tratamiento con SEB, LPS, Pn14TS, PsaA, GC, CNP blancas y GC-CNP. Las PBMCs se trataron con los componentes equivalentes a las GC-CNP de 50 µg/mL durante 48 h. El análisis de citometría de flujo se realizó para cuantificar los linfocitos (A) y (B) monocitos positivos para TNF-α. Los resultados se presentan como media ± desviación estándar de 4 donantes. La diferencia estadística entre los grupos es *, P <0.05; **, P <0,01; ***, P <0,001; ****, P <0,0001.

La capacidad de las CNP (blancas y GC-CNP) para inducir la secreción de TNF-α principalmente por monocitos se relaciona con la capacidad de estas nanopartículas para activar APC (como se sugirió anteriormente para las DCs) y sus precursores (es decir, monocitos) dando lugar a una mayor activación del sistema inmune adaptativo (de linfocitos T) e induciendo actividad protectora contra los patógenos.

Para determinar el papel de las CNP y mPsaA en la actividad aloestimuladora de las DCs, las iDCs se pretrataron con mPsaA, CNP blancas y una mezcla de mPsaA y CNP blancas, y posteriormente se incubaron con linfocitos de sangre periférica (PBLs) alogénicos. Las iDCs no tratadas y tratadas con LPS se usaron como controles negativos y positivos, respectivamente. La expresión de CD25 y CD28 se midió para determinar la activación de los linfocitos T alogénicos CD4 y CD8. Como se puede ver en la **Figura 11A**, hay un aumento significativo en las células T alogénicas CD4+ CD25 cuando las DCs se trataron con CNP blancas, en comparación con la expresión de CD25 cuando se usaron DCs incubadas con LPS o el antígeno PsaA (**Figura 11A**).

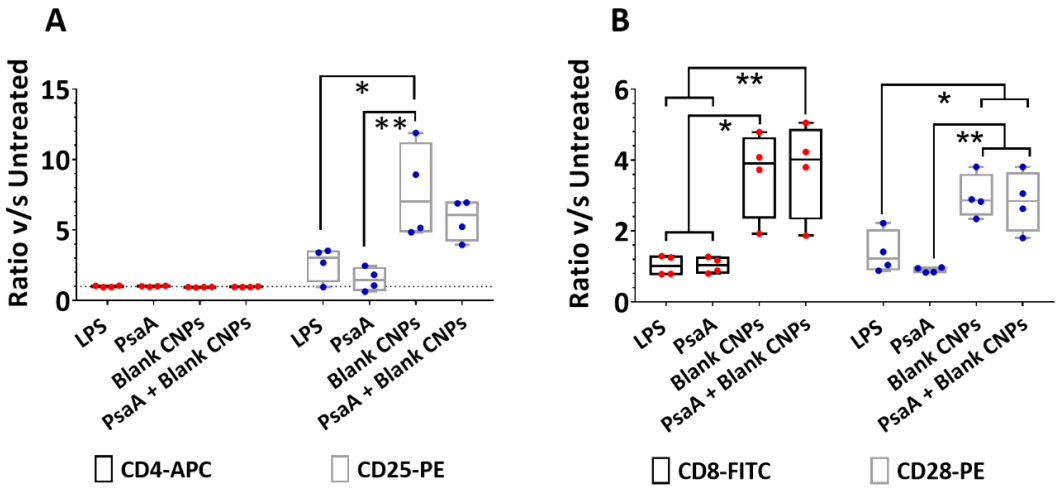

Figura 11: las DCs tratadas con CNP inducen la proliferación de células T en una reacción mixta de linfocitos, las DCs se incubaron durante 24 h en presencia de LPS, PsaA, CNP blancas y PsaA + CNP blancas, después se cultivaron con PBLs alogénicos en una proporción de 1:10 durante 48 h. El número de CD4 y CD25 positivos (A), y CD8 y CD28 positivos (B), se analizaron por citometría de flujo. Los resultados se presentan como media ± D.E. de 4 donantes. La diferencia estadística entre los grupos es *, P <0.05; **, P <0,01; ***, P <0,001; ****, P <0,0001.

Dado que estas últimas no promovieron la activación (es decir, la regulación positiva de CD25) de las células T CD4, se puede pensar que las CNP por sí mismas son capaces de activar las iDCs. Por otro lado, cuando se examinó la activación de los linfocitos T CD8 (**Figura 11B**), se puede detectar una activación clara de estos linfocitos usando DCs pretratadas con CNP blancas o una mezcla de CNP blancas y PsaA. La regulación ascendente de CD28 es significativamente mayor en los linfocitos T CD8 estimulados por DCs tratadas con CNP o CNP + PsaA, en comparación con las DCs pretratadas con LPS o PsaA solo (Figura 5B; azul). Se observó un mayor porcentaje de linfocitos T CD8 + en cultivos en los que las DCs se pretrataron con CNP, en comparación con las observadas en cultivos que utilizan DCs pretratadas con LPS o PsaA (Figura 5B; rojo).

Estudios de inmunización en ratones.

Se realizó una primera serie de experimentos para evaluar el papel de la nanoencapsulación en la inmunogenicidad del GC. Se inmunizaron grupos de 6 ratones por vía subcutánea (S.C)

un total de dos veces a intervalos de dos semanas con GC, GC-CNP o PBS adyuvados con α-GalCer. El nivel de la respuesta de anticuerpos originada por las diferentes formulaciones se determinó mediante ELISA. Este estudio se realizó para ver si la encapsulación de GC dentro de las CNP mejora la inmunogenicidad contra el GC. Se determinó la respuesta inmune, tanto la IgG como la IgM generadas contra los componentes de polisacárido capsular (CP) y proteína (PsaA) del glicoconjugado. Ni GC ni GC-CNP indujeron una respuesta IgM anti-mPsaA tras la segunda inmunización, mientras que se observó una respuesta baja de IgM anti-CP. Al comparar la respuesta IgG de GC y GC-CNPs administradas vía S.C, las GC-CNPs mostraron entre 10 y 100 veces mayor respuesta DE IgG anti-CP y anti-PsaA en comparación con el GC (**Figura 12**). Sorprendentemente, la respuesta de IgG inducida por las GC-CNP en ratones también fue mayor que la observada previamente para el GC administrado a una dosis seis veces mayor [11]. Los resultados muestran que la encapsulación del GC en CNP mejora la respuesta de IgG contra la proteína y el polisacárido capsular.

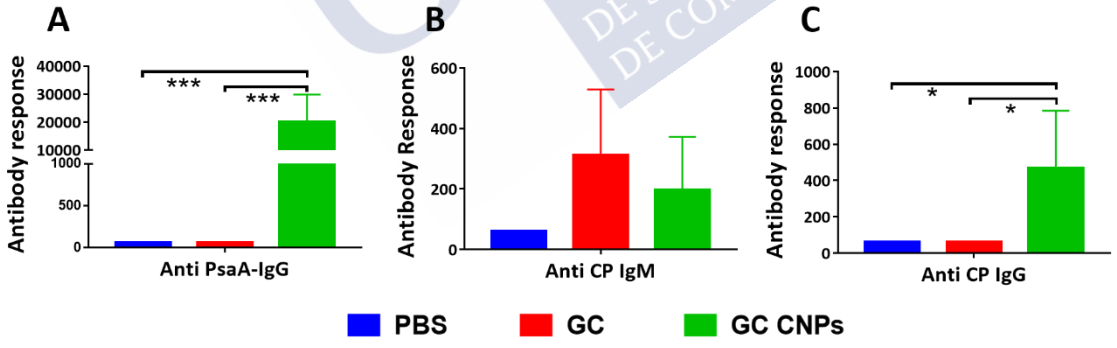

Figura 12: La respuesta de anticuerpos en los ratones inmunizados con PBS, GC y GC-CNP una semana después de la inmunización final. La inmunización se realizó dos veces en los días 0 y 14 y la respuesta de anticuerpos en suero se determinó en el día 21. Los resultados obtenidos se representan como respuesta anti-mPsaA IgG (A), respuesta anti-CP IgM (B) y respuesta anti-CP IgG (C). El análisis estadístico se realizó mediante la prueba U de Mann-Whitney. La diferencia estadística entre los grupos es *, P <0.01; **, P <0,001; ***, P <0,0005. Los datos representan la media ± desviación estándar (n = 6).

También fue interesante conocer las subclases de IgG que se producían predominantemente en el grupo tratado con GC-CNP. Las muestras de suero de ratones inmunizados con GC-CNP

mostraron un alto nivel de anticuerpos de la subclase IgG1 y en un grado mucho menor de IgG2b contra mPsaA y CP (**Figura 13**). No hubo activación de otras subclases de IgG como IgG2a. En la literatura se observa que los anticuerpos de la subclase IgG1 son inducidos principalmente por proteínas bacterianas, mientras que para IgG2 son inducidos por polisacáridos capsulares [30]. La generación de anticuerpos anti IgG1 contra PsaA y CP puede atribuirse a la activación de la fagocitosis por los macrófagos [31].

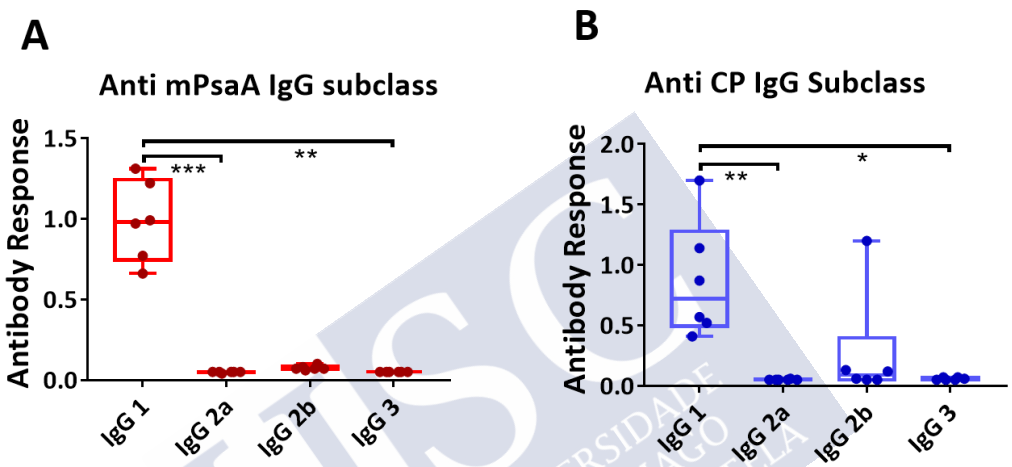

Figura 13: La subclase de respuesta de anticuerpos anti IgG en los ratones inmunizados con GC-CNP una semana después de la inmunización final. La inmunización se realizó dos veces en los días 0 y 14 y la respuesta de anticuerpos en suero se determinó en el día 21. Los resultados obtenidos se representan como respuesta IgG anti-mPsaA (A) e IgG anti-CP IgG (B). El análisis estadístico se realizó mediante ANOVA unidireccional con análisis de Kruskal-Wallis mediante las comparaciones múltiples de Dunn. La diferencia estadística entre los grupos es *, P <0.05; **, P <0.01;. Los datos representan la media ± desviación estándar (n = 6).

Tras la infección por neumococo (**Figura 14**) en ratones, se observó un 50% de supervivencia en el día 20 en el grupo inmunizado por vía SC con GC-CNP mientras que el grupo inmunizado con una cantidad equivalente de GC mostró solo un 17% de supervivencia. Curiosamente, hubo un 100% de supervivencia hasta el día 13 en los ratones tratados con GC-CNP, mientras que en los grupos tratados con GC, la supervivencia se redujo al 50% en el día 10.

En una segunda serie de experimentos, nuestro objetivo fue determinar la respuesta humoral de IgG e IgM inducida en ratones por las GC-CNP, en función de la vía de administración, ya

sea subcutánea o intranasal (I.N). Se inmunizaron grupos de 6 ratones (C57BL/6) un total de tres veces a intervalos de 2 semanas con GC-CNP (S.C), CNP blancas (SC), Prevnar 13 (S.C), GC (I.N), GC-CNP (I.N), CNP blancas (I.N), y CNP blancas GC + (I.N) adyuvantes con α-GalCer.

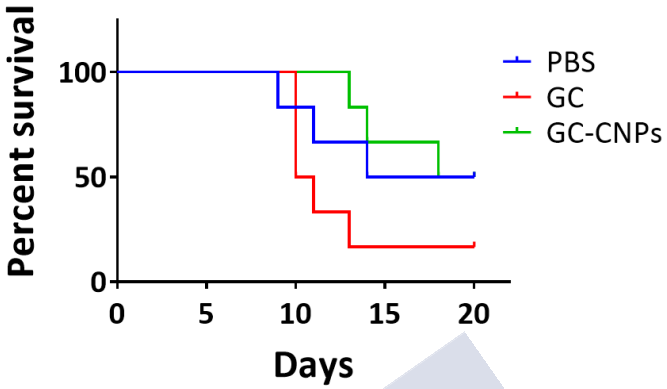

Figura 14: Supervivencia de ratones vacunados por vía intranasal mediante la administración de 30 UFC de H3N2 seguido de $1x10^6$ de *S. pneumoniae* serotipo 14.

Los sueros de ratones inmunizados con CNP blancas, así como el de ratones inmunizados con Prevnar 13 (que no contiene PsaA como inmunógeno) no muestran ninguna respuesta anti-mPsaA IgG en ninguna de las vías. Mientras que las GC-CNP no lograron producir IgG anti-PsaA cuando se administraron a través de la mucosa nasal (**Figura 15A**), las mismas GC-CNP produjeron una respuesta de IgG anti-PsaA 100 veces mayor cuando se administraron por vía S.C. Esto muestra que las GC-CNP fueron capaces de inducir una respuesta IgG anti-PsaA por vía S.C pero no I.N. Los resultados de la inmunización I.N muestran que la respuesta de IgG anti-mPsaA es más alta en el grupo inmunizado con GC y se observa una reducción en la actividad al mezclar el GC con CNP e inmunizar a los ratones. Se observó una reducción adicional de la actividad en la encapsulación de la GC en las CNP. Esto muestra la influencia de las CNP en la reducción de la respuesta inmune contra el GC mientras se administra I.N. Este hallazgo plantea la necesidad de investigar más a fondo la influencia de la naturaleza y

la estructura de las CNP en la inmunogenicidad y el efecto del aclaramiento mucociliar en la disminución de la respuesta inmune contra el GC encapsulado.

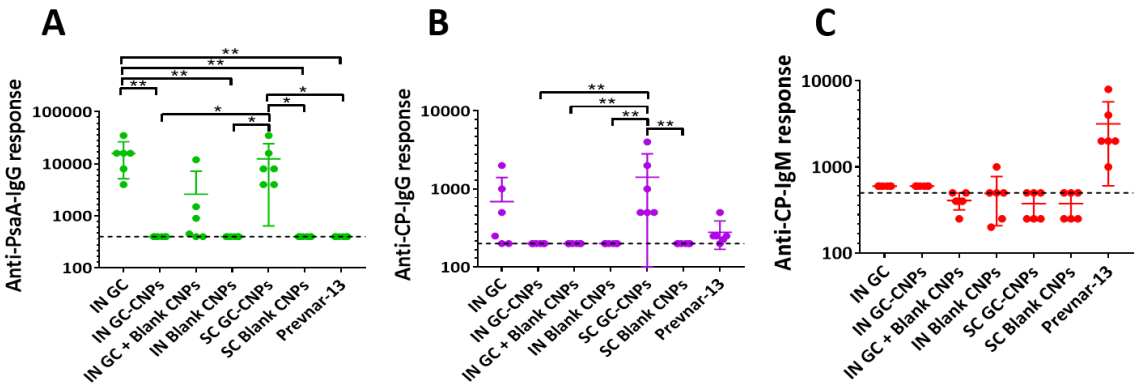

Figura 15: Se estudió la respuesta de anticuerpos en los ratones inmunizados con GC-CNP (S.C), CNP blancas (SC), Prevnar 13 (SC), GC (I.N), GC-CNP (I.N), CNP blancas (I.N) y GC + CNP blancas (I.N). La inmunización se realizó tres veces en el período de un mes (0, 14 y 28 días) y la respuesta de anticuerpos en suero en los ratones se determinó 2 semanas después de la inmunización final. Los resultados se muestran como respuesta anti-mPsaA IgG (A), respuesta anti-CP IgG (B) y respuesta anti-CP IgM (C). Los datos de las muestras de suero se presentaron como media ± DE de seis ratones por grupo. El análisis estadístico se realizó mediante ANOVA unidireccional con análisis de Kruskal-Wallis mediante las comparaciones múltiples de Dunn. La diferencia estadística entre los grupos es *, P <0.05; **, P <0,01; ***, P <0,001.

La respuesta de IgM anti-CP 14 fue muy baja y solo se observó en los ratones inmunizados con Prevnar 13 (**Figura 15C**). Mientras, tanto el GC (I.N) como las GC-CNP (S.C) pudieron inducir una respuesta de IgG anti-CP. Esta respuesta fue muy baja en el grupo de ratones inmunizados con Prevnar 13 y no se observó en los otros grupos.

Además, los estudios sobre la cuantificación de anticuerpos IgA de los fluidos bronquiales de ratones inmunizados no mostraron respuesta de IgA (datos no mostrados). Sin embargo, el estudio final sobre la opsonofagocitosis a partir del suero de los ratones inmunizados está en marcha. Estos resultados serían críticos para concluir el papel de la nanoencapsulación de GC y la vía de inmunización.

Referencias:

[1] Institute for Health Metrics and Evaluation (IHME), Findings from the Global Burden of Disease Study 2017, Seattle, 2018. http://www.healthdata.org/sites/default/files/files/policy_report/2019/GBD_2017_Booklet.pdf (accessed September 23, 2019).

[2] Streptococcus pneumoniae : Vaccines for AMR, (n.d.). https://vaccinesforamr.org/review-of-pathogens/pathogen-profiles/streptococcus-pneumoniae/#impacte8a5-9923a88f-af42 (accessed September 23, 2019).

[3] K.A. Geno, G.L. Gilbert, J.Y. Song, I.C. Skovsted, K.P. Klugman, C. Jones, H.B. Konradsen, M.H. Nahm, Pneumococcal capsules and their types: Past, present, and future, Clin. Microbiol. Rev. 28 (2015) 871–899. doi:10.1128/CMR.00024-15.

[4] K.P. Klugman, R. Dagan, R. Malley, C.G. Whitney, Pneumococcal Conjugate Vaccine and Pneumococcal Common Protein Vaccines, Plotkin's Vaccines. (2013) 504–541. doi:10.1016/B978-1-4557-0090-5.00032-X.

[5] D.M. Weinberger, R. Malley, M. Lipsitch, Serotype replacement in disease after pneumococcal vaccination, Lancet. 378 (2011) 1962–1973. doi:10.1016/S0140-6736(10)62225-8.

[6] N. Li, X.Y. Yang, Z. Guo, J. Zhang, K. Cao, J. Han, G. Zhang, L. Liu, X. Sun, Q.Y. He, Varied metal-binding properties of lipoprotein PsaA in Streptococcus pneumoniae, J. Biol. Inorg. Chem. 19 (2014) 829–838. doi:10.1007/s00775-014-1114-9.

[7] J.S. Sampson, Z. Furlow, A.M. Whitney, D. Williams, R. Facklam, G.M. Carlone, Limited diversity of Streptococcus pneumoniae psaA among pneumococcal vaccine serotypes, Infect. Immun. 65 (1997) 1967–1971.

[8] K.E. Morrison, D. Lake, J. Crook, G.M. Carlone, E. Ades, R. Facklam, J.S. Sampson, Confirmation of psaA in all 90 serotypes of Streptococcus pneumoniae by PCR and potential of this assay for identification and diagnosis, J. Clin. Microbiol. 38 (2000) 434–437.

[9] P. Schmid, S. Selak, M. Keller, B. Luhan, Z. Magyarics, S. Seidel, P. Schlick, C. Reinisch, K. Lingnau, E. Nagy, B. Grubeck-Loebenstein, Th17/Th1 biased immunity to the pneumococcal proteins PcsB, StkP and PsaA in adults of different age, Vaccine. 29 (2011) 3982–3989. doi:10.1016/j.vaccine.2011.03.081.

[10] C. Entwisle, A. Mcilgorm, W. Chan, J.S. Brown, C.A. Colaco, C.R. Bailey, S.W. Clarke, Next Generation Vaccines: Development of a Novel Streptococcus pneumoniae Multivalent Protein Vaccine, (2017). doi:10.12665/J143.Colaco.

[11] M. Prasanna, D. Soulard, E. Camberlein, N. Ruffier, A. Lambert, F. Trottein, N. Csaba, C. Grandjean, Semisynthetic glycoconjugate based on dual role protein/PsaA as a pneumococcal vaccine, Eur. J. Pharm. Sci. 129 (2019) 31–41. doi:10.1016/J.EJPS.2018.12.013.

[12] D. Safari, H.A.T. Dekker, J.A.F. Joosten, D. Michalik, A.C. De Souza, R. Adamo, M. Lahmann, A. Sundgren, S. Oscarson, J.P. Kamerling, H. Snippe, Identification of the Smallest Structure Capable of Evoking Opsonophagocytic Antibodies against Streptococcus pneumoniae Type 14, 76 (2008) 4615–4623. doi:10.1128/IAI.00472-08.

[13] A. Vartak, S.J. Sucheck, Recent advances in subunit vaccine carriers, Vaccines. 4 (2016). doi:10.3390/vaccines4020012.

[14] L.A. Brito, D.T. O'Hagan, Designing and building the next generation of improved vaccine adjuvants, J. Control. Release. (2014). doi:10.1016/j.jconrel.2014.06.027.

[15] J. Banchereau, F. Briere, C. Caux, J. Davoust, S. Lebecque, Y.J. Liu, B. Pulendran, K. Palucka, J. Banchereau, F. Briere, F. Briere, C. Caux, C. Caux, J. Davoust, J. Davoust, S. Lebecque, S. Lebecque, Y.J. Liu, Y.J. Liu, B. Pulendran, B. Pulendran, K. Palucka, K. Palucka, Immunobiology of Dendritic Cells, Immunology. 18 (2000) 767–811. doi:10.1146/annurev.immunol.18.1.767.

[16] R.M. Steinman, Dendritic cells: Understanding immunogenicity, Eur. J. Immunol. 37 (2007). doi:10.1002/eji.200737400.

[17] K. Palucka, J. Banchereau, Linking innate and adaptive immunity, Nat. Med. 5 (1999) 868–870. doi:10.1038/11303.

[18] P. Calvo, C. Remuñan-López, J.L. Vila-Jato, M.J. Alonso, Chitosan and Chitosan/Ethylene Oxide-Propylene Oxide Block Copolymer Nanoparticles as Novel Carriers for Proteins and Vaccines, Pharm. Res. 14 (1997) 1431–1436. doi:10.1023/A:1012128907225.

[19] N. Csaba, M. Garcia-Fuentes, M.J. Alonso, Nanoparticles for nasal vaccination, Adv. Drug Deliv. Rev. 61 (2009) 140–157. doi:10.1016/j.addr.2008.09.005.

[20] H.B.T. Moran, J.L. Turley, M. Andersson, E.C. Lavelle, Immunomodulatory properties of chitosan polymers, Biomaterials. 184 (2018) 1–9. doi:10.1016/j.biomaterials.2018.08.054.

[21] V. Dodane, M. Amin Khan, J.R. Merwin, Effect of chitosan on epithelial permeability and structure, Int. J. Pharm. 182 (1999) 21–32. doi:10.1016/S0378-5173(99)00030-7.

[22] R. Rosenthal, D. Günzel, C. Finger, S.M. Krug, J.F. Richter, J.-D. Schulzke, M. Fromm, S. Amasheh, The effect of chitosan on transcellular and paracellular mechanisms in the intestinal epithelial barrier, Biomaterials. 33 (2012) 2791–2800. doi:10.1016/J.BIOMATERIALS.2011.12.034.

[23] D.A. Zaharoff, C.J. Rogers, K.W. Hance, J. Schlom, J.W. Greiner, Chitosan solution enhances both humoral and cell-mediated immune responses to subcutaneous vaccination., Vaccine. 25 (2007) 2085–94. doi:10.1016/j.vaccine.2006.11.034.

[24] M.F. Bachmann, G.T. Jennings, Vaccine delivery: A matter of size, geometry, kinetics and molecular patterns, Nat. Rev. Immunol. 10 (2010) 787–796. doi:10.1038/nri2868.

[25] C. Foged, B. Brodin, S. Frokjaer, A. Sundblad, Particle size and surface charge affect particle uptake by human dendritic cells in an in vitro model, Int. J. Pharm. 298 (2005) 315–322. doi:10.1016/J.IJPHARM.2005.03.035.

[26] R.P. Gala, M. D'Souza, S.M. Zughaier, Evaluation of various adjuvant nanoparticulate formulations for meningococcal capsular polysaccharide-based vaccine, Vaccine. 34 (2016) 3260–3267. doi:10.1016/J.VACCINE.2016.05.010.

[27] A.L. Silva, R.A. Rosalia, E. Varypataki, S. Sibuea, F. Ossendorp, W. Jiskoot, Poly-(lactic-co-glycolic-acid)-based particulate vaccines: Particle uptake by dendritic cells is a key parameter for immune activation, Vaccine. 33 (2015) 847–854. doi:10.1016/J.VACCINE.2014.12.059.

[28] T. López-León, E.L.S. Carvalho, B. Seijo, J.L. Ortega-Vinuesa, D. Bastos-González, Physicochemical characterization of chitosan nanoparticles: electrokinetic and stability behavior, J. Colloid Interface Sci. 283 (2005) 344–351. doi:10.1016/J.JCIS.2004.08.186.

[29] A.L. Larentis, A.P.C. Argondizzo, G.D.S. Esteves, E. Jessouron, R. Galler, M.A. Medeiros, Cloning and optimization of induction conditions for mature PsaA (pneumococcal surface adhesin A) expression in Escherichia coli and recombinant protein stability during long-term

storage, Protein Expr. Purif. 78 (2011) 38–47. doi:10.1016/j.pep.2011.02.013.

[30] C. Papadea, I.J. Check, Human Immunoglobulin G and Immunoglobulin G Subclasses: Biochemical, Genetic, and Clinical Aspects, Crit. Rev. Clin. Lab. Sci. 27 (1989) 27–58. doi:10.3109/10408368909106589.

[31] M. González-Miro, L. Rodríguez-Noda, M. Fariñas-Medina, D. García-Rivera, V. Vérez-Bencomo, B.H.A. Rehm, Self-assembled particulate PsaA as vaccine against Streptococcus pneumoniae infection., Heliyon. 3 (2017) e00291. doi:10.1016/j.heliyon.2017.e00291.

Introduction

Approaches for design and delivery of subunit pneumococcal vaccines

USC
UNIVERSIDADE
DE SANTIAGO
DE COMPOSTELA

Approaches for design and delivery of subunit pneumococcal vaccines

Abstract

Pneumococcal vaccines have proven to be effective candidates for the prevention of pneumococcal infectious diseases. The global pneumonia burden was significantly reduced by the promotion of pneumococcal polysaccharide (PPSV23) and pneumococcal conjugate (PCV7, 10 and 13) vaccines. Despite their undoubted effectiveness, the serotype dependence of these vaccines still needs to be improved. The serotype replacement phenomenon has led to the development of protein-based vaccines, consisting of highly conserved pneumococcal protein antigens (PPAs). Further improvements rely on understanding the molecular mechanism of immune recognition and optimizing the delivery to the antigen-presenting cells for eliciting both cellular and humoral responses. The use of innovative delivery systems is a new and exciting strategy. In this review, we address the current status of different pneumococcal subunit vaccines and nanotechnological approaches employed for their delivery.

Keywords: Glycoconjugates, Capsular polysaccharides, Protein antigens, Nanotechnology, Pneumonia, Infection, Immunology

1. Introduction

Pneumonia is the leading cause of death among infectious diseases. According to the global health burden of disease study 2017, pneumonia was responsible for 2.6 million deaths in that year. 75% of these deaths were among the children younger than 5 years (809, 000 deaths) and elderly over 70 years (1.1 million deaths) [1,2]. *Streptococcus pneumoniae* is the leading cause for the occurrence of pneumonia. Besides, *S. pneumoniae* is responsible for bacterial meningitis, sepsis and otitis media. The Institute for Health Metrics and Evaluation (IHME) estimates that infections due to *S. pneumoniae* alone are responsible for ~1.2 million deaths annually. Out of these, pneumococcal meningitis and pneumococcal pneumonia were estimated to be responsible for 23,000 and 300,000 cases, respectively [1,3]. Two-thirds of these deaths are concentrated in Sub-Saharan Africa, South Asia, and South-East Asia. In the year 2015, just five countries (India, China, Pakistan, Nigeria and Indonesia) contributed to 54% of all pneumonia cases [4]. For the year 2017, pneumococcal vaccine market was valued at 7,083 million USD and is expected to grow at 5% compound annual growth rate (CAGR) between 2018 and 2025 to reach the market value of 10,215 million USD by the year 2025 [5].

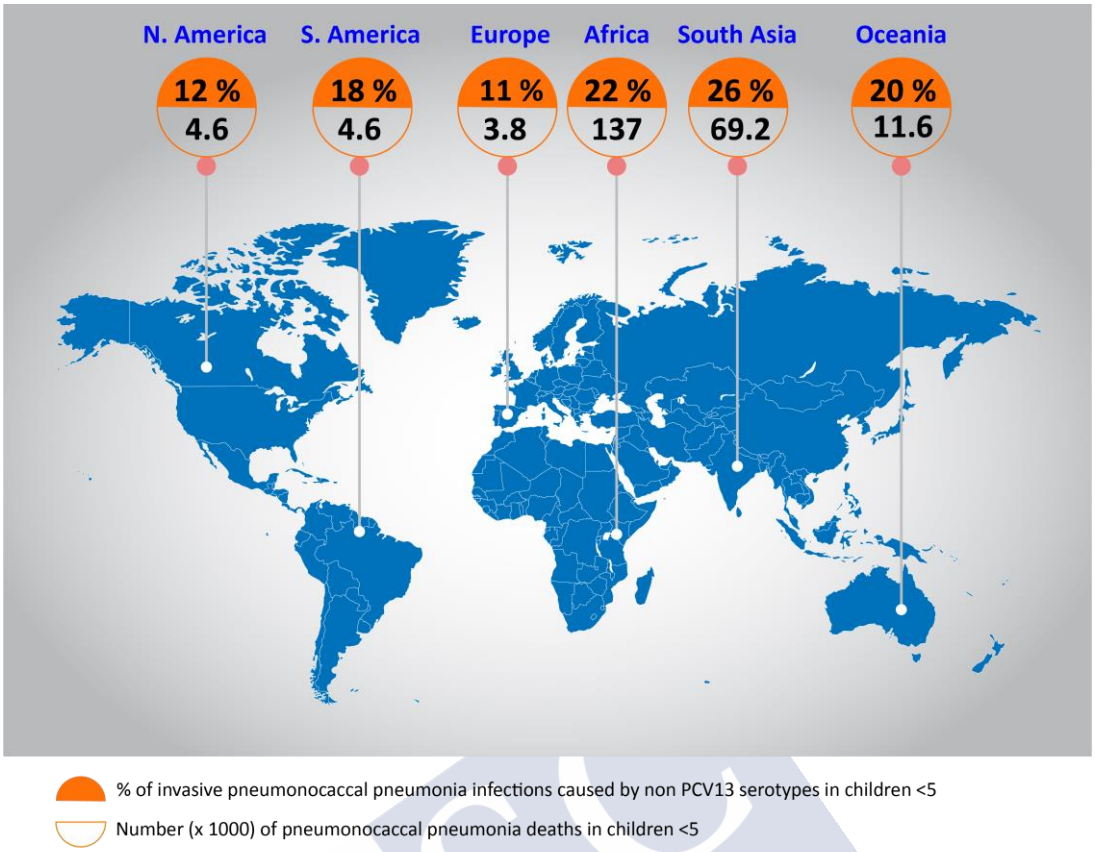

Figure 1: Epidemiology of Pneumonia. The figure illustrates the mortality and morbidity occurred due to pneumococcal pneumonia infections in the children under 5 years. The data was compiled using the report on the global burden of *S. pneumonia* 2000 – 15, Lancet [6]. The values in the upper hemisphere (orange) indicates the % of infections caused by the serotypes that are not included in the PCV. The values in the lower hemisphere (transparent) indicates the number (x 1000) of deaths caused by pneumococcal pneumonia in the children under 5 years.

Over 96 *S. pneumoniae* serotypes have been identified based on differences in the composition of surface-exposed large polysaccharides which form a capsule around the bacteria [7]. Available pneumococcal vaccines target these capsular polysaccharides. Two types of pneumococcal vaccines are currently in use; a 23 valent pneumococcal polysaccharide vaccine (PPSV23) and 7, 10 or 13 valent pneumococcal conjugate vaccines (PCV-7, 10, 13). Although the introduction of the conjugate vaccines has reduced the global burden of pneumonia, the currently available pneumococcal vaccines protect against a limited number of serotypes. An efficient strategy to improve the coverage and immunogenicity is the incorporation of common pneumococcal proteins that are present in all the serotypes. These pneumococcal proteins have been effective in generating a protective

response in the immunized individuals but whether anti-surface protein Abs are useful to diminish the carriage is still debated.

However efficient the vaccine is, its effective delivery is essential to induce a proper immune response. The immunogenicity of subunit vaccines can be enhanced by improving their presentation to dendritic cells (DCs). To achieve this, the use of nanoparticulate systems is a potential alternative. Within this regard, the insights from immunology and microbiology, the advances in the nanotechnology and material science have paved the way for the effective delivery of subunit pneumococcal vaccines.

In this review, we are discussing the current progress in the field of subunit pneumococcal vaccines, together with the factors that influence the generation of an immune response against such vaccines. Also, their uptake by antigen-presenting cells (APCs) when given in nanoparticulate form over the free form are elucidated. This understanding of the mechanisms discussed in the review provides an insight into the importance of using the particulate systems in the subunit vaccine delivery.

2. Pneumococcal vaccine development

The *S. pneumoniae* was first observed by Klebs (1875) in course of his work with lung fluids and sputum from pneumonia patients, while Eberth and Matry (1880) have first coined the term Pneumoniekokken. Later, Louis Pasteur and Miller Sternberg (1881), independently isolated *S. pneumoniae* and the possible serological diversity of the pneumococcal serotypes were described by Benzancon and Griffin in 1897. However, in 1902, Friedrich Neufeld identified the presence of multiple pneumococcal serotypes. In 1917, the landmark papers published by Dochez and Avery described an immunologically active soluble substance of pneumococcus, and six years later Heidelberger and Avery identified these soluble substances

as polysaccharides from the pneumococcal capsule. These investigations eventually led to the identification of the polysaccharide components of the bacterial capsules as possible targets for pneumococcal vaccine development [8]. Since then, substantial progress has occurred in the development of pneumococcal polysaccharide and conjugate vaccines. It is not difficult to imagine the enormous impact of these vaccines on human lives. However, there is a continuous effort in developing novel pneumococcal vaccines that are cost-effective and can offer broader coverage among all the serotypes. To achieve this, researchers are developing vaccines based on common proteins and using nanotechnological approaches for efficient delivery of subunit vaccines.

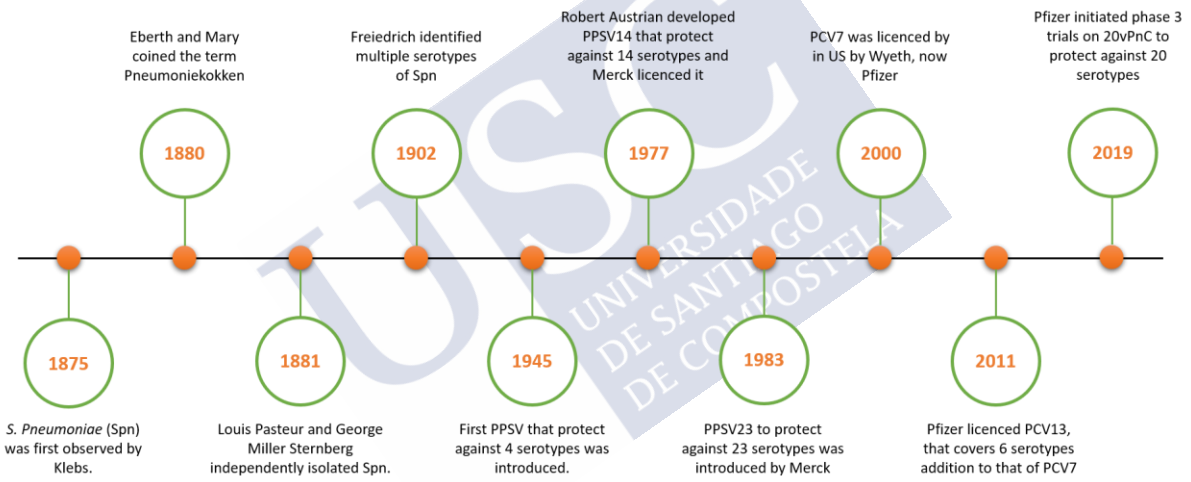

Figure 2: Timeline of pneumococcal vaccine development.

2.1. Polysaccharide vaccines

These vaccines are composed of purified polysaccharide components of the bacterial capsule. The capsular polysaccharides act both as virulence determinants and targets for protective antibodies. Carbohydrates are abundant on the cell surfaces and exist in the form of oligo- or polysaccharides attached to lipids or proteins [9]. They are involved in the invasion and the attachment process [10,11]. In turn, the immune system recognizes the carbohydrates from pathogenic microbes and often elicits an immune response by producing carbohydrate

specific protective antibodies [8,11,12]. The first successful subunit vaccine consisting of capsular polysaccharides from 4 serotypes was introduced in 1945. The importance of this discovery was not credited due to the availability of newly introduced antibiotics. However, Robert Austrian has done extensive research in identifying new serotypes and developed a vaccine that offers protection against 14 serotypes. By expanding this work, in 1983, the vaccine consisting of polysaccharides from 23 serotypes was developed by Merck to cover more than 80 – 90% infectious serotypes. This 23 valent pneumococcal polysaccharide vaccine (PPSV23) contains the components from following serotypes: 1, 2, 3, 4, 5, 6B, 7F, 8, 9N, 9V, 10A, 11A, 12F, 14, 15B, 17F, 18C, 19F, 19A, 20, 22F, 23F, and 33F. It is still in use and is recommended for all the adults over 65 years of age. Although the PPSV23 reduced the rate of invasive pneumococcal disease in immunized patients, it failed to reduce the nasopharyngeal carriage. In addition, due to its inability to produce the B cell memory and switching from IgM to IgG isotypes or producing the antibodies with higher affinity during the primary immune response, PPSV23 failed to be successful in children younger than 2 years and immunocompromised patients. These problems fostered the development of glycoconjugate vaccines that could produce long-lasting immunity.

Isolation of carbohydrate antigens with defined length and specific functional groups from natural sources is challenging. The duties of culture, processing, isolation and purification include laborious, time-consuming and costly activities. Besides, it is not feasible to cultivate all pathogenic bacteria to generate carbohydrate antigens *in-vitro*. Further to this, indeed, the down-stream processing generates glycans with varying lengths that can affect epitope integrity. Synthetic oligosaccharides mimicking native capsular polysaccharides have been proposed to avoid these shortcomings of carbohydrate antigens [13–17]. The progress in immunology and synthetic carbohydrate chemistry has helped in the development of

synthetic glycan approaches, which make the precise identification of the antigenic determinants expressed within the bacterial polysaccharide possible. The chemical synthesis of glycans enables to tune the length, structure, ease of characterization, reduces bacterial contaminants and increases batch-to-batch reproducibility. This complete understanding of polysaccharide vaccines aids in drawing a more robust correlation of the elicited immune response by the chemical structure [18].

In contrast to the native polysaccharides, synthetic glycans can be equipped with a unique functional group that enables its coupling to a protein carrier giving rise to neoglycoconjugates, that can be more easily characterized [19,20]. Besides, such coupling strategy is likely to retain the integrity of sugar epitopes. The site-specific chemical modifications paved a path for linking the adjuvants, which can exhibit improved immuno-stimulant properties [21]. Still, it is often challenging to synthesize the carbohydrate in large scale with low manufacturing costs and without process convolution. However, some approaches could circumvent these problems [18,22].

2.1.1. General mechanism: focus on bacterial antigens

The prerequisite for the adaptive immunity is the activation of T lymphocytes by the DCs, which process the antigen and present it in the MHC complex. Intracellularly synthesized antigens (*e.g.* viral and tumoral origin) are presented by MHC I molecules, that activate $CD8^+$ T cells. MHC II molecules present extracellular antigens to the $CD4^+$ T cells. In addition, the mechanism of cross-presentation also permits such antigens to enter the MHC I pathway and stimulate $CD8^+$ T cells. The adaptive immune system mainly comprises humoral (antibodies) and cell-mediated mediated responses. Upon activation, the naive $CD4^+$ T cells differentiate into Th1 cells (produces INF- γ and IL-2) and Th2 (secrete IL 4, IL 5, IL 10). On the other hand,

$CD8^+$ T cells become cytotoxic T lymphocytes (CTLs), which can kill the altered host cells and secrete cytokines like INF-γ and TNF-α. Excellent reviews on the detailed mechanism of antigen processing by APCs can be found elsewhere [23–26].

2.1.2. Immune cell activation by polysaccharide vaccines

For polysaccharide vaccines, the APCs use distinct endocytosis mechanisms and process the carbohydrates to smaller sizes by endo-lysosomes, but these fragments fail to bind directly MHCII, and hence, glycans are considered as T cell-independent (TI) [23,27]. However, the polysaccharide vaccines generate an immune response on their interaction with B lymphocytes [28,29]. Based on their interaction with the B lymphocytes, antigens are either classified into TI type 1 or TI type 2. TI type 1 antigens (LPS) are capable of proliferating and differentiating both naive and mature B lymphocytes. TI type 1 antigens are effective both in neonates and the elderly [30]. TI type 2 antigens (PPSV) are high molecular weight repetitive polysaccharides that do not exhibit intrinsic B lymphocyte stimulation. However, they interact with the surface immunoglobulins of mature B lymphocytes to generate an immune response. Unlike TI type 1 antigens, TI type 2 antigens are not suitable as vaccine candidates in neonates and elderly [29]. However, as an exception, zwitterionic polysaccharides can be processed and presented by MHCII pathway, that questions this paradigm [31].

2.2. Conjugate vaccines

Glycoconjugate vaccines are prepared by coupling or conjugating the polysaccharide moieties to the carrier proteins. The development of glycoconjugates was driven by the ineffectiveness of the polysaccharide vaccines to generate a strong immune response in the children. The commonly used protein carriers are tetanus toxoid (TT), diphtheria toxoid (DT) and cross-reacting material-197 (CRM-197, a non-toxic mutant of diphtheria toxoid). The coupling of

polysaccharide moieties to carrier proteins enhances T cell-dependent responses against the polysaccharides. In the late 1920s and early 1930s, the synthesis of glycoconjugates using covalent conjugation was pioneered by Avery and Goebel [32]. This early work formed the basis for the further development of the glycoconjugate vaccines. Applying this principle, several investigators have made significant contributions to the development of the glycoconjugates [33–36]. Pfizer launched the first glycoconjugate vaccine covering 7 (PCV7) serotypes in the year 2000. The PCV7 greatly reduced the rate of infections in vaccinated children under 2 years and the non-immunized people within the community through herd effect. Later in 2010, PCV7 was replaced by PCV13 that covers the 13 serotypes.

The PCV13 increased the serotype coverage to 80% and showed broader protection against the pneumococcal infections. As a result, the rate of invasive and non-invasive pneumococcal infections reduced further. Despite their undoubted success in reducing the number of invasive pneumococcal disease in infants and children < 5 years of age, the concern of serotype replacement is still haunting the pneumococcal vaccines [37,38]. The term serotype replacement has been coined to describe the increase in the rate of infections caused by serotypes not covered in PCV7 and PCV13. Serotype replacement thus leads to the emergence of infections caused by serotype, which were not prevalent until then as observed for serotype 35B. Besides this, currently employed technologies in the synthesis of glycoconjugates involve multi-step processes and are cost intense. Seeberger and his coworkers have done significant work in developing semi-synthetic glycoconjugates (serotype 1, 2, 3, 5, 7F and 8) to protect against the serotypes that are not included in the marketed PCVs [39–44]. Their work demonstrates synthetic oligosaccharides can be used as an alternative for purified polysaccharides that are commonly in use. Semi-synthetic glycoconjugates were prepared by conjugating these synthetic oligosaccharides to CRM-197.

Besides, these researchers have also formulated pentavalent semisynthetic vaccines based on purely synthetic oligosaccharide antigens and claimed that adding these to the marketed pneumococcal vaccines can increase their coverage [45]. Despite several advantages and extensive research, only one glycoconjugate based on a synthetic carbohydrate antigen is available in the market. It was developed and licensed in 2003 by Heber Biotech developed and licensed as Quimi-Hib in Cuba [13,46,47]. It consists of a fully synthetic oligosaccharide Hib vaccine conjugated to tetanus toxoid. Overall, Quimi-Hib proved the possibility of translating the synthetic approach from the bench to the industrial scale.

2.2.1. Conjugation methods

The approaches employed to engineer the glycoconjugates aim to produce vaccines with higher batch-to-batch consistency and enhanced potential or biological activity [48]. This involves three major areas (i) glycan assembly, (ii) conjugation approaches, and (iii) construction of multicomponent glycoconjugates. The first approach focuses on obtaining a series of glycans from the pathogens or producing synthetic mimics of the glycans. Glycan assembly involves methods like chemoenzymatic approaches [49], one-pot protocols [50], and automated solid-phase synthesis [51–53]. Conjugation approaches are based on both random and selective methods [22]. In random conjugation, reactive functional groups of the proteins are targeted, such as the amines of lysines, thiols of cysteines, the carboxyl groups from the aspartates/glutamates or the tyrosine residues. While the selective conjugation is performed depending on the targeted functional group frequency and its surface accessibility, this leads to heterogeneous conjugates of different sugar/protein ratios [54]. In the case of multicomponent glycoconjugates, the method involves the attachment of multiple antigens to the same protein, using different linkers and coupling methods [22].

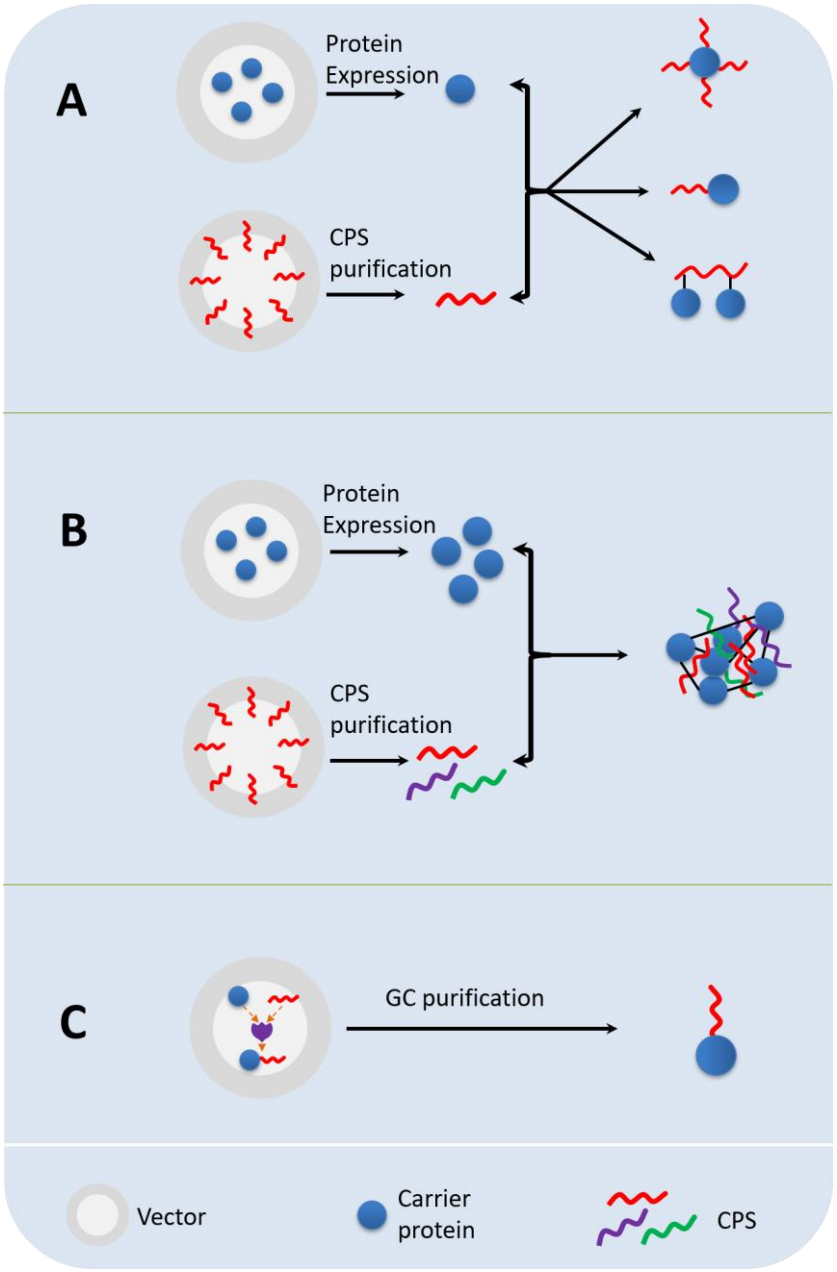

Figure 3: Schematic representation of glycoconjugate (GC) synthesis; A) a simple glycoconjugation method where the carrier protein and the capsular polysaccharides (CPS) are separately produced and conjugated by using the linkers; B) Protein capsular matrix vaccine (PCMV) in which multiple polysaccharide antigens are entrapped in a cross-linked protein matrix; C) Protein glycan coupling technology (PGCT), production of conjugate vaccines *via in vivo* biosynthesis.

Furthermore, advances in the glycoengineering approach pioneered new techniques like protein glycan coupling technology (PGCT), developed by GlycoVaxyn (now acquired by GSK) [22,48,55,56]. In PGCT, polysaccharide antigens are synthesized by the stepwise action of glycosyltransferases at the cytoplasmic side of the bacterial membrane and polymerized after flipping in engineered *E. coli* strains (Figure 3). They are then transferred to an asparagine

residue of the carrier protein synthesized within the same bacterial cell by PglB, an *N*-oligosaccharyltransferase from *Campylobacter jejuni's* protein glycosylation system [57–60]. Alternative approaches such as protein capsular matrix vaccine (PCMV) technology are used in the preparation of GCs, where CPS is non covalently trapped in the protein matrix. Currently, Matrivax is developing a pneumococcal vaccine based on PCMV which is in late preclinical phase [61]. Affinivax Inc has developed a multiple antigen-presenting system (MAPS) platform technology that simplifies the preparation of GCs. The MAPS technology involves highly specific and non-covalent binding between biotinylated polysaccharides and biotin-binding proteins. In contrast to marketed pneumococcal vaccines, MAPS offers a unique way to present the key epitopes of the desired antigens to induce potent immune response [62,63]. Recently, Affinivax Inc and Aestellas have jointly initiated phase 1 clinical trials on pneumococcal vaccine based on MAPS technology.

2.2.2. Uptake and processing of glycoconjugates

The carbohydrate moieties of the conjugate vaccines are key for the induction of pathogen-specific responses. Carbohydrates alone are T cell-independent antigens and cannot be presented to the MHC II after processing by APCs. The covalent linkage to a carrier protein enables the carbohydrates to take a T cell-dependent pathway, that involves the binding of the glycoconjugate complex to the B cell receptor. The glycoconjugate is internalized by the APCs and processed by proteolytic enzymes. The small fragmented peptides or the carbohydrate fragments associated with the peptides are represented by MHC II complex and are recognized by T cells. However, the carbohydrate fragments alone will not be presented by MHC II complex and will follow T cell-independent pathway. T cells produce signals either by direct interaction of surface proteins (CD40 and CD40L) or by secreting cytokines like

Interleukin 2 (IL2) or by inducing the maturation of B cells into antibody-producing plasma cells [23,64].

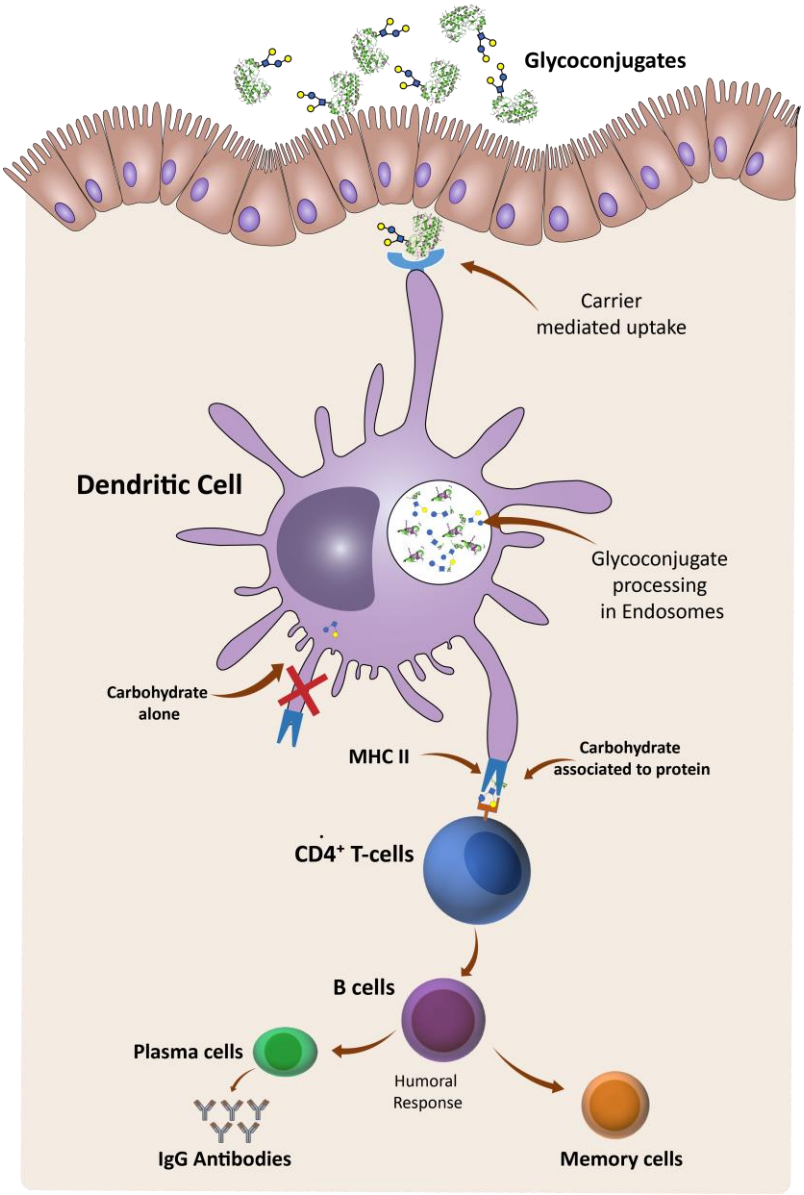

Figure 4: Processing and presentation of glycoconjugate vaccines by immune cells. The schematic representation shows the carrier-mediated uptake GCs. The internalized GCs are processed inside the endosomes and presented to T cells via MHC complexes. The carbohydrate associated with peptide or the peptide fragments alone is presented to CD4 T cells via MHC II, and the activated CD4 T cells stimulate B cells. The B cells activated by CD4 T cells either transform memory cells or antibody-secreting plasma cells.

For soluble antigens, the APCs use distinct endocytosis mechanisms. The strong covalent linkage in glycoconjugates is unlikely to be broken in the endosome, and thus the presentation of the corresponding peptides by MHCII enables that the conjugated glycans can be

recognized by the T cells. This undersells the hypothesis of “peptide only” presentation. T cells fail to respond to the glycans due to the inability of the MHCII to present them, rather than due to their inability to recognize the glycans [65].

2.3. Pneumococcal protein vaccines

Despite the enormous success of PCVs, the increasing incidence of infections caused by the non-vaccine serotype strains have led the search of alternative vaccine candidates. Pneumococci express highly conserved protein-based antigens that are present in all serotypes. This approach hopes to offer broad cross-protection against multiple pneumococcal strains. Pneumococcal protein candidates are T cell-dependent antigens which are highly immunogenic and can elicit immunologic memory. These protein antigens can either be used alone, in association or as a protein carrier in conjugate vaccines. Protein antigens can be engineered and expressed in a relatively simple and cost-effective manner. An extensive list of PPAs has been evaluated for their potential as vaccine candidates, importantly PspA, PsaA, PspC, PcpA, Ply, and PhtD are at the forefront of the investigation (see in table 1).

Table 1: Commonly investigated pneumococcal protein antigens

Protein	Description
PsaA **Pneumococcal surface adhesin A**	Surface-exposed 37-kD multi-functional lipoprotein [66]. Lipoprotein belonging to ABC-type protein complex that transports Mn2+ [67] Helps attachment to the host cell and virulence [68]
PspA **Pneumococcal surface protein A**	66 to 99 kDa surface-exposed choline-binding protein Helps survival and host-to-host invasion by interfering with complement activation [69]
PspC **Pneumococcal surface protein C**	85 kDa surface protein present in 75% of all pneumococcal serotypes Plays a major role in the colonization of nasopharynx
PhtD **Polyhistidine triad D**	95 kDa surface-expressed polyhistidine triad protein Helps attachment to the bronchial epithelium
Ply	53 kDa intracellular toxin present in all serotypes

Pneumolysin	Cholesterol dependent pore-forming cytolysin Helps surface adhesion and forms pores in target cells
PcpA **Pneumococcal choline-binding protein A**	79 kDa choline binding protein The surface protein expressed in more than 90% of serotypes PcpA is ideal candidate against invasive disease as it is expressed during invasive disease but not in the nasal mucosa.
IgA1 protease	130 to 200 kDa endopeptidase [70] Promotes adherence and persistence at mucosal surfaces
SP0148	31 kDa member of ABC transport system Plays an important role in nasopharyngeal colonization [71]
PcsB	38 – 41 kDa protein Hydrolase essential in separation of dividing cells [72]
PavA **Adherence and virulence protein A**	63 kDa surface protein involved in adherence and colonization [73]
StkP **Serine/ threonine-protein kinase**	72 kDa protein kinase Plays a crucial role in regulating cell shape and cell division Plays an important role in providing resistance during the stress conditions and virulence [74]
GlpO **Alpha-glycerophosphate oxidase**	67 kDa protein involved in the metabolism of glycerophospholipid [75]
PfbA **Plasma and fibronectin binding protein**	79 kDa protein that binds to human serum proteins Helps in fibronectin dependent adhesion and invasion [76]
ZmpB **Zinc metalloprotease B**	213 kDa surface bound metalloprotease present in all serotypes Strongly contribute to infection and virulence. Inhibits complement activation [77,78]
PrtA **cell wall associated serine protease A**	240 kDa surface-associated subtilisin-like serine protease Contribute to virulence by cleaving host proteins [79]
Hyl **Hyaluronate lyase**	120 kDa hyaluronidase protein Helps in breaking down the important component of connective tissue during the invasion [80]
NanA **Neuramidase A**	110 -140 kDa neuramidase present in all serotypes It modifies host glycoconjugates, including immune defense proteins [81]
PepO **Pneumococcal endopeptidase O**	72 kDa plasminogen and fibronectin binding protein Plays important role in invasion of host cells and immune evasion [82]
GHIP **Pneumococcus-specific glycosyl hydrolase 25**	30 kDa protein Helps in nasopharyngeal colonization and invasion of host epithelial cells [83]
PotD **Polyamine transporter D**	41 kDa membrane protein Helps in polyamine transport and plays significant role in pathogenesis [84]
PitB **Pilus backbone protein B**	37 kDa protein It is a backbone unit of pili and plays significant role in adherence to host cell [85]

PsrP **pneumococcal serine-rich repeat protein**	412 kDa, extremely large glycosylated cell surface protein Promotes adherence to nasopharyngeal epithelial cells and lung cells [86]
CbpE **Choline binding protein E**	72 kDa protein choline binding protein Helps in nasopharynx colonization and adherence to epithelial cells [87]
EndA **Endonuclease A**	30 kDa membrane nuclease [88] Helps in escaping from nuclear extracellular traps [89]
PD **Protein D**	Non lipidated cell surface lipoprotein

PPAs are increasingly being tested as potential vaccine candidates both in pre-clinical and clinical trials. Currently, Sanofi S.A is working to develop new pneumococcal protein vaccines for pneumonia, solely based on the PPAs like PhtD/dPly/PcpA (NCT01446926, NCT01764126), which are in phase 2 clinical trials (see Table 2). Genocea Biosciences, Inc. was working on developing a trivalent protein vaccine (NCT02116998) comprising of maltose/maltodextrin-binding protein (SP2108), ABC transporter substrate-binding protein (SP0148), and surface-exposed T cell protein antigen (SP1912). The studies successfully demonstrated safety and immunogenicity of the vaccine during the phase II trials. However, due to the lack of statistical significance between the placebo and immunized groups, the studies were terminated. GSK is working on developing a monovalent protein vaccine based on PhtD alone or divalent protein vaccine consisting of dPly and PhtD.

Furthermore, efforts are made to co-administer existing PCVs with pneumococcal proteins. GSK together with PATH is developing vaccines (GSK2189242A) based on the combination of pathogen-specific protein (PhtD/ PlyD1) and Prevenar 13 (NCT01262872). This vaccine combination should not only offer protection against the 13 serotypes whose polysaccharide components are incorporated but, would also provide cross-protection against other serotypes of *S. pneumoniae* that are not included in the existing pneumococcal vaccines. Researchers have also tried pathogen-specific proteins alone and have been successful in

evoking the immune response [90,91]. Some investigators also used fusion proteins which are conjugates of two different proteins (PsaA-PspA) of the same pathogen [92]. Mucosis had developed a platform technology (PneuGEM), in which pneumococcal proteins (PpmA, SlrA and IgA1-protease) are anchored to a bacterium like particles (BLPs) for mucosal immunization. The detailed list of pneumococcal vaccines under development is elaborated in Table 2.

Table 2: Subunit pneumococcal vaccines in pipeline/ clinical trials

Vaccine Type	Prototype	Company	Composition	Development phase
Pneumococcal conjugate vaccines (PCV)	V114	Merck, SII	15-valent PCV	Phase 3 NCT03950622
	GSK218942A	GSK	PCV 13 + dPly-PhtD	Phase 2 NCT01545375
	20vPnc	Pfizer	PCV 20 PCV 13 + 8, 10A, 11A, 12F, 15BC, 22F and 33F	Phase 3 NCT03760146
	PNEUMOSIL	SII, PATH	10 valent PCV	Phase 3 NCT03896477
	-	Beijing Minhai Biotechnology Co., Ltd	13 valent PCV	Phase 3 NCT02494999
	PROPEL	London School of Hygiene and Tropical Medicine	13 valent PCV	Phase 3 NCT02628886
	LBVE	LG Chem	-	Phase 2 NCT03467984
	-	Tergene	15 valent PCV	Pre-clinical
Protein Based vaccines	-	Sanofi S.A, icddrb	PhtD/dPly/PcpA	Phase 2 NCT01764126
		Sanofi S.A	PhtD + PcpA	Phase 1 NCT001444339
	GEN-004	Genocea Biosciences	SP0148 + SP1912 + SP2108	Phase 2 NCT02116998
	IC47	Valneva Austria GmbH	PcsB + Stkp + PsaA	Phase I NCT00873431
	PBPV	CanSino Biologics Inc.	PspA + PlyLD	Phase 1a NCT04087460

	ASP3772	Affinivax, Astellas Pharma Inc	unknown	Phase 1/2 NCT03803202
	PneuBioVax	Immunobiology Ltd	PspA + PlyD1	Phase 1 NCT02572635
	-	GSK	PhtD	Phase 1/ 2 NCT01767402
	GSK2231395 A	GSK	PhtD + Ply + PD	Phase 1 NCT00849069
PCV + common proteins	-	GSK + PATH	PCV 10 + PhtD/ PlyD1	Phase 2 completed NCT00985751

SII: Serum Institute of India; icddrb: International Centre for Diarrhoeal Disease Research, Bangladesh; GSK: GlaxoSmithKline

3. Nanotechnology approaches for pneumococcal vaccine delivery

Although conventional pneumococcal vaccines have significantly reduced the disease burden, there are certain unmet concerns such as sub-optimal immunogenicity profile and intrinsic instability. These subunit vaccines need repeated administrations (two injections at two months interval followed by a boost several months later) to generate an optimal immune response. Besides, available subunit vaccines are administered by a parenteral route that involves the use of needles and these vaccines in their free form are thermolabile. They often require to be co-administered with adjuvants to elicit the promising immune response. Over the past decades, many drug delivery systems, including polymeric micro- and nanoparticles, have been studied to overcome the bottlenecks mentioned above. Apart from encapsulating and delivering the antigens, particulate delivery systems can act as adjuvants [93]. Their ability to mimic the pathogens and interact with the immune cells makes them an attractive strategy for vaccine delivery [94]. Rapid progress in the pharmaceutical field has provided insights for the selection of biodegradable and biocompatible polymers from natural and synthetic sources [95]. In general, particles larger than 500 nm are readily internalized by APCs through phagocytosis, with the upper limit of 5 – 10 microns. Smaller nanoparticles can easily

drain to the lymph nodes and preferably taken up by lymph node resident DCs [96]. Besides, it is also believed that only the particles in the nanometer range transport via the lysosomal pathway and are consistent with their uptake mechanism [97]. More importantly, targeting DCs with an antigen-loaded particulate system can play a substantial role in activating the T cell-mediated immune system by processing the antigens through MHCs. Presenting the fragmented antigen peptides to CD4+ and CD8+ cells result in a humoral and cell-mediated response. Among the nanocarriers used for the delivery of vaccines, relevant examples are polymeric nanoparticles, liposomes, nanoemulsions, nanocapsules and VLPs. However, the mechanism at molecular/cellular levels is poorly understood. It is known that the inherent immunogenicity of the particulate structures can be enhanced by engineering chemical composition (immunostimulating ligands, multiple antigens) and/or the physicochemical properties of the delivery system.

3.1. Nanotechnology strategies for the delivery of subunit pneumococcal vaccines

In the field of vaccine delivery, nanoparticulate systems offer several advantages over the traditional formulations. The strategy like encapsulation or surface conjugation is employed for the incorporation of the carbohydrate antigens (CAs) or protein antigens or glycoconjugates into the nanoparticles. The encapsulation of glycoconjugates into the nanoparticles protect them from the degradation, increases the density of antigens and control the rate of antigen release. In general, the glycoconjugates or protein antigens are incorporated during the fabrication of nanoparticulate vaccines [98,99]. To deliver the pneumococcal antigens, Liposomes were either used as a vehicle or co-administered with the antigens. In 2018, Tada *et al.* developed liposomes based on DOTAP that was co-administered as an adjuvant with antigen PspA intranasally [100]. The liposomal formulation was also able

to elicit PsaA specific Th17 responses, which played a pivotal role in controlling the infection [101] and proved superior to PspA administered alone in inducing a protective immune response. In 2018, Hill *et al*. developed liposomes that mimic the structure of the pathogen (**Figure 5A**), in which, 20 CPS were encapsulated in the core and surface decorated with protein antigens GlpO and PncO [102]. This liposomal vaccine platform was claimed to be capable of surpassing the effectiveness of the best-in-class commercial pneumococcal glycoconjugate vaccine. However, these studies are preclinical and further progress on the work is not reported.

Apart from this, there is substantial literature, in which the pathogen-specific proteins are delivered using nanotechnologies based on the polymers like chitosan [103], polyanhydride [104], PLGA [105] and PLA [106]. Xu *et al.* showed that nanoparticles made of chitosan and encapsulating the PsaA were effective in protecting the mice against an invasive pneumococcal challenge after mucosal immunization [98]. Mott *et al*., used PLGA nanoparticles to ferry the pneumococcal CPS and were effective in generating immune response after intranasal immunization in mice [105]. Similarly, researchers were successful in developing self-assembled nanoparticles [94] or nanocomplexes for the delivery of PPAs [107]. Researchers also explored virus-like particles based on synthetic lipopeptide and they were successful in generating significant protection against the lethal doses of *S. pneumoniae* [94]. Alginate microparticles have been widely explored for the delivery of both the CPS and PPA based pneumococcal vaccines [108–110]. The PspA encapsulated in the alginate microparticles were effective in inducing cross-protection against five serotypes of *S. pneumoniae* after oral immunization [108]. In addition, attempts have been made to deliver the PPAs using the nano in microparticle approach (**Figure 5C**) which were prepared by spray-

drying [111,112]. These formulations claimed to maintain the stability, integrity and antigenicity of the encapsulated protein antigen.

Conjugation strategies have been equally explored to attach of the glycoconjugates or CAs or protein antigens to the nanoparticles [103,113,114]. In most of the cases, functionalized nanoparticles are attached to the glycoconjugate using a linker, which can be either one or two-step processes [113]. In a single-step process, the nanoparticles are directly associated with glycoconjugate using a linker. Whereas in a two-step process the nanoparticles are initially linked with the protein, and then CAs are associated with the protein nanoparticle conjugate. Safari *et al.* in 2012, conjugated a synthetic oligosaccharide known to mimic *S. pneumoniae* serotype 14 capsular polysaccharide (Pn14PS) and the ubiquitous OVA T-helper peptide to GNPs [114]. The intracutaneous injection of these glyco-nanoparticles with MPLA and Quilla saponin as adjuvants promoted the immune response. However, the phagocytic titer was higher in the case of the glycoconjugate [114]. Recently, the same group prepared the nano glycoconjugates by surface conjugating OVA, Pn14PS, D-glucose and a synthetic trisaccharide mimic of *S. pneumoniae* serotype 19F (**Figure 5B**). The glyco-nanoparticles were administered intracutaneously with Quil-A as an adjuvant and PCV 13 was used as a positive control. The results showed an enhanced IgG response against Pn14PS when co-administered with Pn19FPS in particulate form, compared to the groups administered with Pn14PS alone. This is a step forward in the delivery of GCs, where the antigens from two different serotypes Pn14 and Pn19F have successfully elicited the immune response when delivered in the same nanoparticles.

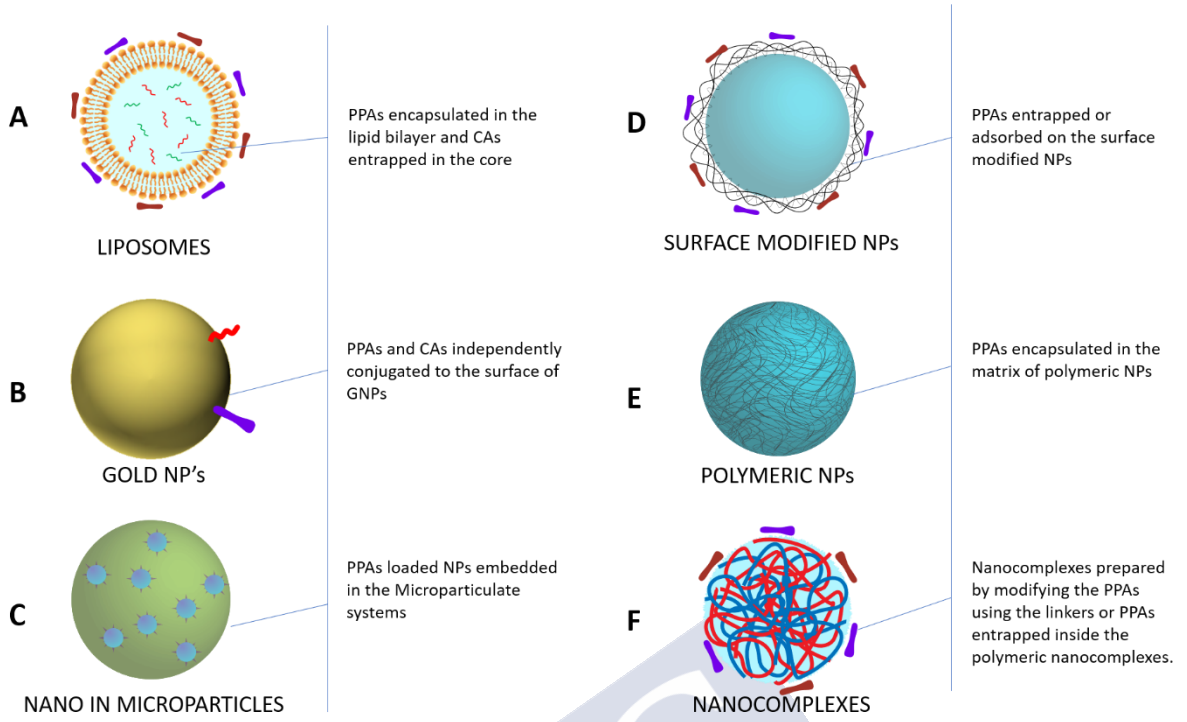

Figure 5: Schematic representation of different nanoparticulate approaches employed for the delivery of pneumococcal vaccine antigens.

The use of nanotechnologies can also help in co-administration of adjuvants and immunomodulatory agents. This can enhance the vaccine efficacy and delivery to the immune cells. They can be incorporated into the nanoparticles either by encapsulation, covalent conjugation or physical adsorption. It has been reported that emulsifying the antigens in an oil-based adjuvant could control the rate of antigen release from the emulsion [115,116], which in turn enhanced the immune potential of the vaccine. Apart from using synthetic or polymeric nanoparticles, the immune system has also been targeted using non-pathogenic bacteria, which themselves can act as a particulate carrier and exhibit adjuvant effects. In 2007, Hanniffy *et al*., investigated the use of *L. lactis* as a particulate vaccine consisting of intracellularly expressed PspA. The results showed that immunization with lactococcal PspA showed better protection against pneumococcal respiratory challenge over the purified PspA [117]. The use of mucoadhesive polymers for surface modification [118] or fabricating the nano-systems [98,119] can enhance the uptake of antigens [120].

Despite several studies being conducted for the effective delivery of the glycoconjugate antigens, we still lack enough literature on the approaches that include both nanotechnology and mucosal targeting for the delivery of pneumococcal antigens. There is a need for research in this area, that can offer multiple benefits like protecting the antigens from degradation, targeting and inducing both mucosal and systemic immunity.

Table 3: Delivery of subunit pneumococcal vaccines that involve particulate technologies

Formulation	Antigen components	Formulation components	Adjuvants	Comments
Polymeric Systems				
Polymeric Nanoparticles	PsaA	Chitosan	-	IN [98]
	PsaA-DNA	Chitosan	CT	IN [121]
	PspA	Polyanhydride	-	S.C [104]
	Lysed components of heat-killed *S. pneumoniae*	PLGA	-	IN [105]
	PsaA, PspA, PS1	PLA		IM [106]
	PspA	PLA, PVA	Alum	IM [122]
	PspA	Cholesteryl group bearing pullulan	-	IN [123]
	PspA	Copolymers CPH, CPTEG	Alum	IN [99]
Metallic Nanoparticles				
Gold Nanoparticles	PS14, OVA	GNPs	MPLA, Quil-A Saponin	ID [114]
	PS14, PS19F, OVA	GNPs	Quil-A	ID [113]
Nanocomplexes				
Nanocomplexes	PspA	Polysorbitol transporter	Polysorbitol transporter	I.N [107]
Polyhydroxy-butyrate beads	Ply, PS19F	Polyhydroxybutyrate	Alum	SC [124]
Lipidic nanosystems				
PCV13 + Liposomes or Nanoparticles	PCV13	Chitosan, Phosphatidylcholine	Quil-A, CNPs, Liposomes	ID [93]
Liposomes	PS19F, GFP	DOPG, Cholesterol, DSPE PEG 2000	-	[125]

	1, 2, 3, 4, 5, 6A, 6B, 7F, 8, 9N, 9V, 12F, 14, 17F, 18C, 19A, 19F, 20, 22F, 23F, GlpO and PncO	DOPC, DOPG, Cholesterol, DSPE PEG2000	-	SC [126]
	PspA	DOTAP, DC-Chol	-	IN [100]
		Microsystems		
Nano in Micro	PspA	PGA-co-PDL, L-leucine	-	IN; PspA adsorbed on PGA-co-PDL NPs were entrapped into L-leucine microparticles by spray drying [111,112]
Alginate Microspheres	PS19-CTB	Alginate	CTB	PO [109,110]
Alginate Microspheres	PsaA-CT or PsaA-CTB	Alginate	CT or CTB	PO [108]
Albumin Microparticles	PS6B, 19F and 23F	Mouse serum albumin, Chitosan	Alum	SC [127]
Latex beads	PS14, PspA	Latex	CpG-ODN	IP [128]
Microcapsules	PS23F or PS23F-OMPC	PVP, Sugar/Starch, MAA	-	IP [129]
		Virus/Bacteria like particles		
SVLPs	PspA	Coiled- coil lipopeptide	Alum	SC [94]
BLPs	PspA	Lactobacillus shell	-	SC / IN [130,131]

PsaA: Pneumococcal surface adhesin A; CT: Cholera toxin; PspA: Pneumococcal surface protein A; PLGA: Poly (lactic-co-glycolic acid); PLA: Polylactic acid; PVA: Polyvinyl alcohol; CPH: 1,6-bis(p-carboxyphenoxy) hexane; CPTEG: 1,8-bis(p-carboxyphenoxy)-3,6-dioxaoctane; PS: Pneumococcal polysaccharide; OVA: Ovalbumin; GNP: Gold nanoparticles; MPLA: Monophoshyl lipid A; Ply: Pneumolysin; PCV: Pneumococcal Conjugate Vaccine; CNP: Chitosan Nanoparticles; GFP: Green Fluorescent Protein; DOPG: 1,2-Dioleoylphosphatidylglycerol; DSPE: 1,2-Distearoyl-sn-glycero-3-phosphoethanolamine; PEG: Polyethylene glycol; GlpO: α-Glycerophosphate oxidase; PncO: bacteriocin ABC transporter transmembrane protein; CpG-ODN: Cytosine phosphate Guanine-oligo deoxynucleotide; OmpC: Outer membrane protein C; PVP: Polyvinylpyrrolidone; MAA: Methacrylic acid; SVLP: Synthetic virus-like particles; BLP: Bacterium-like particles.

3.2. **Nanoparticle properties that affect the delivery of subunit vaccines**

There is a substantial influence of the size of nano vaccines on their biodistribution, lymph node trafficking, cross-protection, and evoking adaptive immune responses. Nanoparticles of larger size will be retained at the site of injection and are transported by the migratory APCs

to the lymph nodes. Studies have shown that without the aid of migratory APCs, smaller nanoparticles (< 100 nm) could traffic directly to the lymph nodes in less than 2 h, by using the convective flow from the interstitium [132]. Usually, the Th1 cell activation (cell-mediated immunity) is induced by particles with a size greater than 1 µm as they are taken up by phagocytosis that enables cross-presentation. The Th2 activation (humoral immunity) is induced by particles smaller than ~600 nm [133]. This is not always true; some studies have reported that particles smaller than ~600 nm have induced the Th1 response when they are co-administered with immunomodulators [134,135]. Also, such small-sized particles have shown to increase the efficiency of cross-presentation [133]. On the other hand, few studies suggested that particles of all ranges up to 1 µm may access the lymph nodes directly via afferent lymphatics, similar to bacterial and virus infection [97,136–138].

Particle charge and shape play a dominant role in the cellular uptake; some studies demonstrate enhanced internalization of spherical particles over rod-shaped nanoparticles [136,139]. However, that is not the only criteria. The spherical nanoparticles were effective in inducing Th1 response, while the rod-shaped particles produced Th2 response [138]. In addition, surface properties like charge and particle hydrophobicity play a crucial role in delivering the antigens through the mucosal route. Positively charged nanoparticles usually bind to the negatively charged mucosal surfaces, increasing the contact with the mucosal epithelium. This can enhance the uptake of nano vaccines and generate mucosal immune responses [140]. Positively charged nanoparticles usually own a higher inflammatory potential than negatively charged or neutral nanoparticles. However, this can also be a disadvantage if the cationic charge is too high as it restricts the route of administration. This generation of an inflammatory response is essential and helps in targeting the nanoparticles to the DCs.

Hydrophobicity of the particles is recognized as a danger signal by the innate immune system. In the human body, hydrophobic materials are mainly exposed to the immune system when there is an abnormal condition such as cellular disruption, against which the immune system is evolved to act on the basic principle of self *vs* non self-recognition [141,142]. This property can be exploited for the activation of the immune system, where the increase in hydrophobicity is associated with enhanced internalization by DCs and induce increased secretion of cytokines. In conclusion, appropriate design in the nano-vaccines can induce the desired immune response. Excellent reviews are available in this field that describes the influence of nanoparticle properties in the vaccine delivery [136,140,143].

3.3. Uptake and processing of glycoconjugates in a nanoparticulate form:

When particulate vaccines are administered, their fate is dependent upon the size, immunomodulators and the adjuvants incorporated in it. Depending on the above parameters, the nanoparticulate vaccines can be either phagocytosed by APCs or will be taken up by carrier-mediated endocytosis. The phagocytic mechanism involves the formation of the pseudopods around the particle, which in turn engulfs the particles forming the phagosomes. Internalization of the particulate vaccines by phagocytosis into phagosomes has an essential consequence because phagosomes are competent organelles for the antigen cross-presentation [144,145]. The process of phagosome formation not only requires the plasma membrane but also involves the contribution of intracellular membranes. The endocytic compartments undergo fission and partial fusion with the phagosome and later mature to form phagolysosome through a so-called kiss and run process.

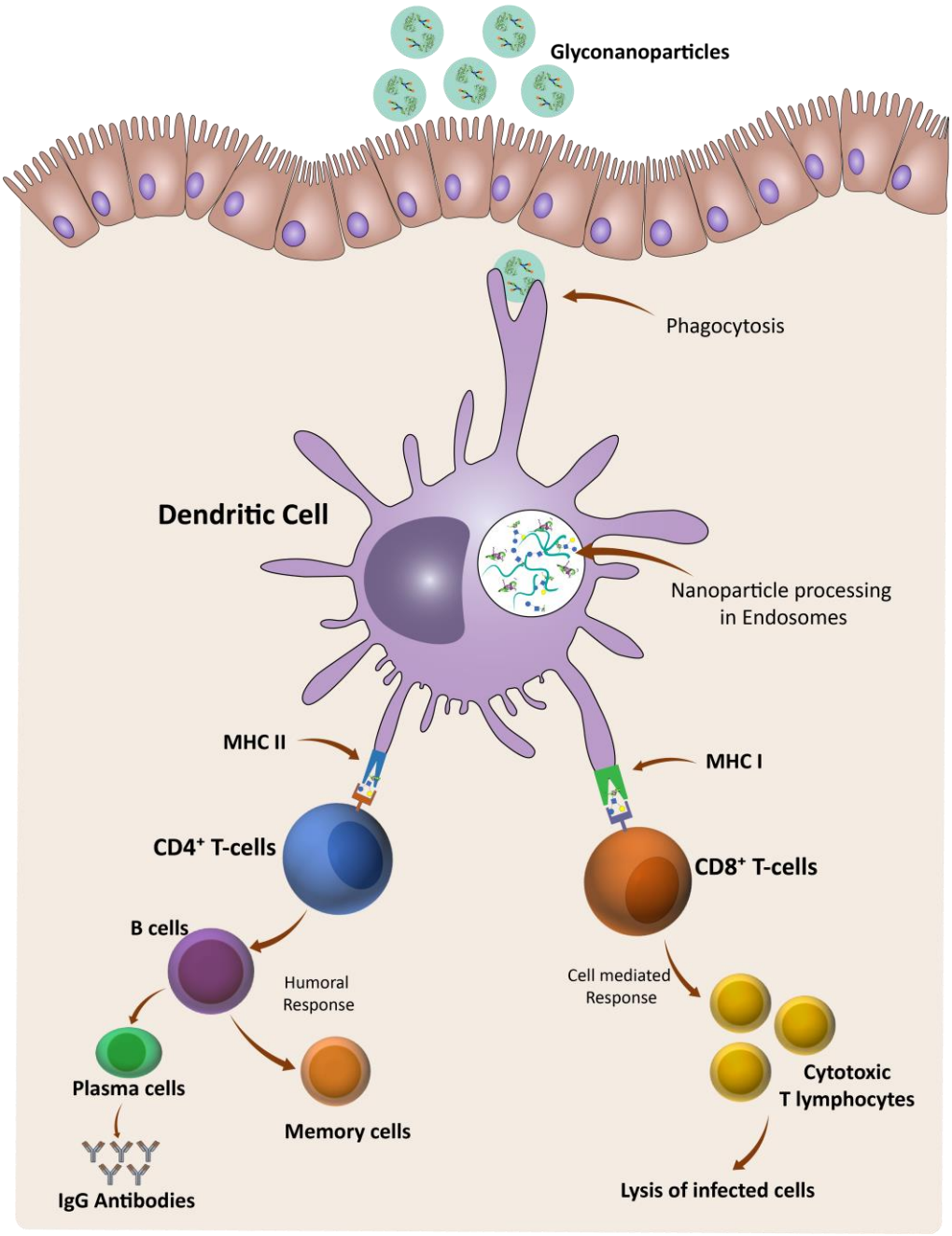

Figure 6: Processing and presentation of antigen-loaded nanoparticle by immune cells. The schematic representation shows the NPs are engulfed by phagocytosis. The internalized particles are processed inside the endosomes and presented to T cells via MHC complexes. The carbohydrates associated with peptides or the peptide fragments are presented to CD4 T cells via MHC II, and the activated CD4 T cells stimulate B cells. The B cells activated by CD4 T cells either transform memory cells or antibody-secreting plasma cells. The peptides presented via MHC I stimulate the CD8 T cells, which in turn activates cytotoxic T lymphocytes that attack the infected cells.

Furthermore, the phagocytosed particulate vaccines will undergo degradation to generate peptide antigens that can be loaded on to the MHC molecules [24]. After the presentation of the antigens on the MHC molecules, when the DCs encounter T cells, the MHC-protein

complex will be recognized by the T-cell receptors (TCRs). In addition to this, a co-stimulatory signal is essential to induce the clonal expression and differentiation of the T-cells into the effector and memory cells. The absence of a co-stimulatory signal may not produce any immune response. The peptide-MHC II complex is recognized by B cells, which are co stimulated by CD4 T cells or cytokines. These B cells will undergo clonal expansion and differentiate to become antibody-secreting plasma cells [24]. The ability of these nanoparticulate vaccines to induce both the cell-mediated and humoral immunity makes them a distinct and appealing strategy for the delivery of the conjugate vaccines.

4. Conclusions and perspectives

Marketed pneumococcal vaccines are either unconjugated polysaccharides or polysaccharide-protein conjugates that contain the capsular polysaccharides from most prevalent serotypes. As the predominant serotype changes with the geographic distribution, the serotype dependent vaccine may not be optimal worldwide. Even though the polysaccharide-based conjugate vaccines have conferred greater protection in the children and elderly. A protein-based vaccine containing several pneumococcal proteins in a single formulation, which is a serotype independent, could be a better and cheaper alternative for existing vaccines. Currently, several subunit pneumococcal vaccines are in the pipeline and clinical market, and they are discussed in detail in this review. However, to date, there are no pneumococcal vaccines based on PPAs available in the market. Recently, there is progress in the use of nanotechnological approaches for encapsulating several pneumococcal proteins and polysaccharides. This advancement using the nanotechnological approach is mainly focused on augmenting the vaccine efficiency and delivery of the sub-unit vaccines. The combination of nanotechnology and the protein-based pneumococcal vaccines, in the near

future, may produce a needle-free and adjuvant free delivery system that can render the protection against all the pneumococcal serotypes. Even though, these novel technologies provide the hope of safer and efficient vaccine delivery, their translation to demonstrate their efficiency in the clinic is still pending.

References:

[1] Institute for Health Metrics and Evaluation (IHME), Findings from the Global Burden of Disease Study 2017, Seattle, 2018. http://www.healthdata.org/sites/default/files/files/policy_report/2019/GBD_2017_Booklet.pdf (accessed September 23, 2019).

[2] JustActions, The Missing Piece. Why Continued Neglect of Pneumonia Threatens the Achievement of Health Goals., New York, USA, 2018. https://stoppneumonia.org/wp-content/uploads/2018/11/The-Missing-Piece_-0611_Spread.pdf (accessed September 23, 2019).

[3] Streptococcus pneumoniae : Vaccines for AMR, (n.d.). https://vaccinesforamr.org/review-of-pathogens/pathogen-profiles/streptococcus-pneumoniae/#impacte8a5-9923a88f-af42 (accessed September 23, 2019).

[4] D.A. McAllister, L. Liu, T. Shi, Y. Chu, C. Reed, J. Burrows, D. Adeloye, I. Rudan, R.E. Black, H. Campbell, H. Nair, Global, regional, and national estimates of pneumonia morbidity and mortality in children younger than 5 years between 2000 and 2015: a systematic analysis., Lancet. Glob. Heal. 7 (2019) e47–e57. doi:10.1016/S2214-109X(18)30408-X.

[5] S. Mukhekar, O. Sumant, Pneumonia Vaccine Market Size, Share and Forecast Analysis By 2025, (2019) 171. https://www.alliedmarketresearch.com/pneumonia-vaccine-market (accessed October 2, 2019).

[6] B. Wahl, K.L. O'Brien, A. Greenbaum, A. Majumder, L. Liu, Y. Chu, I. Lukšić, H. Nair, D.A. McAllister, H. Campbell, I. Rudan, R. Black, M.D. Knoll, Burden of Streptococcus pneumoniae and Haemophilus influenzae type b disease in children in the era of conjugate vaccines: global, regional, and national estimates for 2000-15., Lancet. Glob. Heal. 6 (2018) e744–e757. doi:10.1016/S2214-109X(18)30247-X.

[7] K.A. Geno, G.L. Gilbert, J.Y. Song, I.C. Skovsted, K.P. Klugman, C. Jones, H.B. Konradsen, M.H. Nahm, Pneumococcal Capsules and Their Types: Past, Present, and Future, Clin. Microbiol. Rev. 28 (2015) 871–899. doi:10.1128/CMR.00024-15.

[8] M. Heidelberger, O.T. Avery, the Soluble Specific Substance of Pneumococcus., J. Exp. Med. 38 (1923) 73–9. doi:10.1084/jem.40.3.301.

[9] K. Bazaka, R.J. Crawford, E.L. Nazarenko, E.P. Ivanova, Bacterial Extracellular Polysaccharides, in: Bact. Adhes., 2011: pp. 213–226. doi:10.1007/978-94-007-0940-9.

[10] S. Dahlberg, S. Normark, B. Henriques-normark, K.A. Kline, S. Falker, Bacterial Adhesins in Host-Microbe Interactions, Cell Host Microbe. 5 (2009) 580–592. doi:10.1016/j.chom.2009.05.011.

[11] S. Ehlers, DC-SIGN and mannosylated surface structures of Mycobacterium tuberculosis: a deceptive liaison, Eur. J. Cell Biol. 89 (2010) 95–101. doi:10.1016/j.ejcb.2009.10.004.

[12] R.D. Astronomo, D.R. Burton, Carbohydrate vaccines: developing sweet solutions to sticky situations?, Nat. Rev. Drug Discov. 9 (2010) 308–324. doi:10.1038/nrd3012.

[13] V. Pozsgay, Recent developments in synthetic oligosaccharide-based bacterial vaccines., Curr. Top. Med. Chem. 8 (2008) 126–40. doi:10.2174/156802608783378864.

[14] V. Pozsgay, C. Chu, L. Pannell, J. Wolfe, J.B. Robbins, Protein conjugates of synthetic saccharides elicit higher levels of serum IgG lipopolysaccharide antibodies in mice than do

those of the O-specific polysaccharide from Shigella dysenteriae type 1, Med. Sci. 96 (1999) 5194–5197.

[15] K.R. Harale, N.B. Dumare, D. Singh, A.K. Misra, M.K. Chhikara, Synthesis of a tetrasaccharide and its glycoconjugate corresponding to the capsular polysaccharide of Neisseria meningitidis serogroup X and its immunochemical studies, RSC Adv. 5 (2015) 41332–41340. doi:10.1039/C5RA02993G.

[16] P.H. Seeberger, C.L. Pereira, N. Khan, G. Xiao, E. Diago-Navarro, K. Reppe, B. Opitz, B.C. Fries, M. Witzenrath, A Semi-Synthetic Glycoconjugate Vaccine Candidate for Carbapenem-Resistant Klebsiella pneumoniae, Angew. Chemie - Int. Ed. (2017). doi:10.1002/anie.201700964.

[17] M. Cavallari, P. Stallforth, A. Kalinichenko, D.C.K. Rathwell, T.M.A. Gronewold, A. Adibekian, L. Mori, R. Landmann, P.H. Seeberger, G. De Libero, A semisynthetic carbohydrate-lipid vaccine that protects against S. pneumoniae in mice, Nat. Chem. Biol. 10 (2014) 950–956. doi:10.1038/nchembio.1650.

[18] L.H. Jones, Recent advances in the molecular design of synthetic vaccines, Nat. Chem. 7 (2015) 952–960. doi:10.1038/nchem.2396.

[19] E.A. Kurbatova, N.K. Akhmatova, E.A. Akhmatova, N.B. Egorova, N.E. Yastrebova, E. V. Sukhova, D. V. Yashunsky, Y.E. Tsvetkov, M.L. Gening, N.E. Nifantiev, Neoglycoconjugate of Tetrasaccharide Representing One Repeating Unit of the Streptococcus pneumoniae Type 14 Capsular Polysaccharide Induces the Production of Opsonizing IgG1 Antibodies and Possesses the Highest Protective Activity As Compared to Hexa- an, Front. Immunol. 8 (2017) 1–13. doi:10.3389/fimmu.2017.00659.

[20] E. V. Sukhova, D. V. Yashunsky, Y.E. Tsvetkov, E.A. Kurbatova, N.E. Nifantiev, Synthesis of oligosaccharide fragments of the Streptococcus pneumoniae type 14 capsular polysaccharide and their neoglycoconjugates with bovine serum albumin, Russ. Chem. Bull. 63 (2014) 511–521. doi:10.1007/s11172-014-0462-5.

[21] W. Qiao, S. Ji, Y. Zhao, T. Hu, Conjugation of β-glucan markedly increase the immunogencity of meningococcal group Y polysaccharide conjugate vaccine, Vaccine. 33 (2015) 2066–2072. doi:10.1016/j.vaccine.2015.02.045.

[22] R. Adamo, Advancing Homogeneous Antimicrobial Glycoconjugate Vaccines, Acc. Chem. Res. 50 (2017) 1270–1279. doi:10.1021/acs.accounts.7b00106.

[23] F.Y. Avci, X. Li, M. Tsuji, D.L. Kasper, A mechanism for glycoconjugate vaccine activation of the adaptive immune system and its implications for vaccine design, Nat. Med. 17 (2011) 1602–1609. doi:10.1038/nm.2535.

[24] M.L. De Temmerman, J. Rejman, J. Demeester, D.J. Irvine, B. Gander, S.C. De Smedt, Particulate vaccines: On the quest for optimal delivery and immune response, Drug Discov. Today. 16 (2011) 569–582. doi:10.1016/j.drudis.2011.04.006.

[25] S. Burgdorf, A. Kautz, V. Böhnert, P. a Knolle, C. Kurts, Distinct pathways of antigen uptake and intracellular routing in CD4 and CD8 T cell activation, Science. 612 (2007) 612–616. doi:10.1126/science.1137971.

[26] S. Burgdorf, C. Kurts, Endocytosis mechanisms and the cell biology of antigen presentation, Curr. Opin. Immunol. 20 (2008) 89–95. doi:10.1016/j.coi.2007.12.002.

[27] R. Rappuoli, E. De Gregorio, P. Costantino, On the mechanisms of conjugate vaccines., Proc. Natl. Acad. Sci. U. S. A. 116 (2019) 14–16. doi:10.1073/pnas.1819612116.

[28] T. Defrance, M. Taillardet, L. Genestier, T cell-independent B cell memory, Curr. Opin. Immunol. 23 (2011) 330–336. doi:10.1016/j.coi.2011.03.004.

[29] A. Weintraub, Immunology of bacterial polysaccharide antigens, Carbohydr. Res. 338 (2003) 2539–2547. doi:10.1016/j.carres.2003.07.008.

[30] S. Bondada, H.-J. Wu, D.A. Robertson, R.L. Chelvarajan, Accessory cell defect in unresponsiveness of neonates and aged to polysaccharide vaccines, Vaccine. 19 (2000) 557–565. doi:10.1016/S0264-410X(00)00161-4.

[31] B.A. Cobb, Q. Wang, A.O. Tzianabos, D.L. Kasper, Polysaccharide processing and presentation by the MHCII pathway, Cell. 117 (2004) 677–687. doi:10.1016/j.cell.2004.05.001.

[32] B.Y.O.T. Avery, W.F. Goebel, C h e m o - i m m u n o l o g i c a l studies on conjugated carbohydrate-proteins, (1931).

[33] H. Geyer, S. Stirm, K. Himmelspach, Immunochemical properties of oligosaccharide-protein conjugates withKlebsiella-K2 specificity, Med. Microbiol. Immunol. 165 (1979) 271–288. http://link.springer.com/article/10.1007/BF02152925.

[34] A.A. Lindberg, L.T. Rosenberg, A. Ljunggren, P.J. Garegg, S. Svensson, N.H. Wallin, Effect of synthetic disaccharide-protein conjugate as an immunogen in Salmonella infection in mice., Infect. Immun. 10 (1974) 541–5.

[35] S.B. Svenson, M. Nurminen, A.A. Lindberg, Artificial Salmonella vaccines: O-antigenic oligosaccharide-protein conjugates induce protection against infection with Salmonella typhimurium, Infect. Immun. 25 (1979) 863–872.

[36] J.B. Robbins, CONJUGATES, 152 (1980) 361–376.

[37] D.M. Weinberger, R. Malley, M. Lipsitch, Serotype replacement in disease after pneumococcal vaccination, Lancet. 378 (2011) 1962–1973. doi:10.1016/S0140-6736(10)62225-8.

[38] W.P. Hanage, Serotype Replacement in Invasive Pneumococcal Disease: Where Do We Go from Here?, J. Infect. Dis. 196 (2007) 1282–1284. doi:10.1086/521630.

[39] B. Schumann, K. Reppe, P. Kaplonek, A. Wahlbrink, C. Anish, M. Witzenrath, C.L. Pereira, P.H. Seeberger, Development of an Efficacious, Semisynthetic Glycoconjugate Vaccine Candidate against *Streptococcus pneumoniae* Serotype 1, ACS Cent. Sci. 4 (2018) 357–361. doi:10.1021/acscentsci.7b00504.

[40] P. Ménová, M. Sella, K. Sellrie, C.L. Pereira, P.H. Seeberger, Identification of the Minimal Glycotope of *Streptococcus pneumoniae* 7F Capsular Polysaccharide using Synthetic Oligosaccharides, Chem. - A Eur. J. 24 (2018) 4181–4187. doi:10.1002/chem.201705379.

[41] M.P. Lisboa, N. Khan, C. Martin, F.-F. Xu, K. Reppe, A. Geissner, S. Govindan, M. Witzenrath, C.L. Pereira, P.H. Seeberger, Semisynthetic glycoconjugate vaccine candidate against *Streptococcus pneumoniae* serotype 5, Proc. Natl. Acad. Sci. 114 (2017) 11063–11068. doi:10.1073/pnas.1706875114.

[42] M. Emmadi, N. Khan, L. Lykke, K. Reppe, S.G. Parameswarappa, M.P. Lisboa, S.M. Wienhold, M. Witzenrath, C.L. Pereira, P.H. Seeberger, A Streptococcus pneumoniae Type 2 Oligosaccharide Glycoconjugate Elicits Opsonic Antibodies and Is Protective in an Animal Model of Invasive Pneumococcal Disease, J. Am. Chem. Soc. 139 (2017) 14783–14791. doi:10.1021/jacs.7b07836.

[43] B. Schumann, H.S. Hahm, S.G. Parameswarappa, K. Reppe, A. Wahlbrink, S. Govindan, P.

Kaplonek, L.-A. Pirofski, M. Witzenrath, C. Anish, C.L. Pereira, P.H. Seeberger, A semisynthetic Streptococcus pneumoniae serotype 8 glycoconjugate vaccine., Sci. Transl. Med. 9 (2017) eaaf5347. doi:10.1126/scitranslmed.aaf5347.

[44] S.G. Parameswarappa, K. Reppe, A. Geissner, P. Ménová, S. Govindan, A.D.J. Calow, A. Wahlbrink, M.W. Weishaupt, B.P. Monnanda, R.L. Bell, L.-A. Pirofski, N. Suttorp, L.E. Sander, M. Witzenrath, C.L. Pereira, C. Anish, P.H. Seeberger, A Semi-synthetic Oligosaccharide Conjugate Vaccine Candidate Confers Protection against Streptococcus pneumoniae Serotype 3 Infection., Cell Chem. Biol. 23 (2016) 1407–1416. doi:10.1016/j.chembiol.2016.09.016.

[45] P. Kaplonek, N. Khan, K. Reppe, B. Schumann, M. Emmadi, M.P. Lisboa, F.-F. Xu, A.D.J. Calow, S.G. Parameswarappa, M. Witzenrath, C.L. Pereira, P.H. Seeberger, Improving vaccines against Streptococcus pneumoniae using synthetic glycans., Proc. Natl. Acad. Sci. U. S. A. 115 (2018) 13353–13358. doi:10.1073/pnas.1811862115.

[46] M. Vella, D. Pace, Glycoconjugate vaccines: an update., Expert Opin. Biol. Ther. 15 (2015) 529–546. doi:10.1517/14712598.2015.993375.

[47] C. Jones, Vaccines based on the cell surface carbohydrates of pathogenic bacteria, An. Acad. Bras. Cienc. 77 (2005) 293–324. doi:10.1590/S0001-37652005000200009.

[48] Q.-Y. Hu, F. Berti, R. Adamo, Towards the next generation of biomedicines by site-selective conjugation, Chem. Soc. Rev. 45 (2016) 1691–1719. doi:10.1039/C4CS00388H.

[49] L. Li, R.L. Woodward, W. Han, J. Qu, J. Song, C. Ma, P.G. Wang, Chemoenzymatic synthesis of the bacterial polysaccharide repeating unit undecaprenyl pyrophosphate and its analogs, Nat. Protoc. 11 (2016) 1280–1298. doi:10.1038/nprot.2016.067.

[50] J. Gao, Z. Guo, Chemical Synthesis of the Repeating Unit of Type V Group B *Streptococcus* Capsular Polysaccharide, Org. Lett. 18 (2016) 5552–5555. doi:10.1021/acs.orglett.6b02796.

[51] F. Berti, R. Adamo, Recent mechanistic insights on glycoconjugate vaccines and future perspectives, ACS Chem. Biol. 8 (2013) 1653–1663. doi:10.1021/cb400423g.

[52] F. Micoli, L. Del Bino, R. Alfini, F. Carboni, M.R. Romano, R. Adamo, Glycoconjugate vaccines: current approaches towards faster vaccine design, Expert Rev. Vaccines. 18 (2019) 881–895. doi:10.1080/14760584.2019.1657012.

[53] M.W. Weishaupt, S. Matthies, M. Hurevich, C.L. Pereira, H.S. Hahm, P.H. Seeberger, Automated glycan assembly of a S. pneumoniae serotype 3 CPS antigen., Beilstein J. Org. Chem. 12 (2016) 1440–6. doi:10.3762/bjoc.12.139.

[54] U. Möginger, A. Resemann, C.E. Martin, S. Parameswarappa, S. Govindan, E. Wamho, F. Broecker, D. Suckau, Cross Reactive Material 197 glycoconjugate vaccines contain privileged conjugation sites, Nat. Sci. Reports. (2016) 1–13. doi:10.1038/srep20488.

[55] V.S. Terra, D.C. Mills, L.E. Yates, S. Abouelhadid, J. Cuccui, B.W. Wren, Recent developments in bacterial protein glycan coupling technology and glycoconjugate vaccine design, J. Med. Microbiol. 61 (2012) 919–926. doi:10.1099/jmm.0.039438-0.

[56] F.Y. Avci, Novel strategies for development of next-generation glycoconjugate vaccines., Curr. Top. Med. Chem. 13 (2013) 2535–40. doi:10.2174/15680266113136660180.

[57] M.M. Kämpf, M. Braun, D. Sirena, J. Ihssen, L. Thöny-Meyer, Q. Ren, In vivo production of a novel glycoconjugate vaccine against Shigella flexneri 2a in recombinant Escherichia coli: identification of stimulating factors for in vivo glycosylation, Microb. Cell Fact. 14 (2015) 12. doi:10.1186/s12934-015-0195-7.

[58] M. Wacker, L. Wang, M. Kowarik, M. Dowd, G. Lipowsky, A. Faridmoayer, K. Shields, S. Park, C. Alaimo, K.A. Kelley, M. Braun, J. Quebatte, V. Gambillara, P. Carranza, M. Steffen, J.C. Lee, Prevention of staphylococcus aureus infections by glycoprotein vaccines synthesized in escherichia coli, J. Infect. Dis. 209 (2014) 1551–1561. doi:10.1093/infdis/jit800.

[59] M. Wacker, D. Linton, P.G. Hitchen, M. Nita-Lazar, S.M. Haslam, S.J. North, M. Panico, H.R. Morris, A. Dell, B.W. Wren, M. Aebi, N-Linked Glycosylation in Campylobacter jejuni and Its Functional Transfer into E. coli, Science (80-.). 298 (2002) 1790 LP – 1793. http://science.sciencemag.org/content/298/5599/1790.abstract.

[60] M.F. Feldman, M. Wacker, M. Hernandez, P.G. Hitchen, C.L. Marolda, M. Kowarik, H.R. Morris, A. Dell, M.A. Valvano, M. Aebi, Engineering N-linked protein glycosylation with diverse O antigen lipopolysaccharide structures in Escherichia coli, Proc. Natl. Acad. Sci. 102 (2005) 3016–3021. doi:10.1073/pnas.0500044102.

[61] K.P. Killeen, Matrivax profile., Hum. Vaccin. Immunother. 14 (2018) 804–806. doi:10.1080/21645515.2017.1400789.

[62] F. Zhang, Y.-J. Lu, R. Malley, Multiple antigen-presenting system (MAPS) to induce comprehensive B-and T-cell immunity, PNAS. 110 (2013) 13564–13569. doi:10.1073/pnas.1307228110.

[63] MAPS Technology Platform | Affinivax, (n.d.). http://affinivax.com/maps-platform/maps-technology-platform/ (accessed October 2, 2019).

[64] Z. Lai, J.R. Schreiber, Antigen processing of glycoconjugate vaccines; the polysaccharide portion of the pneumococcal CRM197 conjugate vaccine co-localizes with MHC II on the antigen processing cell surface, Vaccine. 27 (2009) 3137–3144. doi:10.1016/j.vaccine.2009.03.064.

[65] F.Y. Avci, X. Li, M. Tsuji, D.L. Kasper, A mechanism for glycoconjugate vaccine activation of the adaptive immune system and its implications for vaccine design, Nat. Med. 17 (2011) 1602–1609. doi:10.1038/nm.2535.

[66] A.M. Berry, J.C. Paton, Sequence heterogeneity of PsaA, a 37-kilodalton putative adhesin essential for virulence of Streptococcus pneumoniae, Infect. Immun. (1996).

[67] J.S. Sampson, Z. Furlow, A.M. Whitney, D. Williams, R. Facklam, G.M. Carlone, Limited diversity of Streptococcus pneumoniae psaA among pneumococcal vaccine serotypes, Infect. Immun. 65 (1997) 1967–1971.

[68] R. Singh, P. Gupta, P.K. Sharma, E.W. Ades, S.K. Hollingshead, S. Singh, J.W. Lillard, Prediction and characterization of helper T-cell epitopes from pneumococcal surface adhesin A, Immunology. 141 (2014) 514–530. doi:10.1111/imm.12194.

[69] F.C.L. Csordas, C.T. Perciani, M. Darrieux, V.M. Gonçalves, J. Cabrera-Crespo, M. Takagi, M.E. Sbrogio-Almeida, L.C.C. Leite, M.M. Tanizaki, Protection induced by pneumococcal surface protein A (PspA) is enhanced by conjugation to a Streptococcus pneumoniae capsular polysaccharide, Vaccine. 26 (2008) 2925–2929. doi:10.1016/J.VACCINE.2008.03.038.

[70] K. Poulsen, J. Reinholdt, C. Jespersgaard, K. Boye, T.A. Brown, M. Hauge, M. Kilian, A comprehensive genetic study of streptococcal immunoglobulin A1 proteases: evidence for recombination within and between species., Infect. Immun. 66 (1998) 181–90. http://www.ncbi.nlm.nih.gov/pubmed/9423856 (accessed September 13, 2019).

[71] J. Huang, S. Luo, M. Huang, T. Zhang, Z. Min, C. Liu, Q. Zhang, J. Yang, X. Min, Protection against fatal pneumonia through mucosal and subcutaneous immunization with the

pneumococcal SP0148 protein, Microb. Pathog. 129 (2019) 206–212. doi:10.1016/j.micpath.2019.02.018.

[72] M.F. Mills, M.E. Marquart, L.S. McDaniel, Localization of PcsB of Streptococcus pneumoniae and its differential expression in response to stress., J. Bacteriol. 189 (2007) 4544–6. doi:10.1128/JB.01831-06.

[73] D. Pracht, C. Elm, J. Gerber, S. Bergmann, M. Rohde, M. Seiler, K.S. Kim, H.F. Jenkinson, R. Nau, S. Hammerschmidt, PavA of Streptococcus pneumoniae Modulates Adherence, Invasion, and Meningeal Inflammation, Infect. Immun. 73 (2005) 2680–2689. doi:10.1128/IAI.73.5.2680-2689.2005.

[74] J. Echenique, A. Kadioglu, S. Romao, P.W. Andrew, M.-C. Trombe, Protein serine/threonine kinase StkP positively controls virulence and competence in Streptococcus pneumoniae., Infect. Immun. 72 (2004) 2434–7. doi:10.1128/iai.72.4.2434-2437.2004.

[75] L.K. Mahdi, H. Wang, M.B. Van der Hoek, J.C. Paton, A.D. Ogunniyi, Identification of a novel pneumococcal vaccine antigen preferentially expressed during meningitis in mice., J. Clin. Invest. 122 (2012) 2208–20. doi:10.1172/JCI45850.

[76] M. Yamaguchi, Y. Terao, Y. Mori, S. Hamada, S. Kawabata, PfbA, a novel plasmin- and fibronectin-binding protein of Streptococcus pneumoniae, contributes to fibronectin-dependent adhesion and antiphagocytosis., J. Biol. Chem. 283 (2008) 36272–9. doi:10.1074/jbc.M807087200.

[77] C.E. Blue, G.K. Paterson, A.R. Kerr, M. Bergé, J.P. Claverys, T.J. Mitchell, ZmpB, a novel virulence factor of Streptococcus pneumoniae that induces tumor necrosis factor alpha production in the respiratory tract., Infect. Immun. 71 (2003) 4925–35. doi:10.1128/iai.71.9.4925-4935.2003.

[78] D. Chiavolini, G. Memmi, T. Maggi, F. Iannelli, G. Pozzi, M.R. Oggioni, The three extra-cellular zinc metalloproteinases of Streptococcus pneumoniae have a different impact on virulence in mice, BMC Microbiol. 3 (2003) 14. doi:10.1186/1471-2180-3-14.

[79] G. Bethe, R. Nau, A. Wellmer, R. Hakenbeck, R.R. Reinert, H.-P. Heinz, G. Zysk, The cell wall-associated serine protease PrtA: a highly conserved virulence factor of *Streptococcus pneumoniae*, FEMS Microbiol. Lett. 205 (2001) 99–104. doi:10.1111/j.1574-6968.2001.tb10931.x.

[80] M.J. Jedrzejas, Pneumococcal virulence factors: structure and function., Microbiol. Mol. Biol. Rev. 65 (2001) 187-207 ; first page, table of contents. doi:10.1128/MMBR.65.2.187-207.2001.

[81] M. Cámara, G.J. Boulnois, P.W. Andrew, T.J. Mitchell, A neuraminidase from Streptococcus pneumoniae has the features of a surface protein., Infect. Immun. 62 (1994) 3688. https://www.ncbi.nlm.nih.gov/pmc/articles/PMC303019/ (accessed September 23, 2019).

[82] V. Agarwal, A. Kuchipudi, M. Fulde, K. Riesbeck, S. Bergmann, A.M. Blom, *Streptococcus pneumoniae* Endopeptidase O (PepO) Is a Multifunctional Plasminogen- and Fibronectin-binding Protein, Facilitating Evasion of Innate Immunity and Invasion of Host Cells, J. Biol. Chem. 288 (2013) 6849–6863. doi:10.1074/jbc.M112.405530.

[83] J. Dong, J. Wang, Y. He, C. Li, A. Zhou, J. Cui, W. Xu, L. Zhong, Y. Yin, X. Zhang, H. Wang, GHIP in *Streptococcus pneumoniae* is involved in antibacterial resistance and elicits a strong innate immune response through TLR2 and JNK/p38MAPK, FEBS J. 281 (2014) 3803–3815. doi:10.1111/febs.12903.

[84] H.R. Pipkins, J.L. Bradshaw, L.E. Keller, E. Swiatlo, L.S. McDaniel, Polyamine transporter

potABCD is required for virulence of encapsulated but not nonencapsulated Streptococcus pneumoniae, PLoS One. 12 (2017) e0179159. doi:10.1371/journal.pone.0179159.

[85] D. Zähner, A.R. Gandhi, O. Stuchlik, M. Reed, J. Pohl, D.S. Stephens, Pilus backbone protein PitB of Streptococcus pneumoniae contains stabilizing intramolecular isopeptide bonds., Biochem. Biophys. Res. Commun. 409 (2011) 526–31. doi:10.1016/j.bbrc.2011.05.038.

[86] C. Muñoz-Almagro, L. Selva, C.J. Sanchez, C. Esteva, M.F. de Sevilla, R. Pallares, C.J. Orihuela, PsrP, a protective pneumococcal antigen, is highly prevalent in children with pneumonia and is strongly associated with clonal type., Clin. Vaccine Immunol. 17 (2010) 1672–8. doi:10.1128/CVI.00271-10.

[87] C. Attali, C. Frolet, C. Durmort, J. Offant, T. Vernet, A.M. Di Guilmi, Streptococcus pneumoniae choline-binding protein E interaction with plasminogen/plasmin stimulates migration across the extracellular matrix., Infect. Immun. 76 (2008) 466–76. doi:10.1128/IAI.01261-07.

[88] A. Puyet, B. Greenberg, S.A. Lacks, Genetic and structural characterization of endA: A membrane-bound nuclease required for transformation of Streptococcus pneumoniae, J. Mol. Biol. 213 (1990) 727–738. doi:10.1016/S0022-2836(05)80259-1.

[89] K. Beiter, F. Wartha, B. Albiger, S. Normark, A. Zychlinsky, B. Henriques-Normark, An Endonuclease Allows Streptococcus pneumoniae to Escape from Neutrophil Extracellular Traps, Curr. Biol. 16 (2006) 401–407. doi:10.1016/j.cub.2006.01.056.

[90] D.F. Talkington, B.G. Brown, J.A. Tharpe, A. Koenig, H. Russell, Protection of mice against fatal pneumococcal challenge by immunization with pneumococcal surface adhesin A (PsaA), Microb. Pathog. 21 (1996) 17–22. doi:10.1006/mpat.1996.0038.

[91] L. Baril, J. Dietemann, M. Essevaz-Roulet, L. Beniguel, P. Coan, D.E. Briles, B. Guy, G. Cozon, Pneumococcal surface protein A (PspA) is effective at eliciting T cell-mediated responses during invasive pneumococcal disease in adults, Clin. Exp. Immunol. 145 (2006) 277–286. doi:10.1111/j.1365-2249.2006.03148.x.

[92] J. Lu, T. Sun, D. Wang, Y. Dong, M. Xu, H. Hou, F.T. Kong, C. Liang, T. Gu, P. Chen, S. Sun, X. Lv, C. Jiang, W. Kong, Y. Wu, Protective Immune Responses Elicited by Fusion Protein Containing PsaA and PspA Fragments, Immunol. Invest. 44 (2015) 482–496. doi:10.3109/08820139.2015.1037956.

[93] A. Haryono, K. Salsabila, W.K. Restu, S.B. Harmami, D. Safari, Effect of Chitosan and Liposome Nanoparticles as Adjuvant Codelivery on the Immunoglobulin G Subclass Distribution in a Mouse Model, J. Immunol. Res. 2017 (2017) 1–5. doi:10.1155/2017/9125048.

[94] M. Tamborrini, N. Geib, A. Marrero-Nodarse, M. Jud, J. Hauser, C. Aho, A. Lamelas, A. Zuniga, G. Pluschke, A. Ghasparian, J. Robinson, A Synthetic Virus-Like Particle Streptococcal Vaccine Candidate Using B-Cell Epitopes from the Proline-Rich Region of Pneumococcal Surface Protein A, Vaccines. 3 (2015) 850–874. doi:10.3390/vaccines3040850.

[95] C. Jones, Glycoconjugate vaccines: The regulatory Framework, in: Carbohydrate-Based Vaccines Methods Protoc., 2015: pp. 229–251. doi:10.1007/978-1-4939-2874-3.

[96] A. Gomes, M. Mohsen, M. Bachmann, Harnessing Nanoparticles for Immunomodulation and Vaccines, Vaccines. 5 (2017) 6. doi:10.3390/vaccines5010006.

[97] H. Yue, W. Wei, Z. Yue, P. Lv, L. Wang, G. Ma, Z. Su, Particle size affects the cellular response in macrophages, Eur. J. Pharm. Sci. 41 (2010) 650–657. doi:10.1016/j.ejps.2010.09.006.

[98] J.H. Xu, W.J. Dai, B. Chen, X.Y. Fan, Mucosal Immunization with PsaA Protein, Using Chitosan

as a Delivery System, Increases Protection Against Acute Otitis Media and Invasive Infection by Streptococcus pneumoniae, Scand. J. Immunol. 81 (2015) 177–185. doi:10.1111/sji.12267.

[99] D.A. Wagner-Muñiz, S.L. Haughney, S.M. Kelly, M.J. Wannemuehler, B. Narasimhan, Room Temperature Stable PspA-Based Nanovaccine Induces Protective Immunity, Front. Immunol. 9 (2018) 325. doi:10.3389/fimmu.2018.00325.

[100] R. Tada, H. Suzuki, S. Takahashi, Y. Negishi, H. Kiyono, J. Kunisawa, Y. Aramaki, Nasal vaccination with pneumococcal surface protein A in combination with cationic liposomes consisting of DOTAP and DC-chol confers antigen-mediated protective immunity against Streptococcus pneumoniae infections in mice, Int. Immunopharmacol. 61 (2018) 385–393. doi:10.1016/J.INTIMP.2018.06.027.

[101] S.P. Jochems, J.N. Weiser, R. Malley, D.M. Ferreira, The immunological mechanisms that control pneumococcal carriage, PLOS Pathog. 13 (2017) e1006665. doi:10.1371/journal.ppat.1006665.

[102] A.B. Hill, M. Beitelshees, R. Nayerhoda, B.A. Pfeifer, C.H. Jones, Engineering a Next-Generation Glycoconjugate-Like Streptococcus pneumoniae Vaccine, ACS Infect. Dis. 4 (2018) 1553–1563. doi:10.1021/acsinfecdis.8b00100.

[103] J.-H. Xu, W.-J. Dai, B. Chen, X.-Y. Fan, Mucosal Immunization with PsaA Protein, Using Chitosan as a Delivery System, Increases Protection Against Acute Otitis Media and Invasive Infection by *Streptococcus pneumoniae*, Scand. J. Immunol. 81 (2015) 177–185. doi:10.1111/sji.12267.

[104] S.L. Haughney, L.K. Petersen, A.D. Schoofs, A.E. Ramer-tait, J.D. King, D.E. Briles, M.J. Wannemuehler, B. Narasimhan, Retention of structure , antigenicity , and biological function of pneumococcal surface protein A (PspA) released from polyanhydride nanoparticles, Acta Biomater. 9 (2013) 8262–8271. doi:10.1016/j.actbio.2013.06.006.

[105] B. Mott, S. Thamake, J. Vishwanatha, H.P. Jones, Intranasal delivery of nanoparticle-based vaccine increases protection against S. pneumoniae, J. Nanoparticle Res. 15 (2013) 1646. doi:10.1007/s11051-013-1646-x.

[106] C. Anish, N. Khan, A.K. Upadhyay, D. Sehgal, A.K. Panda, Delivery of Polysaccharides Using Polymer Particles: Implications on Size-Dependent Immunogenicity, Opsonophagocytosis, and Protective Immunity, Mol. Pharm. 11 (2014) 922–937. doi:10.1021/mp400589q.

[107] Y.-C. Kye, S.-M. Park, B.-S. Shim, J. Firdous, G. Kim, H.W. Kim, Y.-J. Ju, C.G. Kim, C.-S. Cho, D.W. Kim, J.H. Cho, M.K. Song, S.H. Han, C.-H. Yun, Intranasal immunization with pneumococcal surface protein A in the presence of nanoparticle forming polysorbitol transporter adjuvant induces protective immunity against the Streptococcus pneumoniae infection, Acta Biomater. 90 (2019) 362–372. doi:10.1016/J.ACTBIO.2019.03.049.

[108] J.-Y. Seo, S.Y. Seong, B.-Y. Ahn, I.C. Kwon, H. Chung, S.Y. Jeong, Cross-protective immunity of mice induced by oral immunization with pneumococcal surface adhesin a encapsulated in microspheres., Infect. Immun. 70 (2002) 1143–9. doi:10.1128/iai.70.3.1143-1149.2002.

[109] N.-H. Cho, S.-Y. Seong, K.-H. Chun, Y.-H. Kim, I. Chan Kwon, B.-Y. Ahn, S.Y. Jeong, Novel mucosal immunization with polysaccharide–protein conjugates entrapped in alginate microspheres, J. Control. Release. 53 (1998) 215–224. doi:10.1016/S0168-3659(97)00255-1.

[110] S.Y. Seong, N.H. Cho, I.C. Kwon, S.Y. Jeong, Protective immunity of microsphere-based mucosal vaccines against lethal intranasal challenge with Streptococcus pneumoniae., Infect. Immun. 67 (1999) 3587–92. http://www.ncbi.nlm.nih.gov/pubmed/10377143 (accessed

August 14, 2019).

[111] N.K. Kunda, I.M. Alfagih, E.N. Miyaji, D.B. Figueiredo, V.M. Gonçalves, D.M. Ferreira, S.R. Dennison, S. Somavarapu, G.A. Hutcheon, I.Y. Saleem, Pulmonary dry powder vaccine of pneumococcal antigen loaded nanoparticles, Int. J. Pharm. 495 (2015) 903–912. doi:10.1016/j.ijpharm.2015.09.034.

[112] T.C. Rodrigues, M.L.S. Oliveira, A. Soares-Schanoski, S.L. Chavez-Rico, D.B. Figueiredo, V.M. Gonçalves, D.M. Ferreira, N.K. Kunda, I.Y. Saleem, E.N. Miyaji, Mucosal immunization with PspA (Pneumococcal surface protein A)-adsorbed nanoparticles targeting the lungs for protection against pneumococcal infection, PLoS One. 13 (2018). doi:10.1371/journal.pone.0191692.

[113] M. Vetro, D. Safari, S. Fallarini, K. Salsabila, M. Lahmann, S. Penadés, L. Lay, M. Marradi, F. Compostella, Preparation and immunogenicity of gold glyco-nanoparticles as antipneumococcal vaccine model., Nanomedicine (Lond). 12 (2017) 13–23. doi:10.2217/nnm-2016-0306.

[114] D. Safari, M. Marradi, F. Chiodo, H.A. Th Dekker, Y. Shan, R. Adamo, S. Oscarson, G.T. Rijkers, M. Lahmann, J.P. Kamerling, S. Penadés, H. Snippe, Gold nanoparticles as carriers for a synthetic Streptococcus pneumoniae type 14 conjugate vaccine., Nanomedicine (Lond). 7 (2012) 651–662. doi:10.2217/nnm.11.151.

[115] S. Martiñón, A. Cisneros, S. Villicaña, R. Hernández-Miramontes, E. Mixcoha, P. Calderón-Vargas, Chemical and Immunological Characteristics of Aluminum-Based, Oil-Water Emulsion, and Bacterial-Origin Adjuvants, J. Immunol. Res. 2019 (2019) 1–9. doi:10.1155/2019/3974127.

[116] R.K. Gupta, G.R. Siber, Adjuvants for human vaccines—current status, problems and future prospects, Vaccine. 13 (1995) 1263–1276. doi:10.1016/0264-410X(95)00011-O.

[117] S.B. Hanniffy, A.T. Carter, E. Hitchin, J.M. Wells, Mucosal Delivery of a Pneumococcal Vaccine Using *Lactococcus lactis* Affords Protection against Respiratory Infection, J. Infect. Dis. 195 (2007) 185–193. doi:10.1086/509807.

[118] G. Barhate, M. Gautam, S. Gairola, S. Jadhav, V. Pokharkar, Enhanced mucosal immune responses against tetanus toxoid using novel delivery system comprised of chitosan-functionalized gold nanoparticles and botanical adjuvant: Characterization, immunogenicity, and stability assessment, J. Pharm. Sci. 103 (2014) 3448–3456. doi:10.1002/jps.24161.

[119] M. Amidi, S.G. Romeijn, J.C. Verhoef, H.E. Junginger, L. Bungener, A. Huckriede, D.J.A. Crommelin, W. Jiskoot, N -Trimethyl chitosan (TMC) nanoparticles loaded with influenza subunit antigen for intranasal vaccination : Biological properties and immunogenicity in a mouse model, 25 (2007) 144–153. doi:10.1016/j.vaccine.2006.06.086.

[120] N. Marasini, A.K. Giddam, Z.G. Khalil, W.M. Hussein, R.J. Capon, M.R. Batzloff, M.F. Good, I. Toth, M. Skwarczynski, Double adjuvanting strategy for peptide-based vaccines: trimethyl chitosan nanoparticles for lipopeptide delivery, Nanomedicine. 11 (2016) 3223–3235. doi:10.2217/nnm-2016-0291.

[121] J. Xu, W. Dai, Z. Wang, B. Chen, Z. Li, X. Fan, C.L.I.N.V.A.I. Mmunol, Intranasal Vaccination with Chitosan-DNA Nanoparticles Expressing Pneumococcal Surface Antigen A Protects Mice against Nasopharyngeal Colonization by Streptococcus pneumoniae □, 18 (2011) 75–81. doi:10.1128/CVI.00263-10.

[122] C. Anish, A.K. Upadhyay, D. Sehgal, A.K. Panda, Influences of process and formulation

parameters on powder flow properties and immunogenicity of spray dried polymer particles entrapping recombinant pneumococcal surface protein A, Int. J. Pharm. 466 (2014) 198–210. doi:10.1016/J.IJPHARM.2014.03.025.

[123] Y. Fukuyama, Y. Yuki, Y. Katakai, N. Harada, H. Takahashi, S. Takeda, M. Mejima, S. Joo, S. Kurokawa, S. Sawada, H. Shibata, E.J. Park, K. Fujihashi, D.E. Briles, Y. Yasutomi, H. Tsukada, K. Akiyoshi, H. Kiyono, Nanogel-based pneumococcal surface protein A nasal vaccine induces microRNA-associated Th17 cell responses with neutralizing antibodies against Streptococcus pneumoniae in macaques, Mucosal Immunol. 8 (2015) 1144–1153. doi:10.1038/mi.2015.5.

[124] M. González-Miró, A.-M. Radecker, L.M. Rodríguez-Noda, M. Fariñas-Medina, C. Zayas-Vignier, M. Hernández-Cedeño, Y. Serrano, F. Cardoso, D. Santana-Mederos, D. García-Rivera, Y. Valdés-Balbín, V. Vérez-Bencomo, B.H.A. Rehm, Design and Biological Assembly of Polyester Beads Displaying Pneumococcal Antigens as Particulate Vaccine, ACS Biomater. Sci. Eng. 4 (2018) 3413–3424. doi:10.1021/acsbiomaterials.8b00579.

[125] R. Nayerhoda, A. Hill, M. Beitelshees, C. Jones, B. Pfeifer, Design Variation of a Dual-Antigen Liposomal Vaccine Carrier System, Materials (Basel). 12 (2019) 2809. doi:10.3390/ma12172809.

[126] A.B. Hill, M. Beitelshees, R. Nayerhoda, B.A. Pfeifer, C.H. Jones, Engineering a Next-Generation Glycoconjugate-Like *Streptococcus pneumoniae* Vaccine, ACS Infect. Dis. (2018) acsinfecdis.8b00100. doi:10.1021/acsinfecdis.8b00100.

[127] B.D. Souza, P. Nagaraja Shastri, G. Hammons, E. Kim, L.P. Kolluru, G.M. Carlone, G. Rajam, M.J.D. Souza, Immune-potentiation of Pneumococcal Capsular Polysaccharide Antigen using Albumin Microparticles, J. Pharmacovigil. 06 (2018) 1–6. doi:10.4172/2329-6887.1000261.

[128] J. Colino, L. Duke, C.M. Snapper, Noncovalent association of protein and capsular polysaccharide on bacteria-sized latex beads as a model for polysaccharide-specific humoral immunity to intact gram-positive extracellular bacteria., J. Immunol. 191 (2013) 3254–63. doi:10.4049/jimmunol.1300722.

[129] M.P. Flanagan, J.G. Michael, Oral immunization with a Streptococcal pneumoniae polysaccharide conjugate vaccine in enterocoated microparticles induces serum antibodies against type specific polysaccharides, Vaccine. 17 (1999) 72–81. doi:10.1016/S0264-410X(98)00118-2.

[130] B. Li, X. Chen, J. Yu, Y. Zhang, Z. Mo, T. Gu, W. Kong, Y. Wu, Protection elicited by nasal immunization with pneumococcal surface protein A (PspA) adjuvanted with bacterium-like particles against Streptococcus pneumoniae infection in mice, Microb. Pathog. 123 (2018) 115–119. doi:10.1016/J.MICPATH.2018.06.041.

[131] D. Wang, J. Lu, J. Yu, H. Hou, K. Leenhouts, M.L. Van Roosmalen, T. Gu, C. Jiang, W. Kong, Y. Wu, A Novel PspA Protein Vaccine Intranasal Delivered by Bacterium-Like Particles Provides Broad Protection Against Pneumococcal Pneumonia in Mice, Immunol. Invest. 47 (2018) 403–415. doi:10.1080/08820139.2018.1439505.

[132] V. Manolova, A. Flace, M. Bauer, K. Schwarz, P. Saudan, M.F. Bachmann, Nanoparticles target distinct dendritic cell populations according to their size, Eur. J. Immunol. 38 (2008) 1404–1413. doi:10.1002/eji.200737984.

[133] A. Mant, F. Chinnery, T. Elliott, A.P. Williams, The pathway of cross-presentation is influenced by the particle size of phagocytosed antigen, Immunology. 136 (2012) 163–175. doi:10.1111/j.1365-2567.2012.03558.x.

[134] M.E.C. Lutsiak, G.S. Kwon, J. Samuel, Biodegradable nanoparticle delivery of a Th2-biased peptide for induction of Th1 immune responses, J. Pharm. Pharmacol. 58 (2006) 739–747. doi:10.1211/jpp.58.6.0004.

[135] C.S.W. Chong, M. Cao, W.W. Wong, K.P. Fischer, W.R. Addison, G.S. Kwon, D.L. Tyrrell, J. Samuel, Enhancement of T helper type 1 immune responses against hepatitis B virus core antigen by PLGA nanoparticle vaccine delivery, J. Control. Release. 102 (2005) 85–99. doi:10.1016/j.jconrel.2004.09.014.

[136] M.F. Bachmann, G.T. Jennings, Vaccine delivery: A matter of size, geometry, kinetics and molecular patterns, Nat. Rev. Immunol. 10 (2010) 787–796. doi:10.1038/nri2868.

[137] T. Fifis, A. Gamvrellis, B. Crimeen-Irwin, G.A. Pietersz, J. Li, P.L. Mottram, I.F.C. McKenzie, M. Plebanski, Size-Dependent Immunogenicity: Therapeutic and Protective Properties of Nano-Vaccines against Tumors, J. Immunol. 173 (2004) 3148–3154. doi:10.4049/jimmunol.173.5.3148.

[138] S. Kumar, A.C. Anselmo, A. Banerjee, M. Zakrewsky, S. Mitragotri, Shape and size-dependent immune response to antigen-carrying nanoparticles, J. Control. Release. 220 (2015) 141–148. doi:10.1016/j.jconrel.2015.09.069.

[139] K. Niikura, T. Matsunaga, T. Suzuki, S. Kobayashi, H. Yamaguchi, Y. Orba, A. Kawaguchi, H. Hasegawa, K. Kajino, T. Ninomiya, K. Ijiro, H. Sawa, Gold nanoparticles as a vaccine platform: Influence of size and shape on immunological responses in vitro and in vivo, ACS Nano. 7 (2013) 3926–3938. doi:10.1021/nn3057005.

[140] K.T. Gause, A.K. Wheatley, J. Cui, Y. Yan, S.J. Kent, F. Caruso, Immunological Principles Guiding the Rational Design of Particles for Vaccine Delivery, (2017). doi:10.1021/acsnano.6b07343.

[141] P. Matzinger, The danger model: A renewed sense of self, Science (80-.). 296 (2002) 301–305.

[142] D.F. Moyano, M. Goldsmith, D.J. Solfiell, D. Landesman-Milo, O.R. Miranda, D. Peer, V.M. Rotello, Nanoparticle hydrophobicity dictates immune response, J. Am. Chem. Soc. 134 (2012) 3965–3967. doi:10.1021/ja2108905.

[143] R. Toy, K. Roy, Engineering nanoparticles to overcome barriers to immunotherapy, Bioeng. Transl. Med. 1 (2016) 47–62. doi:10.1002/btm2.10005.

[144] A.L. Ackerman, C. Kyritsis, R. Tampe, P. Cresswell, Early phagosomes in dendritic cells form a cellular compartment sufficient for cross presentation of exogenous antigens, Proc. Natl. Acad. Sci. 100 (2003).

[145] S.W. Howland, K.D. Wittrup, E. Alerts, Antigen Release Kinetics in the Phagosome Are Critical to Cross-Presentation Efficiency, J. Immunol. 180 (2008) 1576–1583. doi:10.4049/jimmunol.180.3.1576.

Background, Hypothesis and Objectives

USC
UNIVERSIDADE
DE SANTIAGO
DE COMPOSTELA

General background:

Polysaccharide vaccines alone are weak antigens and fail to generate the strong immune response in the children and immunocompromised patients [1] and therefore, they are generally conjugated to carrier proteins like TT, DT or CRM 197. In diseases like Pneumonia, 96 different pneumococcal serotypes are responsible for causing the infection [2]. In this case, the polysaccharide component from each serotype needs to be incorporated in the vaccine to elicit the protection. However, the preparation of the vaccine comprising of capsular polysaccharide components from each serotype is highly difficult, expensive and time consuming. Currently, two types of pneumococcal vaccines are in use; a 23 valent pneumococcal polysaccharide vaccine (PPV23) that consists of mixture of polysaccharide antigens from different pneumococcal serotypes; and the other group consists of pneumococcal conjugate vaccines (PCV-7, 10, 13), in which the polysaccharide antigens are conjugated to carrier proteins to generate potent immune response in children. However, these pneumococcal vaccines can protect only against the infections caused by a limited number of serotypes, whose polysaccharides are incorporated in the vaccine and at the same time, they are associated with the problem of serotype replacement.

In this line, researchers have identified proteins that are commonly present in all the pneumococcal serotypes and can act as an antigen [3]. These pneumococcal proteins have been effective in generating a protective response in the immunized individuals [4–6]. As the protein antigens are sub-unit vaccines, they should be either accompanied with suitable adjuvant, carrier or both. However, the major hurdle lies in developing an efficient vaccine delivery system. In recent years, the use of biocompatible and biodegradable polymers has been investigated as adjuvants and antigen carriers. Amongst them, chitosan continues to show tremendous potential as it is non-toxic, biocompatible, biodegradable polymer that has mucoadhesive and immunostimulatory properties [7]. Use of these particulate systems will help in protecting the antigen from degradation and the mimic the pathogen in size, shape or by carrying the antigens on the surface. Therefore, in our studies, we adopted chitosan nanoparticles as suitable carriers for the delivery of synthesized glycoconjugate antigens.

Hypothesis:

- The use of common pneumococcal protein, Pneumococcal surface adhesin A (PsaA), as a carrier protein for preparation of glycoconjugate, might produce serotype-independent immune response. We hypothesize that it would be possible to replace the traditional carrier proteins like TT, DT and CRM 197 with PsaA. The PsaA conjugated to tetrasaccharide in this study can act both as carrier and the antigen.

- Further encapsulation of these glycoconjugates into the polymeric nano-systems could improve their presentation to the immune cells, thereby generating enhanced immune response. The utilization of chitosan nanoparticles that are biocompatible, biodegradable, mucoadhesive and immunostimulatory properties can help in the effective delivery of the glycoconjugate antigens via mucosal route.

- Targeting of glycoconjugates via mucosal routes using the chitosan nanoparticles might generate both systemic (IgG) and mucosal (IgA) immune responses and offer protection against invasive pneumococcal infections.

In summary, we hypothesize that the strategies proposed in this thesis might result in an improved pneumococcal vaccine formulation that enables needle free vaccine delivery and protect against invasive pneumococcal infections.

Objectives:

The overall goal of this thesis is to develop a improved pneumococcal vaccine formulation based on semisynthetic glycoconjugate antigen. In order accomplish this, studies are organised into several specific goals as shown below.

Objective 1: Preparation and characterization of a semisynthetic glycoconjugate antigen, including:

- Synthesis of the tetrasaccharide antigen that mimic the capsular polysaccharide of *Streptococcus pneumoniae* serotype 14 (Pn14TS).
- Expression and purification of Pneumococcal surface adhesin A (PsaA) using recombinant DNA technology in *E. coli.*
- Synthesis and characterization of glycoconjugate vaccine (GC) using produced Pn14TS and PsaA.

The results corresponding to this objective are presented in the chapter 1: "Semisynthetic glycoconjugate based on dual role protein/PsaA as a pneumococcal vaccine" and have already been published.

Objective 2: Development and characterization of polymeric nanosystems encapsulating the synthesised glycoconjugate antigen.

- Preparation of glycoconjugate loaded chitosan nanoparticles using ionic gelation method, and their characterization.
- To study the ability of the nanosystems to enhance the immune response against the glycoconjugate antigens.
- To compare the immune response obtained after systemic and mucosal immunizations.

The results corresponding to this objective are presented in the chapter 2: "Chitosan nanoparticles as carriers for the delivery of semisynthetic glycoconjugate antigen".

Objective 3: Evaluation of *in vitro* efficiency of glycoconjugate loaded nanoparticles

- To study the cytocompatibility and internalization of prepared nanoparticles with the human monocyte-derived dendritic cells.
- To study the interaction of the prepared nanosystems with the dendritic cells.

The results corresponding to this objective are presented in the chapter 3: “Interaction of glycoconjugate loaded chitosan nanoparticles with human dendritic cells”.

References:

[1] A. Weintraub, Immunology of bacterial polysaccharide antigens, Carbohydr. Res. 338 (2003) 2539–2547. doi:10.1016/j.carres.2003.07.008.

[2] K.A. Geno, G.L. Gilbert, J.Y. Song, I.C. Skovsted, K.P. Klugman, C. Jones, H.B. Konradsen, M.H. Nahm, Pneumococcal Capsules and Their Types: Past, Present, and Future, Clin. Microbiol. Rev. 28 (2015) 871–899. doi:10.1128/CMR.00024-15.

[3] K.P. Klugman, R. Dagan, R. Malley, C.G. Whitney, Pneumococcal Conjugate Vaccine and Pneumococcal Common Protein Vaccines, Plotkin's Vaccines. (2013) 504–541. doi:10.1016/B978-1-4557-0090-5.00032-X.

[4] M. González-Miro, L. Rodríguez-Noda, M. Fariñas-Medina, D. García-Rivera, V. Vérez-Bencomo, B.H.A. Rehm, Self-assembled particulate PsaA as vaccine against Streptococcus pneumoniae infection., Heliyon. 3 (2017) e00291. doi:10.1016/j.heliyon.2017.e00291.

[5] A. David Ogunniyi, R.L. Folland, D.E. Briles, S.K. Hollingshead, J.C. Paton, N. Adelaide, Immunization of Mice with Combinations of Pneumococcal Virulence Proteins Elicits Enhanced Protection against Challenge with Streptococcus pneumoniae, 2000. http://iai.asm.org/ (accessed September 14, 2018).

[6] Q. Xu, J.R. Casey, M.E. Pichichero, Higher levels of mucosal antibody to pneumococcal vaccine candidate proteins are associated with reduced acute otitis media caused by Streptococcus pneumoniae in young children, Mucosal Immunol. 8 (2015) 1110–1117. doi:10.1038/mi.2015.1.

[7] H.B.T. Moran, J.L. Turley, M. Andersson, E.C. Lavelle, Immunomodulatory properties of chitosan polymers, Biomaterials. 184 (2018) 1–9. doi:10.1016/J.BIOMATERIALS.2018.08.054.

USC
UNIVERSIDADE
DE SANTIAGO
DE COMPOSTELA

Chapter 1

Semisynthetic glycoconjugate based on dual role protein/PsaA as a pneumococcal vaccine

This work was done in collaboration with Center for Infection and Immunity of Lille, Institut Pasteur de Lille (France). The results from this chapter have already been published.

USC
UNIVERSIDADE
DE SANTIAGO
DE COMPOSTELA

Semisynthetic glycoconjugate based on dual role protein/PsaA as a pneumococcal vaccine

Abstract

Pneumococcal infections remain a major public health concern worldwide. The currently available vaccines in the market are based on pneumococcal capsular polysaccharides but they still need to be improved to secure an optimal coverage notably in population at risk. To circumvent this, association of virulence pneumococcal proteins to the polysaccharide valencies has been proposed with the hope to observe an additive - if not synergistic - protective effect. Along this line, the use of the highly conserved and ubiquitous pneumococcal surface adhesin A (PsaA) as a protein carrier for a synthetic pneumococcal oligosaccharide is demonstrated herein for the first time. A tetrasaccharide mimicking functional antigenic determinants from the *S. pneumoniae* serotype 14 capsular polysaccharide (Pn14TS) was chemically synthesised. The mature PsaA (mPsaA) was expressed in *E. coli* and purified using affinity chromatography. The Pn14PS was conjugated to mPsaA using maleimide-thiol coupling chemistry to obtain mPsaA-Pn14PS conjugate (protein/sugar molar ratio: 1/5.4). The mPsaA retained the structural conformation after the conjugation and lyophilisation. The prepared glycoconjugate adjuvanted with α-galactosylceramide, a potent activator of invariant Natural Killer T cells, was tested in mice for its immunological response upon subcutaneous injection in comparison with mPsaA alone and a model BSA conjugate (BSA-Pn14PS, used here as a control). Mice immunised with the mPsaA-Pn14TS produced a robust IgG response against mPsaA and against the capsular polysaccharide from pneumococcal serotype 14. These data provide the basis for novel pneumococcal vaccine development.

Keywords: Glycoconjugate vaccine, Carbohydrate antigens, pneumococcal surface adhesin A. Pneumococcal vaccine

Graphical Abstract

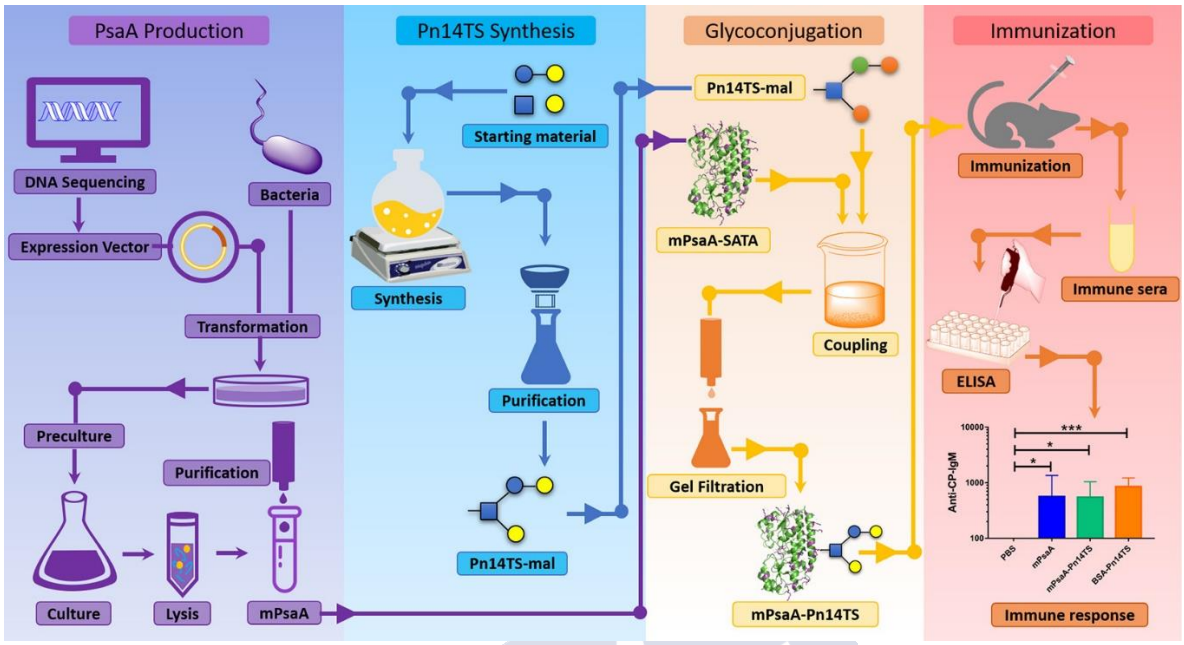

1. Introduction

Streptococcus pneumoniae is a leading cause of mortality and morbidity in children and the elderly population. It is responsible for infections like pneumonia, otitis media, meningitis and bacteraemia which accounts for an estimated number of 800,000 deaths in children annually [1]. The polysaccharide subunits expressed by pneumococci are anchored to the cell wall surface and preventing the clearance of pneumococci from the lung and protecting them from complement-mediated opsonophagocytosis [2]. Polysaccharide chains act as early target antigens as their production is essential for pneumococcal colonisation and virulence. These polysaccharides are highly immunogenic and induce the production of antibodies that react with homologous serotype [3].

Capsular polysaccharide (CP) vaccines currently in use for adults have only weak or no efficacy towards pneumonia and bronchitis caused by *S. pneumoniae* [3]. The protection level of a vaccinated individual varies depending on the location as the prevalence of serotype varies significantly among the continents. Due to this phenomenon, the capsular serotypes used as vaccine antigens are monitored internationally [1]. The inability of the polysaccharide vaccines to elicit a protective immune response in toddlers and young children have given way for the development of improved vaccines. Polysaccharides are T-cell independent antigens, and they do not elicit any protective immune response in infants and children, but conjugating them to a protein makes them T-cell dependent and immunogenic in the same population [4]. Researchers have tried conjugating capsular polysaccharide to carrier proteins like tetanus toxoid, diphtheria toxin, and cross-reactive material of diphtheria toxoid (CRM197) to overcome this issue. The prepared glycoconjugates can generate T-cell

dependent antibody response and higher antibody titers in children and high-risk individuals [5,6]. Glycoconjugate vaccines such as the heptavalent (PCV7) vaccine and the more recent tridecavalent (PCV13) pneumococcal vaccine are promising in preventing pneumonia caused by the corresponding serotypes. However, it is still not clear whether it is by preventing nasopharyngeal colonisation or by improving adaptive immune response in the lungs. The overall protection mechanism against the *S. pneumoniae* infection is not clearly understood, which hinders the design of more efficacious novel vaccines [7].

There is a need for pneumococcal vaccines with broader coverage against the pneumococcal serotypes. As capsular polysaccharides are serotype specific, researchers have focused on identifying protein immunogens which can offer complete serotype coverage and generate enhanced protection. Along with this line, pneumococcal surface adhesin A (PsaA) is a membrane-associated metal binding lipoprotein [8], which is highly conserved and essential for the survival and virulence of the bacteria [9]. PsaA is involved in the adhesion and colonisation of nasopharyngeal epithelium by the pneumococci. Its presence in all serotypes of pneumococci along with its ability to generate robust responses in infants or elderly population further contribute to make it an ideal candidate for pneumococcal vaccine formulations [10,11]. Indeed, PsaA used as immunogen was able to prevent entry of the pathogen noticeably by reducing the nasal carriage of the pathogen and even to confer protection when combined with adjuvants in animal models [12–15]. Alternatively, PsaA has also been used as a carrier protein in glycoconjugate vaccines which has already demonstrated protection in animal models [16,17]. Additionally, the concomitant administration of PsaA with PCV7 reduced the colonization in the murine models [18]. In these reports, glycoconjugates were acquired from bacterial source[16,17], but the utility of

PsaA as a carrier for synthetic oligosaccharides mimicking full-length CP remains to be documented. To this aim, the capsular polysaccharide of the *S. Pneumoniae* type 14 consists of the repeating units of {6)-[β-D-Galp-(1→4)-]β-D-GlcpNAc-(1→3)-β-D-Galp-(1→4)-β-D-Glcp-(1→}n [19]. The tetrasaccharide β-D-Galp-(1→4)-β-D-Glcp-(1→6)-[β-D-Galp-(1→4)]-β-D-GlcpNAc (referred to as Pn14TS) has been identified as the smallest oligosaccharide of the serotype 14 that is capable of inducing opsonophagocytic response when coupled to the carrier proteins like CRM197 [20]. It possesses higher protective properties as compared to related hexa- or octasaccharides when conjugated [21]. In this study, we thus propose to produce this synthetic mimic of *S. pneumoniae* type 14 CP and to conjugate it to pneumococcal PsaA, using thiol maleimide coupling chemistry to obtain a semisynthetic glycoconjugate vaccine. The immunogenicity of the obtained glycoconjugate was studied in BALB/c mice. As an adjuvant, we chose α-galactosylceramide (α-GalCer), a potent activator of invariant Natural Killer T (*i*NKT) cells [22,23].

2. Materials and Methods

2.1. Mice and ethics statement

Specific pathogen-free C57BL/6 mice (6 week-old, female) were purchased from Janvier (Le Genest-St-Isle, France). Mice were maintained in a biosafety level 2 facility in the Animal Resource Centre at the Lille Pasteur Institute for at least two weeks prior to usage, to allow appropriate acclimation. Mice were fed a standard rodent chow (SAFE A04) (SAFE, Augy, France) and water *ad libitium*. The diet contains ~11.8% fiber including ~10% water-insoluble fiber (3.6% cellulose) and 1.8% water-soluble fiber. All the animal experiments were performed at Lille Pasteur institute according to the ethical guidelines (agreement number AF 16/20090 and 00357.03).

2.2. Materials and general methods

The antibiotic ampicillin was purchased from PanReac Applichem, chloramphenicol and kanamycin were purchased from Sigma Aldrich, and the LB culture medium was purchased from VWR. The isopropyl thiogalactoside (IPTG) used in the induction of protein was obtained from Alfa-Aesar. The NiNTA beads used in the affinity chromatography for the purification of the PsaA were obtained from Macherey-Nagel. The linker *S*-acetylthioacetate *N*-Hydroxy succinimide (SATA-NHS) and 6-maleimidocaproic acid succinimidyl ester were obtained from Merck and Interchim, respectively. The adjuvant α-GalCer was produced by Dr. B. Frisch (University of Strasbourg). All reagents were purchased from commercial sources and used without further purification. Reactions were monitored by thin-layer chromatography (TLC) on 0.25 mm silica gel plates with fluorescent indicator (GF254) and visualised under UV light. Detection was done by charring with vanillin in sulfuric acid/ethanol (1.5:95 v/v). Flash-chromatography purifications were made on silica gel columns (4 to 80 g, 240-400 mesh) using an automated Reveleris Flash Chromatography System (Grace Alltech) equipped by both ELS (Evaporative Light Scattering) and UV/diode array allowing the simultaneous use of two customizable wavelength detectors.

RP-HPLC separation was performed on a Uptisphere Strategy 100 Å C18HQ (Interchim, France) (5 µm, 21.2 × 250 mm) column at a flow rate of 6 mL min^{-1} with ELSD and UV (225 nm) detection. Gradient: 0% B for 5 min, 0–5% B over 5 min, 10–80% B over 30 min, 80% B for 5 min; Solvent system A: H_2O; solvent system B: MeOH.

All NMR experiments were performed at 400 MHz using Bruker Avance 400 MHz spectrometers equipped with a DUAL+ $^{1}H/^{13}C$ ATMA grad 5 mm probe. Assignments were performed by stepwise identification using COSY, and HSQC experiments using standard pulse

programs from the Bruker library. Chemical shifts are given relative to external TMS with calibration involving the residual solvent signals.

High-resolution mass spectra were recorded in positive mode on Waters SYNAPT G2-Si HDMS with detection with a hybrid quadrupole time of flight (Q-TOF) detector. The compounds were individually dissolved in MeOH at a concentration of 1 mg/mL and then infused into the electrospray ion source at a flow rate of 10 µl.min^{-1} at 100°C. The mass spectrometer was operated at 3 kV while scanning the magnet at a typical range of 4000-100 Da. The mass spectra were collected as continuum profile data. An accurate mass measurement was achieved based on every five-second auto-calibration using leucine-enkephalin ([M+H]$^{+}$ = 556.2771 *m/z*) as an internal standard. PsaA mass spectra were determined on an Autoflex III MALDI-TOF/TOF spectrometer (Bruker Daltonics) in positive ionisation modes and with a linear detection. 75 pmol of each sample was deposited on the MALDI target plate and were mixed with sinapinic acid as the matrix (10 mg mL−1; H_2O–CH_3CN–TFA, 50:50:0.1). The mass spectrometer was calibrated with a standard of BSA (15 pmol on target) on dimer and different charge states of the protein.

2.3. Synthesis of Pneumococcal serotype 14 tetrasaccharide (Pn14TS)

2.3.1. 2-azidoethyl (2,3,4,6-tetra-*O*-benzoyl-β-D-galactopyranosyl)-(1→4)-6-O-tert-butyldimethylsilyl-2-deoxy-2-phtalimido-β-D-glucopyranoside 3

2,3,4,6-tera-O-benzoyl-D-galactopyranose trichloroacetimidate donor **1** (446 mg, 0.60 mmol) and 2-azidoethyl 2-deoxy-6-*O*-TBDMS-2-phtalimido-β-D-glucopyranoside acceptor **2** (270 mg, 0.55 mmol) were mixed with molecular sieves (MS4Å) in CH_2Cl_2 (5 mL). The mixture was cooled to 0°C, then TMSOTf (32 µl) was added and the reaction mixture stirred at this temperature for 1h. The reaction was quenched upon addition of Et_3N (0.1 mL), and the resulting mixture was filtered through a Celite pad. The filtrate was concentrated, and the crude residue was purified by flash-chromatography on silica gel (eluent gradient of cyclohexane/EtOAc) to give disaccharide **3** (352 mg, 60%). (R_f = 0.63, EtOAc/Cyclohexane = 6:4); ^{1}H NMR (400 MHz, $CDCl_3$): δ 8.02-7.15 (m, 24H), 5.88 (d, *J* = 3.5 Hz, 1H), 5.77 (dd, *J* = 8.0, 10.5 Hz, 1H), 5.49 (dd, *J* = 3.5, 10.5 Hz, 1H), 5.18 (d, *J* = 8.5 Hz, 1H), 4.94 (d, *J* = 8.0 Hz, 1H), 4.63-4.49 (m, 2H), 4.32-4.27 (m, 2H), 4.19 (d, *J* = 1.5 Hz, 1H), 4.10 (dd, *J* = 8.5, 10.8 Hz, 1H), 3.85 (ddd, *J* = 3.6, 5.3, 10.6 Hz, 1H), 3.74 (t, *J* = 8.7 Hz, 1H), 3.60-3.55 (m, 1H), 3.52 (ddd, *J* = 3.6, 7.6, 10.6 Hz, 1H), 3.43 (dt, *J* = 2.2, 9.7 Hz, 1H), 3.27 (ddd, *J* = 3.7, 7.8, 13.3 Hz, 1H), 3.07 (ddd, *J* = 3.6, 5.3, 13.3 Hz, 1H), 0.76 (s, 9H), -0.14 (s, 3H), -0.15 (s, 3H); HR-ESI-MS: *m/z* Calcd for $C_{56}H_{58}N_4O_{16}Si$. $[M+Na]^+$ 1093.3539, found 1093.3508.

2.3.2. 2-azidoethyl 2,3,4,6-tetra-*O*-acetyl-(2,3,4,6-tetra-*O*-benzoyl-β-D-galactopyranosyl)-(1→4)-2-deoxy-2-phtalimido-β-D-glucopyranoside 4

To disaccharide **3** (250 mg, 0.23 mmol) dissolved in CH_3CN (5.8 mL) in a 15 mL teflon tube, was added aqueous solution of HF (48%, 306 µl) at 0°C. The reaction mixture was stirred for 30 min at RT and then neutralized upon addition of solid $NaHCO_3$. The mixture was diluted in EtOAc and washed with H_20 and brine. The organic layer was dried (Na_2SO_4), filtered and

concentrated under reduced pressure. The crude residue was purified by flash-chromatography on silica gel (eluent gradient of cyclohexane/EtOAc) to give disaccharide **4** (169 mg, 76%). (R_f = 0.40, EtOAc/Cyclohexane = 4:6); ^{1}H NMR (400 MHz, $CDCl_3$): δ 8.08-7.23 (m, 24H), 5.97 (d, *J* = 3.4 Hz, 1H), 5.87 (dd, *J* = 8.0, 10.4 Hz, 1H), 5.60 (dd, *J* = 3.4, 10.4 Hz, 1H), 5.32 (d, *J* = 8.5 Hz, 1H), 5.04 (d, *J* = 8.0 Hz, 1H), 4.67 (dd, *J* = 3.4, 11.5 Hz, 1H), 4.60 (broad d t, *J* = 9.5 Hz, 1H), 4.43-4.32 (m, 3H), 4.23 (dd, *J* = 8.6, 10.7 Hz, 1H), 3.85 (ddd, *J* = 2.4, 5.2, 10.7 Hz, 1H), 3.74 (t, *J* = 8.9 Hz, 1H), 3.60-3.50 (m, 4H), 3.33 (ddd, *J* = 3.4, 5.8, 13.3 Hz, 1H), 3.17 (ddd, *J* = 3.4, 5.2, 13.3 Hz, 1H); ^{13}C NMR (100 MHz, $CDCl_3$): δ 168.0, 166.1, 165.8, 165.3, 133.9, 133.7, 133.6, 133.3, 133.2, 131.9, 130.0, 129.9, 129.8, 129.0, 128.8, 128.7, 128.7, 128.6, 128.4, 128.3, 102.2, 98.4, 82.1, 74.3, 72.4, 71.5, 69.6, 69.6, 68.6, 68.1, 62.7, 60.6, 55.8, 50.4; HR-ESI-MS: *m/z* Calcd for $C_{56}H_{58}N_4O_{16}Si$. $[M+Na]^+$ 979.2650, found 979.2642.

2.3.3. 2-azidoethyl (2,3,4,6-tetra-O-acetyl-β-D-galactopyranosyl)-(1→4)-(2,3,6-tri-O-acetyl-β-D-galactopyranosyl)-(1→6)-[(2,3,4,6-tetra-*O*-benzoyl-β-D-galactopyranosyl)-(1→4)]-2-deoxy-2-phtalimido-β-D-glucopyranoside 6

Imidate donor **5** (134 mg, 0.17 mmol, 1.2 equiv) and acceptor **4** (137 mg, 0.143 mmol) were mixed with molecular sieves (MS 4 Å) in CH_2Cl_2 (5 mL). Then TMSOTf (28 µl) was added and the reaction mixture stirred at RT overnight. The reaction was quenched upon addition of Et_3N (0.1 mL), and the resulting mixture was filtered through a Celite pad. The filtrate was concentrated, and the crude residue was purified by flash-chromatography on silica gel (eluent gradient of cyclohexane/EtOAc) to give tetrasaccharide **6** (124 mg, 55%). (R_f = 0.48, EtOAc/Cyclohexane = 6:4); ^{1}H NMR (400 MHz, $CDCl_3$): δ 7.98-7.13 (m, 24H), 5.87 (d, *J* = 3.50 Hz, 1H), 5.76 (dd, *J* = 7.9, 10.4 Hz, 1H), 5.57 (dd, *J* = 3.5, 10.4 Hz, 1H), 5.28 (d, *J* = 3.6 Hz, 1H), 5.15 (d, *J* = 10.5 Hz, 1H), 5.04 (dd, *J* = 7.9, 10.4 Hz, 1H), 4.93-4.87 (m, 3H), 4.75 (dd, *J* = 7.5, 8.8 Hz, 1H), 4.46 (dd, *J* = 4.00, 11.9 Hz, 1H), 4.52-4.42 (m, 3H), 4.40 (d, *J* = 8.0 Hz, 1H), 4.33 (dd, *J*

= 2.2, 12.9 Hz, 1H), 4.26 (dd, *J* = 8.4, 11.6 Hz, 1H), 4.10 (dd, *J* = 8.6, 10.9 Hz, 1H), 4.04-3.99 (m, 2H), 3.95 (dd, *J* = 5.4, 12.0 Hz, 1H), 3.89-3.81 (m, 2H), 3.70-3.59 (m, 3H), 3.54-3.42 (m, 2H), 3.28 (ddd, *J* = 3.5, 8.1, 13.5 Hz, 1H), 3.17-3.14 (ddd, *J* = 3.4, 5.8, 13.3 Hz, 1H), 3.08 (ddd, *J* = 3.4, 5.2, 13.3 Hz, 1H), 2.23 (s, 3H), 2.08 (s, 3H), 2.06 (s, 3H), 2.00 (s, 6H), 1.97 (s, 3H), 1.96 (s, 3H), 1.89 (s, 3H); ^{13}C NMR (100 MHz, $CDCl_3$): δ 171.0, 170.5, 170.4, 170.2, 170.1, 169.9, 169.5, 169.2, 168.0, 166.2, 166.4, 166.4, 164.9, 134.1, 133.9, 133.7, 133.4, 130.8, 130.0, 129.9, 129.9, 129.8, 129.7, 128.0, 128.9, 128.8, 128.7, 128.7, 128.5, 128.4, 128.3, 126.1, 101.9, 101.2, 100.4, 98.2, 83.1, 76.1, 73.5, 72.9, 72.5, 72.3, 71.8, 71.4, 71.0, 70.6, 69.8, 69.2, 68.5, 68.2, 66.8, 62.7, 62.0, 60.9, 60.4, 55.7, 55.5, 50.4, 21.0, 20.9, 20.8, 20.6, 20.5, 19.8; HR-ESI-MS: *m/z* Calcd for $C_{76}H_{78}N_4O_{33}$. $[M+Na]^+$ 1597.4446, found 1597.4384.

2.3.4. 2-azidoethyl (β-D-galactopyranosyl)-(1→4)-(β-D-galactopyranosyl)-(1→6)-[(β-D-galactopyranosyl)-(1→4)]-2-deoxy-2-acetamido-β-D-glucopyranoside 8

Per acetylated tetrasaccharide **7** (45 mg, 0.035 mmol) dissolved in MeOH (400 µl) was reacted with a 2.5M solution of sodium methoxide in MeOH (5 µl) overnight at RT. The reaction mixture was quenched with Amberlite® resin IR120 (H+ form), filtered and concentrated to reduced pressure to furnished tetrasaccharide **8** (27 mg, quantitative); (R_f = 0.50, *n*BuOH/EtOH/H_2O = 5:5:3); ^{1}H NMR (400 MHz, D_2O): δ 4.58 (d, *J* = 8.2 Hz, 1H), 4.53 (d, *J* = 8.0 Hz, 1H), 4.50 (d, *J* = 7.8 Hz, 1H), 4.42 (d, *J* = 7.8 Hz, 1H), 4.27 (dd, *J* = 2.7, 11.2 Hz, 1H), 4.02 (ddd, *J* = 3.1, 5.5, 11.4 Hz, 1H), 3.97-3.92 (m, 2H), 3.90 (d, *J* = 3.3 Hz, 1H), 3.84-3.77 (m, 2H), 3.76-3.67 (m, 11H), 3.66-3.62 (m, 5H), 3.60-3.55 (m, 1H), 3.54-3.47 (m, 2H), 3.42 (ddd, *J* = 3.1, 7.3, 10.4 Hz, 1H), 3.36 (ddd, *J* = 3.1, 4.5, 13.3 Hz, 1H), 2.01 (s, 3H); ^{13}C NMR (100 MHz, D_2O): δ 174.7, 103.0, 102.8, 102.5, 101.1, 78.5, 77.9, 75.4, 75.3, 74.8, 74.3, 73.6, 72.7, 72.6, 72.6, 72.4, 71.0, 71.0, 68.9, 68.6, 68.6, 67.5, 61.1, 61.0, 60.1, 55.1, 50.4, 22.3.

2.3.5. 2-aminoethyl (β-D-galactopyranosyl)-(1→4)-(β-D-galactopyranosyl)-(1→6)-[(β-D-galactopyranosyl)-(1→4)]-2-deoxy-2-acetamido-β-D-glucopyranoside 9

To a mixture of $NaBH_4$ (2.60 mg) and 10% Pd/C (1.15 mg) in H_2O was added azide derivative **8** (25 mg) dissolved in aqueous NaOH 0.1M (305 µl). The reaction mixture was stirred until complete reduction of the azide (monitored by TLC). Then the reaction mixture is filtered over a Celite pad, neutralized with amberlite IR120 (H^+ form), filtered and lyophilised to furnish **9** (22 mg, 91%); R_f = 0, nBuOH/EtOH/H_2O = 5:5:3); ^{1}H NMR (400 MHz, D_2O): δ 4.55 (d, *J* = 8.3 Hz, 1H), 4.52 (d, *J* = 8.0 Hz, 1H), 4.49 (d, *J* = 7.8 Hz, 1H), 4.42 (d, *J* = 7.8 Hz, 1H), 4.27 (dd, *J* = 2.2, 11.4 Hz, 1H), 4.03-3.92 (m, 3H), 3.89 (d, *J* = 3.3 Hz, 1H), 3.86-3.60 (m, 19H), 3.60-3.55 (m, 1H), 3.54-3.47 (m, 2H), 3.36-3.31 (m, 1H), 3.16-3.15 (m, 2H), 2.01 (s, 3H); ^{13}C NMR (100 MHz, D_2O): δ 174.9, 103.0, 102.8, 102.4, 101.1, 78.5, 77.7, 75.4, 75.3, 74.7, 74.4, 73.3, 72.7, 72.6, 72.5, 72.2, 71.0, 71.0, 68.6, 68.6, 67.4, 66.4, 61.1, 61.0, 60.1, 55.0, 39.5, 22.2; HR-ESI-MS: *m/z* Calcd for $C_{28}H_{50}N_2O_{21}$ $[M+H]^+$ 751.2984, found 751.3016.

2.3.6. 2-(*N*-6-maleimidocaproyl)ethyl (β-D-galactopyranosyl)-(1→4)-(β-D-galactopyranosyl)-(1→6)-[(β-D-galactopyranosyl)-(1→4)]-2-deoxy-2-acetamido-β-D-glucopyranoside 10 (Pn14TS-mal)

To a solution of compound **9** (20 mg, 0.026 mmol, 1.03 equiv) in DMSO were successively added 6-maleimido-caproic acid succinimidyl ester (8 mg, 1 equiv) and DIEA (10 µl) at RT. The reaction mixture was stirred at 30°C overnight, diluted in water and freeze-dried. The crude residue was purified by RP-HPLC to provide **10** (Pn14TS-mal) (11.5 mg, 46% yield); ^{1}H NMR (400 MHz, D_2O): δ 4.54-4.50 (m, 3H), 4.43 (d, *J* = 7.8 Hz, 1H), 4.26 (dd, *J* = 2.4, 11.2 Hz, 1H), 3.97-3.47 (m, 24H), 3.38-3.31 (m, 3H), 2.21 (t, *J* = 7.4 Hz, 2H), 2.00 (s, 3H), 1.61-1.62 (m, 4H), 1.31-1.23 (m, 2H); HR-ESI-MS: *m/z* Calcd for $C_{38}H_{61}N_3O_{24}$ $[M+Na]^+$ 966.3543, found 966.3556.

2.4. mPsaA expression vector

The HtTEV-mPsaA plasmid, consisting of the gene coding for mature PsaA (without signal peptide) from *S. pneumonia*e in fusion with a histidine tag separated by a TEV protease cleavage site cloned between NdeI and BamHI sites of the pEt11a vector, was purchased from Genscript. The recombinant plasmid was transformed into *Escherichia coli* BL21(DE3) using the heat shock method, and the stocks were maintained at -80°C in 20% glycerol. The host bacteria *E. coli* strains XL1 blue and BL21(DE3), used for cloning and protein expression were obtained from Millipore.

2.5. Expression and purification of HtTEV-mPsaA

The expression of HtTEV-mPsaA protein was performed according to the following protocol. Briefly, 1000 mL of fresh LB medium with 25 µg/mL ampicillin were inoculated with 50 mL of overnight pre-culture and left to grow at 37°C, 180 rpm until they reached an exponential phase (approximately OD of 0.6/0.7) and at this point the HtTEV-mPsaA expression in the cultures was induced with IPTG (1mM final concentration). The cultures were left to grow for another 4h at 37°C and 180 rpm. The cells were harvested by centrifugation at 10 000 rpm. The pellet was resuspended in 50 mL cold lysis buffer (50 mM NaH_2PO_4, 150 mM NaCl, pH 8.0) and was subjected to sonication (10-20 min, 50% amplitude, pulse of 5 sec ON/OFF) in ice, and the cell debris was removed by centrifugation (20 min, 13,000 rpm). The protein was then purified by affinity chromatography as follows. The obtained supernatant was incubated with 1 mL of preconditioned NiNTA beads for 1h on rotating disk at 4°C, 12 rpm. Unbound fraction was collected, and the beads were washed with a lysis buffer containing 20 mM imidazole. The elution was performed with a lysis buffer containing different fractions of Imidazole up to 300 mM. The eluted fractions were subjected to SDS-PAGE to identify the

fractions containing target protein. The eluted fractions, containing the target protein (40 mg/l of culture), were pooled and dialysed against 0.1 M PBS at 4°C.

2.6. Removal of histidine tag from HtTEV-mPsaA and western blot analysis

The enzymatic cleavage of the histidine tag from the HtTEV-mPsaA was performed using the AcTEV™ protease (Invitrogen) flanked with a 6-histidine tag. The removal of the histidine tag was performed using at 8:1 HtTEV-mPsaA/ AcTEV™ protease ratio in the reaction buffer (50 mM Tris-HCl (pH 7.6), 1 mM EDTA, 1 mM DTT), for 4h at 4°C. The reaction mixture was incubated with the NiNTA beads for the separation of the cleaved mPsaA from the histidine tag, not digested HtTEV-mPsaA and the TEV protease. The eluate was collected and subjected to SDS-PAGE, western blot and MALDI TOF mass spectrometry to confirm the complete removal of the histidine tag.

For the western blot, the vertical SDS-PAGE was carried out using 12% acrylamide gels with the loadings of the reaction mixture and HtPsaA and AcTEV™ protease as controls using the Bio-rad system. The proteins were transferred to a nitrocellulose membrane at 200 V for 60 min. For the antibody probing, the nitrocellulose membrane was initially blocked with PBS containing 5% skimmed milk and 0.1% tween 20 for 1 h at room temperature. A primary antibody to mouse anti-poly his (Sigma H1029, diluted 1:1000) was applied to the membrane and incubated for 1h at RT. The membranes were washed thrice with PBS containing 0.1% Tween 20® and incubated with secondary antibody (Goat anti-Mouse IgG (H+L) Secondary Antibody, Alexa Fluor 680) for 30 min at RT on a shaker. Membranes were subjected to a final wash with PBS, and the detection was performed using an Odyssey CLx scanner (LI-COR) at 700 nm.

2.7. Glycoconjugate synthesis

S-acetyl-thioacetate succinimidyl ester was added to a solution of purified mPsaA (10 mg) in PBS 0.2M, pH 7.4 (1mL), in three portions every 45 min (3× 2.85 mg, 3×40 equiv) and the resulting mixture stirred for further 45min to give rise to mPsaA-SATA. The excess of reagents was removed by dialysis using 0.1M potassium phosphate buffer, pH 6.6. Later, a 2M solution of NH_2OH-HCl (4.61 µl) was to a mixture of mPsaA-SATA (3 mg) and Pn14TS-maleimide (1.31 mg) (1:15 ratio) in 0.1M potassium phosphate buffer, pH 6.6. The reaction mixture was stirred at RT for 1 h and then purified by gel filtration using a HiLoad 15/600 Superdex™ 75pg (GE Healthcare) column and PBS 0.1M, pH7.3 as eluent. BSA-Pn14TS conjugate was prepared analogously.

The colorimetric methods were used to determined sugar/protein ratios in the glycoconjugates. (i) Bradford assay (BioRad protein assay) was used to determine the concentration of the protein. (ii) The anthrone /sulphuric acid method [24] was used for the quantification of the tetrasaccharide.

2.8. Conformational stability of the PsaA derivatives

The conformational stability of the protein at different storage conditions was monitored by Circular Dichroism (CD) spectroscopy (Jasco J-810 spectropolarimeter). The PsaA samples with the concentration of 0.05 mg/mL in 0.1M PBS were prepared and measured using the quartz cells with 1 mm path length. The instrument parameters were 0.1 nm bandwidth, with a scanning range between 190 to 250 nm at the scanning speed of 50 nm/min, a temperature of 20°C. The baseline was subtracted using the blank solution containing the same buffer.

2.9. Immunizations and preparation of the hyperimmune serum

Female BALB/c mice were injected sub-cutaneously (s.c.) with PBS, mPsaA, mPsaA-Pn14TS or BSA-Pn14TS, (25 µg protein/dose). All mice were administered with 250 ng of α-GalCer as an adjuvant. The mice were immunized on day 0 and boosted at day 21, 90 and 120. The serum was collected on day 28, 98 and 128. To obtain anti-Sp14 Abs, mice were infected (*i.n*.) at day 0 and 15 with *S. pneumoniae* serotype 14 ($1x10^6$ c.f.u.). Two weeks off the last challenge, mice were bled. Sera were stored at -80 °C.

2.10. Measurement of humoral response

The Ab responses induced upon immunisation were assessed one week after the second, the third and the fourth injections by ELISA. mPsaA, mPsaA-Pn14TS, mPsaA-BSA and CP14 (Alliance Bio Expertise), were used as coated antigens to define the anti-mPsaA, anti-Pn14TS, and anti-CP14 Ab titers. mPsaA (0.1 µg/well) or conjugates (0.2 µg/well) in 10mM PBS, pH 7.3 (100 µl/well), were coated on 96 wells microtitre Nunc Maxisorp (ThermoFisher Scientific) plates overnight at 4 °C. CP14 (1 µg/well) was coated for 48h at 4°C in in 10mM PBS, pH 7.3 (100 µg/well). Plates were then washed with PBS 0.05% Tween ® 20 (3×200 µl), saturated using PBS containing 10% skimmed milk at 37°C for 2h, then washed using PBS -Tris-Tween ® 20 (TBST, 50mM Tris, 150mM NaCl, 0,1% Tween 20) (3×200 µl). Series of dilution of sera in PBS containing 10% skimmed milk (100 µl/well), were incubated at 37°C for 2h. Plates were then washed with TBST (3×200 µl) and then incubated with goat anti-mouse IgG(H+L)-horse radish peroxidase-labelled conjugate (CliniSciences) used as secondary Ab at a dilution of 1/6,000, for 1h at 37°C and further washed with TPBS (5×200 µl). The enzyme substrate, o-phenylenediamine dihydrochloride (100 µL at 0.4 mg mL−1) in 0.1 M sodium citrate (pH 5.2), containing 0.02% hydrogen peroxide, was added to each well and the plate incubated for 20

min at RT in the dark. The reaction was terminated by adding 3 M HCl (1000 µL per well), and the A492 was read in an Infinite M1000 spectrophotometer (TECAN). The Ab titer was defined as the dilution of immune serum that gave an OD (405 nm) at least twice that observed with pre-immune serum.

2.11. Statistical analysis

Statistical analysis was done using Graph pad 7. To analyse multiple serum samples, the follow-up study Kruskal-Wallis analysis with Dunn's test was adopted, and the comparison of paired values was performed with the use of the analysis of variance (ANOVA for repeated measures test. Two-tailed p values less than 0.05 were considered significant.

3. Results

3.1. Synthesis of antigen tetrasaccharide

Chemo-enzymatic and chemical synthesis of the pneumococcal serotype 14 tetrasaccharides have been previously reported in the literature. The former relies on the beta-(1-->4)-connection of the galactose residue to the *N*-acetyl-β-D-glucosamine residue by using bovine milk β-1,4-galactosyltransferase [25,26]. Chemical synthesis is based on an obvious [2+2] approach consisting in the glycosylation of lactose donor with a lactosamine acceptor which, in turn, is obtained from a glycosylation between a galactose donor and a glucosamine acceptor [20,27–31]. Our synthetic strategy was inspired mainly by that reported by Deng *et al.* [31] without improved yield but lesser synthetic steps. We elected to carry out the first glycosylation using perbenzoylated trichloracetimidate donor **1** [32] with diol **2** (Scheme 1). Indeed, the full protection of the glucosamine acceptor is not required as the glycosylation is known to take place precisely at the 4-OH position thanks to the steric hindrance generated

by the 2-naphthamido protecting group in derivative **2** [27,33]. Thus, glycosylation of **1** and **2** in the presence of trimethylsilyl trifluoromethanesulfonate (TMSOTf) gave rise to disaccharide **3** in 60% yield, further treated with HF-pyridine complex to remove the silyl protecting group at the 6-OH position of the glucosamine moiety to furnish the disaccharide acceptor **4** in 76% yield. Next, acceptor **4** was glycosylated with imidate **5** used in slight excess using TMSOTf as the promoter to give tetrasaccharide **6** in 55% yield. Exchange of naphthamide to acetamide group was carried out according to Deng et al. procedure [31] to give intermediate **7** which was treated under Zemplén condition to provide target Pn14TS antigen **8** equipped with a 2-azidoethyl spacer arm downstream. Derivative **10** ready for conjugation was finally obtained after azide reduction in **8** to give amine intermediate **9** followed by coupling with a caproyl maleimide functional linker (28% overall yield for 6 steps).

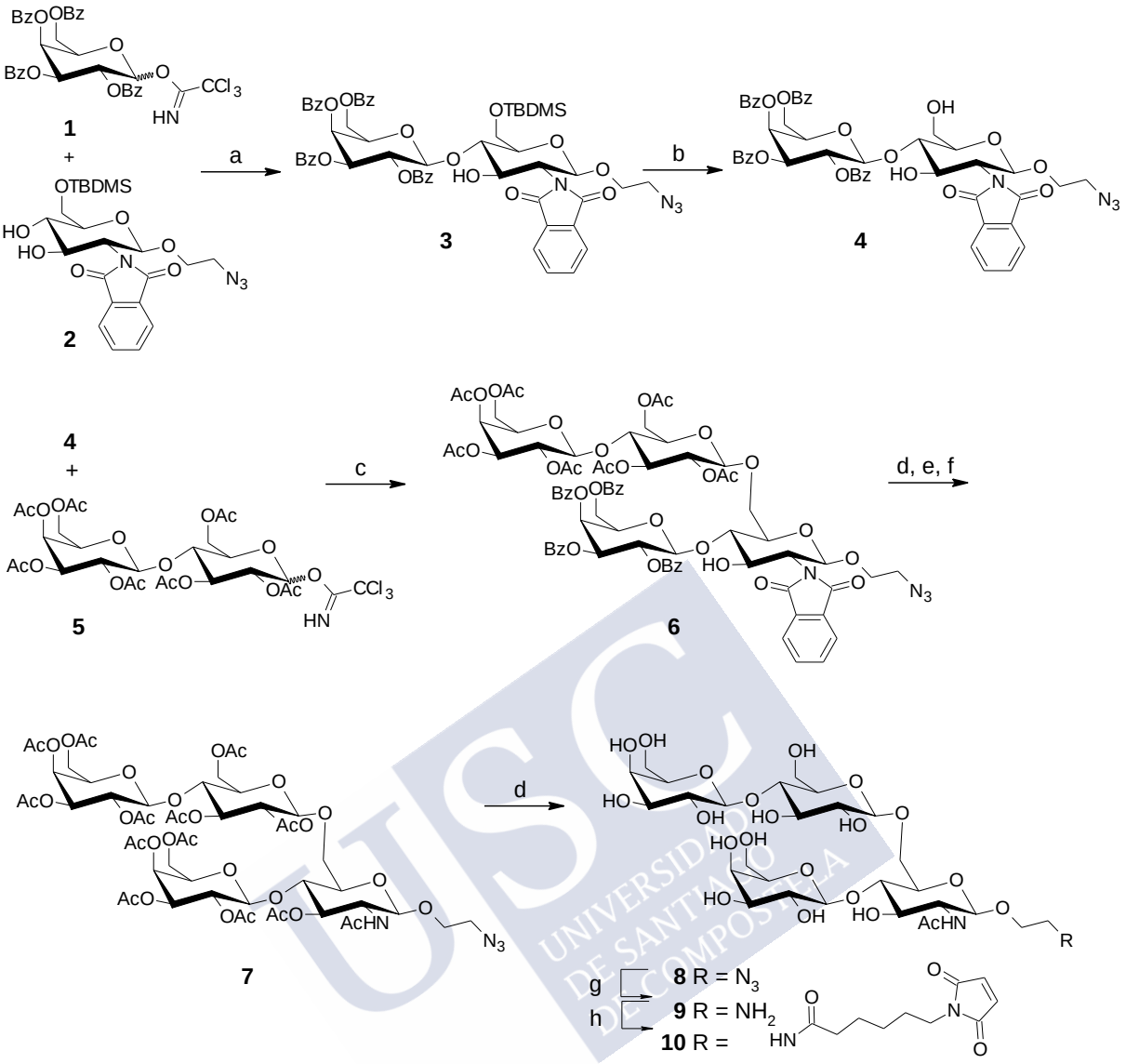

Scheme 1. Synthesis of Pn14TS antigen. *Reagents and conditions:* a, cat TMSOTf , MS4Å, CH_2Cl_2, 0°C, 1h, 60%; b) HF.pyridine, CH_3CN, RT, 30min, 76%; c) cat TMSOTf , MS4Å, CH_2Cl_2, RT, overnight, 55%; d) MeONa, MeOH, RT, 2h; e) H_2N-NH_2, MeOH, RT, 12h; f) Ac_2O, Et_3N, cat DMAP, CH_2Cl_2, 0°C to RT, 12h, 66%; g) $NaBH_4$, cat 10% Pd/C, aqueous NaOH, 30 min, 91%; h) *N*-ε-maleimidocaproyl-oxysuccinimide ester,DIEA, DMSO,30°C, overnight, 46%.

3.2. Expression and purification of mPsaA

PsaA is a 37-kDa protein composed of 309 amino acid residues. The full-length protein possesses a signal peptide at its N-terminus as a transmembrane region. The presence of this leader sequence significantly reduces the expression of the protein [34]. To circumvent this limitation, mature PsaA (mPsaA or $PsaA^{21-309}$), *i.e.*, deprived of the terminal peptide signal was

produced. pET11a plasmid harbouring the *PsaA* gene along with a poly-histidine tag (HHHHHH) and TEV sequence (ENLYFQS) at the N-terminus was constructed and transformed into *E. coli* BL21(DE3) by heat shock method. This extra sequence was introduced to facilitate the purification of the protein, although its expression and purification in the absence of tag have been reported [34] enabling its removal to ensure the absence of interference with the immune response. Interestingly, the TEV protease operates at the Q-S peptide bond leaving in place a serine residue. This serine residue naturally occurs at this position meaning that native mPsaA will be recovered after TEV protease digestion. SDS-PAGE confirmed the expression of the PsaA by visualising the protein band at an expected molecular weight (Fig. 1, Lanes 2). The histidine tag from the HtTEV-mPsaA was cleaved using AcTEV™ protease, and the resultant mPsaA was purified using NiNTA beads to remove the histidine tag. The experimental results obtained from the western blot technique using anti-histidine tag antibodies confirmed the identity and purity of HtTEV-mPsaA and the removal of the poly-histidine tag. The sample corresponding to the unbound fraction of affinity chromatography shows a band appearing slightly below that of HtTEV-mPsaA SDS-PAGE when revealed by Coomassie blue, which is absent in western blot analysis (Fig.1A and B, Lanes 4). A band corresponding to HtTEV protease and a second one corresponding to uncleaved HtTEV-mPsaA with very low intensity - meaning that the cleavage was efficient - are detected in the eluate after purification on NiNTA beads (Fig. 1, Lane 5B). The identity of both forms of PsaA was confirmed by MALDI-TOF mass experiments (Fig. 1 C). The molecular weight of the two proteins differs from 1751 mass unit which corresponds to the tag and the terminal methionine residue. The molecular weight of mPsaA was found equal to 32,395 Da, 1 mass unit superior to the theoretical calculated average mass (32,394 Da).

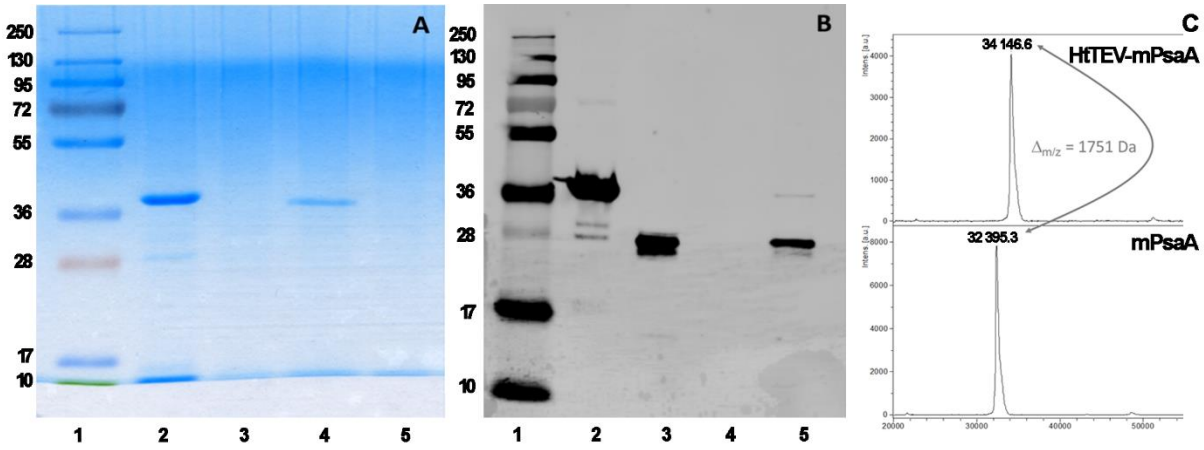

Figure 1: mPsaA characterisation. Analysis of histidine tag removal from HtTEV-mPsaA by SDS-PAGE (A) and by Western blot (B)**.** Lane 1: unstained protein marker; Lane 2: HtTEV-mPsaA; Lane 3: AcTEV™ protease used for the cleavage; Lane 4: purified mPsaA after removal of poly-histidine tag; Lane 5: eluate after purification of mPsaA protein on NiNTA beads; MALDI-TOF-MS spectra of PsaA before and after histidine tag removal (C)

3.3. Preparation and identification of PsaA-Pn14TS and BSA-Pn14TS conjugates

The mPsaA was conjugated to Pn14TS by thiol/maleimide coupling chemistry (Scheme 2). To this aim, free amine functional groups of the surface exposed lysines of this protein was derivatised by treatment with excess (120 molar ratio) of SATA-NHS reagent. The excess of the unreacted reagent was removed by dialysis.

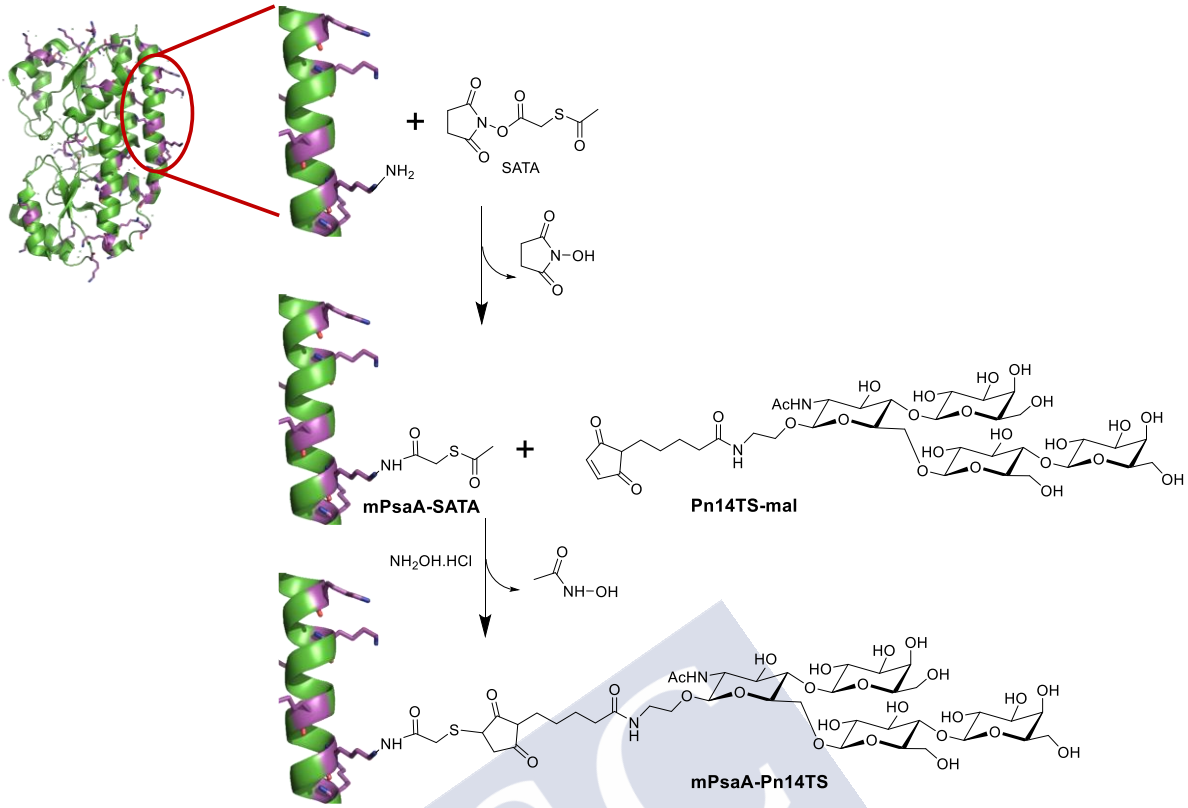

Scheme 2: Schematic representation of the basic conjugation strategy used to couple Pn14TS to mPsaA. (mPsaA structure PDB 3ZK9 is from Counago *et al*., 2014 and was drawn in PyMol)

Subsequently, the modified carrier was conjugated to Pn14TS-mal in a 1:16 molar ratio in the presence of excess hydroxylamine hydrochloride to generate *in situ* thiol-reactive groups. The resultant PsaA-Pn14TS conjugate was purified by gel filtration (Figure 2A), lyophilised and stored at -80°C. Similarly, a control BSA-Pn14TS conjugate was prepared to evaluate the importance of PsaA as a carrier moiety. SDS-PAGE of the conjugates and synthetic intermediates thereof was consistent with increasing molecular weight at every incremental step of the process (Figure 2B).

The analysis of chemical composition of the glycoconjugates by the phenol-sulphuric method and Bradford assay revealed that the sugar/protein molar ratios of the two conjugates were both equal to 5.4/1.

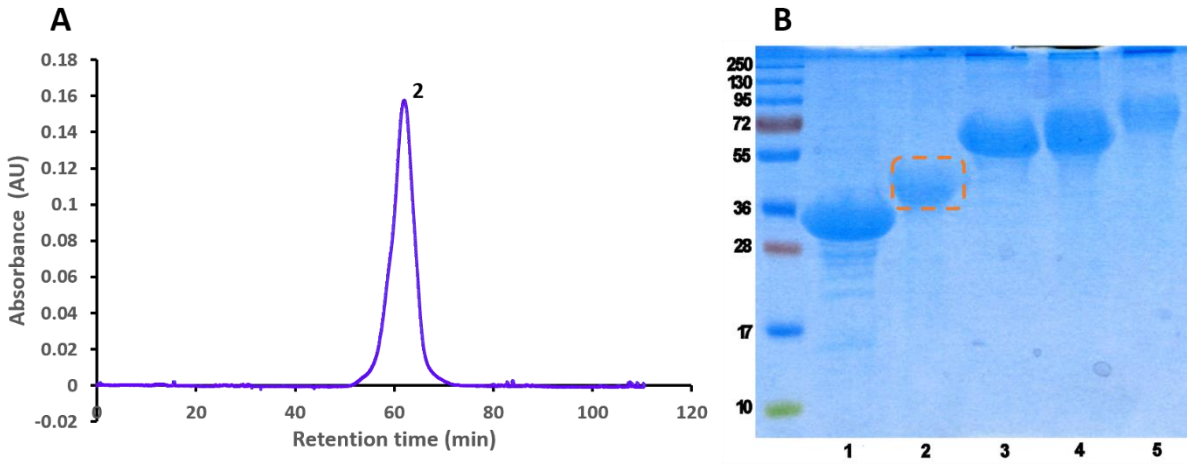

Figure 2. (A) Size exclusion chromatography profile of mPsaA-Pn14TS conjugate; (B) 12% SDS-PAGE; Lane 1: mPsaA; Lane 2: mPsaA-Pn14TS; Lane 3: BSA; Lane 4: BSA-SATA; Lane 5: BSA-Pn14TS. Column HiLoad 15/600 Superdex™ 75pg (GE Healthcare) column and PBS 0.1M, pH7.3 as eluent.

The CD analysis of mPsaA-Pn14TS conjugate and the intermediates in comparison to the mPsaA revealed that there is no change in the secondary structure of the protein. The PsaA exhibited negative peaks at 208 nm and 222 nm in all the stages of conjugation and lyophilisation, which is indicative of similar protein folding and possess a significant number of alpha helixes, beta sheets in agreement with the determined mPsaA structure [35]. The similar folding pattern observed after the superimposition of the CD spectra of HtTEV-PsaA, mPsaA and mPsaA-Pn14TS confirms the stability in the protein during the process of conjugation (Figure 3). The conservation of mPsaA and mPsaA-Pn14TS was done by storing them at -80 °C after lyophilisation or in 40% glycerol and both cases the mPsaA has maintained its secondary structure even after a 12-month storage at -80 °C (data not shown).

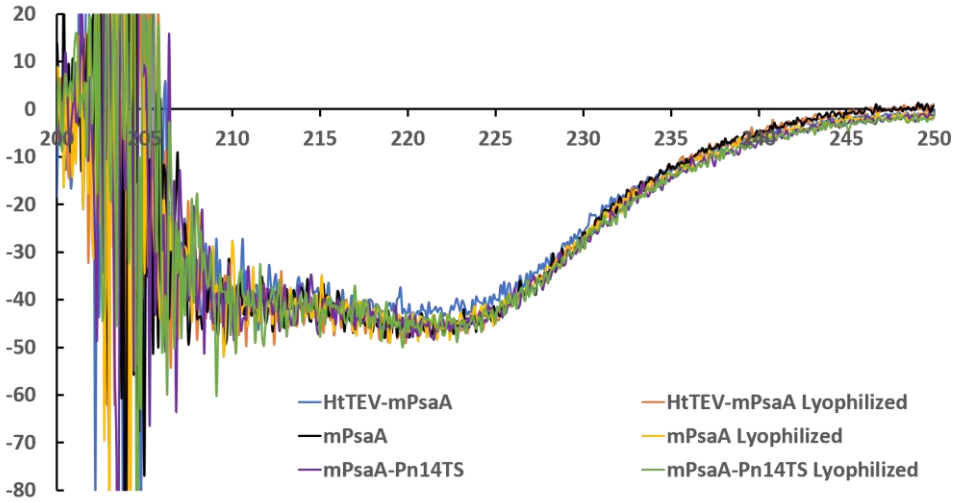

Figure 3: The overlay of the CD spectra of the protein at the different stages of purification, conjugation and lyophilisation

3.4. Immunization of mice and antibody response

The immunisation efficiency of the different formulations was evaluated by the determination of the humoral IgG response in the mice antisera immunised subcutaneously with mPsaA, mPsaA-Pn14TS, BSA-Pn14TS, and PBS four times at 25 µg of protein/dose.

3.4.1. Anti-mPsaA response

The titers of anti-mPsaA IgG were first measured using mPsaA as a coating antigen (Figure 4A). Both mPsaA and mPsaA-Pn14TS conjugates were able to induce anti-mPsaA IgGs while such response was not observed for either BSA conjugate or PBS control. High level of Abs was detected after the second immunisation (Day 28, blue bars) and maintained after the boosts in the groups immunised with mPsaA. Anti-mPsaA Abs were also raised in the sera of mice immunised with mPsaA-Pn14TS albeit at a much lower extent and wider variability with no boost effect (green bars Day 28 *vs* Day 98 *vs* Day 128). Comparison of these observations suggests that mPsaA derivatisation followed by conjugation to Pn14TS antigen might have hampered accessibility of mPsaA B epitopes to the immune system (blue *vs* green bars in fig.

4A). However, this hypothesis was not confirmed when sera of mice immunized with mPsaA alone were tested against mPsaA-Pn14TS conjugate coated on the microtiter plate (Figure 4B, blue bars). Indeed, the level of Ab titers was comparable to that observed when mPsaA was the coated antigen (1/1000 -1/10,000; compare blue bars in Figure 4A and 4B). Moreover, the Abs seemed to be mPsaA specific as no titer (<1/100) could be measured when assessed against BSA-Pn14TS as the coated antigen (Figure 4C, blue bars). Taken together, these results are in favour of a competition between the mPsaA B epitopes and the antigenic determinants expressed by Pn14TS rather than epitope masking to explain the observed difference in anti-mPsaA response whether mPsaA or mPsaA-Pn14TS was the immunogen.

3.4.2. Anti-carbohydrate response

We next turned our attention to the anti-carbohydrate response first focusing on the anti-synthetic tetrasaccharide IgG response. The BSA conjugate was used as the coated antigen to reveal the anti-Pn14TS IgG raised in mice immunized with the corresponding mPsaA-Pn14TS conjugate (Figure 4C). Anti-Pn14TS IgG response was present at Day 28 (Figure 4C, green bar) and consistently increased after the first (Day 98) and the second boost (Day 128 $P<0.01$). Conversely, mPsaA-Pn14TS conjugate was used as the coated antigen to measure the anti-Pn14TS response raised by the BSA conjugate and the global anti-IgG directed against both tetrasaccharide and protein valences in mice immunized with mPsaA-Pn14TS (Figure 4B). A 10^3-10^4 anti-Pn14TS IgG titer range was measured only after the fourth immunization in mice immunized with the BSA conjugate (orange bars Day 28 and Day 98 *vs* Day 198). Besides, a significant ($P<0.05$) global anti-IgG titer was measured after booster dose, in the immune sera of mice administered with the mPsaA-Pn14TS conjugate (Day 98 and Day 128, green bars).

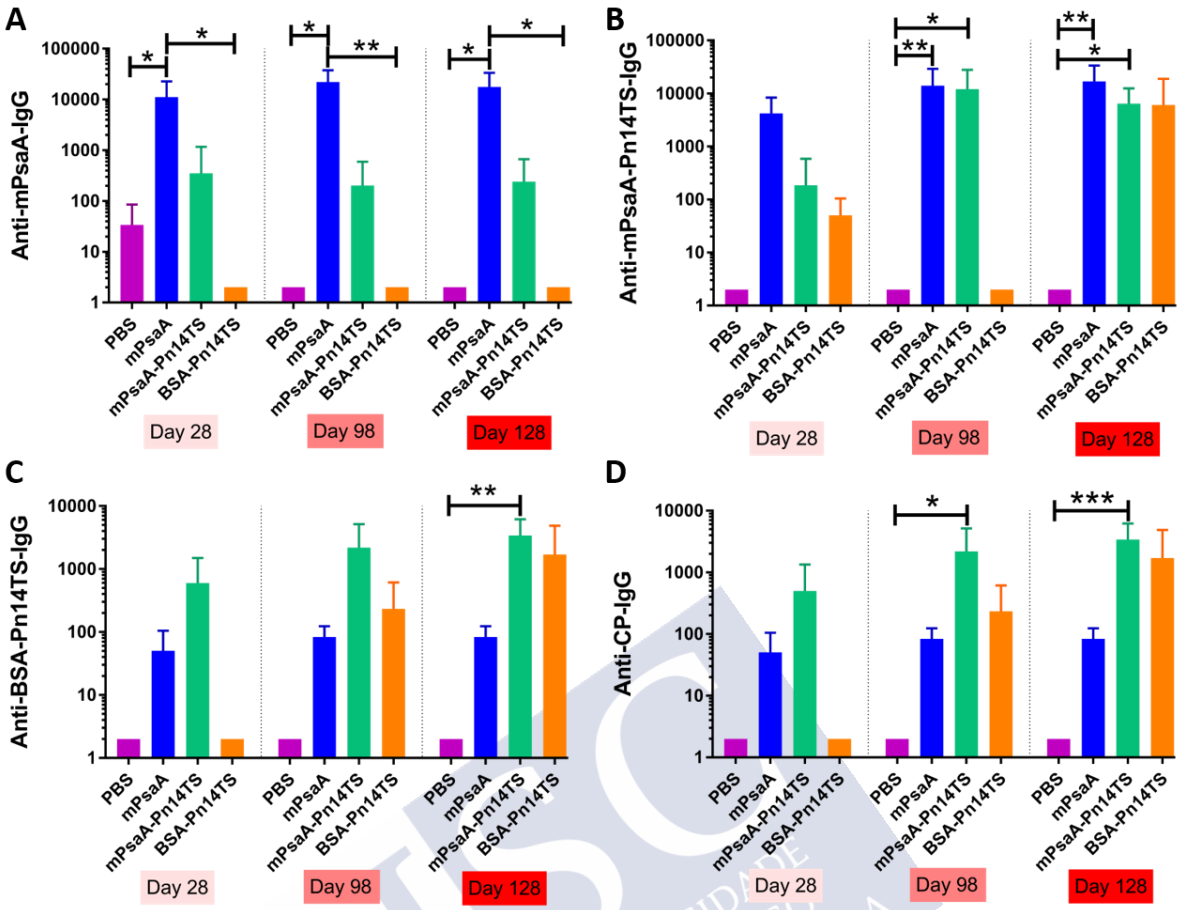

Figure 4. Titers of IgG Abs of mice immunised with PBS, mPsaA, mPsaA-Pn14TS conjugate, BSA-Pn14TS-conjugate, and Sp14 one week after the 2nd (J28), the 3rd (J98) and the 4th (J128) immunisation. (A) Against mPsaA (coated on a microtiter plate); (B) against mPsaA-Pn14TS; (C) against BSA-Pn14TS; (D) against *S. pneumoniae* serotype 14 capsular polysaccharide (CP). The serum samples data presented as geometric mean titer ± standard deviation of six mice per group. Statistical analysis was performed using one-way ANOVA with Kruskal-Wallis analysis for multiple comparisons. Statistical difference between the groups is *, $p < 0.05$; **, $p < 0.01$; ***, $p < 0.001$.

To investigate whether the conjugates were able to induce the production of anti-CP Abs, CP from serotype 14 was coated on ELISA microtiter plates (Figure 4D). As expected, no anti-CP Abs could be measured in the sera of mice immunized with PBS or mPsaA. The anti-CP response induced by the mPsaA-Pn14TS conjugate was significant after the first ($P<0.05$) and the second boost ($P<0.001$) (Figure 4D, green bars at Day 28 and Day 128). 4 out of 6 mice immunised with the mPsaA-Pn14TS conjugate raised anti-CP-titers superior or equal to 1/1000 after the first boost and 5 out of 6 after the second one. Anti-CP titers were also

measured in mice sera immunised with BSA-Pn14TS, but these titers were less consistent and accompanied by high variability from one mouse to another (Figure 4D, orange bar Day128). Mice immunised with the BSA-Pn14TS were administered twice as less carbohydrate antigen than those immunised with mPsaA-Pn14TS (1.5 *vs* 3.1 µg/dose, respectively) to keep the amount of protein dose equal. This might explain the apparent discrepancy between the immunogenicity of the two conjugates. To summarise, these results confirm that Pn14TS can be considered as an immune mimic of the *S. pneumoniae* serotype 14 CP (Safari *et al*., 2008; Kurbatova *et al*., 2017).

4. Discussion

The advent of glycoconjugate vaccines has been a breakthrough for the prophylactic treatment of infectious diseases caused by encapsulated bacteria including *S. pneumoniae* [36]. The pneumococcal glycoconjugate vaccine is safe and effective but faces serotype replacement phenomenon: Initially composed of 7 polysaccharides corresponding to 7 different serotypes, it has been implemented to protect against 13 pneumococcal and soon 15 serotypes. These have been selected by geographic prevalence and virulence but still, vaccination results in colonisation by non-vaccine serotypes. While it is envisaged to increase the CP valency of the vaccine further – *e.g.*, the licensed pneumococcal polysaccharide vaccine comprises 23 serotypes – to circumvent this drawback, researchers have moved on to the identification of novel surface exposed or secreted pneumococcal antigens [37]. On these lines, much attention has been paid to the identification of proteins which are i) targets of antibodies in the field, ii) highly conserved across the serotypes, iii) shared by all pneumococcal strains and iv) involved in virulence and colonisation, thereby limiting possible by-pass by the pathogen to provide novel vaccine formulations with broad coverage. Hence,

among others, pneumolysin, pneumococcal histidine triad protein D or pneumococcal surface protein A (PspA) is now under clinical investigation. However, to maximise the efficacy, such formulations will undoubtedly be composed not of one but several antigens. This has been suggested to be crucial for vaccines that aim to generate broad mucosal protection against this highly heterogeneous pathogen [38]. We believe that these novel vaccine targets would advantageously be combined with the current, effective glycoconjugate vaccines. They can be added merely as extra components or used as carriers [16,18,39–43]. It has even been shown for PspA that its conjugation to CP 23F induced higher survival than PspA alone in an infection challenge providing the basis for, at least, an additive if not a synergistic protective effect [40]. Herein, we have elected to investigate PsaA in a dual role of immunogen and carrier. The role of PsaA in inducing protective immunity against systemic infection or once bacteria have colonised the lungs has been controversial [12,13,44] but its beneficial role in reducing colonization cannot be disputed noticeably when co-administered with PCV7 [12,18,45]. Besides, PsaA had already been used as a carrier for purified bacterial polysaccharide to prepare pneumococcal [16] and even hybrid Hib/pneumococcus [17] glycoconjugate vaccines. However, its use to access to semi-synthetic glycoconjugate vaccines which have recently appeared as a credible alternative to traditional glycoconjugates [46] remained uninvestigated before this study. Production and characterisation of conjugate whereby mPsaA is conjugated to a synthetic CP serotype 14 mimicking tetrasaccharide Pn14TS was the first objective of the study. Recombinant native mPsaA has thus been produced in high yield and purify using NiNTA affinity column followed by complete histidine tag removal, aware that an optimised production process, in the absence of a tag, has been developed for possible scale-up [34]. Most importantly, conjugation and further purification steps, as well as long-term storage, did not alter the secondary structure of mPsaA monitored

by circular dichroism analysis suggesting that potential conformational B-epitopes are conserved.

The immunization efficiency of the conjugate mPsaA-Pn14TS adjuvanted with α-GalCer was next examined in mice in comparison with mPsaA and a model conjugate BSA-Pn14TS. The conjugate elicited anti-mPsaA antibodies but at a lesser extent than unconjugated mPsaA. This situation is not found for the reported glycoconjugates which make use of either PsaA [16] or PspA [40,41] as carrier proteins which, differ by the nature of the conjugated antigens (polysaccharide *vs* tetrasaccharide). Since mice sera raised against mPsaA bind to mPsaA-Pn14TS when coated on the microtiter plates at a high level, these observations are more likely due to B epitope competition than to masking of the mPsaA B epitope by Pn14TS after conjugation. In summary, these observations suggest that the mode of presentation of PsaA to the immune system as well as its chemical-physical structure might strongly influence the fate of the immune response. This indicates that special care should be given to the design of future mPsaA-based glycoconjugates.

On the other hand, both mPsaA-based and BSA-based conjugates elicited anti-CP14 antibodies mainly after the 2nd boost for BSA-Pn14TS. However, these data cannot be compared as the mice were immunized with a distinct amount of tetrasaccharide whether they received the mPsaA (3.1 µg/dose) or the BSA (1.5 µg/dose) conjugates to keep the amount of administered protein constant. Dose and sugar to protein ratio effects were beyond the scope of the study, which is focused on the design of a mPsaA conjugate prototype. Titers were nevertheless in the same range (1:1000 to 1:8000) to those observed for reported Pn14TS conjugates using carriers whose use is approved in humans such as CRM_{197} which, noticeably, is present in commercial PCV7 and PCV13 [20] or BSA [21].

5. Conclusion

In summary, the first semi-synthetic glycoconjugate vaccine solely composed of pneumococcal antigens, *i.e*., of a synthetic tetrasaccharide mimicking the capsule of serotype 14 coupled to PsaA has been reported. The latter has been selected as it should contribute to control pneumococcal colonisation and ensure herd immunity. The conjugate has been prepared in high yield and purity and proved to be stable during long-term storage. The conjugate was able to induce the production of IgGs against both synthetic oligosaccharide and protein moieties. This study suggests further modifications in term of glycoconjugate design (*e.g.* using tyrosine-directed conjugation for finely tuning the anti-mPsaA/anti-tetrasaccharide humoral response) [47] and route of administration (*i.e.* mucosal for an optimal adjuvantation of □-GalCer) [48] for its future improvement.

Mucosal surfaces are the common entry points for the Streptococcus pneumoniae. Therefore, the change of the administration route from parenteral Immunization to a mucosal route is expected to enhance the production of mucosal IgA antibodies. This may significantly contribute to protection against mucosal infections by acting as the first line of defence. Combination of T-cell dependent immunogenicity of glycoconjugate vaccines with mucosal immunization could be an attractive strategy for preventing pneumococcal infections.

6. Acknowledgements

Maruthi Prasanna acknowledges his doctoral fellowship from the European Commission, Education, Audiovisual and Culture Executive Agency (EACEA), under the Erasmus Mundus programme, “NanoFar: European Doctorate in Nanomedicine and Pharmaceutical Innovation” (Project: 2015-01-C4). We would like to thank Dr. B. Frisch (University of Strasbourg) for the production of α-GalCer.

REFERENCES

[1] R. Wilson, J.M. Cohen, R.J. Jose, C. de Vogel, H. Baxendale, J.S. Brown, Protection against Streptococcus pneumoniae lung infection after nasopharyngeal colonization requires both humoral and cellular immune responses, Mucosal Immunol. 8 (2015) 627–639. doi:10.1038/mi.2014.95.

[2] C. Hyams, J. Yuste, K. Bax, E. Camberlein, J.N. Weiser, J.S. Brown, Streptococcus pneumoniae resistance to complement-mediated immunity is dependent on the capsular serotype., Infect. Immun. 78 (2010) 716–25. doi:10.1128/IAI.01056-09.

[3] C.C. Daniels, P.D. Rogers, C.M. Shelton, A Review of Pneumococcal Vaccines: Current Polysaccharide Vaccine Recommendations and Future Protein Antigens, J. Pediatr. Pharmacol. Ther. 21 (2016) 27–35. doi:10.5863/1551-6776-21.1.27.

[4] H. Jakobsen, I. Jonsdottir, Mucosal vaccination against encapsulated respiratory bacteria - New potentials for conjugate vaccines?, Scand. J. Immunol. 58 (2003) 119–128. doi:10.1046/j.1365-3083.2003.01292.x.

[5] H. Jakobsen, S. Hannesdottir, S.P. Bjarnarson, D. Schulz, E. Trannoy, C.A. Siegrist, I. Jonsdottir, Early life T Cell responses to pneumucoccal conjugates increase with age and determine the polysaccharide-specific antibody response and protective efficacy, Eur. J. Immunol. 36 (2006) 287–295. doi:10.1002/eji.200535102.

[6] Z. Lai, J.R. Schreiber, Antigen processing of glycoconjugate vaccines; the polysaccharide portion of the pneumococcal CRM197 conjugate vaccine co-localizes with MHC II on the antigen processing cell surface, Vaccine. 27 (2009) 3137–3144. doi:10.1016/j.vaccine.2009.03.064.

[7] C. Entwisle, A. Mcilgorm, W. Chan, J.S. Brown, C.A. Colaco, C.R. Bailey, S.W. Clarke, Next Generation Vaccines: Development of a Novel Streptococcus pneumoniae Multivalent Protein Vaccine, (2017). doi:10.12665/J143.Colaco.

[8] N. Li, X.Y. Yang, Z. Guo, J. Zhang, K. Cao, J. Han, G. Zhang, L. Liu, X. Sun, Q.Y. He, Varied metal-binding properties of lipoprotein PsaA in Streptococcus pneumoniae, J. Biol. Inorg. Chem. 19 (2014) 829–838. doi:10.1007/s00775-014-1114-9.

[9] G. Rajam, D.J. Phillips, E. White, J. Anderton, C.W. Hooper, J.S. Sampson, G.M. Carlone, E.W. Ades, S. Romero-Steiner, A functional epitope of the pneumococcal surface adhesin A activates nasopharyngeal cells and increases bacterial internalization, Microb. Pathog. 44 (2008) 186–196. doi:10.1016/j.micpath.2007.09.003.

[10] K.E. Morrison, D. Lake, J. Crook, G.M. Carlone, E. Ades, R. Facklam, J.S. Sampson, Confirmation of psaA in all 90 serotypes of Streptococcus pneumoniae by PCR and potential of this assay for identification and diagnosis, J. Clin. Microbiol. 38 (2000) 434–437.

[11] S. Rapola, V. Jäntti, R. Haikala, R. Syrjänen, G.M. Carlone, J.S. Sampson, D.E. Briles, J.C. Paton, A.K. Takala, T.M. Kilpi, H. Käyhty, Natural Development of Antibodies to Pneumococcal Surface Protein A, Pneumococcal Surface Adhesin A, and Pneumolysin in Relation to Pneumococcal Carriage and Acute Otitis Media, J. Infect. Dis. 182 (2000) 1146–1152. doi:10.1086/315822.

[12] S. Wang, Y. Li, H. Shi, G. Scarpellini, A. Torres-Escobar, K.L. Roland, R. Curtiss, Immune responses to recombinant pneumococcal PsaA antigen delivered by a live attenuated

Salmonella vaccine, Infect. Immun. 78 (2010) 3258–3271. doi:10.1128/IAI.00176-10.

[13] D.O. Gor, X. Ding, Q. Li, D. Sultana, S.S. Mambula, R.J. Bram, N.S. Greenspan, Enhanced immunogenicity of pneumococcal surface adhesin A (PsaA) in mice via fusion to recombinant human B lymphocyte stimulator (BLyS), Biol. Direct. 6 (2011) 9. doi:10.1186/1745-6150-6-9.

[14] J. Lu, T. Sun, D. Wang, Y. Dong, M. Xu, H. Hou, F.T. Kong, C. Liang, T. Gu, P. Chen, S. Sun, X. Lv, C. Jiang, W. Kong, Y. Wu, Protective Immune Responses Elicited by Fusion Protein Containing PsaA and PspA Fragments, Immunol. Invest. 44 (2015) 482–496. doi:10.3109/08820139.2015.1037956.

[15] T.A. Olafsdottir, K. Lingnau, E. Nagy, I. Jonsdottir, Novel protein-based pneumococcal vaccines administered with the Th1-promoting adjuvant IC31 induce protective immunity against pneumococcal disease in neonatal mice, Infect. Immun. 80 (2012) 461–468. doi:10.1128/IAI.05801-11.

[16] H. Lin, Z. Lin, C. Meng, J. Huang, Y. Guo, Preparation and immunogenicity of capsular polysaccharide-surface adhesin A (PsaA) conjugate of Streptococcus pneumoniae, Immunobiology. 215 (2010) 545–550. doi:10.1016/j.imbio.2009.08.008.

[17] Z. Chen, Immunogenicity and protective immunity against otitis media caused by pneumococcus in mice of Hib conjugate vaccine with PsaA protein carrier, 10 (2016) 490–498. doi:10.1007/s11684-016-0470-y.

[18] M.J. Whaley, J.S. Sampson, S.E. Johnson, G. Rajam, A. Stinson-Parks, P. Holder, E. Mauro, S. Romero-Steiner, G.M. Carlone, E.W. Ades, Concomitant administration of recombinant PsaA and PCV7 reduces Streptococcus pneumoniae serotype 19A colonization in a murine model, Vaccine. 28 (2010) 3071–3075. doi:10.1016/j.vaccine.2010.02.086.

[19] C.A. Laferriere, R.K. Sood, J.D.E. Muys, F. Michon, H.J. Jennings, Streptococcus pneumoniae Type 14 Polysaccharide-Conjugate Vaccines : Length Stabilization of Opsonophagocytic Conformational Polysaccharide Epitopes †, 66 (1998) 2441–2446.

[20] D. Safari, H.A.T. Dekker, J.A.F. Joosten, D. Michalik, A.C. De Souza, R. Adamo, M. Lahmann, A. Sundgren, S. Oscarson, J.P. Kamerling, H. Snippe, Identification of the Smallest Structure Capable of Evoking Opsonophagocytic Antibodies against Streptococcus pneumoniae Type 14 , 76 (2008) 4615–4623. doi:10.1128/IAI.00472-08.

[21] E.A. Kurbatova, N.K. Akhmatova, E.A. Akhmatova, N.B. Egorova, N.E. Yastrebova, E. V. Sukhova, D. V. Yashunsky, Y.E. Tsvetkov, M.L. Gening, N.E. Nifantiev, Neoglycoconjugate of Tetrasaccharide Representing One Repeating Unit of the Streptococcus pneumoniae Type 14 Capsular Polysaccharide Induces the Production of Opsonizing IgG1 Antibodies and Possesses the Highest Protective Activity As Compared to Hexa- an, Front. Immunol. 8 (2017) 1–13. doi:10.3389/fimmu.2017.00659.

[22] C. Paget, F. Trottein, Role of type 1 natural killer T cells in pulmonary immunity, Mucosal Immunol. 6 (2013) 1054–1067. doi:10.1038/mi.2013.59.

[23] A. Bendelac, P.B. Savage, L. Teyton, The Biology of NKT Cells, Annu. Rev. Immunol. 25 (2007) 297–336. doi:10.1146/annurev.immunol.25.022106.141711.

[24] D. Herbert, P.J. Phipps, R.E. Strange, Chapter III Chemical Analysis of Microbial Cells, Methods Microbiol. 5 (1971) 209–344. doi:10.1016/S0580-9517(08)70641-X.

[25] J. Niggemann, J.P. Kamerling, J.F.G. Vliegenthart, β-1,4-Galactosyltransferase-catalyzed Synthesis of the Branched Tetrasaccharide Repeating Unit of Streptococcus pneumoniae Type 14, Bioorg. Med. Chem. 6 (1998) 1605–1612. doi:10.1016/S0968-0896(98)00095-9.

[26] J.A.F. Joosten, B.J. Lazet, J.P. Kamerling, J.F.G. Vliegenthart, fragments of the capsular polysaccharide of Streptococcus pneumoniae type 14, 338 (2003) 2629–2651. doi:10.1016/S0008-6215(03)00292-1.

[27] Y.-X. Chen, W. Zhao, L. Zhao, Y.-F. Zhao, Y.-M. Li, Facile synthesis of a pentasaccharide mimic of a fragment of the capsular polysaccharide of Streptococcus pneumoniae type 15C, Carbohydr. Res. 343 (2008) 607–614. doi:10.1016/J.CARRES.2007.12.002.

[28] W. Zou, H.J. Jennings, Mimics of the structural elements of type III group B Streptococcus capsular polysaccharide. Part III: two repeating units (octasaccharide) with (S)-1-carboxyethyl groups replacing sialic acids, Bioorg. Med. Chem. Lett. 7 (1997) 647–650. doi:10.1016/S0960-894X(97)00077-2.

[29] A. Demchenko, G.-J. Boons, A highly convergent synthesis of a hexasaccharide derived from the oligosaccharide of group B type III Streptococcus, Tetrahedron Lett. 38 (1997) 1629–1632. doi:10.1016/S0040-4039(97)00106-8.

[30] P. Pornsuriyasak, N.P. Rath, A. V. Demchenko, 4-(Pyridin-2-yl)thiazol-2-yl thioglycosides as bidentate ligands for oligosaccharide synthesis via temporary deactivation, Chem. Commun. 0 (2008) 5633. doi:10.1039/b810569c.

[31] S. Deng, L. Bai, R. Reboulet, R. Matthew, D.A. Engler, L. Teyton, A. Bendelac, P.B. Savage, A peptide-free, liposome-based oligosaccharide vaccine, adjuvanted with a natural killer T cell antigen, generates robust antibody responses in vivo., Chem. Sci. 5 (2014) 1437–1441. doi:10.1039/C3SC53471E.

[32] S. Rio, J.-M. Beau, J.-C. Jacquinet, Synthesis of glycopeptides from the carbohydrate-protein linkage region of proteoglycans, Carbohydr. Res. 219 (1991) 71–90. doi:10.1016/0008-6215(91)89043-F.

[33] J. Dion, F. Deshayes, N. Storozhylova, T. Advedissian, A. Lambert, M. Viguier, C. Tellier, C. Dussouy, F. Poirier, C. Grandjean, Lactosamine-Based Derivatives as Tools to Delineate the Biological Functions of Galectins: Application to Skin Tissue Repair, ChemBioChem. 18 (2017) 782–789. doi:10.1002/cbic.201600673.

[34] A.L. Larentis, A.P.C. Argondizzo, G.D.S. Esteves, E. Jessouron, R. Galler, M.A. Medeiros, Cloning and optimization of induction conditions for mature PsaA (pneumococcal surface adhesin A) expression in Escherichia coli and recombinant protein stability during long-term storage, Protein Expr. Purif. 78 (2011) 38–47. doi:10.1016/j.pep.2011.02.013.

[35] R.M. Couñago, M.P. Ween, S.L. Begg, M. Bajaj, J. Zuegg, M.L. O'Mara, M.A. Cooper, A.G. McEwan, J.C. Paton, B. Kobe, C.A. McDevitt, Imperfect coordination chemistry facilitates metal ion release in the Psa permease, Nat. Chem. Biol. 10 (2014) 35–41. doi:10.1038/nchembio.1382.

[36] P. Costantino, R. Rappuoli, F. Berti, The design of semi-synthetic and synthetic glycoconjugate vaccines, Expert Opin. Drug Discov. 6 (2011) 1045–1066. doi:10.1517/17460441.2011.609554.

[37] C. Feldman, R. Anderson, Review: Current and new generation pneumococcal vaccines, J. Infect. 69 (2014) 309–325. doi:10.1016/J.JINF.2014.06.006.

[38] A.M. Roche, J.N. Weiser, Identification of the targets of cross-reactive antibodies induced by Streptococcus pneumoniae colonization., Infect. Immun. 78 (2010) 2231–9. doi:10.1128/IAI.01058-09.

[39] K. Pauksens, A.C. Nilsson, M. Caubet, T.G. Pascal, P. Van Belle, J.T. Poolman, P.G.

Vandepapelière, V. Verlant, P.E. Vink, Randomized controlled study of the safety and immunogenicity of pneumococcal vaccine formulations containing PhtD and detoxified pneumolysin with alum or adjuvant system AS02V in elderly adults., Clin. Vaccine Immunol. 21 (2014) 651–60. doi:10.1128/CVI.00807-13.

[40] F.C.L. Csordas, C.T. Perciani, M. Darrieux, V.M. Gonçalves, J. Cabrera-Crespo, M. Takagi, M.E. Sbrogio-Almeida, L.C.C. Leite, M.M. Tanizaki, Protection induced by pneumococcal surface protein A (PspA) is enhanced by conjugation to a Streptococcus pneumoniae capsular polysaccharide, Vaccine. 26 (2008) 2925–2929. doi:10.1016/j.vaccine.2008.03.038.

[41] R. Santamaria, C. Goulart, C.T. Perciani, G.C. Barazzone, R.J. Carvalho, V.M. Gonçalves, L.C.C. Leite, M.M. Tanizaki, Humoral immune response of a pneumococcal conjugate vaccine: Capsular polysaccharide serotype 14—Lysine modified PspA, Vaccine. 29 (2011) 8689–8695. doi:10.1016/J.VACCINE.2011.08.109.

[42] C.T. Perciani, G.C. Barazzone, C. Goulart, E. Carvalho, J. Cabrera-Crespo, V.M. Gonçalves, L.C.C. Leite, M.M. Tanizaki, Conjugation of polysaccharide 6B from Streptococcus pneumoniae with pneumococcal surface protein A: PspA conformation and its effect on the immune response., Clin. Vaccine Immunol. 20 (2013) 858–66. doi:10.1128/CVI.00754-12.

[43] M.A. da Silva, T.R. Converso, V.M. Gonçalves, L.C.C. Leite, M.M. Tanizaki, G.C. Barazzone, Conjugation of PspA4Pro with Capsular Streptococcus pneumoniae Polysaccharide Serotype 14 Does Not Reduce the Induction of Cross-Reactive Antibodies., Clin. Vaccine Immunol. 24 (2017) e00118-17. doi:10.1128/CVI.00118-17.

[44] A. David Ogunniyi, R.L. Folland, D.E. Briles, S.K. Hollingshead, J.C. Paton, N. Adelaide, Immunization of Mice with Combinations of Pneumococcal Virulence Proteins Elicits Enhanced Protection against Challenge with Streptococcus pneumoniae, 2000. http://iai.asm.org/ (accessed September 14, 2018).

[45] Q. Zhang, S. Choo, A. Finn, Immune Responses to Novel Pneumococcal Proteins Pneumolysin, PspA, PsaA, and CbpA in Adenoidal B Cells from Children, Infect. Immun. 70 (2002) 5363–5369. doi:10.1128/IAI.70.10.5363-5369.2002.

[46] V. Verez-Bencomo, V. Fernández-Santana, E. Hardy, M.E. Toledo, M.C. Rodríguez, L. Heynngnezz, A. Rodriguez, A. Baly, L. Herrera, M. Izquierdo, A. Villar, Y. Valdés, K. Cosme, M.L. Deler, M. Montane, E. Garcia, A. Ramos, A. Aguilar, E. Medina, G. Toraño, I. Sosa, I. Hernandez, R. Martínez, A. Muzachio, A. Carmenates, L. Costa, F. Cardoso, C. Campa, M. Diaz, R. Roy, A synthetic conjugate polysaccharide vaccine against Haemophilus influenzae type b., Science. 305 (2004) 522–5. doi:10.1126/science.1095209.

[47] A. Nilo, L. Morelli, I. Passalacqua, B. Brogioni, M. Allan, F. Carboni, A. Pezzicoli, F. Zerbini, D. Maione, M. Fabbrini, M.R. Romano, Q.-Y. Hu, I. Margarit, F. Berti, R. Adamo, Anti-Group B Streptococcus Glycan-Conjugate Vaccines Using Pilus Protein GBS80 As Carrier and Antigen: Comparing Lysine and Tyrosine-directed Conjugation, ACS Chem. Biol. 10 (2015) 1737–1746. doi:10.1021/acschembio.5b00247.

[48] A.N. Courtney, P. Thapa, S. Singh, A.M. Wishahy, D. Zhou, J. Sastry, Intranasal but not intravenous delivery of the adjuvant α-galactosylceramide permits repeated stimulation of natural killer T cells in the lung, Eur. J. Immunol. 41 (2011) 3312–3322. doi:10.1002/eji.201041359.

USC
UNIVERSIDADE
DE SANTIAGO
DE COMPOSTELA

Chapter 2

Chitosan nanoparticles as carriers for the delivery of semisynthetic glycoconjugate antigen

This work was done in collaboration with Center for Infection and Immunity of Lille, Institut Pasteur de Lille (France).

USC
UNIVERSIDADE
DE SANTIAGO
DE COMPOSTELA

Chitosan nanoparticles as carriers for the delivery of a semisynthetic glycoconjugate antigen

Abstract

Subunit vaccines are the promising candidates for immunization against infectious diseases. However, the development of effective subunit vaccines formulation requires a combination of potent adjuvants, a suitable delivery system and an efficient route of delivery. In this chapter, we prepared semisynthetic glycoconjugate (GC) loaded chitosan nanoparticles to enhance the immune response generated against the glycoconjugate. The glycoconjugate was encapsulated into the chitosan nanoparticles (GC-CNPs) by simple ionic gelation method and the resultant nanoparticles had the size of ~150 nm with a zeta potential of ~30 mV. The nanoparticles had an encapsulation efficiency of 70% and in the presence of cryoprotectant, they could be lyophilized and reconstituted without altering their size. The colloidal stability studies were performed in simulated nasal mucosal medium and the results showed that nanoparticles were stable for a period of 24h. A comparative study was performed in mice, to evaluate the potential of nano-encapsulation on immune response generated against the glycoconjugates. The *in vivo* studies showed that the mice injected with the GC-CNPs (S.C), in combination with α-GalCer as an adjuvant has displayed 100 folds higher IgG response and 10 folds higher IgM response over the groups treated with GC (S.C). However, the same GC-CNPs did not show potential IgG response when administered *via* intranasal route. Overall, the study demonstrates the potential use of nanoparticulate systems to deliver semisynthetic glycoconjugate antigens effectively.

Keywords: Pneumococcal surface adhesin A, Chitosan, Nanoparticles, Glycoconjugate vaccine, *Streptococcus pneumoniae*, Immunology

USC
UNIVERSIDADE
DE SANTIAGO
DE COMPOSTELA

1. INTRODUCTION

Streptococcus pneumoniae is the leading cause of mortality in children under the age of 5 years. In the year 2017, *S. pneumoniae* was responsible for 1.2 million deaths globally and 300,000 deaths were due to pneumococcal pneumonia [1,2]. There are more than 96 serotypes of *S. pneumoniae* based on the diversity of capsular polysaccharides [3]. The marketed vaccines employed in the prevention of pneumococcal infection are based on these capsular polysaccharides. Pneumococcal polysaccharide vaccines (PPSV23) and pneumococcal conjugate vaccines (PCV7 and PCV13) are commonly used marketed vaccines. The introduction of conjugate vaccines has significantly reduced the global burden of pneumococcal infections across many communities [4]. Still, conjugate vaccines offer protection against limited serotypes whose polysaccharide components are incorporated in the vaccines. Due to this, immunizing with the existing vaccines fail to protect against *S. pneumoniae* infections caused by serotypes not included in the formulations. Polysaccharide or conjugate vaccine requires complex manufacturing, purification and dose optimization steps, and introduction of further serotypes in the formulations will result in an escalation of the vaccine costs. To circumvent these limitations, vaccines based on pneumococcal proteins have been investigated. The proteins like pneumococcal surface adhesin A (PsaA) [5–7], pneumococcal surface protein A (PspA) [8], pneumolysin (Ply) [9], and pneumococcal histidine traid D (PhtD) [10] have been extensively studied as the potential vaccines against pneumococcal infections as they are expected to offer broad protection against all the pneumococcal serotypes [11].

In our earlier study, the combination of protein and sugar valences have been proposed to induce an additional or synergistic effect. In this line, we have successfully synthesized a semisynthetic glycoconjugate vaccine where PsaA plays a dual role as both immunogen and

carrier. PsaA was covalently linked to a synthetic tetrasaccharide mimic of capsular polysaccharide (CP) from pneumococcal serotype 14 (Pn14TS) to obtain a glycoconjugate (Pn14TS-mPsaA/GC) [12]. Pn14TS is a synthetic tetrasaccharide derived from the capsular polysaccharide of *S. pneumoniae* serotype 14, that was able to evoke the opsonophagocytic response [13]. PsaA is a highly conserved, 37-kDa protein that is commonly present in all the 96 serotypes of *S. pneumoniae* [14]. PsaA is a member of the ATP- binding cassette (ABC) protein that transports manganese. Additionally, PsaA is a surface-exposed protein that is reported to play a significant role in the adhesion and colonization of *S. pneumoniae* [14,15]. This makes the PsaA an ideal candidate for vaccination against pneumococcal infections [16,17].

While most subunit vaccines alone are poor immunogens and fail to generate T and B cell responses, glycoconjugate vaccines can induce better immune protection on their own. Nevertheless, their co-administration with an adjuvant can further heighten the immune response. Several adjuvants like aluminium salts, cholera toxin (CT) [18,19], α-galactosyl ceramide (α-GalCer) [20] have been explored for this purpose. However, strong adjuvant activity is often associated with increased toxicity and adverse effects. As an alternative strategy, the use of particulate carriers offer multiple benefits as a vaccine delivery system: i) they can act as an adjuvant; ii) they enhance the stability of antigens; iii) they reduce the need of administering multiple doses; iv) they are suitable for needle-free vaccine delivery via mucosal routes [21–23]. Several particulate systems like polymeric nanoparticles [24], metallic nanoparticles [25], liposomes [26] and microparticles [27] have been explored for the delivery of pneumococcal antigens. Nanoencapsulation helps the antigens to cross the epithelial barrier and presents them to the immune cells [21]. In most of the cases, the subunit vaccines have been encapsulated into the nanoparticles or co-administered with antigens as

an adjuvant [28]. The increasing use of particulate systems in the delivery of the antigens has led to the deeper understandings in cellular and molecular mechanisms by which vaccines stimulate the immune adaptive response.

Earlier studies have demonstrated chitosan nanoparticles as an adequate carrier for the delivery of protein subunit vaccines [29]. Chitosan is a biocompatible, biodegradable and a mucoadhesive polymer with adjuvant properties [30]. The preparation of chitosan nanoparticles (CNPs) involves a solvent-free and simple ionic gelation method and this makes it attractive for the encapsulation of delicate macromolecules such as protein-based antigens. In this study, GC was encapsulated into CNPs (GC-CNPs) and the characterization of GC-CNPs was performed. A comparative study on the immunogenicity of GC and GC-CNPs was performed to identify the importance of nanoencapsulation in enhancing the immunogenicity of the glycoconjugates. In summary, we demonstrate the use of chitosan nanoparticles for the delivery of semisynthetic glycoconjugate antigens.

2. Methods

2.1. Preparation and characterization of CNPs

Chitosan nanoparticles were prepared by ionic gelation technique that was previously developed by our group [29]. First, the chitosan (2 mg/mL) and poloxamer (20 mg/mL) solutions were prepared under magnetic stirring using ultrapure water. Then 0.5 mL each of chitosan and poloxamer solutions were mixed in a reaction vial to form a 0.1% and 1% (w/v) mixture of chitosan and poloxamer, respectively. Next, 0.5 mL of a TPP solution (0.4 mg/mL) was added at once to the mixture of chitosan and poloxamer under magnetic stirring (700 rpm). After 30 min of the reaction, the nanoparticles were concentrated by centrifugation at 12000 RCF, for 12 min, at 15 °C, using 10 µl of glycerol bed. After the centrifugation, the pellet

in the bottom was carefully collected and resuspended in ultrapure water. For GC loaded CNPs, the TPP solution (0.5 mL of 0.4 mg/mL) containing GC (50 µg) was added to 1 mL of 0.1% w/v chitosan in 1% poloxamer kept under magnetic stirring at 700 rpm.

The particle size and polydispersity index of the nanoparticles were measured by dynamic light scattering (DLS) and the zeta potential was calculated from the electrophoretic mobility values obtained by laser Doppler anemometry using a Zetasizer Nano-ZS90 (Malvern Instruments; Malvern, UK). All the measurements were performed at 25 °C with a detection angle of 173° in distilled water unless otherwise indicated. The nanoparticle concentration and stability in cell culture medium was evaluated by nanoparticle tracking analysis using NanoSight NS500 (Malvern instruments; Malvern, UK).

The surface morphology of the GC-CNPs was examined by field emission scanning electron microscopy (FESEM, ZEISS FESEM ULTRA Plus, Germany). For FESEM studies, 10 µl of the GC-CNPs suspension (10,000 times diluted) was placed on the silicon wafer and left to dry overnight in the desiccator. Prior to the analysis, the samples were sputter-coated with iridium (10 nm thickness).

The blank and GC-CNPs (0.5% & 1% w/v) were lyophilized in the presence of 5% and 10 % (w/v) trehalose as a cryoprotectant in the Eppendorf tubes. The samples were frozen overnight at -20 °C and then transferred to the freeze-dryer Genesis 25 ES, VirTis Model-Wizard 2.0 (SP Industries, USA). The primary drying step lasted for 35 h during which the temperature was gradually increased from -40 to -20 °C. This was followed by a secondary drying step in which the temperature was increased to RT from 0 °C. After the freeze-drying, the nanoparticles were resuspended in the ultrapure water and were analysed for their particle size and PDI. A similar freeze-drying process was used to determine the formulation process yield.

2.2. Encapsulation of GC into CNPs and release studies

The encapsulation efficiency (EE) of GC in CNPs was determined by calculating the amount of free GC present in the collected supernatant after the centrifugation. The amount of free GC was determined using the micro BCA assay kit (Thermo Fischer scientific) by measuring the absorbance at 562 nm. The quantification was performed using the linear standard curve produced with the solutions of GC solubilized in the supernatant of CNPs in the concentration range of 0.5 - 10 µg/mL. The % EE was calculated as follows: % EE = A – B/A × 100, where A is the total GC and B is the free GC in the supernatant.

To perform the *in-vitro* release studies, GC-CNPs were incubated in the SNF (pH 6.5) at 37 °C kept under constant agitation in a shaking incubator at 300 rpm. At different time points (0, 1, 2, 4, 8 and 24 h) the supernatant was collected by centrifugation. The micro BCA protein assay kit determined the amount of the GC released at different time points.

2.3. Fluorescent labelling of chitosan

The Cy5 labelled GC-CNPs were prepared to visualize the GC-CNPs during the *in vitro* studies. Briefly, chitosan (50 mg; 0.3 mmol monomer units; 1 eq) was placed in a reaction vial and dissolved in deionized water (5mL). Cyanine (Cy5) (1 mg; 0.015 mmol; 0.050 eq), in dimethyl sulfoxide (DMSO) (0.3mL) was added to the chitosan solution under continuous stirring. After sealing, the vial was stirred for 16 h at RT, protected from light. After the reaction, the labelled chitosan was purified using PD10 columns (Centri Pure P10; Zetadex Gel Filtration columns). The yield of the reaction was measured afterwards by weighing the freeze-dried product in the eppendorf and subtracting the weights. The labelling of the GC-CNPS was simply performed by substituting 2% of chitosan with the Cy5-labelled chitosan (Cy5-chitosan) during the synthesis of the CNPs.

2.4. Colloidal stability of chitosan

The colloidal stability of the GC-CNPs was studied by monitoring the particle size and the mean count rate (MCR) in the simulated nasal fluid (SNF) containing 0.1% mucin (Type III mucosa from Sigma Aldrich) using DLS. The SNF with different concentrations of mucin (0.001, 0.01 & 0.1 % w/v) was used to mimic the nasal environment for the intra-nasal delivery. In brief, 200 µL of 1mg/mL GC-CNPs were mixed with 800 µl of mucin in SNF, while nanoparticles suspended in water and SNF at same concentrations are used as controls. The GC-CNPs in the different media are shaken at 100 rpm at 37 °C using a constant-temperature shaker, at different time points (0, 0.5, 1, 2, 4 and 24h) the size and mean count rate of samples are measured using DLS. To study the stability of GC-CNPs in cell culture medium, the GC-CNPs at the concentration of 0.5 mg/mL were incubated in RPMI + 10% FCS (R10 media) for 4h. Later, the change in the nanoparticles was measured using NTA as mentioned in section 2.1.

2.5. *In vivo* studies Immunization studies in mice

Specific pathogen-free C57BL/6 mice (6 weeks-old, female) were purchased from Janvier (Le Genest-St-Isle, France). Mice were maintained in a biosafety level 2 facility in the Animal Resource Centre at the Lille Pasteur Institute for at least two weeks prior to usage, to allow appropriate acclimation. Mice were fed a standard rodent chow (SAFE A04) (SAFE, Augy, France) and water *ad libitum*. The diet contains ~11.8% fibre including ~10% water-insoluble fibre (3.6% cellulose) and 1.8% water-soluble fibre. All the animal experiments were performed at Lille Pasteur institute according to the ethical guidelines (agreement number AF 16/20090 and 00357.03).

Groups of 6 female C57BL/6 mice were injected subcutaneously (S.C.) with GC or GC-CNPs, (1 µg carbohydrate antigen/5 µg protein/dose). All mice were administered with 250 ng of α-GalCer as an adjuvant. Two series of immunizations were carried out: Firstly, mice were

immunised S.C. on day 0 and boosted at day 14 with either PBS, GC or GC-CNP. Second, in a subsequent study 7 groups of mice were immunized with GC-CNPs (S.C), blank CNPs (S.C), Prevnar 13 (S.C), GC (I.N), GC-CNPs (I.N), blank CNPs (I.N), and GC + blank CNPs (I.N), thrice at day 0, 14 and 28). Mice were bled one week after every immunization. Sera were stored at −80 °C until the quantification of Ab response by ELISA.

2.6. Measurement of humoral response

The Ab responses induced upon immunization were assessed by using enzyme-linked immunosorbent assay (ELISA) as described previously, with slight modifications [1]. In brief, the samples with different serial dilutions were loaded into individual 96 wells microtiter Nunc Maxisorp (ThermoFisher Scientific) where the plates were coated with mPsaA (0.1 µg/well) or Pn14TS (0.2 µg/ well) and plates overnight at 4 °C. The goat anti-mouse IgA, IgM and IgG(H+L)- HRP-labelled conjugate (CliniSciences) used as secondary Ab at a dilution of 1/6000, was used as secondary antibodies. The reactions were read in an Infinite M1000 spectrophotometer (TECAN). Similarly, anti-mouse IgG1, IgG2a, IgG2b and IgG3 were used to determine the predominant IgG subclass expressed. To determine the anti-CP14 response the purified capsular polysaccharide (CP14) (Alliance Bio Expertise, France) was coated in the wells. While the killed pneumococcal serotype 14 (Sp14) were coated in the plates to determine the anti-Sp 14 antibody response. The Ab titer was defined as the dilution of immune serum that gave an OD (405 nm) at least twice that observed with pre-immune serum.

2.7. Influenza A virus (IAV) infection

The *S. pneumoniae* (serotype 14) strain used in this study was a gift from Dr M. de Jonge (Nijmegen University, The Netherlands). The mouse-adapted H3N2 IAV strain Scotland/20/1974 was described in [31]. For infection with IAV, 50 µl of phosphate-buffered saline containing (or not, in a mock sample) 30 plaque-forming units (p.f.u.) of the H3N2 IAV strain Scotland/20/1974 were intranasally administered to anesthetized mice. This dose corresponds to a sub-lethal dose, which is necessary to investigate secondary bacterial infection. For secondary pneumococcal infection post-influenza, mice were challenged (I.N) at 7 dpi with *S. pneumoniae* ($1x10^6$ c.f.u.). The survival of the mice was monitored for 20 days [32].

2.8. Statistical Analysis

All values are presented as geometric mean ± standard deviation. The statistical analysis was performed using Graphpad Prism 7 software. The statistical significance of the observed differences was assessed by Mann Whitney U test and Kruskal Wallis analysis by Dunns multiple comparisons. A probability value of $P < 0.05$ was considered statistically significant.

3. Results

3.1. Nanoparticle preparation and characterization

The schematic representation of the CNPs formation is shown in **Figure 1**. DLS analysis of CNPs suspensions revealed the formation of nanoparticles with an average diameter of 142 ±18 nm and zeta potential of +27 ±3 mV. The PDI of the GC-CNPs was lower than 0.2, indicating the homogeneity of the nanoparticle population. The incorporation of poloxamers in the formulation and the use of glycerol bed during nanoparticle separation is attributed for its ability to maintain the stability of the nanoparticles [33] and improving the *in vivo* efficiency of the nanoparticles [34,35].

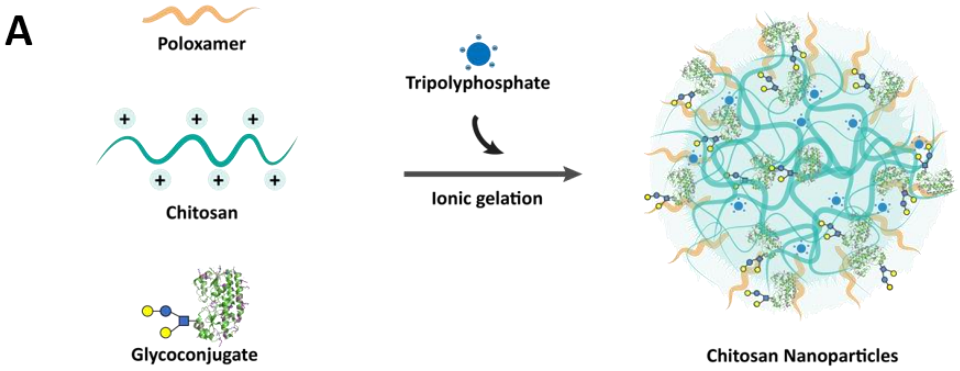

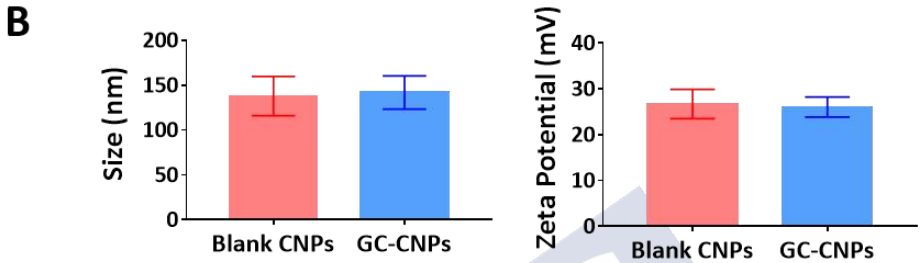

C

	Size (nm)	PDI	Zeta Potential (mV)	% Encapsulation Efficiency
Blank CNPs	134 ±18	< 0.2	29 ±3	-
PsaA CNPs	142 ±9	< 0.2	35 ±2	12 ±2
GC-CNPs	142 ±18	< 0.2	27 ±3	70 ±3
CY5-GC-CNPs	150 ±9	< 0.2	30 ±2	-

Figure 1: Schematic representation of chitosan nanoparticle preparation by ionic gelation method (A); Particle size and zeta potential of blank CNPs and GC-CNPs analysed by Malvern zeta sizer (B); Physico-chemical properties of the prepared nanoparticles (C).

The nanoparticle tracking analysis (NTA) displayed that the blank CNPs and GC-CNPs had similar average particle size around 150 nm (**Figure 2A**), close values to those obtained previously by DLS. The results from scanning electron microscopy presented in **Figure 2B** confirm that the CNPs and GC-CNPs have narrow size distribution. The SEM micrographs show that CNPs presented near spherical morphology and showed no signs of aggregation.

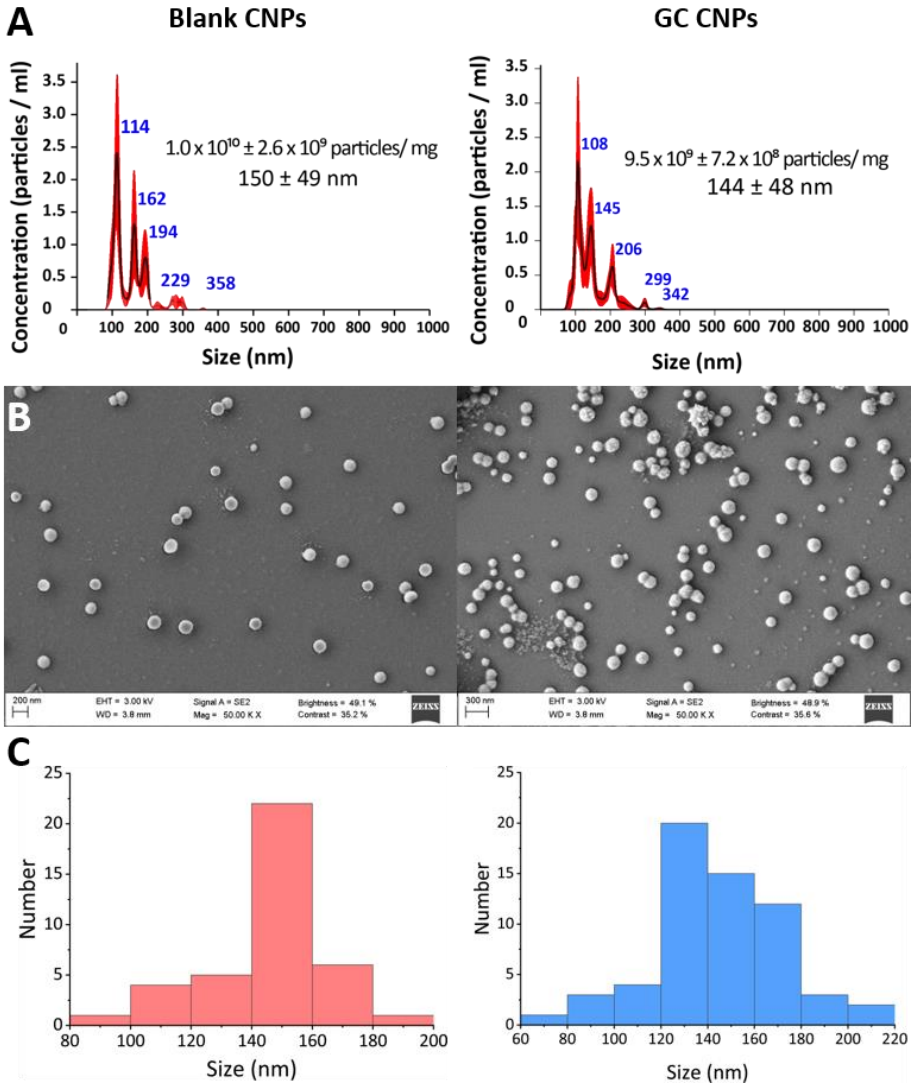

Figure 2: Particle size determination by nanoparticle tracking analysis (NTA) and field emission scanning electron microscopy (FESEM) of the blank CNPs and GC-CNPS; A) The figure represents the particle size distribution and the nanoparticle concentration of blank and GC-CNPs, determined by NTA; B) The surface morphology of blank CNPs and GC-CNPs determined by FESEM and shows the CNPs had spherical shape; C) The particle size distribution from the FESEM images calculated using image J software and plotted by graph pad prism.

The diameter of a hundred particles from the micrographs of both the blank CNPs and GC-CNPs was measured using the Image J software. The size distribution of the measured particles is plotted as shown in **Figure 2C.** The average particle size was 147 ±19 nm and 145 ±28 nm for the blank CNP and GC-CNPs respectively. No significant difference in the distribution pattern of the NPs was observed, even though the GC-CNPs had a slightly higher number of particles in the size range below 100 nm. For cell studies, the nanoparticles were

labelled by conjugating Cy5 to chitosan. The particle size analysis shows that the Cy5-GC-CNPs had an average diameter of 150 ±9 nm and zeta potential of 30 ±2 mV. The use of the Cy5 labelled chitosan exhibited a slight increase in the size of the CNPs. The formulation contained approximately ~8-15 thousand Cy5 molecules per particle as calculated from particle numbers obtained by NTA.

3.2. Encapsulation efficiency and antigen release studies

Encapsulation efficiency (EE) of GC in the CNPs was found to be 70 ±3% that corresponds to 35 µg of protein per milligram of NPs, while the EE of mPsaA was < 20%. When compared to PsaA, the GC contains the tetrasaccharide and the acetyl thioacetate molecules associated with it. The higher encapsulation of GC into the nanoparticles, when compared to PsaA, might be attributed to its tetrasaccharide chains. The prepared GC-CNPs contained approximately 6,000 GCs per particle as calculated with particle numbers measured by nanoparticle tracking analysis (~1.9 x 10^{10} particles per mg of GC-CNPs)**.** The nanoparticles freeze-dried in the absence of cryoprotectant were dispersible in water but showed an increase in the particle size. Both the blank and GC-CNPs that were freeze-dried in the presence of 5% and 10% trehalose as a cryoprotectant were easily re-dispersible after 1 week of storage at 4° C. This helps in the storage of nano vaccines in the powder form.

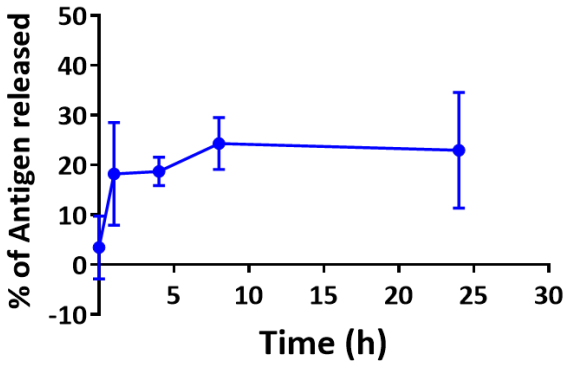

Figure 3: The percentage of antigen released after incubating the GC-CNPs in SNF for a period of 24h (N=3)

The amount of the GC released at different time points from the CNPs was quantified against the supernatant of the blank CNPs. Approximately 18% of antigen was released after 1 h of incubation in SNF. Afterwards, there was no significant increase in the percentage of the antigen released. At the end of 24 h, the percentage of antigen released was 24 ±9%, as seen in **Figure 3**.

3.3. Stability of chitosan nanoparticles in simulated nasal fluid

The stability of GC-CNPs in the mucosal medium was studied for a period of 24 h. The results obtained from the interaction of chitosan nanoparticles with mucin in SNF are represented in different plots as shown in **Figure 4A & 4B**.

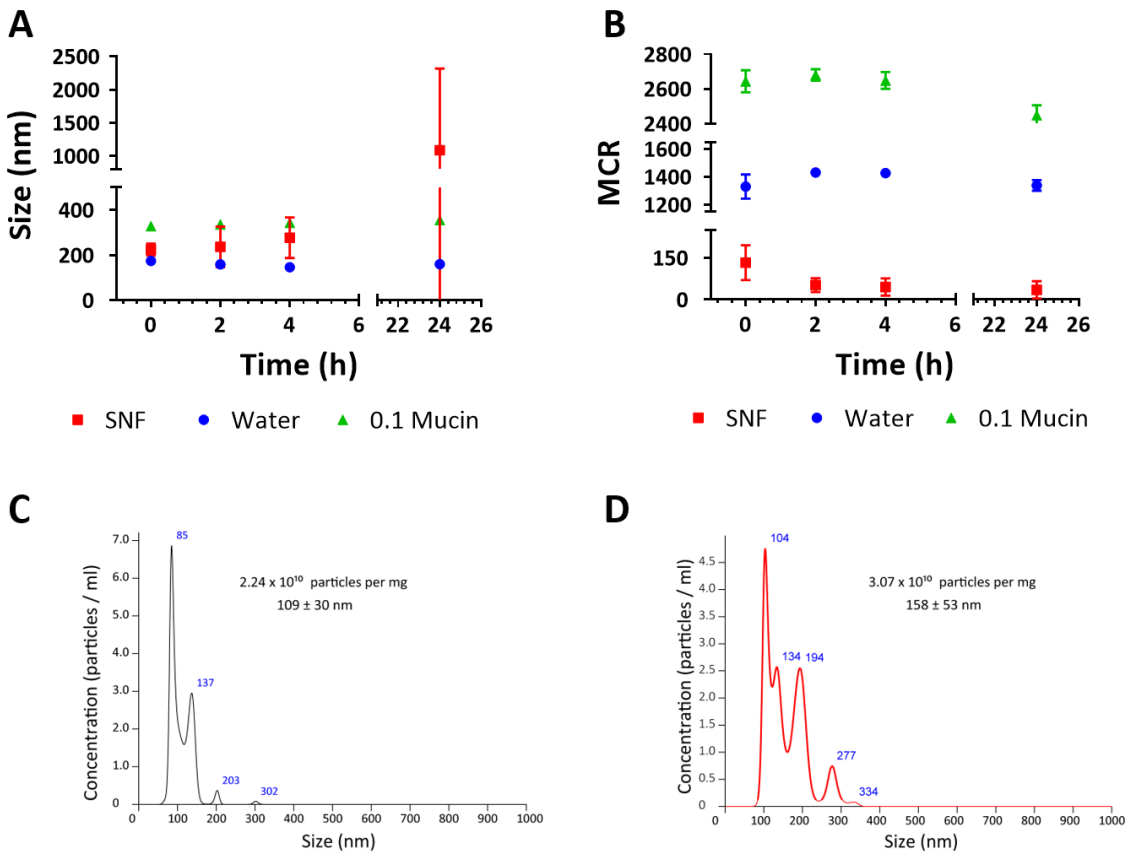

Figure 4: Colloidal stability of GC-CNPs in the mucosal and cell culture medium. Particle size (A) and mean count rate (B) characterization of the GC-CNPs measured at different time points during 24 hours, to evaluate their stability in mucosal medium (SNF + 0.1% mucin); The particle size distribution measured by NTA to compare the stability of GC-CNPs while in water (C) and after incubation in RPMI with 10 % FCS (D).

Particle sizes in SNF containing 0.1% mucin were measured around 320 nm thereafter t=0 *i. e.* twice as much as the mean particle sizes observed when NPs are dispersed in water (**Figure 4A & 4B**). While the nanoparticles incubated in SNF, the particle size increased with time, and the count rate of the particles reduced drastically. The results show that even though the nanoparticles are not stable in SNF, their stability in this medium increased in the presence of mucin. The reason for the initial increase in the size of nanoparticles with 0.1% mucin in SNF, even though they were stable thereafter, might be due to the mucoadhesive property of the chitosan nanoparticles. The higher viscosity of the mucosal medium can also reduce the Brownian motion of the GC-CNPs due to which the particles appear larger and this phenomenon cannot be ruled out with this method. Taken together the results obtained suggest that the chitosan nanoparticles might have enough stability in the nasal mucosa. The colloidal stability of the nanoparticles was evaluated by measuring their size and PDI in the R10 cell culture medium and was found to be concentration dependent. The data obtained by NTA confirms that the GC-CNPs showed no signs of aggregation in the R10 media at the concentrations below 500 µg/mL **(Figure 4C & 4D)**.

3.4. *In vivo* studies

3.4.1. The effect of nanoencapsulation on GC immunogenicity

In the first series of experiments groups of 6 mice were immunized S.C. twice at two weeks interval with GC, GC-CNP or PBS adjuvanted with α-GalCer to test the effect of encapsulation on GC immunogenicity. ELISA determined the levels of the IgG and IgM antibody response raised by the different formulations.

To investigate whether the GC and GC-CNPs were able to induce the production of anti-mPsaA Abs, the ELISA microtiter plates were treated with mPsaA as a coating antigen. Neither GC

alone nor GC-CNP induced an anti-mPsaA IgM response after the second immunization (data not shown). Contrasting to this result, both GC and GC-CNPs were able to induce anti-mPsaA IgGs in mice. Notably, this anti-mPsaA IgG response at least, 100-fold higher in the GC-CNPs treated mice in comparison to the GC treated mice (P<0.0005) **(Figure 5A)**.

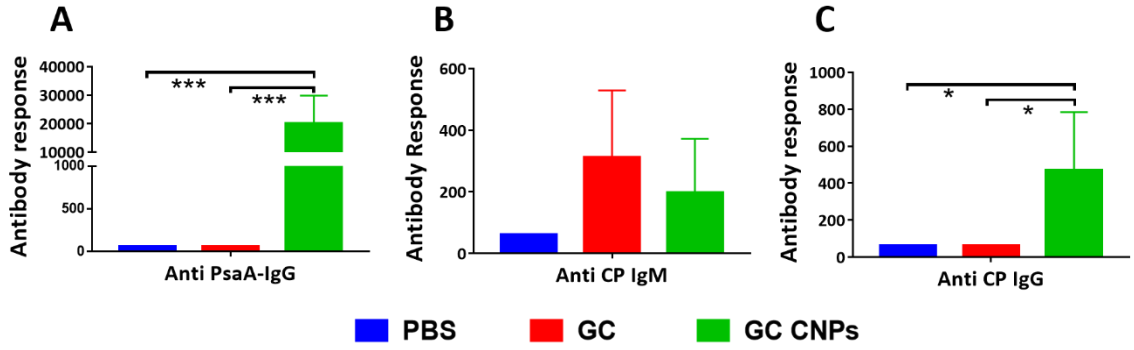

Figure 5: The antibody response in the mice immunised with PBS, GC and GC-CNPs one week after the final immunization. The immunization was performed twice at day 0 and 14 and the serum antibody response in the mice was determined at day 21. The obtained results are represented as anti-PsaA IgG response (A), anti-CP14 IgM response (B) and anti-CP14 IgG response (C). Statistical difference between the groups is *, P < 0.01; **, P < 0.001; ***, P < 0.0005. Data represent mean ± SD (n=6).

To investigate whether the GC and GC-CNPs were able to induce the production of anti-CP14 Abs, CP from serotype 14 was coated on ELISA microtiter plates. A low anti-CP14 IgM response was observed in both groups with high variability and no significant difference. However, the increase in anti-CP14 IgG in the mice treated with GC-CNPs was 10 folds higher than the mice treated with GC alone **(Figure 5B).** The results show that the encapsulation of the GC in CNPs enhance the IgG response against both the protein and the capsular polysaccharide. Finally, we tested whether the IgG induced in the sera of mice immunized with GC-CNP were able to bind to the bacteria. To this aim killed *S. pneumoniae* bacteria were used as coated antigen. A significantly higher anti-Sp14 IgG titers were detected on ELISA plates (data not shown).

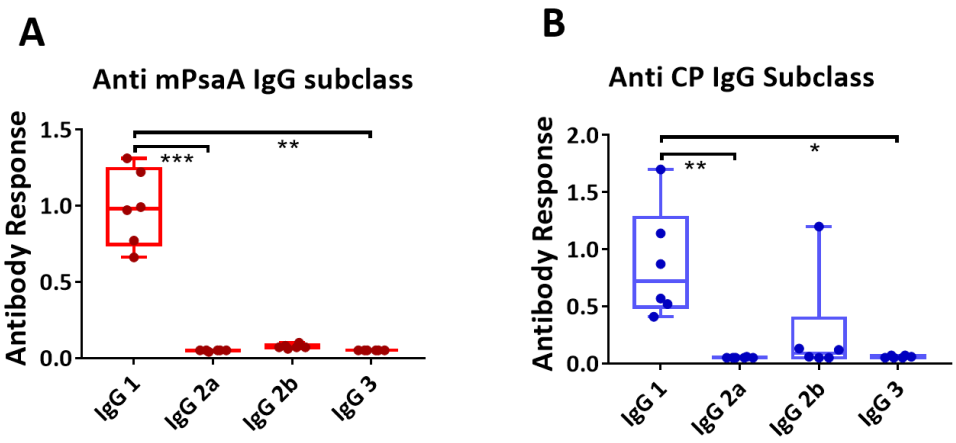

Figure 6: The subclass of anti-IgG antibody response in the mice immunised with GC-CNPs one week after the final immunization. The immunization was performed twice at day 0 and 14 and the serum antibody response in the mice was determined at day 21. The obtained results are represented as anti-mPsaA IgG subclass response (A), anti-CP IgG subclass response (B). Statistical difference between the groups is *, $P < 0.05$; **, $P < 0.01$; ***, $P< 0.001$. Data represent mean ± SD (n=6).

In addition, studies were performed to determine which subclass of the IgG was predominantly expressed in the groups immunized with GC-CNPs. The serum samples of mice immunized with GC-CNPs displayed a high level of Abs of the IgG1 subclass and at a much lower extent of the IgG2b against both PsaA and CP14 (**Figure 6**). There was no activation of other IgG subclasses in particular of the IgG2a one. However, the IgG2b was the second predominant IgG subclass that was in the mice immunized with GC-CNPs.

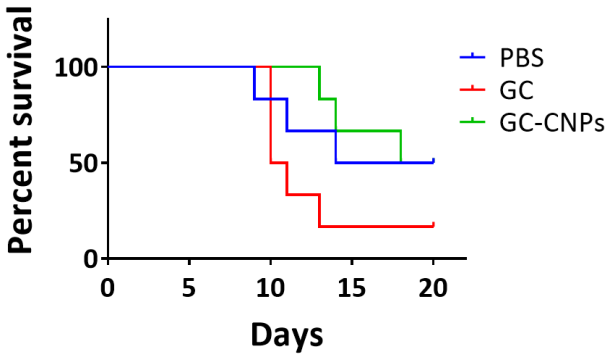

Figure 7: Survival of vaccinated mice challenged intranasally by administering 30 CFU of H_3N_2 followed by $1x10^6$ of *S. pneumoniae* serotype 14. The survival of the mice was monitored for 20 days. The differences between survival rates of 6 mice per group were analysed by Kaplan–Meier survival curve. Log-rank (Mantel–Cox) test p = 0.0714, no significant difference.

The invasive pneumococcal challenge (**Figure 7**) in the mice displayed 50% of survival on day 20, in the group immunized S.C with GC-CNPs while the group immunized with an equivalent amount of GC showed only 17% survival. Interestingly, there was 100% survival until day 13 in the mice treated with GC-CNPs. Whereas, in the groups treated with GC the survival reduced to 50% in day 10. Overall, the results demonstrated that the mice immunized with GC-CNPs exhibited higher protection against the invasive pneumococcal challenge.

3.4.2. The role of administration route on the immunogenicity of GC

In the second set of experiments, we aimed at determining the humoral IgG and IgM response induced in mice by the GC-CNP depending on their route of administration, either S.C. or I.N. The serum samples of different groups of mice immunized with GC (I.N), GC-CNPs (I.N), GC + blank CNPs (I.N), blank CNPs (I.N), GC-CNPs (S.C), blank CNPs (S.C) and Prevnar 13 (S.C) adjuvanted with α-GalCer. The serum analysis shows no anti-mPsaA IgM response in any groups (data not shown). Sera of mice immunized with blank CNPs by either route, as well as that of mice immunized with Prevnar 13 (which does not contain PsaA as an immunogen) do not show any anti-mPsaA IgG response.

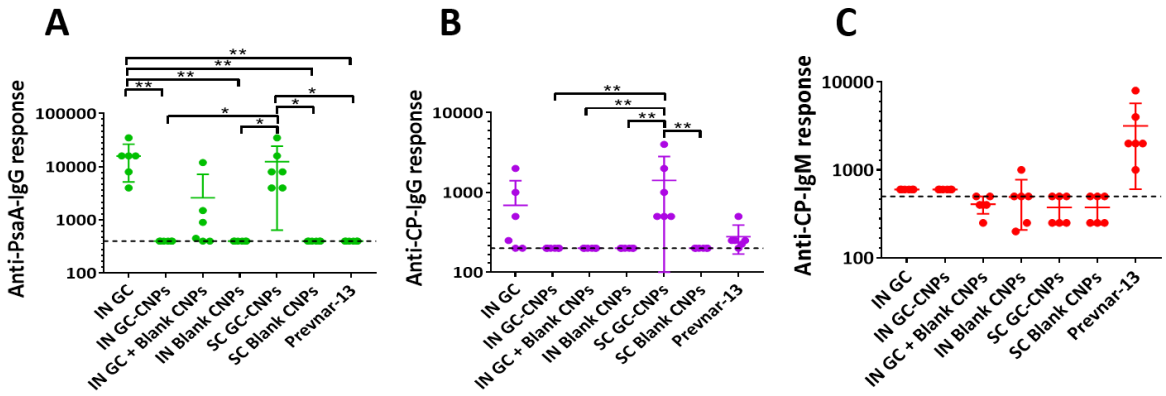

Figure 8: The antibody response in the mice immunised with GC (I.N), GC-CNPs (I.N), GC + blank CNPs (I.N), blank CNPs (I.N), GC-CNPs (S.C), blank CNPs (S.C) and Prevnar 13 (S.C). The results are displayed as anti-mPsaA IgG response (A), anti-CP IgG response (B), and anti-CP IgM response (C). The serum samples data are presented as geometric mean titer ± standard deviation of six mice per group. Statistical difference between the groups is *, $P < 0.05$; **, $P < 0.01$; ***, $P < 0.001$.

High anti-mPsaA IgG response was raised against GC-CNPs via S.C. administration, confirming the results observed during the first series of immunization. The anti-PsaA IgG response was similar to GC-CNPs (S.C) when GC was administered intranasally. However, the group treated with a physical mixture of GC & blank CNPs showed a marked decrease in the anti-PsaA IgG (about 2 folds) compared to the groups treated with GC (I.N) and GC-CNPs (S.C) while the response was absent in GC-CNPs (I.N.) **(Figure 8A)**. The results obtained from quantifying the anti-PsaA IgG in the groups immunized I.N clearly show that the anti-PsaA IgG response is highest in the group immunized with GC and a reduction in activity is seen when physically mixing the GC with CNPs prior to immunization. Further reduction in the activity was observed on encapsulation of the GC in the CNPs. This indicates the influence of the CNPs in reducing the immune response against the GC while injected I.N. However, the same GC-CNPs when injected S.C increased anti-PsaA IgG several folds compared to GC (S.C).

Considering the anti-CP14 IgG response, both the GC (I.N) and the GC-CNPs (S.C) were able to induce an anti-CP14 IgG response (**Figure 8B**). While, the GC-CNPs (S.C) showed significantly higher anti-CP14 IgG response against other groups (GC-CNPs (I.N), blank CNPs (I.N), and GC + blank CNPs (I.N)) except GC (I.N). The group treated with Prevnar 13 showed very low anti-CP14 IgG response ($P<0.01$). To study the production of anti-CP14 Abs in the mice immunized with different formulations, CP from serotype 14 was coated on ELISA microtiter plates. The anti-CP14 IgM response was very low in all the groups, except in the group immunized with Prevnar 13 **(Figure 8C)**.

4. **Discussion**

Chitosan nanoparticles (CNPs) have earlier been investigated as a carrier for numerous vaccines [36–38], including pneumococcal protein vaccines [24] and have been tested as an adjuvant in mixture with PCV13 [39]. To the best of our knowledge, chitosan or any other polymeric nanoparticles have never been used as a carrier for the delivery of pneumococcal conjugate vaccines. The knowledge on the influence of the nanocarriers on the immunogenicity of the glycoconjugate is still missing. The current study provides significant data to understand the influence of the CNPs in altering/enhancing the immunogenicity of the glycoconjugates.

CNPs have a proven track record in the delivery of therapeutic proteins and vaccines *via* mucosal route [40–42]. In addition, the CNPs have demonstrated to possess adjuvant activity in S.C immunization and thus, also appear as promising carriers for systemic administration [43]. CNPs carry the advantage of mild and solvent-free preparation, that is ideal for preserving protein integrity during the encapsulation step. The stability study to access the nanoparticle behaviour in the mucosal and cell culture media and to proceed with the further experimentation showed that the nanoparticles remained suspended for 24h. Even though there was a slight increase in the size of the nanoparticles in the mucosal medium, there was no reduction in the particle count. The slight increase in the particle size might be the result of higher viscosity of the mucosal medium that reduces the brownian moment of the nanoparticles. The incorporation of poloxamers in the formulation maintains the stability [33]. The nanoparticles freeze-dried in the presence of cryoprotectant did not show any increase in the hydrodynamic diameter of the nanoparticles after re-dispersing. This helps in long term storage of the nanoparticles in the powder form. In addition, the presence of the cryoprotectant is known to protect protein conformation and structural integrity [44]. In our

study, approximately 35 µg of GC was associated with per mg of CNPs. GC-CNPs released < 30% of GC over 24h. The reason for this might be due to the strong association of the GC to the CNPs. The initial burst release might either correspond to the un-associated GC or the GC that is adsorbed on the surface of the CNPs. A similar phenomenon is seen in the literature where the CNPs were strongly associated with the antigen [45,46].

Our study aimed to evaluate the role of nanoencapsulation in enhancing the immunogenicity against the GC. The groups immunized with GC-CNPs (S.C) displayed 10 and 100 folds greater anti-CP14 and anti-PsaA, respectively, IgG response in comparison to the GC (S.C). Strikingly, the IgG response induced by the GC-CNPs in mice was also higher than that previously observed for GC administered at a six times higher dose [12]. This is in agreement with published results where the encapsulation of antigen in the chitosan nanoparticles led to a ten-fold antigen dose reduction without affecting the level of the immune response [48]. In the first series of experiments, the functionality of Abs induced in mice was assessed using IAV infection challenge. The mice immunized with the GC-CNPs displayed greater protection over its counterparts immunized with GC. However, α-GalCer stimulates a non-specific immune response in control groups which protects against Flu and then Sp infection [47]. The α-GalCer, an adjuvant used in this study is a glycosphingolipid that can potentially activate the NKT cells [48] and been explored as an adjuvant in both systemic and mucosal immunizations [49–51]. The adjuvant effect of chitosan is usually enhanced in the presence of an additional adjuvant.

The generated IgG antibodies in the group treated with GC-CNPs were predominantly IgG1 subclass. In the literature, it is seen that IgG1 subclass of antibodies are mainly induced by bacterial proteins, while the IgG2 antibodies are induced by capsular polysaccharides [52]. The results obtained from our studies showed greater IgG1 production against both PsaA and

CP, while no IgG2a or IgG3 response was observed. Similar results were observed by Bal *et al*., when antigen-loaded trimethyl chitosan nanoparticles were injected intradermally [53]. The mice treated with GC-CNPs also displayed CP14 specific IgG1 response this is classically ascribed to the conjugation of the carbohydrate hapten herein Pn14TS to the carrier protein herein mPsaA. Interestingly, IgG2b against the CP14 was second prevalent subtype. The results are in agreement with the studies performed by Majela *et al*., [54] where the mice immunized with self-assembled PsaA particles produced predominantly IgG1 and IgG2b as a second predominant response. The generation of anti IgG1 Abs against both PsaA and CP can be attributed to the activation of phagocytosis by the macrophages [54]. The generation of IgG1 subclass antibodies corresponds to the Th2 (humoral) immune response and the IgG2b subclass is identified as a part of Th1 (cell-mediated) immune response [54,55]. The results are in agreement with the hypothesis that a vaccine based on PsaA can elicit both humoral and cellular immune response [56].

The second set of immunizations were performed to understand if the GC-CNPs can generate a greater immune response via I.N over S.C immunization. In this study, the GC-CNPs failed to produce anti-PsaA IgGs when administered through I.N **(Figure 8A).** Whereas the same CNPs, when administered via S.C route, produced 100 folds higher anti-PsaA IgG response. This clearly displays that GC-CNPs were able to induce an anti-PsaA IgG response via S.C but not via I.N. It is well established that systemic routes of immunization are more efficient than intranasal one since they do not face to the mucosal barriers. Generally, the nanoparticles administered via mucosal routes tend to undergo mucosal clearance and hence the dose should be increased for mucosal immunization. In agreement with these observations, ovalbumin-loaded N-trimethyl CNPs administered S.C generated higher immune response

compared to the same CNPs administered I.N [57]. Herein it is surprising that GC was superior as an immunogen than GC-CNPs when administered I.N. On the contrary, the results show that the presence of CNPs is reducing the immune response produced against the GC when administered intranasally. The results displayed in the **figure 8A**, clearly demonstrate that the anti-PsaA IgG response is decreasing when the GC is co-administered with CNPs as a physical mixture *via* I.N. The anti-PsaA IgG response further reduced when the GC-CNPs were administered *via* I.N. It is surprising that the mice immunized with Prevenar 13 as control did not exhibit any IgG response against the CP14, while the GC administered via IN and GC-CNPs administered via S.C. produced IgG response. The studies on the quantification of IgA antibodies from the bronchial fluids of immunized mice show no IgA response (data not shown). However, the final study on the opsonophagocytosis from the serum of the immunized mice is underway. These results would be critical in concluding the role of nanoencapsulation of GC and the immunization route.

Xu *et al* (2015) demonstrated that encapsulating the PsaA in chitosan nanoparticles and immunizing mice intranasally enhanced the IgG response against the PsaA and protected against pneumococcal infection challenges [58]. The results obtained from our study contradict these findings. In our study where the equal number of animals were used, the unencapsulated glycoconjugate (GC) displayed significantly higher IgG response when compared to the GC-CNPs. However, the number of injections made by Xu *et al*., were two times more (6 *vs* 3 injections) and the amount of protein (15 µg *vs* 5 µg/dose) was three times more than our study. Moreover, the mean particle sizes (695 nm *vs* 145 nm) as well as the composition of the CNPs (no poloxamer added in the literature protocol), were different. This finding brings the need to investigate further the influence of both nature and structure of the CNPs on the immunogenicity and possibly the mucosal clearance in lowering the immune

response against the encapsulated GC. Considering the latter parameter, we cannot, of course, be sure that mucosal clearance is the only reason for reduction in IgG response in the groups treated with GC-CNPs *via* I.N. route. We do not know, how, GC interacts with CNPs when simply co-administered within a formulation and, beyond, whether CNPs facilitate the mucosal clearance of the glycoconjugate. To date, there is no literature supporting this phenomenon while there are several studies that demonstrated the chitosan or CNPs as potential immunostimulants [59–62].

Conclusions

In this study, we reported chitosan nanoparticles as a potential carrier for semisynthetic glycoconjugate antigen. The nanoparticles were rationally prepared to encapsulate, control the release of antigen and maintain the stability in the mucosal medium. Moreover, the nanoparticles could be easily freeze-dried and reconstituted. The results obtained from the immunization studies suggest that the CNPs can enhance the immune response of GC when administered S.C. while the same CNPs were not effective via I.N administration. Overall, this study revealed that CNPs could enhance the immunological properties of both pneumococcal protein and carbohydrate components of glycoconjugate vaccine, encouraging the further study of the formulation as nanoparticulate vaccine delivery systems for preventing the infections against *S. pneumoniae*.

5. Acknowledgements

This work was supported by the grant from European Commission, Education, Audiovisual and Culture Executive Agency (EACEA), under the Erasmus Mundus programme, “NanoFar: European Doctorate in Nanomedicine and Pharmaceutical Innovation” (Project: 2015-01-C4). We would like to thank Dr. B. Frisch (University of Strasbourg) for the production of α-GalCer.

6. References

[1] Institute for Health Metrics and Evaluation (IHME), Findings from the Global Burden of Disease Study 2017, Seattle, 2018. http://www.healthdata.org/sites/default/files/files/policy_report/2019/GBD_2017_Booklet.pdf (accessed September 23, 2019).

[2] Streptococcus pneumoniae : Vaccines for AMR, (n.d.). https://vaccinesforamr.org/review-of-pathogens/pathogen-profiles/streptococcus-pneumoniae/#impacte8a5-9923a88f-af42 (accessed September 23, 2019).

[3] K.A. Geno, G.L. Gilbert, J.Y. Song, I.C. Skovsted, K.P. Klugman, C. Jones, H.B. Konradsen, M.H. Nahm, Pneumococcal Capsules and Their Types: Past, Present, and Future, Clin. Microbiol. Rev. 28 (2015) 871–899. doi:10.1128/CMR.00024-15.

[4] A. Torres, P. Bonanni, W. Hryniewicz, M. Moutschen, R.R. Reinert, T. Welte, Pneumococcal vaccination: what have we learnt so far and what can we expect in the future?, Eur. J. Clin. Microbiol. Infect. Dis. 34 (2014) 19–31. doi:10.1007/s10096-014-2208-6.

[5] G. Rajam, J.M. Anderton, G.M. Carlone, J.S. Sampson, E.W. Ades, Pneumococcal Surface Adhesin A (PsaA): A Review, Crit. Rev. Microbiol. 34 (2008) 131–142. doi:10.1080/10408410802275352.

[6] T.A. Olafsdottir, K. Lingnau, E. Nagy, I. Jonsdottir, Novel protein-based pneumococcal vaccines administered with the Th1-promoting adjuvant IC31 induce protective immunity against pneumococcal disease in neonatal mice, Infect. Immun. 80 (2012) 461–468. doi:10.1128/IAI.05801-11.

[7] S. Rapola, V. Jäntti, R. Haikala, R. Syrjänen, G.M. Carlone, J.S. Sampson, D.E. Briles, J.C. Paton, A.K. Takala, T.M. Kilpi, H. Käyhty, Natural Development of Antibodies to Pneumococcal Surface Protein A, Pneumococcal Surface Adhesin A, and Pneumolysin in Relation to Pneumococcal Carriage and Acute Otitis Media, J. Infect. Dis. 182 (2000) 1146–1152. doi:10.1086/315822.

[8] F.C.L. Csordas, C.T. Perciani, M. Darrieux, V.M. Gonçalves, J. Cabrera-Crespo, M. Takagi, M.E. Sbrogio-Almeida, L.C.C. Leite, M.M. Tanizaki, Protection induced by pneumococcal surface protein A (PspA) is enhanced by conjugation to a Streptococcus pneumoniae capsular polysaccharide, Vaccine. 26 (2008) 2925–2929. doi:10.1016/J.VACCINE.2008.03.038.

[9] Q. Zhang, S. Choo, A. Finn, Immune Responses to Novel Pneumococcal Proteins Pneumolysin, PspA, PsaA, and CbpA in Adenoidal B Cells from Children, Infect. Immun. 70 (2002) 5363–5369. doi:10.1128/IAI.70.10.5363-5369.2002.

[10] K. Pauksens, A.C. Nilsson, M. Caubet, T.G. Pascal, P. Van Belle, J.T. Poolman, P.G. Vandepapelière, V. Verlant, P.E. Vink, Randomized controlled study of the safety and immunogenicity of pneumococcal vaccine formulations containing PhtD and detoxified pneumolysin with alum or adjuvant system AS02V in elderly adults., Clin. Vaccine Immunol. 21 (2014) 651–60. doi:10.1128/CVI.00807-13.

[11] A.D. Ogunniyi, J.C. Paton, Vaccine Potential of Pneumococcal Proteins, Streptococcus Pneumoniae. (2015) 59–78. doi:10.1016/B978-0-12-410530-0.00004-1.

[12] M. Prasanna, D. Soulard, E. Camberlein, N. Ruffier, A. Lambert, F. Trottein, N. Csaba, C. Grandjean, Semisynthetic glycoconjugate based on dual role protein/PsaA as a pneumococcal vaccine, Eur. J. Pharm. Sci. 129 (2019) 31–41. doi:10.1016/J.EJPS.2018.12.013.

[13] D. Safari, H.A.T. Dekker, J.A.F. Joosten, D. Michalik, A.C. De Souza, R. Adamo, M. Lahmann, A. Sundgren, S. Oscarson, J.P. Kamerling, H. Snippe, Identification of the Smallest Structure Capable of Evoking Opsonophagocytic Antibodies against Streptococcus pneumoniae Type 14 , 76 (2008) 4615–4623. doi:10.1128/IAI.00472-08.

[14] K.E. Morrison, D. Lake, J. Crook, G.M. Carlone, E. Ades, R. Facklam, J.S. Sampson, Confirmation of psaA in all 90 serotypes of Streptococcus pneumoniae by PCR and potential of this assay for identification and diagnosis, J. Clin. Microbiol. 38 (2000) 434–437.

[15] J.S. Sampson, Z. Furlow, A.M. Whitney, D. Williams, R. Facklam, G.M. Carlone, Limited diversity of Streptococcus pneumoniae psaA among pneumococcal vaccine serotypes, Infect. Immun. 65 (1997) 1967–1971.

[16] P. Schmid, S. Selak, M. Keller, B. Luhan, Z. Magyarics, S. Seidel, P. Schlick, C. Reinisch, K. Lingnau, E. Nagy, B. Grubeck-Loebenstein, Th17/Th1 biased immunity to the pneumococcal proteins PcsB, StkP and PsaA in adults of different age, Vaccine. 29 (2011) 3982–3989. doi:10.1016/j.vaccine.2011.03.081.

[17] C. Entwisle, S. Hill, Y. Pang, M. Joachim, A. McIlgorm, C. Colaco, D. Goldblatt, P. De Gorguette D'Argoeuves, C. Bailey, Safety and immunogenicity of a novel multiple antigen pneumococcal vaccine in adults: A Phase 1 randomised clinical trial, Vaccine. 35 (2017) 7181–7186. doi:10.1016/j.vaccine.2017.10.076.

[18] X. Shen, T. Lagergård, Y. Yang, M. Lindblad, M. Fredriksson, G. Wallerström, J. Holmgren, Effect of pre-existing immunity for systemic and mucosal immune responses to intranasal immunization with group B Streptococcus type III capsular polysaccharide-cholera toxin B subunit conjugate, Vaccine. 19 (2001) 3360–3368. doi:10.1016/S0264-410X(00)00532-6.

[19] J.-Y. Seo, S.Y. Seong, B.-Y. Ahn, I.C. Kwon, H. Chung, S.Y. Jeong, Cross-protective immunity of mice induced by oral immunization with pneumococcal surface adhesin a encapsulated in microspheres., Infect. Immun. 70 (2002) 1143–9. doi:10.1128/iai.70.3.1143-1149.2002.

[20] A. Donadei, C. Balocchi, M.R. Romano, L. Panza, R. Adamo, F. Berti, D.T. O'Hagan, S. Gallorini, B.C. Baudner, Optimizing adjuvants for intradermal delivery of MenC glycoconjugate vaccine, Vaccine. 35 (2017) 3930–3937. doi:10.1016/j.vaccine.2017.06.018.

[21] T. Storni, M.K. Thomas, G. Senti, P. Johansen, Immunity in response to particulate antigen-delivery systems, 57 (2005) 333–355. doi:10.1016/j.addr.2004.09.008.

[22] B. Bernocchi, R. Carpentier, D. Betbeder, Nasal nanovaccines, Int. J. Pharm. 530 (2017) 128–138. doi:10.1016/j.ijpharm.2017.07.012.

[23] N. Csaba, M. Garcia-Fuentes, M.J. Alonso, Nanoparticles for nasal vaccination, Adv. Drug Deliv. Rev. 61 (2009) 140–157. doi:10.1016/j.addr.2008.09.005.

[24] J.H. Xu, W.J. Dai, B. Chen, X.Y. Fan, Mucosal Immunization with PsaA Protein, Using Chitosan as a Delivery System, Increases Protection Against Acute Otitis Media and Invasive Infection by Streptococcus pneumoniae, Scand. J. Immunol. 81 (2015) 177–185. doi:10.1111/sji.12267.

[25] D. Safari, M. Marradi, F. Chiodo, H.A. Th Dekker, Y. Shan, R. Adamo, S. Oscarson, G.T. Rijkers, M. Lahmann, J.P. Kamerling, S. Penadés, H. Snippe, Gold nanoparticles as carriers for a synthetic Streptococcus pneumoniae type 14 conjugate vaccine., Nanomedicine (Lond). 7 (2012) 651–662. doi:10.2217/nnm.11.151.

[26] R. Tada, H. Suzuki, S. Takahashi, Y. Negishi, H. Kiyono, J. Kunisawa, Y. Aramaki, Nasal vaccination with pneumococcal surface protein A in combination with cationic liposomes consisting of DOTAP and DC-chol confers antigen-mediated protective immunity against

Streptococcus pneumoniae infections in mice, Int. Immunopharmacol. 61 (2018) 385–393. doi:10.1016/J.INTIMP.2018.06.027.

[27] N.-H. Cho, S.-Y. Seong, K.-H. Chun, Y.-H. Kim, I. Chan Kwon, B.-Y. Ahn, S.Y. Jeong, Novel mucosal immunization with polysaccharide–protein conjugates entrapped in alginate microspheres, J. Control. Release. 53 (1998) 215–224. doi:10.1016/S0168-3659(97)00255-1.

[28] J. Mosafer, A. Badiee, Z. Mohammadamini, A. Komeilinezhad, M. Tafaghodi, Immunization against PR8 influenza virus with chitosan-coated ISCOMATRIX nanoparticles, Artif. Cells, Nanomedicine, Biotechnol. 46 (2018) 587–593. doi:10.1080/21691401.2018.1464460.

[29] P. Calvo, C. Remuñan-López, J.L. Vila-Jato, M.J. Alonso, Chitosan and Chitosan/Ethylene Oxide-Propylene Oxide Block Copolymer Nanoparticles as Novel Carriers for Proteins and Vaccines, Pharm. Res. 14 (1997) 1431–1436. doi:10.1023/A:1012128907225.

[30] N. Riteau, A. Sher, Chitosan: An Adjuvant with an Unanticipated STING, Immunity. 44 (2016) 522–524. doi:10.1016/J.IMMUNI.2016.03.002.

[31] C. Paget, S. Ivanov, J. Fontaine, F. Blanc, M. Pichavant, J. Renneson, E. Bialecki, J. Pothlichet, C. Vendeville, G. Barba-Spaeth, G. Barba-Speath, M.-R. Huerre, C. Faveeuw, M. Si-Tahar, F. Trottein, Potential role of invariant NKT cells in the control of pulmonary inflammation and CD8+ T cell response during acute influenza A virus H3N2 pneumonia., J. Immunol. 186 (2011) 5590–602. doi:10.4049/jimmunol.1002348.

[32] K. Kosai, M. Seki, A. Tanaka, Y. Morinaga, Y. Imamura, K. Izumikawa, H. Kakeya, Y. Yamamoto, K. Yanagihara, K. Tomono, S. Kohno, Increase of apoptosis in a murine model for severe pneumococcal pneumonia during influenza A virus infection., Jpn. J. Infect. Dis. 64 (2011) 451–7. http://www.ncbi.nlm.nih.gov/pubmed/22116322 (accessed October 17, 2019).

[33] M.J. Santander-Ortega, A.B. Jódar-Reyes, N. Csaba, D. Bastos-González, J.L. Ortega-Vinuesa, Colloidal stability of Pluronic F68-coated PLGA nanoparticles: A variety of stabilisation mechanisms, J. Colloid Interface Sci. 302 (2006) 522–529. doi:10.1016/J.JCIS.2006.07.031.

[34] M.L. Kang, H.-L. Jiang, S.G. Kang, D.D. Guo, D.Y. Lee, C.-S. Cho, H.S. Yoo, Pluronic® F127 enhances the effect as an adjuvant of chitosan microspheres in the intranasal delivery of Bordetella bronchiseptica antigens containing dermonecrotoxin, Vaccine. 25 (2007) 4602–4610. doi:10.1016/J.VACCINE.2007.03.038.

[35] C.M. Coeshott, S.L. Smithson, E. Verderber, A. Samaniego, J.M. Blonder, G.J. Rosenthal, M.A.J. Westerink, Pluronic® F127-based systemic vaccine delivery systems, Vaccine. 22 (2004) 2396–2405. doi:10.1016/J.VACCINE.2003.11.064.

[36] M. Amidi, S.G. Romeijn, J.C. Verhoef, H.E. Junginger, L. Bungener, A. Huckriede, D.J.A. Crommelin, W. Jiskoot, N -Trimethyl chitosan (TMC) nanoparticles loaded with influenza subunit antigen for intranasal vaccination : Biological properties and immunogenicity in a mouse model, 25 (2007) 144–153. doi:10.1016/j.vaccine.2006.06.086.

[37] N. Csaba, M. Köping-Höggård, M.J. Alonso, Ionically crosslinked chitosan/tripolyphosphate nanoparticles for oligonucleotide and plasmid DNA delivery, Int. J. Pharm. 382 (2009) 205–214. doi:10.1016/J.IJPHARM.2009.07.028.

[38] J. Xu, W. Dai, Z. Wang, B. Chen, Z. Li, X. Fan, Intranasal vaccination with chitosan-DNA nanoparticles expressing pneumococcal surface antigen A protects mice against nasopharyngeal colonization by Streptococcus pneumoniae, Clin. Vaccine Immunol. 18 (2011) 75–81. doi:10.1128/CVI.00263-10.

[39] A. Haryono, K. Salsabila, W.K. Restu, S.B. Harmami, D. Safari, Effect of Chitosan and Liposome

Nanoparticles as Adjuvant Codelivery on the Immunoglobulin G Subclass Distribution in a Mouse Model, J. Immunol. Res. 2017 (2017) 1–5. doi:10.1155/2017/9125048.

[40] D. Pawar, K.S. Jaganathan, Mucoadhesive glycol chitosan nanoparticles for intranasal delivery of hepatitis B vaccine : enhancement of mucosal and systemic immune response Mucoadhesive glycol chitosan nanoparticles for intranasal delivery of hepatitis B vaccine : enhancement of muco, 7544 (2016). doi:10.3109/10717544.2014.908427.

[41] W. Xu, Y. Shen, Z. Jiang, Y. Wang, Intranasal delivery of chitosan – DNA vaccine generates mucosal SIgA and anti-CVB3 protection, 22 (2004) 3603–3612. doi:10.1016/j.vaccine.2004.03.033.

[42] R. Fernández-Urrusuno, P. Calvo, C. Remuñán-López, J.L. Vila-Jato, M. José Alonso, Enhancement of Nasal Absorption of Insulin Using Chitosan Nanoparticles, Pharm. Res. 16 (1999) 1576–1581. doi:10.1023/A:1018908705446.

[43] T. Neimert-Andersson, A.C. Hällgren, M. Andersson, J. Langebäck, L. Zettergren, J. Nilsen-Nygaard, K.I. Draget, M. van Hage, A. Lindberg, G. Gafvelin, H. Grönlund, Improved immune responses in mice using the novel chitosan adjuvant ViscoGel, with a Haemophilus influenzae type b glycoconjugate vaccine, Vaccine. 29 (2011) 8965–8973. doi:10.1016/j.vaccine.2011.09.041.

[44] S.L. Nail, S. Jiang, S. Chongprasert, S.A. Knopp, Fundamentals of Freeze-Drying, in: Springer, Boston, MA, 2002: pp. 281–360. doi:10.1007/978-1-4615-0549-5_6.

[45] S. Gordon, A. Saupe, W. McBurney, T. Rades, S. Hook, Comparison of chitosan nanoparticles and chitosan hydrogels for vaccine delivery, J. Pharm. Pharmacol. 60 (2008) 1591–1600. doi:10.1211/jpp.60.12.0004.

[46] C. Bulmer, A. Margaritis, A. Xenocostas, Production and characterization of novel chitosan nanoparticles for controlled release of rHu-Erythropoietin, Biochem. Eng. J. 68 (2012) 61–69. doi:10.1016/J.BEJ.2012.07.007.

[47] T. Nakamura, D. Yamazaki, J. Yamauchi, H. Harashima, The nanoparticulation by octaarginine-modified liposome improves α-galactosylceramide-mediated antitumor therapy via systemic administration, J. Control. Release. 171 (2013) 216–224. doi:10.1016/j.jconrel.2013.07.004.

[48] L.J. Carreño, S.S. Kharkwal, S.A. Porcelli, Optimizing NKT cell ligands as vaccine adjuvants, Immunotherapy. 6 (2014) 309–320. doi:10.2217/imt.13.175.

[49] S.-Y. Ko, H.-J. Ko, W.-S. Chang, S.-H. Park, M.-N. Kweon, C.-Y. Kang, α-Galactosylceramide Can Act As a Nasal Vaccine Adjuvant Inducing Protective Immune Responses against Viral Infection and Tumor, J. Immunol. 175 (2005) 3309–3317. doi:10.4049/jimmunol.175.5.3309.

[50] C.J.H. Davitt, S. Longet, A. Albutti, V. Aversa, S. Nordqvist, B. Hackett, C.P. McEntee, M. Rosa, I.S. Coulter, M. Lebens, J. Tobias, J. Holmgren, E.C. Lavelle, Alpha-galactosylceramide enhances mucosal immunity to oral whole-cell cholera vaccines, Mucosal Immunol. 12 (2019) 1055–1064. doi:10.1038/s41385-019-0159-z.

[51] G. Lu, A. Zhou, M. Meng, L. Wang, Y. Han, J. Guo, H. Zhou, H. Cong, Q. Zhao, X.Q. Zhu, S. He, Alpha-galactosylceramide enhances protective immunity induced by DNA vaccine of the SAG5D gene of Toxoplasma gondii, BMC Infect. Dis. 14 (2014). doi:10.1186/s12879-014-0706-x.

[52] C. Papadea, I.J. Check, Human Immunoglobulin G and Immunoglobulin G Subclasses: Biochemical, Genetic, and Clinical Aspects, Crit. Rev. Clin. Lab. Sci. 27 (1989) 27–58. doi:10.3109/10408368909106589.

[53] S.M. Bal, B. Slütter, R. Verheul, J.A. Bouwstra, W. Jiskoot, Adjuvanted, antigen loaded N-trimethyl chitosan nanoparticles for nasal and intradermal vaccination: Adjuvant- and site-dependent immunogenicity in mice, Eur. J. Pharm. Sci. 45 (2012) 475–481. doi:10.1016/J.EJPS.2011.10.003.

[54] M. González-Miro, L. Rodríguez-Noda, M. Fariñas-Medina, D. García-Rivera, V. Vérez-Bencomo, B.H.A. Rehm, Self-assembled particulate PsaA as vaccine against Streptococcus pneumoniae infection., Heliyon. 3 (2017) e00291. doi:10.1016/j.heliyon.2017.e00291.

[55] C.F.M. Vadesilho, D.M. Ferreira, A.T. Moreno, C. Chavez-Olortegui, R.A. Machado de Avila, M.L.S. Oliveira, P.L. Ho, E.N. Miyaji, Characterization of the antibody response elicited by immunization with pneumococcal surface protein A (PspA) as recombinant protein or DNA vaccine and analysis of protection against an intranasal lethal challenge with Streptococcus pneumoniae, Microb. Pathog. 53 (2012) 243–249. doi:10.1016/J.MICPATH.2012.08.007.

[56] R. Palaniappan, S. Singh, U.P. Singh, S.K.K. Sakthivel, E.W. Ades, D.E. Briles, S.K. Hollingshead, J.C. Paton, J.S. Sampson, J.W. Lillard, Jr., Differential PsaA-, PspA-, PspC-, and PdB-specific immune responses in a mouse model of pneumococcal carriage., Infect. Immun. 73 (2005) 1006–13. doi:10.1128/IAI.73.2.1006-1013.2005.

[57] S.M. Bal, B. Slütter, R. Verheul, J.A. Bouwstra, W. Jiskoot, Adjuvanted, antigen loaded N-trimethyl chitosan nanoparticles for nasal and intradermal vaccination: Adjuvant- and site-dependent immunogenicity in mice, Eur. J. Pharm. Sci. 45 (2012) 475–481. doi:10.1016/j.ejps.2011.10.003.

[58] J.-H. Xu, W.-J. Dai, B. Chen, X.-Y. Fan, Mucosal Immunization with PsaA Protein, Using Chitosan as a Delivery System, Increases Protection Against Acute Otitis Media and Invasive Infection by *Streptococcus pneumoniae*, Scand. J. Immunol. 81 (2015) 177–185. doi:10.1111/sji.12267.

[59] R. Scherließ, S. Buske, K. Young, B. Weber, T. Rades, S. Hook, In vivo evaluation of chitosan as an adjuvant in subcutaneous vaccine formulations, Vaccine. 31 (2013) 4812–4819. doi:10.1016/J.VACCINE.2013.07.081.

[60] P. Watts, A. Smith, M. Hinchcliffe, ChiSys® as a Chitosan-Based Delivery Platform for Nasal Vaccination, in: Mucosal Deliv. Biopharm., Springer US, Boston, MA, 2014: pp. 499–516. doi:10.1007/978-1-4614-9524-6_23.

[61] D.A. Zaharoff, C.J. Rogers, K.W. Hance, J. Schlom, J.W. Greiner, Chitosan solution enhances both humoral and cell-mediated immune responses to subcutaneous vaccination, Vaccine. 25 (2007) 2085–2094. doi:10.1016/J.VACCINE.2006.11.034.

[62] Z.-S. Wen, Y.-L. Xu, X.-T. Zou, Z.-R. Xu, Chitosan nanoparticles act as an adjuvant to promote both Th1 and Th2 immune responses induced by ovalbumin in mice., Mar. Drugs. 9 (2011) 1038–55. doi:10.3390/md9061038.

USC
UNIVERSIDADE
DE SANTIAGO
DE COMPOSTELA

Chapter 3

Interaction of glycoconjugate loaded chitosan nanoparticles with human dendritic cells

This work was performed in collaboration with Department of Biochemistry and Molecular Biology, School of Pharmacy (USC).

USC
UNIVERSIDADE
DE SANTIAGO
DE COMPOSTELA

Interaction of glycoconjugate loaded chitosan nanoparticles with human dendritic cells

Abstract

Nanoparticle delivery systems have been extensively studied for vaccination, as they can enhance the immunogenicity of antigens by protecting them from degradation and increasing their uptake by antigen presenting cells. Despite their potential utilisation, their clinical application is limited due to the lack of knowledge on the interaction of the nanoparticles with the immune system. This study was focused on understanding the presentation of glycoconjugate (GC) loaded chitosan nanoparticles (CNPs) by human monocyte-derived dendritic cells (MoDCs). For this purpose, GC loaded chitosan nanoparticles (GC-CNPs) were investigated for their compatibility with immune cells, uptake and immuno-stimulatory properties. The glycoconjugate (Pn14TS-PsaA/GC) encapsulated in the CNPs was earlier synthesised and characterized in our laboratory. The nanoparticles were compatible with DCs. Flow cytometry and confocal microscopy analysis confirmed that DCs internalized GC-CNPs within 2h. GC-CNPs promoted DC maturation and enhanced expression of the co-stimulatory molecules CD80, CD83 and CD86. Furthermore, significant activation of CD8+ T cells was observed in the DCs treated with the CNPs. The GC-CNPs treated DCs showed an increased proinflammatory cytokine (TNF-α) response in comparison to the GC alone. In conclusion, the encapsulation of the GC in CNPs showed the enhanced uptake and displayed better immunostimulatory properties in comparison to the naked GC.

Keywords: Chitosan, Nanoparticles, Glycoconjugate**,** Dendritic cells, Pneumococcal surface adhesin-A, Immunology

Graphical Abstract

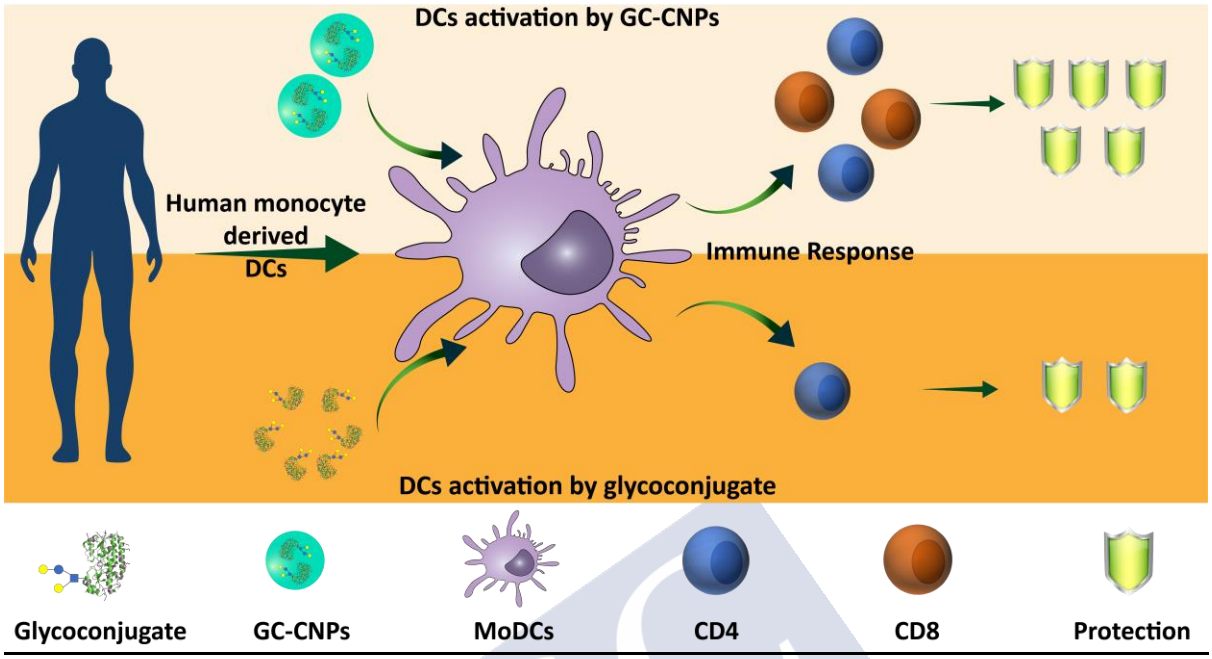

1. Introduction

The central hallmark for effective vaccination is to prime the adaptive immune response. This requires the activation of naive B and T lymphocytes into effectors cells that translate into protective immunity. Dendritic cells (DCs) are the primary antigen presenting cells (APCs) that play a key role in the orchestration of the humoral and cell-mediated immunity [1,2]. As APCs, DCs act as the connection between innate and adaptive arms of the immune system [2,3]. For the presentation of the antigens by DCs, it is crucial that the DCs undergo maturation and express high levels of MHC-II and other co-stimulatory molecules like CD80 and CD86. Having the capacity to capture and process the exogenous antigens, DCs can effectively stimulate naive T cells against them.

The quest for safer vaccines has increased the demand for the subunit vaccines that are composed of purified bacterial or viral components. Most of these newly developed sub-unit vaccines are weakly immunogenic [4,5]. Their poor immunogenicity is attributed to the small size and the lack of pathogen-associated molecular patterns that are essential for antigen recognition. In order to trigger the immune response, the subunit vaccines are co-administered with the adjuvants or delivered via particulate systems. The major hurdle of developing an effective and successful vaccine is to design antigen delivery systems showing broad protective immune responses.

The nanoparticle-based delivery systems offer several advantages due to their physicochemical characteristics like particle size, surface charge, and immunostimulatory properties [6,7]. They tend to mimic the pathogens with their size, shape and often by carrying the antigens at the surface [8,9]. They can form a depot at the site of administration

and control the release of the antigen [10,11]. In recent years, the use of biocompatible and biodegradable polymers has been investigated as adjuvants and antigen carriers. Polymers like chitosan, alginate, protamine, dextran, hyaluronic acid, and poly(lactic-co-glycolic acid) (PLGA) have been investigated for protein/peptide [12] or DNA-based vaccines [13]. Amongst them, chitosan is a nontoxic, biocompatible, biodegradable and mucoadhesive natural polymer, that is considered as an excellent biomaterial for the design of antigen carriers [14]. As an immune adjuvant, chitosan is known to enhance humoral and cellular immunity [15]. Despite their positive attributes, limitations such as burst release, poor mechanical properties and stability in biological media pose a stiff challenge to their universal acceptability as a drug carrier [16]. However, the previously mentioned positive attributes of the chitosan nanoparticles dominate its shortcomings. Therefore, these properties fostered researchers to adopt chitosan nanoparticles (CNPs) as a carrier for vaccine delivery.

In our previous studies, we produced a synthetic mimic of *S. pneumoniae* type 14 capsular polysaccharide (Pn14TS) and conjugated it to pneumococcal surface adhesin A (PsaA), using thiol maleimide coupling chemistry to obtain a semisynthetic glycoconjugate. The immunization studies in mice have shown that synthesized glycoconjugate (Pn14TS-PsaA/GC) was able to induce the production of IgGs against both the synthetic oligosaccharide and the protein moieties [17]. In the present study, the GC loaded CNPs were prepared by the ionic gelation method [12], and a systematic study was performed to understand the influence of the CNPs in presenting the GC to the APCs. For this purpose, PsaA, GC, blank CNPs and GC loaded CNPs (GC-CNPs), were compared in a systematic study. This included the *in vitro* evaluation of antigen uptake and their localization in the DCs and upregulation of the costimulatory markers. To further demonstrate the applicability of CNPs as a potential

antigen carrier, the studies on DC stimulation and DC-mediated T lymphocyte stimulation were performed.

2. Materials and Methods

2.1. Materials

Pneumococcal surface adhesin A (PsaA) and GC were produced and synthesised respectively at UFIP, University of Nantes [17]. The cytokines IL-4, GM-CSF, INF-γ were procured from Miltenyi Biotech. PBS (pH 7.2), RPMI 1640, PSG 100X and fetal bovine serum (FBS) were obtained from Gibco, Life technologies. Ficoll Histopaque 1077, paraformaldehyde, DAPI, Triton X-100 and pentasodium tripolyphosphate were procured from Sigma Aldrich. The pharmaceutical grade water-soluble chitosan with an acetylation degree of 80% was purchased from HMC^{+} biopolymers. Kolliphor P 188 was obtained as a gift sample from BASF. All the antibodies used for FACS analysis were either obtained from Miltenyi Biotech or Sigma Aldrich. Pierce Chromogenic Endotoxin Quant Kit (A39552) was procured from Thermo Fischer Scientific. The Cy5-NHS was purchased from Lumiprobe. The gel filtration columns (centripure PD10 columns) were obtained from EMP Biotech. All the other chemicals and reagents used were analytical grade.

2.2. Preparation of antigen loaded chitosan nanoparticles

Chitosan nanoparticles (CNPs) were prepared by the ionotropic gelation of chitosan with tripolyphosphate (TPP), according to the method previously reported by our group [12]. In brief, glycoconjugate-loaded chitosan nanoparticles (GC-CNPs) were fabricated by adding 500 µL of TPP (0.4 mg/mL) to 1 mL of chitosan (0.1% w/v) in 1% poloxamer 188 containing 50 µg of GC and kept under magnetic stirring (1000 rpm) for 1h. The polymer to antigen ratio was 20:1 and the polymer to crosslinker ratio was 5:1. Nanoparticles were separated by

centrifugation at 12,000 g for 12 min. Supernatants were discarded, and particles were resuspended in ultrapure water.

The hydrodynamic diameter and polydispersity index (PDI) of the particles were determined by dynamic light scattering (DLS) and the zeta potential was measures by laser doppler anemometry using a Zetasizer Nano-ZS90 (Malvern Instruments; Malvern, UK). All the measurements were performed at 25 °C with a detection angle of 173° in distilled water, unless otherwise indicated.

2.3. Preparation of Cy5 labelled nanoparticles

For *in vitro* studies the CNPs were fluorescently labelled with Cy5. For this, during the preparation of the CNPs, 2% of chitosan was replaced with the Cy5-labelled chitosan (Cy5-chitosan). The detailed synthesis of Cy5-chitosan is mentioned in the previous chapter (Chapter 2; Section 2.3).

2.4. Endotoxin testing

The quantification of endotoxins in the samples used for DC cell studies was performed using the Pierce Chromogenic Endotoxin Quant Kit (A39552). Briefly, 2 micrograms of antigen (PsaA or GC) or 50 micrograms of chemicals (Chitosan, Kolliphor-188 or TPP) were suspended in water and tested for the presence of endotoxin according to the manufacturer's instructions [18]. The calibration curve (0.1–8 EU/mL) was constructed using a stock solution of 10 EU/mL. To avoid external endotoxin interference, all the dilutions were prepared in endotoxin-free water, which was also used as blank. All the tubes and tips used to perform this quantification were endotoxin-free and the entire procedure was performed inside of a laminar flow cabinet.

2.5. Donor selection and blood collection

Buffy-coats used in the experiments were obtained from anonymous donors and were kindly donated by the Agency for the Donation of Organs and Blood (ADOS, Santiago de Compostela) with the approval of the Director of the Agency and the Clinical Research Ethics Committee of Galicia (2014/543). Freshly obtained buffy coats were used within 24h. Heparinized blood samples were obtained from healthy volunteers among the staff of Faculty of Pharmacy, University of Santiago de Compostela, and CiMUS. Before the collection, informed consent was obtained from the volunteers in accordance with the guidelines of the Ethical Committee of Clinical Research of Galicia.

2.6. Dendritic Cell (DC) and Peripheral blood lymphocytes (PBLs) generation

Peripheral blood mononuclear cells (PBMCs) were isolated by Ficoll gradient centrifugation method. Adherent monocytes were isolated by incubating PBMCs in culture plates (2h, 37 °C) in R2 culture media (RPMI-1640 completed with 2% of FBS). After the incubation period, non-adherent cells were washed thrice with PBS and adherent monocytes were cultured for six days in R10 media (RPMI-1640 completed with 10% FBS) supplemented with GM-CSF and IL-4 (100 ng/mL each). After three days, half of the media was replaced with fresh R10 supplemented with equal amounts of cytokines. The resultant immature DCs (iDCs) were scraped and collected from the culture plates on day 6. These iDCs were used for further experimentation.

Mature DCs (mDCs) were obtained by incubation of iDCs with bacterial lipopolysaccharide (LPS) (10 ng/mL) and interferon-γ (IFN-γ) (100 U/mL) for 48h. The peripheral blood lymphocytes (PBLs) required for the allogenic stimulation experiments were collected by

washing the non-adherent cells after incubating the PBMCs for 2h at 37 °C and these non-adherent PBLs were stored in liquid nitrogen until further use.

2.7. Cytocompatibility Studies

The cytocompatibility assay of GC-CNPs in the DCs was performed by MTS (3-(4,5-dimethylthiazol-2-yl)-5-(3-carboxymethoxyphenyl)-2-(4-sulfophenyl)-2H-tetrazolium) assay. The generated iDCs (1 x 10^5 cells/mL) were incubated with different concentrations of the CNPs (25, 50, 100, 200, 400 and 900 µg/mL) for 24h. The untreated iDCs were used as a positive control. After 24h incubation with the CNPs, the cells were washed with PBS and were incubated with fresh R10 media for another period of 24h, and 20 µL of MTS reagent was added to each well after 20h and incubated for another 4h. The intensity of colour was quantified by measuring the absorbance at 490 nm using a spectrophotometer. The results were plotted as percentage (%) viability v/s the nanoparticle concentration. The percentage viability is a difference of metabolically active cells in the untreated group and the groups treated with the nanoparticles.

The cytocompatibility of blank CNPs and GC-CNPs was also studied using 7-amino actinomycin D (7-AAD). Briefly, following the incubation of iDCs with blank CNPs or GC-CNPs (25, 50, 100, 200, 400 and 900 µg/mL) for 24h, cells were harvested, washed twice with PBS and stained with 7 AAD (1 µL per tube (0.05 µg/µL)), for 30 min at 4 °C. After washing 3 times with PBS containing 2% BSA, the cells were analysed by flow cytometry (BD FACS Calibur™ cytometer). Data were analysed using Flowing software (Cell Imaging Core, Turku Centre for Biotechnology, Finland). Data are shown as the percentage of cells viable after incubating with the different concentrations of nanoparticles.

2.8. The study on internalization of nanoparticles by DCs

To evaluate the time-dependent uptake of CNPs by human MoDCs, iDCs ($5x10^5$ per well) were plated into a 24-well plate with 0.5 mL of R10 media. Immediately, Cy5-labelled GC-CNPs (Cy5-GC-CNPs) were added at a concentration of 50 µg/mL. At different time intervals (0, 0.5, 1, 2 and 4h of incubation), cells were collected for uptake analysis. The collected cells were washed immediately with PBS and fixed in a flow cytometry tube using 200 µL of PBS containing 1% paraformaldehyde (1% PFA). As a control, the MoDCs treated with an equal amount of CNPs at 4 °C was used. The samples were diluted with 500 µL of PBS, and the suspension was analysed by flow cytometry (BD FACS Calibur™ cytometer). The surface morphology of the macrophages incubated with the nanoparticles (50 µg/mL, for 0.5 h, at 37 °C) was performed using FESEM, (ZEISS FESEM ULTRA Plus, Germany).

In addition, uptake studies were performed in the cells ($5 x 10^5$ cells per well) pre-treated with chlorpromazine (CLO), cytochalasin D (Cit-D), dimethyl amiloride (DHA) in R10 medium for 1h at 37 °C. Next, the Cy5-GC-CNPs (50 µg/mL) were added to iDCs and incubated for 4h at 37 °C. Afterwards, the iDCs were collected by pipetting, washed twice (300 x g, 7 min, 4 °C) with PBS and fixed using 4% PFA (15 min, RT). The uptake of the nanoparticles in the DCs treated with inhibitors was determined using flow cytometry and compared against uptake in the untreated iDCs.

For CSLM analysis, the DCs ($5x10^5$ per well) were plated into a 24-well plate with 0.5 mL of R10 media and incubated for 30 min. Following that the DCs were incubated with the Cy5 labelled GC-CNPs for 1h. After the incubation time, the DCs were washed with PBS and seeded at a density of $1 x 10^5$ onto the poly-L-lysine coated coverslips and allowed to adhere for 15

min. Afterwards, the cells were fixed with 4% PFA for 15 min. The DCs were permeabilized/ fixed using 100 µL of BD Citofix / Citoperm™ (15 min, RT, in the dark) and were washed twice with PBS. The cells were stained using DAPI and phalloidin-488 and fixed on the glass slide using mounting medium (Vectashield® Antifade Mounting Medium, Vector Labs, USA). The image acquisition was made using CLSM (Leica SP5, Mannheim, Germany). Excitation wavelengths were 670 nm for Cy5 and 488 nm for Alexa 488.

2.9. Study on effect of GC-CNPs on DC maturation by phenotypic analysis

For the phenotypic analysis, the iDCs were seeded on 24 well plates at a density of 5 x 10^5 cells per well 0.5 mL of R10 media. The DCs were incubated for 48 h at 37 °C in R10 with blank or GC-CNPs using LPS (10 ng/mL) as a positive control. After 48 h of incubation, the generated DCs were collected, washed twice (300 x g, 7 min, 4 °C) with PBS containing 0.1% BSA. DCs were resuspended in 200 µL of PBS with 1% FCS (1% PBS), of this 100 µL of the DCs were incubated with 50x diluted anti-CD83-PE, anti-CD86-APC and anti-CD1a, another 100 µL with 50× diluted anti-CD80-PE, anti-HLA-APC and anti-CD1a-FITC (in all cases, for 30 min, in dark, on ice). CD1a was included as a DC marker to verify correct monocyte differentiation. After the 30-minute staining period, the cells were harvested, washed thrice with 1% PBS and resuspended in 500 µL of PBS. The DCs were quantified for the expression of CD80, CD83, CD86 and HLA using flow cytometry (BD FACS Calibur ™ flow cytometer; BD Biosciences, Madrid). The cytometry data were analysed using the Flowing software program (Cell Imaging Core, Turku Centre for Biotechnology, Finland). The forward versus side scattering was used for gating the live cells and the CD1a positive cells were picked for the quantification of co-stimulatory markers. The expression of cytokines from the CNPs treated DCs were compared against the LPS treated DCs, assuming 100% maturation.

2.10. T cell stimulation by GC-CNPs

Heparinized whole blood was taken from 4 healthy human volunteers and the peripheral blood mononuclear cells (PBMCs) were collected by Ficoll Histopaque density gradient centrifugation and washed twice with ice-cold PBS. Collected PBMCs were seeded in 24 well plates at a density of 1.0×10^6 per well using 0.5 mL of R10 media. The PBMCs were treated with different components of formulation (Pn14TS, PsaA, GC, Blank CNPs and GC-CNPs). The DCs treated with Staphylococcus Enterotoxin-B (SEB), LPS were used as positive controls and the untreated DCs were used as control and incubated for 48h at 37 °C. After 48h incubation, brefeldin (5 µg/mL) was added to block the cytokine secretion and incubated at 37 °C overnight. The following day, the cells were harvested, washed with 1% PBS. Further, the cells were stained with 5 µL CD3-FITC, washed twice with 1% PBS and were fixed using 1% PFA for 15 min at RT. The cells were centrifuged and permeabilized with BD Citofix / Citoperm™ (15 min, RT, in the dark), and the cells were resuspended in 100 µL of Citofix / Citoperm™. The staining was performed by adding 5 µL of TNF-α-PE for each tube (30 min, on ice, in the dark). The cells were washed twice using Citofix / Citoperm™ and resuspended in 0.5 mL of PBS and analysed by using flow cytometry (BD FACS Calibur™ flow cytometer; BD Biosciences, Madrid).

2.11. Activation of allogenic T cells by antigen primed DCs

The immature DCs (iDCs) and the non-adherent cells (peripheral blood lymphocytes, PBLs) were obtained according to the methods mentioned (**Section 2.6)**. Mature DCs (mDCs) were obtained by incubation of iDCs with bacterial lipopolysaccharide (LPS) (10 ng/mL) and interferon-γ (IFN-γ) (100 U/mL) for 48h. The capacity of iDCs pre-incubated with the PsaA, NPs and in combination (PsaA + CNPs) to activate CD4+ and CD8+ T lymphocytes in an

allogenic culture was determined by flow cytometry. Briefly, after incubation of iDCs with the CNPs (50 µg/mL) and PsaA (2 µg/mL) for 24h, cells were harvested, washed with PBS and plated with allogenic T cells (non-adherent PBLs) at a 1: 10 ratio (DC: T) for 7-10 days. After the activation and proliferation period, cells were harvested, washed and stained with 5 µL of CD8-FITC and CD28-PE or CD4-APC and CD25-PE antibodies and analysed by using flow cytometry (BD FACS Calibur™ flow cytometer; BD Biosciences, Madrid).

2.12. Statistical Analysis

The statistical analysis was performed using GraphPad prism 7 software. The 2way ANOVA Bonferroni's multiple comparison test, one-way ANOVA with Kruskal-Wallis analysis by Dunn's multiple comparison test and one-way ANOVA with Bonferroni's multiple comparison test were used to calculate statistical significance.

3. Results and Discussion

3.1. Nanoparticles preparation and characterization

The aqueous dispersion of CNPs had an average diameter of 140 ± 4 nm and the zeta potential of 32.3 ±0.2 mV. The PDI of the GC-CNPs was shown to be less than 0.2, indicating the homogeneity of the nanoparticles. Next, encapsulation efficiency of the protein GC loaded in the CNPs was analysed and was found to be 70 ±3%. To track the uptake of CNPs, the nanoparticles were prepared by using Cy5-labelled chitosan. The particle size analysis showed the Cy5-GC-CNPs had an average diameter of 150 ±9 nm and zeta potential of 30 ±2 mV. All the components used in the preparation of CNPs were assayed for the detection of endotoxin activity using the end-point chromogenic Limulus Amoebocyte assay (LAL test). Endotoxin content was lower than 0.5 EU/µg in all the cases (**Figure 1**), which are far below the maximum recommended endotoxin levels for recombinant subunit vaccines (20 EU/mL) [19]. The

colloidal stability of the nanoparticles was evaluated by measuring their size and PDI in the R10 medium and was found to be concentration dependent. The aggregation of the CNPs was observed when the concentrations were above 500 µg/mL in R10 media after 24h. Below this concentration, the NPs showed no signs of aggregation (data not shown).

A

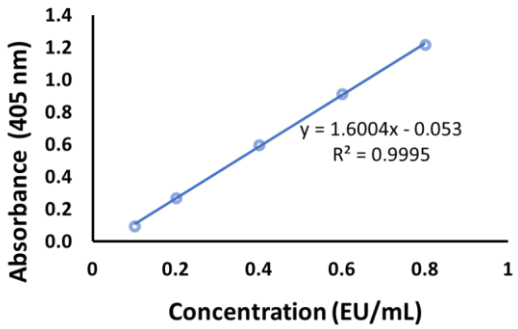

B

Formulation Components	ng/µg	EU/ µg
mPsaA	0.000734	0.007342
GC	0.035147	0.351475
Chitosan	0.000004	0.000037
Poloxamer	0.000009	0.000095
TPP	0.000003	0.000033

Figure 1. Endotoxin analysis of CNPs formulation components. A) The calibration curve used to quantify the endotoxin level in the formulation components. **B)** Endotoxin quantification in the different CNPs components. As can be seen, all of them shows levels below 0.5 EU/µg.

3.2. In vitro evaluation of dendritic cells viability in the presence of chitosan nanoparticles

To study the influence of the GC-CNPs concentration on the metabolic activity and/or survival of iDC an MTS assay was performed. As seen in **Figure 2A**, the GC-CNPs displayed the dose-dependent reduction in the metabolic activity of iDCs. Over 80% of the iDCs were metabolically active when treated with GC-CNPs in the concentration range of 25 to 100 µg/mL. Whereas, the metabolic activity was reduced to 60% in the concentrations of 200 to 400 µg/mL and significantly reduced down to 40% when treated with 900 µg/mL of GC-CNPs. The results suggest that the GC-CNPs at a concentration of 25 to 100 µg/mL were in the acceptable non-toxic range. The toxicity seen at the higher concentrations might be due to the possibility of the nanoparticle aggregation at higher concentrations after 12h. However, to mitigate the risk of the nanoparticle aggregation, the CNPs were used in the concentrations

of 0.1 mg/mL or lower. In this regard, the GC-CNPs at a concentration of 50 µg/mL was adopted for further studies.

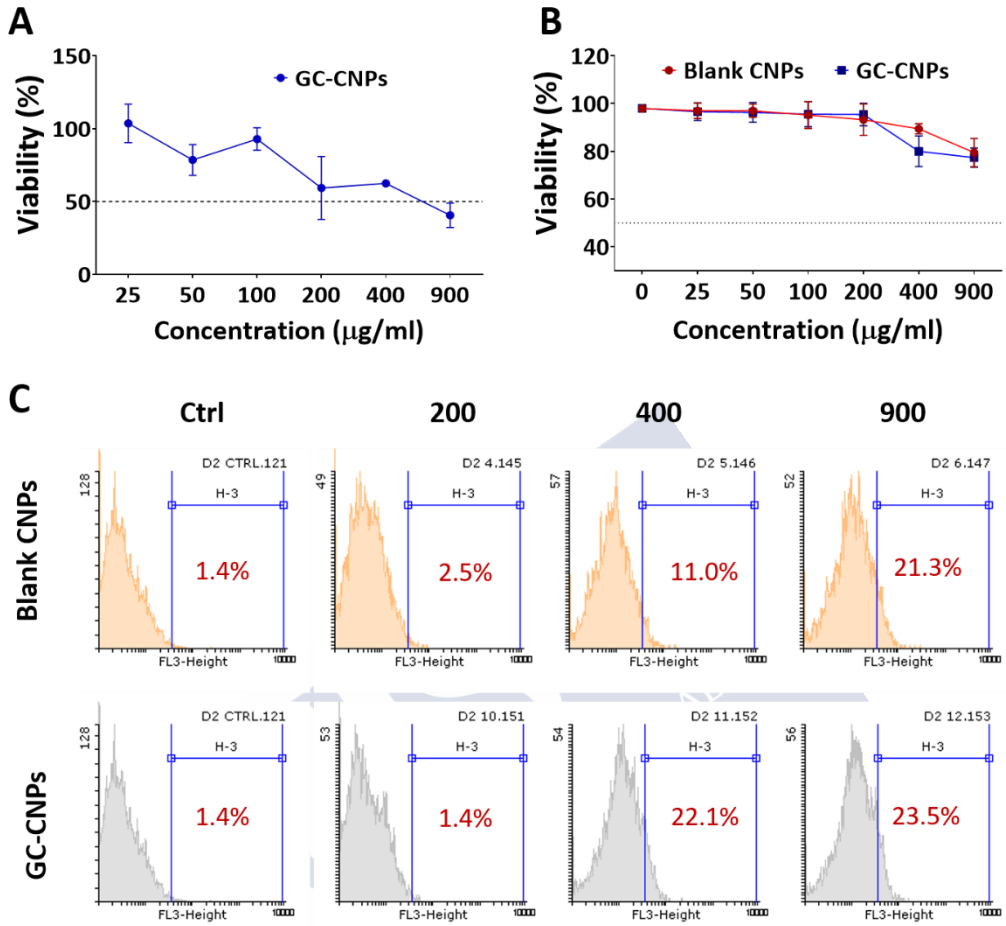

Figure 2. **Chitosan Nanoparticles (CNPs) cytotoxicity on immature dendritic cells (iDCs). A)** MTS staining assay; **B)** 7-AAD assay was performed for both GC-CNPs (blue lines) and blank CNPs (red lines) and **C)** Representative histograms obtained from flow cytometric analysis after 7-AAD staining. Results are presented as mean± SD from 4 donors.

In a likely manner, the cytocompatibility of the nanoparticles with DCs was studied using 7 AAD assay. 7 AAD is a fluorescent DNA dye that can pass the plasma membrane of the cell which is apoptotic or dead. The dose-dependent mortality of the DCs was observed in **Figure 2B**. The GC-CNPs at the concentration range of 25 to 200 µg/mL displays over 90% survival and 80% at 400 µg/mL. At the highest concentration of 900 µg/mL, the DCs displayed 75% survival (see also **Figure 2C** for representative histograms). However, the mortality of the DCs were not more than 25% in any case. Both the blank CNPs and GC-CNPs had a similar profile

of cytocompatibility and considered to be least toxic to DCs at the concentrations below 200 µg/mL.

3.3. The GC-CNPs are effectively internalized by the DCs

The uptake of GC-CNPs in DCs was studied as the function of incubation time at different temperatures of incubation. As can be seen in **Figure 3A**, the pattern of GC-CNPs (50 µg/mL) internalization in DCs at 37 °C shows greater uptake with the increase in incubation time. However, only 10% increase in the GC-CNPs uptake was observed between 2h and 4h of incubation at 37 °C. While the DCs incubated at 4 °C as a control (treated with 50 µg/mL of GC-CNPs), did not show any significant uptake of GC-CNPs even after 4h, showing a specific energy-dependent nanoparticle uptake at 37 °C.

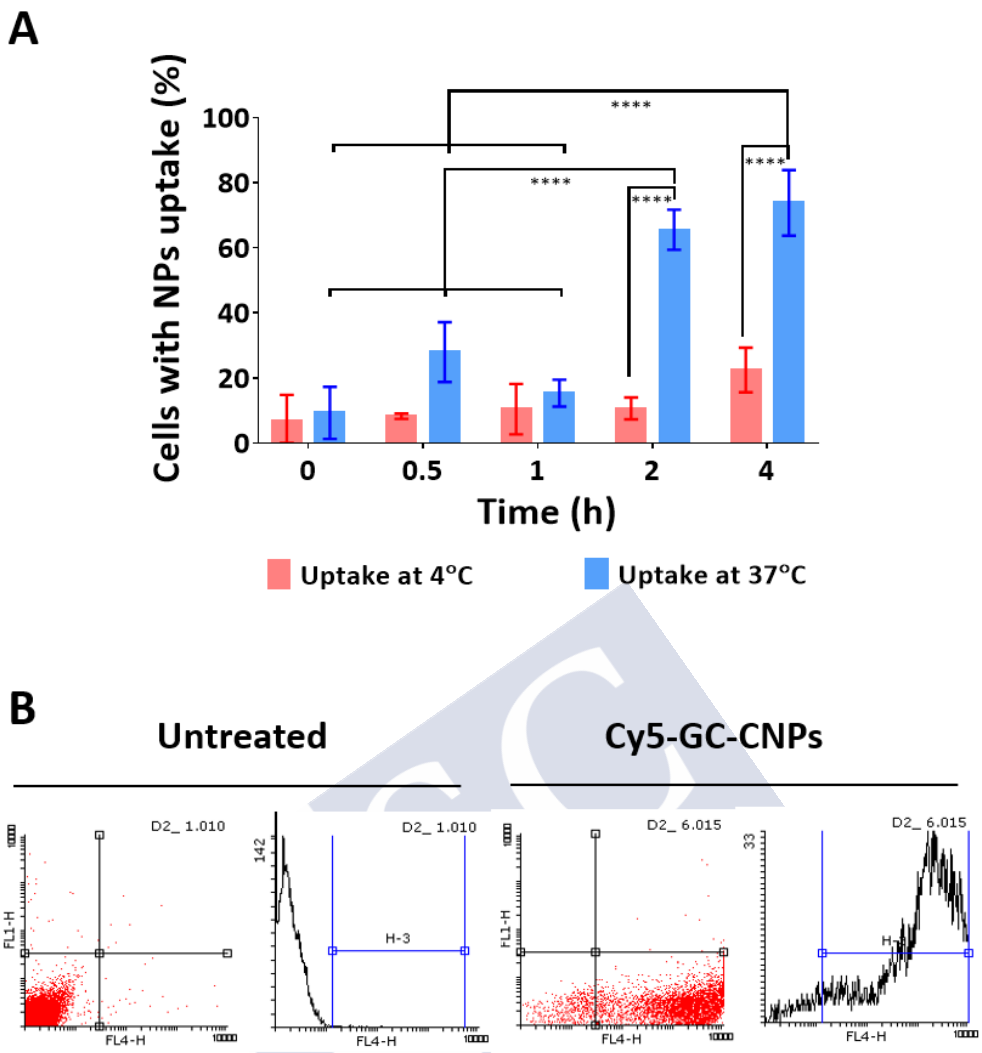

Figure 3: The internalization of the Cy5-GC-CNPs are studied in MoDCs. As shown in **(A)** Time-dependent uptake of Cy5-labeled GC-CNPs (50 µg/mL) at 4 °C and 37 °C analyzed by flow cytometry. **(B)** Comparison of untreated DCs with Cy5-GC-CNPs (50 µg/mL for 2 h at 37 °C) treated DCs, is represented as dot plot and histogram. Results are presented as mean± SD from 3 donors. Statistical difference between the groups is *, $P < 0.05$; **, $P < 0.01$; ***, $P < 0.001$; ****, $P < 0.0001$.

Further to this, the CLSM was used to examine the localization of GC-CNPs in DCs. For the intracellular localization the nanoparticles were probed with Cy5. In the **Figure 4A** the co-localization of Cy5-GC-CNPs (red) and the nucleus stain (blue) confirms the uptake of nanoparticles by the DCs. The z-stack of the images in **Figure 4A** confirms the internalization of the nanoparticles by DCs. Further, cytoskeleton labelling (phalloidin-488, green) of the DCs were performed to see if the nanoparticles were associated with the cell membrane or completely internalized. The Z-stack of the images in the **Figure 4B** confirms that the

nanoparticles were mostly inside the DCs with very slight or no adsorption to the surface of DCs.

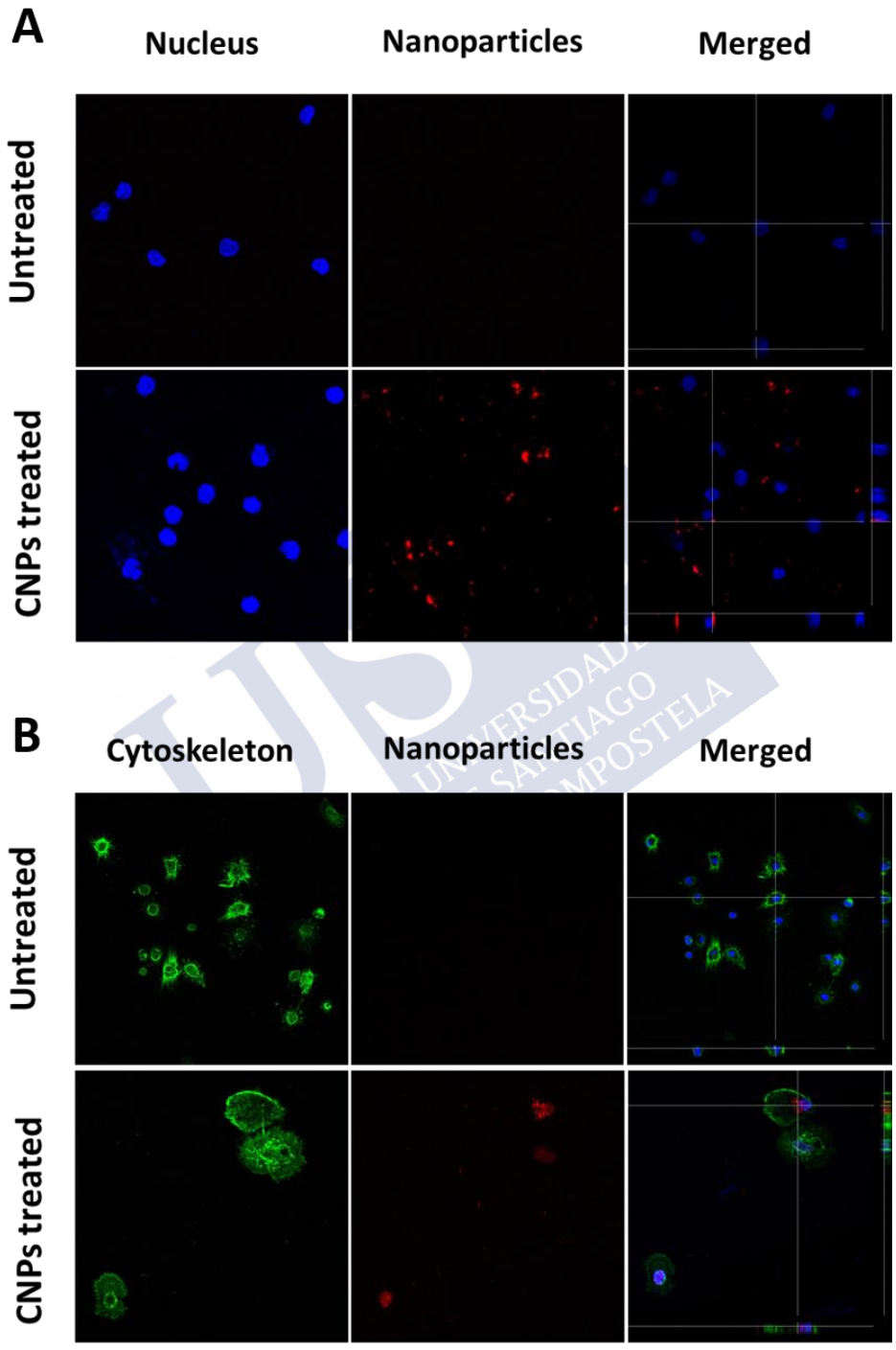

Figure 4: **Internalization of the Cy5-GC-CNPs in DCs.** Confocal microscopy images of the DCs incubated without or with Cy5-GC-CNPs. **(A)** DCs with DAPI staining and **(B)** DCs with cytoskeleton staining using phalloidin-488 (F-actin) and nucleus staining using DAPI. Red channel: Cy5-GC-CNPs; blue channel: cell nuclei; green channel: cytoskeleton.

In the **Figure 5B**, from the micrographs obtained from FEG-SEM, we can visualize the uptake of GC-CNPs by the DCs. This was observed after 0.5h of co-incubation of the GC-CNPs with the DCs. During the sample preparation for imaging, the monocytes undergo a series of washings to retain only the GC-CNPs firmly attached to the cell membrane and this helps in visualization of the nanoparticles that are being internalized by the DCs and not the nanoparticles that are adsorbed to the cell surface. The red arrow marks in the **Figure 5B** indicate the nanoparticles that are being internalized by DCs. In addition, the film that can be observed on the nanoparticles might be the cell membrane that is ruffling around the nanoparticle for their internalization. However, these studies are preliminary and further studies are in progress to understand this in detail.

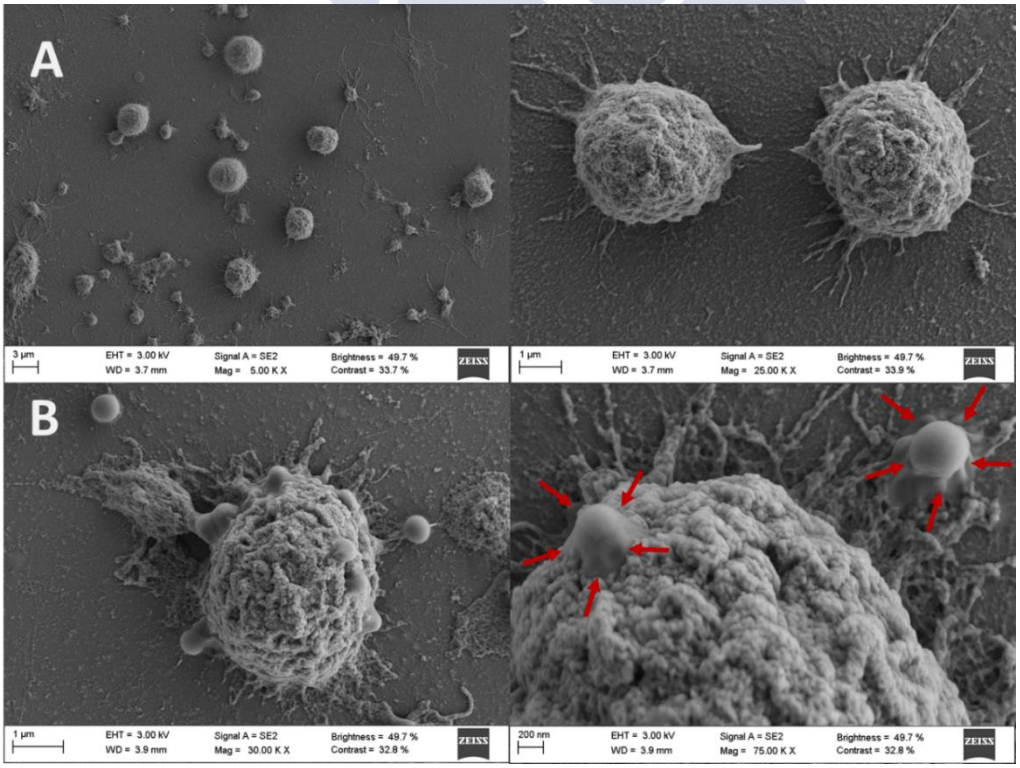

Figure 5: **Assessment of GC-CNPs uptake by monocytes using FEG-SEM**. **A)** untreated monocytes **B)** Monocytes treated with GC-CNPs. The GC-CNPs are pointed with the red arrow marks.

Next, we investigated the pathways by which the GC-CNPs were internalized. To perform this, the different internalization pathways were blocked using selective inhibitors like

chlorpromazine (Clathrin-mediated endocytosis, CLO), cytochalasin D (actin-mediated phagocytosis, Cit-D) and dimethyl amiloride (micropinocytosis, DHA). The uptake of the nanoparticles was not affected by the presence of CLO or DHA, while the GC-CNPs uptake was slightly reduced in the presence of Cit-D as seen in **Figure 6A**, which indicates phagocytosis as a possible mechanism of uptake. Next, we further tried to block the uptake by a combination of different inhibitors (DHA+CLO, DHA+Cit-D, CLO+Cit-D and DHA+CLO+Cit-D). The DCs pre-treated with the DHA+Cit-D and CLO+Cit-D showed a slight reduction in the uptake of GC-CNPs. This indicates the phagocytosis as the critical mechanism of nanoparticle uptake. However, the results obtained are not statistically significant. Altogether, results show that the GC-CNPs are probably internalized by multiple uptake pathways and blocking one of them might force the DCs to internalize the GC-CNPs by alternative routes. However, the detailed study on the uptake mechanism should be performed using the inhibitors like dextran sulfate, nystatin or methyl-β-cyclodextrin.

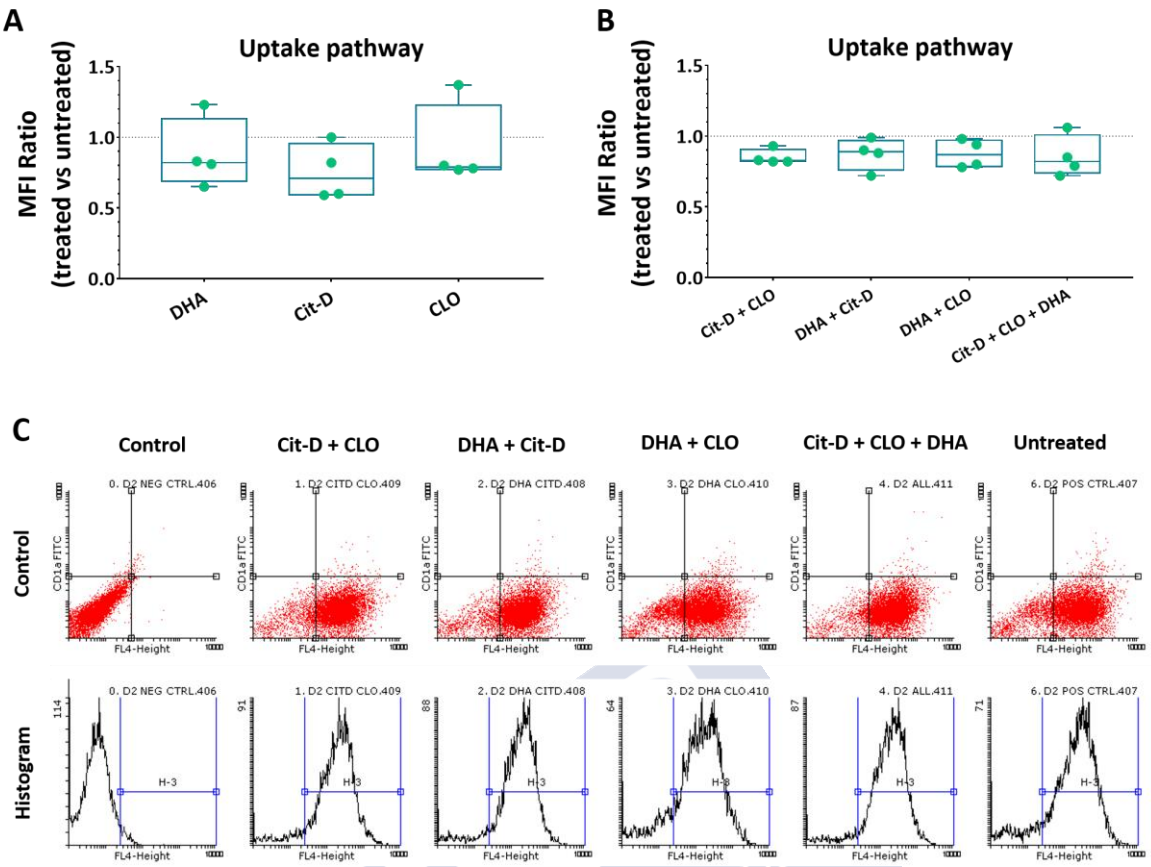

Figure 6: Effect of endocytic inhibitors on the internalization of GC-CNPs in the MoDCs. MoDCs were either untreated or pre-treated with chlorpromazine (10 µg/mL, clathrin-mediated endocytosis), cytochalasin D (10 µg/mL, phagocytosis), or amiloride (50 µM, micropinocytosis) and were incubated with GC-CNPs (50 µg/mL, 4h). Results are presented as mean± SD from 4 donors.

3.4. Chitosan nanoparticles enhance expression of the co-stimulatory molecules CD80 and CD86 on DCs

The study on the expression of co-stimulatory markers was undertaken to elucidate the effect of GC-CNPs on DC maturation. The co-stimulatory marker CD86 designates to be a marker of primary DC maturation, while CD80 only increases in mature DC. Many studies have shown that antigen delivery to DCs upregulates expression of both CD80 and CD86 that are known to induce T cell receptor signalling and promote T cell activation [20]. The CD83 is most characteristic of cell surface markers for fully matured DCs, whose role is regulating the maturation of B and T- lymphocytes [21].

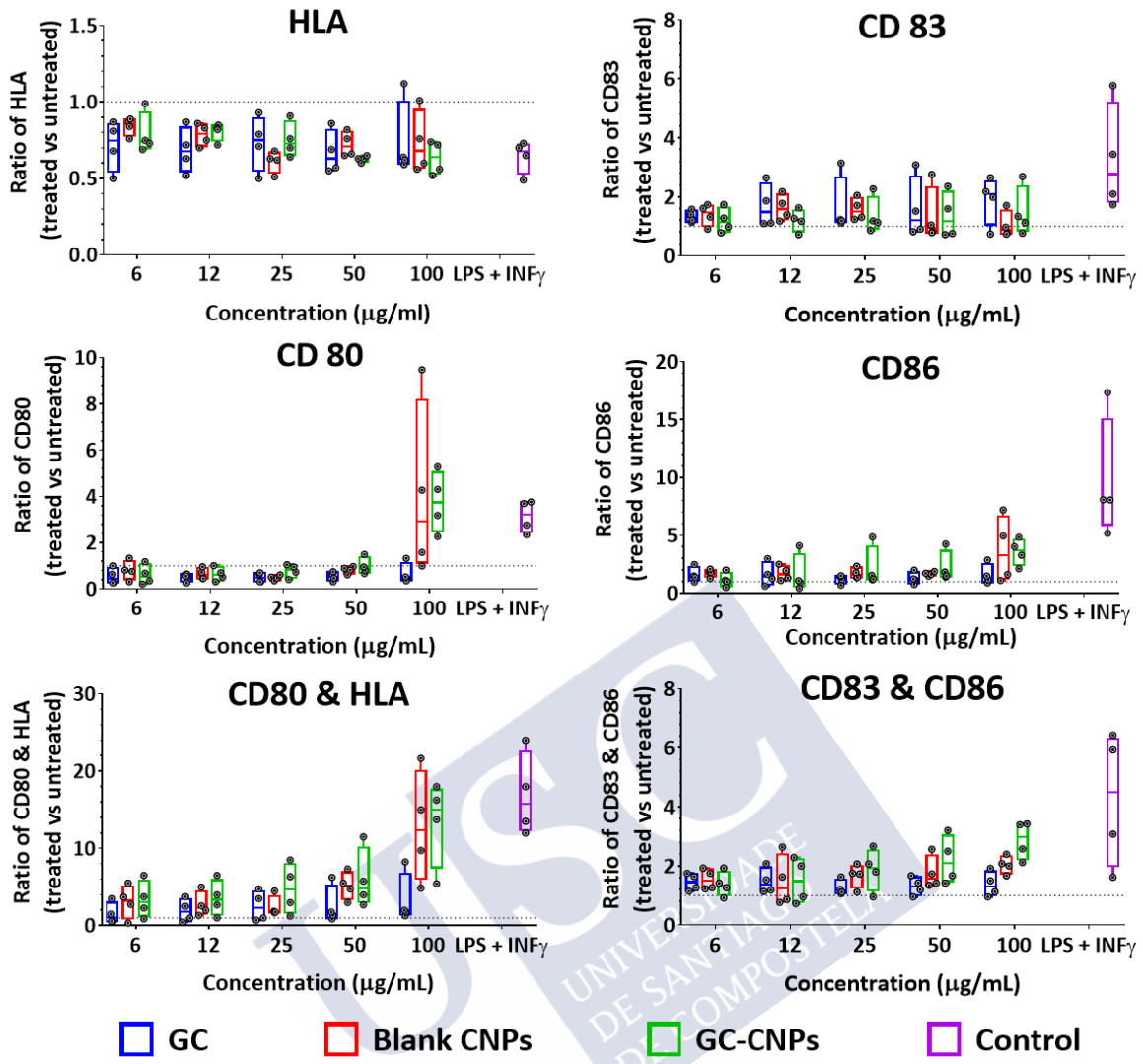

Figure 7: **GC-CNPs induce moDC activation and maturation.** The bars in the different colors indicate GC (Blue), Blank CNPs (Red), GC-CNPs (green) and the control with LPS+ INF-γ treatment (Purple). The data represent the mean ±SD of the results obtained from the 4 donors.

As illustrated in **Figure 7**, iDCs treated with blank CNPs and GC-CNPs showed an enhanced expression of CD80, CD83 and CD86 markers, although this upregulation does not reach statistical significance probably due to the variability seen among the different donors. Moreover, there was no marked increase in the HLA expression with the same treatments probably due to the high expression level seen already in untreated iDCs.

The stimulation of DCs with different concentrations of nanoparticles showed that the upregulation and the expression of CD86 occurred in a concentration-dependent manner and

was highest at 100 µg/mL concentration. The CD80 upregulation was observed only at 100 µg/mL and not at the lower concentrations. The CD83 upregulation was observed when treated with nanoparticles and was independent of their concentration. The DCs treated with blank CNPs and GC-CNPs displayed a similar profile of activation marker expression, but the upregulation was always higher in the case of GC-CNPs. This suggests that the presence of GC in the CNPs potentiate the stimulation of the CD80, CD83 and CD86 by the DCs. The DCs treated with the GC alone, showed similar CD83, lower CD86 and no CD80 upregulation when compared to the GC-CNPs treated DCs. Finally, a clear upregulation of all co-stimulatory molecules is seen when iDCs were treated with LPS and INF-γ (**Figure 7**, violet columns) and higher for both CD83 and CD86 when compared to CNP-treated DCs but not for CD80.

These results can emphasize the role of CNPs as an adjuvant in DC stimulation. Chitosan is known for its role in macrophage activation, and upregulation of the cytokines. There were low levels of endotoxin detected in our formulations (see **Figure 1**) and the results obtained are not due to the endotoxin activation. Overall, the results suggest that the nanoparticles alone or in combination with GC can upregulate the co-stimulatory markers in comparison to the GC alone, suggesting the adjuvant property of the CNPs.

3.5. DCs matured by the CNPs stimulate T cells

Next the role of different components of the CNPs in the stimulation of both peripheral lymphocytes and monocytes was determined by the quantification of TNF-α secreted by these cell types. SEB was used as a positive control for T lymphocyte stimulation, whereas LPS was used as a positive control for monocyte stimulation (**Figure 8**). When PBMCs were incubated with CNPs or their components no significant activation of T lymphocytes (measured as TNF-α-positive cells) was seen for any treatment. However, a different picture

was seen in the case of peripheral monocytes. Treatment with blank CNPs stimulate more TNF-α production by monocytes compared to the untreated iDCs, but to a lesser extent when compared to the GC-CNP treated PBMCs. iDCs incubated with GC-CNP synthesise more TNF-α compared to their individual antigenic components (Pn14TS and mPsaA; **Figure 8**, monocytes). However, it is interesting to notice that the GC alone induce the secretion of TNF-α by monocytes to a level similar seen using LPS. This increase in the TNF-α by monocytes might be associated with the conjugation of tetrasaccharide to the carrier protein. The ability of the CNPs (either blank and GC-CNPs) to induce TNF-α secretion mainly by monocytes indicates the capacity of these nanoparticles to activate APCs (as suggested above for DCs) and their precursors (*i.e*. monocytes) to trigger a significantly higher activation of the adaptive immune system (*i.e*. T lymphocytes) and induce protective activity against the pathogens.

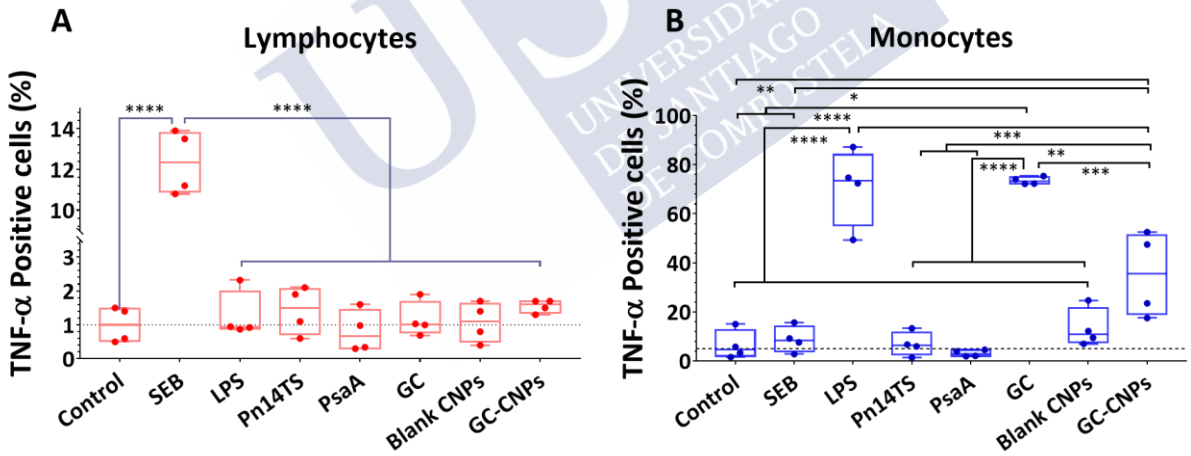

Figure 8: **The graphs indicate the percentage of TNF-α positive cells after treatment with SEB, LPS, Pn14TS, PsaA, GC, Blank CNPs and GC-CNPs. A)** Lymphocytes and **B)** Monocytes. Results are presented as mean ± SD from 4 donors. Statistical difference between the groups is *, P < 0.05; **, P < 0.01; ***, P < 0.001; ****, P < 0.0001.

To determine the role of CNPs and PsaA on the allo-stimulatory activity of DCs, iDCs were pre-treated with either PsaA, Blank CNPs and a mixture of PsaA and Blank CNPs and incubated with allogeneic PBLs. Untreated and LPS-treated iDCs were used as negative and positive

controls, respectively. The expression of either CD25 or CD28 was used to determine the activation of both CD4+ and CD8+ allogeneic T lymphocytes.

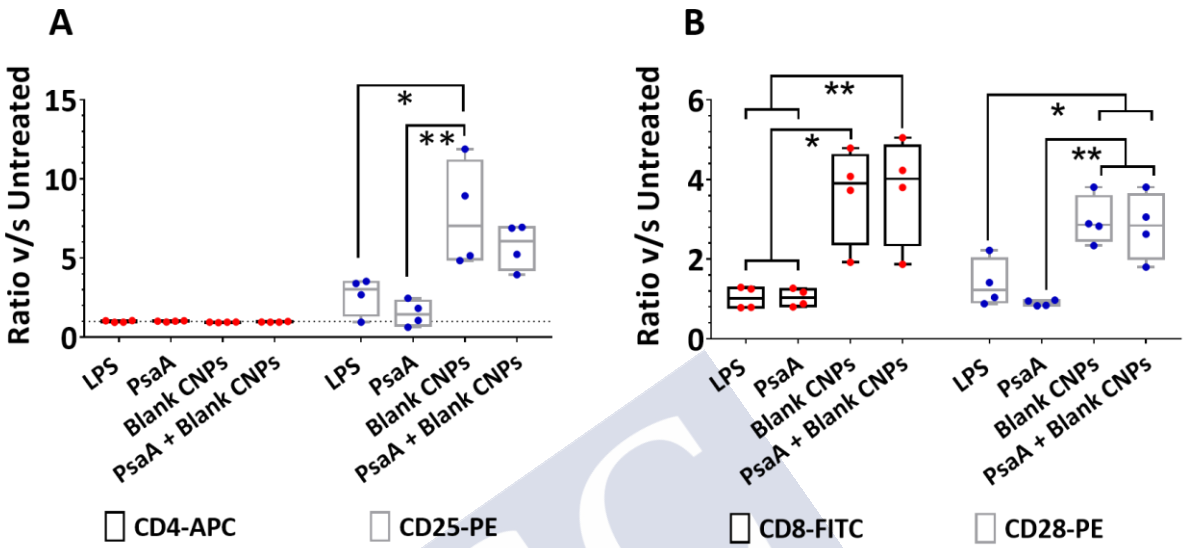

Figure 9: **CNPs treated DCs induce the proliferation of T cells in mixed lymphocyte reaction. A)**. The number of CD4 & CD25 positives, **B)** and the CD8 & CD28 positives**,** were analysed. Results are presented as mean ± SD from 4 donors. Statistical difference between the groups is *, P < 0.05; **, P < 0.01; ***, P < 0.001; ****, P < 0.0001.

As can be seen in **Figure 9A**, there is a significant increase in the CD25 positive CD4+ allogenic T cells when DCs were pre-treated with blank CNPs, compared to the CD25 expression when using DCs pre-treated with either LPS or the antigen PsaA (**Figure 9A**). Moreover, an increase in the level of CD4+ T cell activation is also seen when DCs used to stimulate T cells were pre-treated with the mixture of blank CNPs and PsaA, although this activation did not reach statistical significance when compared to either LPS- or PsaA-treated DCs. Since DCs treated with PsaA alone did not promote the activation of CD4+ T cells, it is tempting to speculate that the CNP by itself is capable of activating iDCs.

On the other hand, when the activation of CD8+ T lymphocytes was examined (**Figure 9B**) a clear activation of these lymphocytes can be detected when using DCs pre-treated with either

blank CNPs or a mixture of blank CNPs and PsaA. The up regulation of CD28 is significantly higher in CD8+ T lymphocytes stimulated by those DCs compared to that seen in CD8+ T lymphocytes stimulated with DCs pre-treated with either LPS or PsaA alone (**Figure 9B**; blue). This sharp stimulation is also seen when the number of CD8+ T lymphocytes is examined, because a higher percentage of this lymphocytes is seen in cultures where DCs pre-treated with CNPs are used, compared to those seen in cultures using either LPS or PsaA-treated DCs (**Figure 9B**; red).

4. Discussion

Dendritic cells are considered as important targets for the vaccine delivery due to their central role in inducing the immune responses. The particulate systems can deliver the antigen to DCs and act as excellent tools for achieving immune activation. In this study, we used chitosan nanoparticles of ~150 nm to deliver the antigen and activate the DCs. The literature suggests that the nanoparticles of this size are optimal for the uptake by DCs. The nanoparticles used in our studies, both blank and antigen loaded nanoparticles produced low levels of toxicity and were free from any endotoxin contamination. The cell viability was more than 80% at concentrations below 100 µg/mL. This was confirmed by both MTS and 7 AAD assays. Performing both MTS and 7 AAD assays helps to know the number of cells that are metabolically active vs non-apoptotic. Similar study was performed by Das et al., to determine the survival of DCs in the presence of chitosan nanoparticles. They reported that percentage DC survival when incubated with 100 µg/mL chitosan nanoparticles was ~40% viability, while in our case, viability was > 80% at the same concentration [22]. However, the chitosan nanoparticles prepared by them had a size >250 nm and had zeta potential of 39 mV. It is

possible that the higher zeta potential of the nanoparticles might have resulted in the increased toxicity.

The results obtained from the confocal microscopy suggests the GC-CNPs are localized in the cytoplasm. This is essential for the processing and presentation of the antigens by the DCs [7]. In addition, we performed nanoparticle uptake studies by blocking different uptake pathways like phagocytosis, micropinocytosis and clathrin-mediated endocytosis to understand the major pathway by which nanoparticles are internalized. Although the results obtained from the uptake studies are not statistically significant when compared to the controls (DCs without inhibitor treatments) and do not indicate any single dominant mechanism by which the GC-CNPs were internalised, they suggest that phagocytosis could be the possible mechanism by which most of the GC-CNPs were captured by iDCs. The studies performed by He et al., have also shown that the nanoparticles in this size range can be phagocytosed and processed by the APCs [23]. In addition, studies performed by Roser et al., suggest that the positive charge of the nanoparticles might influence phagocytosis mediated uptake [24]. Overall, our studies suggest that the nanoparticles were internalised by different uptake pathways, in particular phagocytosis.

In the body, the DCs are present in an immature state, which in the presence of foreign bodies undergo a maturation process. As a result of this activation process, the DCs undergo physiological changes, which include among others the upregulation of different costimulatory markers, including CD80, CD83 and CD86 [25]. The ability of antigens to induce the DC activation is pivotal in inducing the adaptive immunity. We found that the GC-CNPs were able to promote the expression of the costimulatory markers like CD80, CD83 and CD86. However, studies performed by Han *et al*., using blank CNPs did not display upregulation of

costimulatory markers like CD80, MHC II and CD86, while the antigen loaded CNPs enhanced the production of these costimulatory markers in comparison to the antigen alone or blank CNPs [26]. In contrary, Molina *et al*., demonstrated CD80 and CD83 upregulation with blank CNPs. They demonstrated the use of CNPs to differentiate human monocytes into immature dendritic cells [27]. The DCs treated with ovalbumin loaded PLGA nanoparticles have also shown the upregulation in these costimulatory markers [28,29]. In our studies, we have used the poloxamer 188 as a stabilizing agent during the nanoparticle preparation and Zupancic et al., reported that Pluronic® F127 (poloxamer 407) used as a stabilizing agent in the nano-formulations has shown inhibitory effect on the stimulation of CD80 and CD86 markers [28]. Interestingly, Thiele et al., has reported that upregulation of CD83 is associated with the nanoparticle uptake by phagocytosis [30], which supports our results that shows the GC-CNPs uptake by phagocytosis. Most of the times endotoxin contamination in the formulation might result in the false positive results. However, it is important to note that the chitosan nanoparticles used in the study were free from endotoxin contamination.

TNF-α is a cytokine secreted by the macrophages, monocytes and activated lymphocytes that act as an inflammatory marker in protecting against infectious pathogens. TNF-α produced by the macrophages can activate the T cells and can be the product of the activated T cells. As a product of effector CD4 and CD8 T cells, TNF-α is best known for its protective activity against several pathogens. The results obtained from our studies showed that the PBMCs primed with the GC-CNPs were able to induce the secretion of TNF-α. However, it is interesting to observe that the DCs treated with PsaA alone did not exhibit the TNF-α stimulation in the monocytes, while its counterpart GC resulted in significant TNF-α stimulation. The higher TNF-α stimulation in the GC may be the result of conjugating the Pn14TS to the PsaA. There are reports that suggests that the glycoproteins can stimulate TNF-α production in the monocytes

[31]. However, we could not find any literature that suggests that conjugating the polysaccharide antigen to carrier protein could enhance the TNF-α stimulation against the protein itself. In contrary, we found that both outer membrane protein complex (OMPC) and the OMPC conjugated to HiB polysaccharide have shown the TNF-α stimulation in the bone marrow derived DCs [32]. In any case, the possibility of the higher TNF-α stimulation in the GC treated cells, due to the traces of endotoxins in the GC cannot be ruled out. Studies from Silva et al., have shown that, for activation and differentiation of T cells the NPs uptake, processing and presentation by DCs is essential [11]. In addition, the stimulation of antigen specific CD4+ and CD8+ T lymphocytes is essential for efficient adaptive immunity. In our study, we have accessed the ability of the DCs primed with GC-CNPs and GC to activate the T cells. The DCs primed with the GC-CNPs induced the stimulation of both CD4+ and CD8+ T lymphocytes. In contrary, the DCs primed with the GC exhibited CD4+ T lymphocytes only. Zupancic et al., reported that DCs treated with ovalbumin loaded PLGA nanoparticles showed the activation of both CD4+ and CD8+ T lymphocytes [28]. The results obtained from our study clearly indicate the role of CNPs in the upregulation of CD25. The expression of the activation markers like CD25 is an indication of the activation of adaptive immunity. The presence of the CD28 signals demonstrates the ability of the CNPs to stimulate the naive T lymphocytes [33]. Our results suggest that the CNPs, in combination with the PsaA, can stimulate adaptive immune responses.

Conclusions:

The study shows that encapsulation of GC in the CNPs enhances the expression of co-stimulatory markers when compared to the naked GC or blank CNPs. In addition, priming the DCs with CNPs significantly enhanced the proliferation and stimulation of both CD4 and CD8

T lymphocytes, in particular, the latter. Overall, the results suggest that chitosan nanoparticles can act as an efficient delivery system for glycoconjugate vaccines targeting the dendritic cells.

5. Acknowledgements:

I would like to acknowledge Cristina Calvino Sanpedro for initially teaching me how to work with human dendritic cells.

6. References:

[1] R.M. Steinman, Dendritic cells: Understanding immunogenicity, Eur. J. Immunol. 37 (2007). doi:10.1002/eji.200737400.

[2] J. Banchereau, F. Briere, C. Caux, J. Davoust, S. Lebecque, Y.J. Liu, B. Pulendran, K. Palucka, J. Banchereau, F. Briere, F. Briere, C. Caux, C. Caux, J. Davoust, J. Davoust, S. Lebecque, S. Lebecque, Y.J. Liu, Y.J. Liu, B. Pulendran, B. Pulendran, K. Palucka, K. Palucka, Immunobiology of Dendritic Cells, Immunology. 18 (2000) 767–811. doi:10.1146/annurev.immunol.18.1.767.

[3] K. Palucka, J. Banchereau, Linking innate and adaptive immunity, Nat. Med. 5 (1999) 868–870. doi:10.1038/11303.

[4] A. Vartak, S.J. Sucheck, Recent advances in subunit vaccine carriers, Vaccines. 4 (2016). doi:10.3390/vaccines4020012.

[5] L.A. Brito, D.T. O'Hagan, Designing and building the next generation of improved vaccine adjuvants, J. Control. Release. (2014). doi:10.1016/j.jconrel.2014.06.027.

[6] M.F. Bachmann, G.T. Jennings, Vaccine delivery: A matter of size, geometry, kinetics and molecular patterns, Nat. Rev. Immunol. 10 (2010) 787–796. doi:10.1038/nri2868.

[7] C. Foged, B. Brodin, S. Frokjaer, A. Sundblad, Particle size and surface charge affect particle uptake by human dendritic cells in an in vitro model, Int. J. Pharm. 298 (2005) 315–322. doi:10.1016/J.IJPHARM.2005.03.035.

[8] T.G. Dacoba, A. Olivera, D. Torres, J. Crecente-Campo, M.J. Alonso, Modulating the immune system through nanotechnology, Semin. Immunol. 34 (2017) 78–102. doi:10.1016/j.smim.2017.09.007.

[9] M. Zaman, S. Chandrudu, I. Toth, Strategies for intranasal delivery of vaccines, Drug Deliv. Transl. Res. 3 (2013) 100–109. doi:10.1007/s13346-012-0085-z.

[10] R.P. Gala, M. D'Souza, S.M. Zughaier, Evaluation of various adjuvant nanoparticulate formulations for meningococcal capsular polysaccharide-based vaccine, Vaccine. 34 (2016) 3260–3267. doi:10.1016/J.VACCINE.2016.05.010.

[11] A.L. Silva, R.A. Rosalia, E. Varypataki, S. Sibuea, F. Ossendorp, W. Jiskoot, Poly-(lactic-co-glycolic-acid)-based particulate vaccines: Particle uptake by dendritic cells is a key parameter for immune activation, Vaccine. 33 (2015) 847–854. doi:10.1016/J.VACCINE.2014.12.059.

[12] P. Calvo, C. Remuñan-López, J.L. Vila-Jato, M.J. Alonso, Chitosan and Chitosan/Ethylene Oxide-Propylene Oxide Block Copolymer Nanoparticles as Novel Carriers for Proteins and Vaccines, Pharm. Res. 14 (1997) 1431–1436. doi:10.1023/A:1012128907225.

[13] N. Csaba, M. Köping-Höggård, M.J. Alonso, Ionically crosslinked chitosan/tripolyphosphate nanoparticles for oligonucleotide and plasmid DNA delivery, Int. J. Pharm. 382 (2009) 205–214. doi:10.1016/J.IJPHARM.2009.07.028.

[14] H.B.T. Moran, J.L. Turley, M. Andersson, E.C. Lavelle, Immunomodulatory properties of chitosan polymers, Biomaterials. 184 (2018) 1–9. doi:10.1016/J.BIOMATERIALS.2018.08.054.

[15] D.A. Zaharoff, C.J. Rogers, K.W. Hance, J. Schlom, J.W. Greiner, Chitosan solution enhances both humoral and cell-mediated immune responses to subcutaneous vaccination, Vaccine. 25 (2007) 2085–2094. doi:10.1016/J.VACCINE.2006.11.034.

[16] T. López-León, E.L.S. Carvalho, B. Seijo, J.L. Ortega-Vinuesa, D. Bastos-González,

Physicochemical characterization of chitosan nanoparticles: electrokinetic and stability behavior, J. Colloid Interface Sci. 283 (2005) 344–351. doi:10.1016/J.JCIS.2004.08.186.

[17] M. Prasanna, D. Soulard, E. Camberlein, N. Ruffier, A. Lambert, F. Trottein, N. Csaba, C. Grandjean, Semisynthetic glycoconjugate based on dual role protein/PsaA as a pneumococcal vaccine, Eur. J. Pharm. Sci. 129 (2019) 31–41. doi:10.1016/J.EJPS.2018.12.013.

[18] Instructions Pierce LAL Chromogenic Endotoxin Quantitation Kit, Thermo Sci. (n.d.). https://assets.thermofisher.com/TFS-Assets/LSG/manuals/MAN0016039_2162445_Pierce_LAL_Chromo_Endotox_Quant_UG.pdf (accessed June 17, 2019).

[19] L.A. Brito, M. Singh, Acceptable Levels of Endotoxin in Vaccine Formulations During Preclinical Research, J Pharm Sci. 100 (2010) 34–37. doi:10.1002/jps.22267.

[20] G.M.Z. Al-Ashmawy, Dendritic Cell Subsets, Maturation and Function, in: Dendritic Cells, InTech, 2018. doi:10.5772/intechopen.79926.

[21] M. Breloer, B. Fleischer, CD83 regulates lymphocyte maturation, activation and homeostasis., Trends Immunol. 29 (2008) 186–94. doi:10.1016/j.it.2008.01.009.

[22] I. Das, A. Padhi, S. Mukherjee, D.P. Dash, S. Kar, A. Sonawane, Biocompatible chitosan nanoparticles as an efficient delivery vehicle for Mycobacterium tuberculosis lipids to induce potent cytokines and antibody response through activation of γδ T cells in mice., Nanotechnology. 28 (2017) 165101. doi:10.1088/1361-6528/aa60fd.

[23] C. He, Y. Hu, L. Yin, C. Tang, C. Yin, Effects of particle size and surface charge on cellular uptake and biodistribution of polymeric nanoparticles, Biomaterials. 31 (2010) 3657–3666. doi:10.1016/J.BIOMATERIALS.2010.01.065.

[24] M. Roser, D. Fischer, T. Kissel, Surface-modified biodegradable albumin nano- and microspheres. II: effect of surface charges on in vitro phagocytosis and biodistribution in rats, Eur. J. Pharm. Biopharm. 46 (1998) 255–263. doi:10.1016/S0939-6411(98)00038-1.

[25] K. Palucka, J. Banchereau, I. Mellman, Designing vaccines based on biology of human dendritic cell subsets., Immunity. 33 (2010) 464–78. doi:10.1016/j.immuni.2010.10.007.

[26] H.D. Han, Y. Byeon, J.H. Jang, H.N. Jeon, G.H. Kim, M.G. Kim, C.G. Pack, T.H. Kang, I.D. Jung, Y.T. Lim, Y.J. Lee, J.W. Lee, B.C. Shin, H.J. Ahn, A.K. Sood, Y.M. Park, In vivo stepwise immunomodulation using chitosan nanoparticles as a platform nanotechnology for cancer immunotherapy, Sci. Rep. 6 (2016). doi:10.1038/srep38348.

[27] M.A. Franco-Molina, E.E. Coronado-Cerda, E. López-Pacheco, D.G. Zarate-Triviño, S.A. Galindo-Rodríguez, M. del Carmén Salazar-Rodríguez, Y. Ramos-Zayas, R. Tamez-Guerra, C. Rodríguez-Padilla, Chitosan Nanoparticles Plus KLH Adjuvant as an Alternative for Human Dendritic Cell Differentiation, Curr. Nanosci. >15 (2018) 532–540. doi:10.2174/1573413714666181008110627.

[28] E. Zupančič, C. Curato, M. Paisana, C. Rodrigues, Z. Porat, A.S. Viana, C.A.M. Afonso, J. Pinto, R. Gaspar, J.N. Moreira, R. Satchi-Fainaro, S. Jung, H.F. Florindo, Rational design of nanoparticles towards targeting antigen-presenting cells and improved T cell priming, J. Control. Release. 258 (2017) 182–195. doi:10.1016/J.JCONREL.2017.05.014.

[29] V.B. Joshi, S.M. Geary, A.K. Salem, Biodegradable Particles as Vaccine Delivery Systems: Size Matters, AAPS J. 15 (2013) 85–94. doi:10.1208/s12248-012-9418-6.

[30] L. Thiele, B. Rothen-Rutishauser, S. Jilek, H. Wunderli-Allenspach, H.P. Merkle, E. Walter,

Evaluation of particle uptake in human blood monocyte-derived cells in vitro. Does phagocytosis activity of dendritic cells measure up with macrophages?, J. Control. Release. 76 (2001) 59–71. doi:10.1016/S0168-3659(01)00412-6.

[31] R. Planès, M. Serrero, K. Leghmari, L. BenMohamed, E. Bahraoui, HIV-1 Envelope Glycoproteins Induce the Production of TNF-α and IL-10 in Human Monocytes by Activating Calcium Pathway, Sci. Rep. 8 (2018). doi:10.1038/s41598-018-35478-1.

[32] E. Latz, J. Franko, D.T. Golenbock, J.R. Schreiber, Haemophilus influenzae Type b-Outer Membrane Protein Complex Glycoconjugate Vaccine Induces Cytokine Production by Engaging Human Toll-Like Receptor 2 (TLR2) and Requires the Presence of TLR2 for Optimal Immunogenicity , J. Immunol. 172 (2004) 2431–2438. doi:10.4049/jimmunol.172.4.2431.

[33] F.A. Harding, J.G. McArthur, J.A. Gross, D.H. Raulet, J.P. Allison, CD28-mediated signalling co-stimulates murine T cells and prevents induction of anergy in T-cell clones, Nature. 356 (1992) 607–609. doi:10.1038/356607a0.

General Discussions

USC
UNIVERSIDADE
DE SANTIAGO
DE COMPOSTELA

General Discussion

Currently available vaccines for pneumonia, either PPSV or PCV are based on polysaccharide antigens from the *S. pneumoniae* and does not protect against all pneumococcal serotypes. As the capsular polysaccharide composition is different among serotypes, researchers should incorporate polysaccharide antigens from all pathogenic serotypes. Due to their high number, this is a complex and costly approach. Several reports describe the incorporation of pneumococcal proteins antigens for the immunization against all pneumococcal serotypes. In this line, we started working on semisynthetic glycoconjugate antigen based on the pneumococcal proteins that are commonly present in all the pneumococcal serotypes [1].

Glycoconjugate development: As a first objective, we focused on developing a semi-synthetic glycoconjugate antigen that can act as a better alternative to the marketed glycoconjugate vaccine. Accordingly, we developed a glycoconjugate that was composed of a pneumococcal protein antigen, Pneumococcal surface adhesin A (PsaA) and a synthetic tetrasaccharide (Pn14TS) that mimic the capsular polysaccharide of pneumococcal serotype 14 [2]. The PsaA has been selected because of its immunogenic nature and its previous use as carrier protein. PsaA used in the study was recombinantly produced in *E. coli* using the methods already mentioned in the literature [3]. To aid in the purification, the PsaA equipped of a poly-histidine tag was produced, although its production in absence of tag had been reported in the literature. We however inserted a sequence specific for the TEV protease between the histidine tag and the PsaA sequence. Later the poly-histidine tag was cleaved, and the resulting protein purified using affinity chromatography. The removal of the poly-histidine tag was confirmed by western blot analysis using anti-histidine tag antibodies. The whole procedure resulted in PsaA with high yield and purity. The conjugation of Pn14TS to the PsaA

by thiol-maleimide coupling gave rise to a glycoconjugate (GC) that retained its secondary structure on long term storage in a lyophilized form. The prepared GC was successful in maintaining its functionality even after lyophilization, while other carrier proteins like diphtheria toxoid and tetanus toxoid or their combination products are freeze sensitive and should always be maintained between 2-8 °C [4–6]. The results from the circular dichroism give the indication that the conformational B-epitopes are conserved during the conjugation process. The immunization efficiency of the glycoconjugate (GC/ Pn14TS-mPsaA) adjuvanted with α-GalCer was compared with mPsaA and model conjugate (Pn14TS-BSA). The studies displayed that mPsaA (S.C.) generated higher anti mPsaA antibodies compared to mPsaA-Pn14TS/ GC (S.C.). The reason for this result might be due to the masking of the B epitopes of mPsaA after conjugating with the Pn14TS or a competition between the protein and polysaccharide B epitopes or a different processing for the protein and the polysaccharide given the route of administration. The overall observations from the study suggest that the synthesized glycoconjugate was effective in generating IgG antibodies against both its protein (mPsaA) and tetrasaccharide counterparts.

Formulation development: Despite the effectiveness of the synthesized GC when administered (S.C.) in the free-from, it is well known that the use of nanocarriers could enhance the immune response generated against the GC. This brings to the second objective of this thesis to design the suitable nanocarriers for the delivery of glycoconjugate antigens. Generally, pneumococcal infections are caused by nasopharyngeal colonization and it is reported that mucosal immunization can generate effective systemic and mucosal immune responses. Bearing this in mind, we have evaluated chitosan nanoparticles (CNPs) as carriers for mucosal delivery of the glycoconjugates.

The use of such CNPs offers various benefits due to their biocompatible, biodegradable and mucoadhesive properties. The developed CNPs had a size of ~150 nm and positive zeta potential. Every milligram of these nanoparticles was able to encapsulate approximately 35 µg of a glycoconjugate, while the encapsulation of PsaA alone was three times lower. Besides, the GC-CNPs were easily freeze-dried and could be re-dispersed in water without changes in their size and zeta potential. Further studies on this are required to see if these nanovaccines could be stored for longer-term without refrigeration, which would help to eliminate the requirement of the cold chain when transporting to remote locations in countries with limited logistic capacity and reducing the overall cost of vaccination. While the nasal delivery of antigens using the mucoadhesive nanoparticles provide significant advantage over unencapsulated antigen, this advantage is limited by the particle aggregation and the mucus adhesion. However, in our studies the nanoparticles displayed slight increase in the particle size but did not show any signs of aggregation when incubated with simulated nasal mucosal fluid.

Release kinetics of the antigen plays important role in presenting the antigens to the immune system. If the antigen release from the nanoparticles is too fast antigens will be presented to the APCs in the soluble form and if the release is too slow there will be not enough antigen for their presentation to APCs. In our study, obtained CNPs were able to release <30% of GC over 24h, of which the majority was released within the first hours. Two mechanisms can explain the initial burst release of antigen from the nanoparticles: either by the release of antigen adsorbed on the nanoparticle surface or the escape of the antigen from the pores of the nanoparticles. This indicates that the initial burst release might correspond to the drug adsorbed on the surface of the CNPs or the non-associated GC. There are previously reported studies where similar release profiles were observed [7,8]. Controlling the antigen release

from the formulations serves as an advantage for the depot formulations. This sustained release of the antigens increases the antigen exposure to the DCs and prolong the antigen presentation.

***In vitro* studies:** We furthermore evaluated the interaction of nanoparticles with antigen-presenting cells (APCs) in generating an effective immune response. To understand, if the GC-CNPs were effective in interacting and activating immune cells, a series of studies with MoDCs were performed. The GC-CNPs showed concentration-dependent toxicity when incubated with these cells. At concentrations below 100 µg/mL, the nanoparticles were highly biocompatible, and they displayed > 80% of survival as shown with both MTT (metabolic activity) and 7-AAD assay (apoptosis). The percentage of metabolically active cells at 100 µg/mL are higher than in reported literature were the same concentrations displayed lower than 50% survival [9]. In our studies, both CNPs and GC-CNPs treatments displayed similar DCs survival. The nanoparticle uptake is pivotal in activation of the DCs that play a substantial role in inducing the adaptive immunity. The internalization studies were performed in the presence of inhibitors that block different uptake pathways (CLO, Cit-D and DHA) and the results did not indicate any dominant mechanism of uptake. Even though the results were not statistically significant, they suggested phagocytosis as a possible uptake mechanism. These results are supported by the literature that shows the chitosan nanoparticles with ~150 nm size range and having zeta potential > 15 mV are internalized by phagocytosis [10]. Confocal microscopy and flow cytometry have confirmed the internalization of the GC-CNPs by the DCs in less than 2h. The GC-CNPs were able to upregulate the production of costimulatory markers (CD80, CD83 and CD86) in the DCs, which indicates their activation. The GC loaded CNPs were successful in the activation of DCs. However, the upregulation of these co-stimulatory markers with blank CNPs is debated [11,12]. The upregulation of CD83 marker is associated

with phagocytosis, which strengthens our hypothesis of phagocytosis as a dominant mechanism of GC-CNPs uptake [13]. Besides, in further experiments, the DCs pulsed with GC-CNPs were able to stimulate T cells and induce the production of TNF-α. The TNF-α is well known as a product of effector CD4 and CD8 T cells and for its protective activity against several pathogens. In our study, we also observed that the DCs pre-treated with a mixture of blank CNPs and PsaA produced higher CD25 activation in CD4 allogenic T cells when compared with either LPS or PsaA alone. However, this activation was even higher with the DCs pre-treated with just blank CNPs. Similarly, the mixture of PsaA and blank CNPs significantly up regulated the CD28 in CD8 allogenic T cells and increased the proliferation of CD8 T cells, in comparison to the DCs treated with either LPS or PsaA. This leads to the belief that the CNPs by itself can activate the DCs. Also, researchers have used CNPs to differentiate human monocytes into immature dendritic cells [11]. Overall, the results suggest that the combination of CNPs and mPsaA, can stimulate adaptive immune responses.

***In vivo* studies:** In this study, two sets of immunizations were performed in mice with the following aims. 1) To evaluate the role of nanoencapsulation in enhancing the immunogenicity against the GCs; 2) To understand if GC-CNPs can generate higher immune response via mucosal administration as compared to subcutaneous immunization.

The GC-CNPs immunized via S.C. route produced 10 folds and 100 folds anti-CP and anti PsaA IgG response, respectively, when compared with the mice treated S.C. with GC alone. Moreover, the group immunized with GC-CNPs displayed the generation of IgG1 subclass predominantly and IgG2b as a second prevalent subtype against the capsular polysaccharides. While only IgG1 subclass of antibodies was produced against PsaA. Studies from Majela *et al.,* showed similar results where self-assembled PsaA particles produced predominantly IgG1

and slightly lower IgG2b antibodies [14]. Also, the group immunized with GC-CNPs displayed higher protection against the systemic pneumococcal challenge, when compared to untreated and groups treated with GC alone. It is important to note that, all the formulations were co-administered along with the adjuvant α-GalCer that can potentially activate NKT cells [15].

The second series of immunizations were performed to compare the immune response generated by GC-CNPs/ GC administered S.C. and I.N. Interestingly, the GC alone I.N. administered produced equivalent anti-PsaA IgG response to that of GC-CNPs S.C. administered. The results suggest that GCs via I.N. were effective in generating the higher immune response when compared to the GC via S.C. However, it is surprising that GC-CNPs administered via I.N. produced 100 folds lower anti-PsaA IgG when compared to the GC alone administered via I.N. or GC-CNPs administered via S.C. The generated anti PsaA IgG response is in the order of GC-CNPs (S.C.) = GC (I.N) > GC+ CNPs (I.N.) > GC-CNPs (I.N.). This shows that the presence of CNPs *via* I.N. is reducing the anti PsaA IgG response generated against the GCs. Additionally, both GC via I.N. and GC-CNPs via S.C. generated anti CP IgG response, while the groups immunized with Prevenar 13 or GC-CNPs (I.N.) failed to do so. This contradicts our hypothesis that the CNPs as a carrier for I.N. delivery of GC would enhance the immune response against the GCs. The possible reason for this phenomenon might be the mucosal clearance of the CNPs. This leads to the conclusion that in our study CNPs were not effective via I.N. An alternative explanation for the higher immunogenicity of GC over GC-CNP when I.N. administered could refer to intrinsic adhesive properties of PsaA, responsible for nasopharynx epithelial cell colonization. However, the further optimization of the formulation to improve the antigen release profiles would help in achieving better results.

In summary, this thesis describes the design of nanoparticles encapsulating the semisynthetic glycoconjugate as a vaccine against pneumococcal infections. Even though, the CNPs were not effective in generating the immune response via I.N. route, they showed promising results via S.C. immunization and offer an opportunity for the future development of improved pneumococcal vaccines.

References:

[1] A.D. Ogunniyi, J.C. Paton, Vaccine Potential of Pneumococcal Proteins, Streptococcus Pneumoniae. (2015) 59–78. doi:10.1016/B978-0-12-410530-0.00004-1.

[2] D. Safari, H.A.T. Dekker, J.A.F. Joosten, D. Michalik, A.C. De Souza, R. Adamo, M. Lahmann, A. Sundgren, S. Oscarson, J.P. Kamerling, H. Snippe, Identification of the Smallest Structure Capable of Evoking Opsonophagocytic Antibodies against Streptococcus pneumoniae Type 14 , 76 (2008) 4615–4623. doi:10.1128/IAI.00472-08.

[3] A.L. Larentis, A.P.C. Argondizzo, G. dos S. Esteves, E. Jessouron, R. Galler, M.A. Medeiros, Cloning and optimization of induction conditions for mature PsaA (pneumococcal surface adhesin A) expression in Escherichia coli and recombinant protein stability during long-term storage, Protein Expr. Purif. 78 (2011) 38–47. doi:10.1016/J.PEP.2011.02.013.

[4] Temperature sensitivity of vaccines Immunization, Vaccines and Biologicals, 2006. www.who.int/vaccines-documents/ (accessed November 21, 2019).

[5] M.M. Ho, F. Mawas, B. Bolgiano, X. Lemercinier, D.T. Crane, R. Huskisson, M.J. Corbel, Physico-chemical and immunological examination of the thermal stability of tetanus toxoid conjugate vaccines, Vaccine. 20 (2002) 3509–3522. doi:10.1016/S0264-410X(02)00342-0.

[6] B. Bolgiano, F. Mawas, S.E. Yost, D.T. Crane, X. Lemercinier, M.J. Corbel, Effect of physico-chemical modification on the immunogenicity of Haemophilus influenzae type b oligosaccharide-CRM197 conjugate vaccines, Vaccine. 19 (2001) 3189–3200. doi:10.1016/S0264-410X(01)00024-X.

[7] S. Gordon, A. Saupe, W. McBurney, T. Rades, S. Hook, Comparison of chitosan nanoparticles and chitosan hydrogels for vaccine delivery, J. Pharm. Pharmacol. 60 (2008) 1591–1600. doi:10.1211/jpp.60.12.0004.

[8] C. Bulmer, A. Margaritis, A. Xenocostas, Production and characterization of novel chitosan nanoparticles for controlled release of rHu-Erythropoietin, Biochem. Eng. J. 68 (2012) 61–69. doi:10.1016/J.BEJ.2012.07.007.

[9] I. Das, A. Padhi, S. Mukherjee, D.P. Dash, S. Kar, A. Sonawane, Biocompatible chitosan nanoparticles as an efficient delivery vehicle for Mycobacterium tuberculosis lipids to induce potent cytokines and antibody response through activation of γδ T cells in mice., Nanotechnology. 28 (2017) 165101. doi:10.1088/1361-6528/aa60fd.

[10] C. He, Y. Hu, L. Yin, C. Tang, C. Yin, Effects of particle size and surface charge on cellular uptake and biodistribution of polymeric nanoparticles, Biomaterials. 31 (2010) 3657–3666. doi:10.1016/J.BIOMATERIALS.2010.01.065.

[11] M.A. Franco-Molina, E.E. Coronado-Cerda, E. López-Pacheco, D.G. Zarate-Triviño, S.A. Galindo-Rodríguez, M. del Carmén Salazar-Rodríguez, Y. Ramos-Zayas, R. Tamez-Guerra, C. Rodríguez-Padilla, Chitosan Nanoparticles Plus KLH Adjuvant as an Alternative for Human Dendritic Cell Differentiation, Curr. Nanosci. >15 (2018) 532–540. doi:10.2174/1573413714666181008110627.

[12] H.D. Han, Y. Byeon, J.H. Jang, H.N. Jeon, G.H. Kim, M.G. Kim, C.G. Pack, T.H. Kang, I.D. Jung, Y.T. Lim, Y.J. Lee, J.W. Lee, B.C. Shin, H.J. Ahn, A.K. Sood, Y.M. Park, In vivo stepwise immunomodulation using chitosan nanoparticles as a platform nanotechnology for cancer immunotherapy, Sci. Rep. 6 (2016). doi:10.1038/srep38348.

[13] L. Thiele, B. Rothen-Rutishauser, S. Jilek, H. Wunderli-Allenspach, H.P. Merkle, E. Walter, Evaluation of particle uptake in human blood monocyte-derived cells in vitro. Does phagocytosis activity of dendritic cells measure up with macrophages?, J. Control. Release. 76 (2001) 59–71. doi:10.1016/S0168-3659(01)00412-6.

[14] M. González-Miro, L. Rodríguez-Noda, M. Fariñas-Medina, D. García-Rivera, V. Vérez-Bencomo, B.H.A. Rehm, Self-assembled particulate PsaA as vaccine against Streptococcus pneumoniae infection., Heliyon. 3 (2017) e00291. doi:10.1016/j.heliyon.2017.e00291.

[15] L.J. Carreño, S.S. Kharkwal, S.A. Porcelli, Optimizing NKT cell ligands as vaccine adjuvants, Immunotherapy. 6 (2014) 309–320. doi:10.2217/imt.13.175.

Conclusions

USC
UNIVERSIDADE
DE SANTIAGO
DE COMPOSTELA

Conclusions

In this thesis, we developed a semisynthetic glycoconjugate antigen against pneumococcal infections. We also evaluated chitosan nanoparticles as carriers for the delivery of the synthesized glycoconjugate antigen. The results obtained from the studies led to the following conclusions.

1) The PsaA was successfully produced in *E. coli* using recombinant DNA technology. A semisynthetic glycoconjugate vaccine solely composed of pneumococcal antigens, i.e., of a synthetic tetrasaccharide mimicking the capsule of serotype 14 coupled to PsaA was synthesized. The conjugate was able to induce the IgGs antibodies against both synthetic oligosaccharide and protein moieties in the immunized mice.

2) Chitosan nanoparticles produced by ionic gelation method had an average size of 150 nm, a narrow size distribution, positive surface charge and over 70% association efficiency of the glycoconjugate. Chitosan nanoparticles exhibited good colloidal stability upon incubation in simulated nasal fluid containing mucin.

3) The studies with monocyte derived dendritic cells indicated that chitosan nanoparticles were compatible with DCs. The interaction of CNPs with the dendritic cells was time dependent and were internalized by multiple uptake pathways. In addition, priming the DCs with CNPs significantly enhanced the proliferation and stimulation of both CD4 and CD8 T lymphocytes, indicating that the CNPs can generate both cellular and humoral immune responses.

4) The GC-CNPs produced specific anti PsaA and anti CP IgG responses that were 100 folds and 10 folds higher than GC when administered *via* S.C. while the same GC-CNPs did not show similar effects via I.N administration.

Overall, our findings suggest that chitosan nanoparticles as carriers could enhance the systemic immune response against the glycoconjugates. Future work will mainly focus on improving mucosal immune response to these nanovaccines.

USC
UNIVERSIDADE
DE SANTIAGO
DE COMPOSTELA

Annex

Super-resolution imaging of nanoparticle uptake by dendritic cells

This work is performed as a part of NanoFar internship in collaboration with Nanoscopy for Nanomedicine group at IBEC, Barcelona, Spain.

USC
UNIVERSIDADE
DE SANTIAGO
DE COMPOSTELA

1. Introduction

Although nanoparticles are widely investigated for the intracellular delivery of the vaccines and the therapeutic molecules, their clinical transition has not progressed as rapidly as preclinical results. Also, most of these investigated nanomedicines fail during the clinical trials [1]. One of the reasons for this is lack of rational design of the nanoparticles and lack of understanding on their interaction with cells [2]. Several experimental challenges need to be addressed to move the nanoparticles from bench to the bedside. Primarily, it is essential to have an adequate understanding of the interaction of the nanoparticles with the cells.

The study of the nanoparticle cell interactions is one of the biggest challenges with the nanomedicines that are currently investigated. The amount of the nanoparticles that are internalised or adsorbed on the surface of the cells determine the efficiency of the nanomedicines. However, the nanoparticle cell interactions are under-investigated due to the lack of user-friendly methods. Generally, the interaction of the nanoparticles with the cellular structures are visualized using either electron microscopy (EM) or confocal laser scanning microscopy (CLSM). In addition, the quantitative analysis to study the interaction of the nanoparticles with the cells can be performed using mass spectrometric techniques like ICP-MS. However, this can be only used for metallic nanoparticles and requires pre-treatment using chemical etching methods [3]. Electron microscopy offers excellent resolution and enables in visualizing the nanoparticles and the subcellular structures in detail, but it is limited to the fixed cells and involves complex sample preparation. On the other hand, CLSM allows the 3D multicolour imaging of the live cells but is restricted due to the limited resolution of 250 nm. This resolution does not allow the visualization of individual nanoparticles. Super-resolution microscopy has been proposed to overcome the limitations of the existing

techniques and act as a bridge between confocal and electron microscopy. Super-resolution microscopy offers the great advantage of multicolour imaging from optical microscopy and the resolution of electron microscopy [4]. Super-resolution techniques enable the analysis at single-cell level and allow the intracellular localization of the nanoparticles. A wide variety of super-resolution techniques like stochastic optical reconstruction microscopy (STORM) [5], stimulated emission depletion (STED) [6], structured illumination microscopy (SIM) [7] and photoactivation localization microscopy (PALM) [8] is used for the identification of the cellular structures in the biological sciences. STORM imaging provides the accurate localization of the nanoparticles based on the stochastically blinking fluorophores and can offer the resolution of 20 nm [5]. This higher resolution of the STORM imaging enables visualization at the molecular level.

Overall, the main objective of this work has been using STORM based imaging technique for intracellular localization of the nanoparticles in the dendritic cells.

2. Methods

2.1. Human dendritic cell and DC 2.4 cell line preparation

The iDCs were obtained from buffy coats according to the method mentioned in **Chapter 3 (2.6 section)**. DC2.4 cells were cultured in RPMI 1640 medium which was supplemented with 10% fetal bovine serum and penicillin/streptomycin antibiotics.

2.2. Internalization of Cy5-GC-CNPs in MoDCs

To track the nanoparticles after internalization by dendritic cells, the nanoparticles and the dendritic cells were labelled with two different dyes. The nanoparticles were labelled with Cy5, as described in **chapter 3 (section 2.3)**. Cy5 is considered as one of the best performing

cyanine-based dyes for STORM imaging. DCs ($5x10^5$ per well) were plated into a 24 well plate with 0.5 mL of R10 media. Following that cells were incubated with the Cy5 labelled GC-CNPs (50 µg/ million cells) for different time periods (0.5, 1, 2, 4 and 24h). After the incubation time, the DCs were washed with PBS. Afterwards, the cells were fixed with 4 % PFA for 15 min. To understand the position of the nanoparticles inside cells, the plasma membrane of the MoDCs was stained with Alexa 488-labelled WGA at 0.2 µg/mL (Wheat Germ Agglutinin, a lectin known to bind to N-acetyl-D-glucosamine and sialic acid on the cell membrane) and the nucleus was stained using DAPI. The staining was performed in Lab-Tek 8 well plates for 10 min, and the DCs were washed twice with PBS after incubation. The cells were suspended in 20-30 µl of STORM buffer (160 µL of PBS + 20 µL of 50% glucose + 20 µL of β-mercaptoethanol + 2 µL of Glucose oxidase) just before imaging.

2.3. Internalization of GC-CNPs in DC2.4 cell lines after different time periods of incubation

The DC2.4 cells (25,000 per well) were seeded on Lab-Tek plates with 0.2 mL of R10 media. Following that cells were incubated with the Cy5 labelled GC-CNPs (0.5 µg of NPs) for different time periods (0.5, 1, 2, 4 and 24h). After the incubation time, the DCs were washed with PBS. Afterwards, the cells were fixed with 4% PFA for 15 min. For imaging, the cells were stained using DAPI and wheat germ agglutinin (WGA, at 0.2 µg/mL) for 10 min, and the DCs were washed twice with PBS after incubation. The cells were suspended in 20-30 µl of STORM buffer.

2.4. The fate of GC-CNPs in DC2.4 cell lines after incubating for 1h

The DC2.4 cells (25,000 per well) were plated into a Lab-Tek plate with 0.2 mL of R10 media. Following that cells were pulsed with the Cy5 labelled GC-CNPs (0.5 and 2.5 µg of NPs) and

incubated at 37 °C for 1h. After the incubation time, the DCs were washed with PBS and then replaced with R10 medium and incubated at 37 °C. At different time points (1, 4 and 24h), the cells were fixed with 4% PFA for 15 min. For imaging, the cells were stained using DAPI and wheat germ agglutinin (WGA, at 0.2 µg/mL). The cells were suspended in Lab-Tek using 20-30 µl of STORM buffer for imaging.

2.5. Endosomal uptake of GC-CNPs in DC2.4 cell lines

The DC2.4 cells (25,000 per well) were plated into a Lab-Tek plate with 0.2 mL of R10 media. Following that cells were incubated with the Cy5 labelled GC-CNPs (2.5 µg of NPs) for 1 h. After the incubation time, the DCs were washed with PBS and then replaced with R10 medium and incubated. At 4 h, the cells were fixed with 4% PFA for 15 min. For imaging, the cells were stained using DAPI and anti-lamp2 antibody (Lamp2-488, at 0.1 µg/mL). The cells were suspended in Lab-Tek using 20-30 µl of STORM buffer for imaging.

3. Results and Discussion

3.1. Internalization of Cy5-GC-CNPs in MoDCs

The images in **Figure 1** shows the internalization of the GC-CNPs increased with time. Each red dot in **Figure 1** represents a nanoparticle that is present in the plane (0.5 µm thick) of the MoDC. Even though there is a gradual increase in the NPs uptake with the time until 4h, it was not maximum. However, a significantly higher NPs inside the cells were observed after 24h **(Figure 2)** and the NPs were inside the cells. The uptake of the chitosan nanoparticles was strictly temperature dependent. The nanoparticles were rapidly internalized at 37 °C. While the DCs incubated at 4 °C displayed only a small number of NPs in the cells and were mostly present on the surface of the DCs. These results are in agreement with our previously performed studies using confocal microscope. As expected, the higher internalization of

chitosan nanoparticles by the DCs might be attributed to the cationic property of the chitosan. Similarly, the studies performed by veronica *et al.,* have shown that PLGA nanoparticles coated with chitosan had higher internalization compared to the uncoated nanoparticles after 4h of incubation [9].

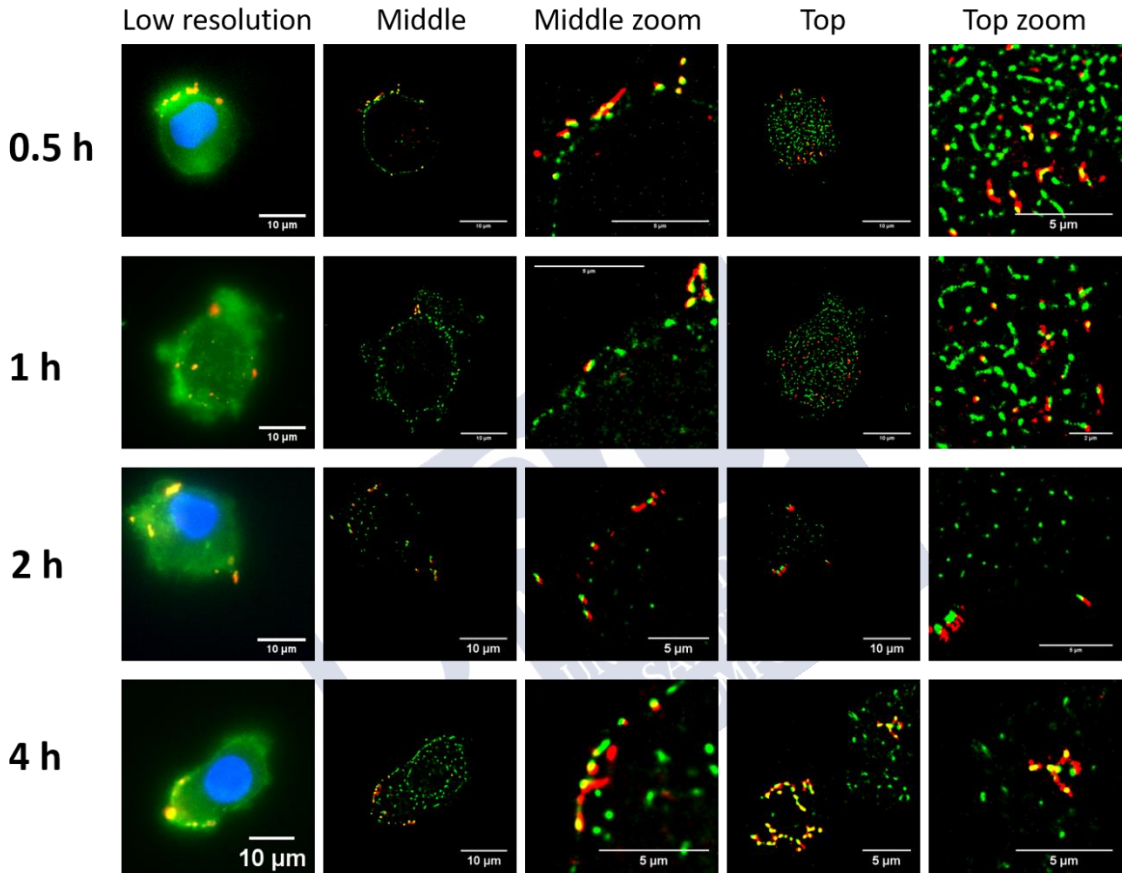

Figure 1- Internalization of Cy5-GC-CNPs (50 µg/ million cells) by MoDCs at different time points (0.5, 1, 2 and 4h). The cell membrane is stained with wheat germ agglutinin-488 (WGA-488; green colour), the nucleus stained with DAPI (blue colour) and the nanoparticles are labelled with Cy5 (red colour).

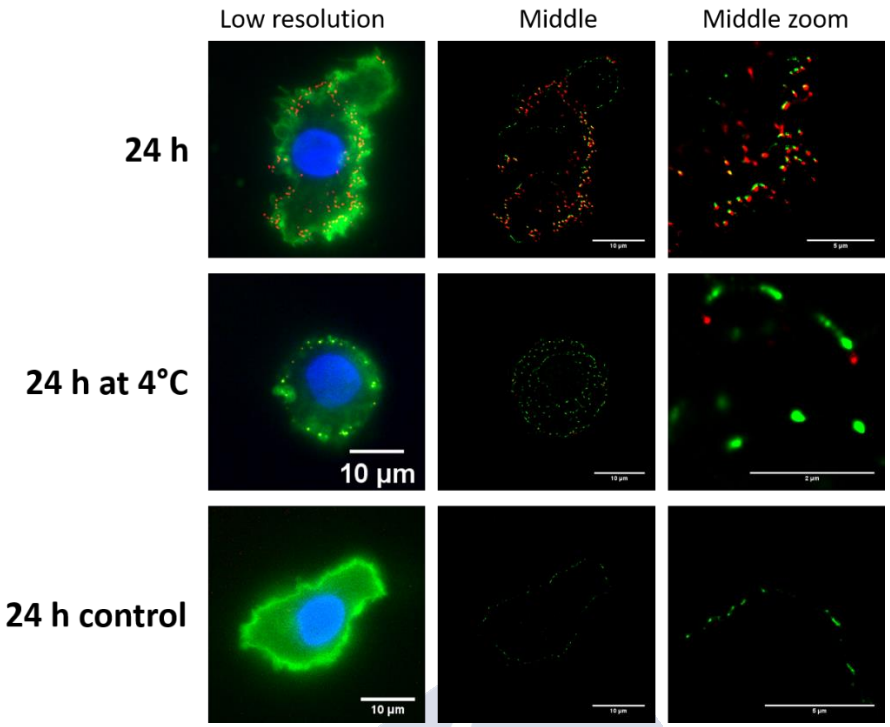

Figure 2- Internalization of the Cy5-GC-CNPs (50 µg/ million cells) by MoDCs at 24h (at 37° C and 4° C). The cell membrane is stained with wheat germ agglutinin-488 (WGA-488; green colour), the nucleus stained with DAPI (blue colour) and the nanoparticles are labelled with Cy5 (red colour).

3.2. Time-dependent internalization of GC-CNPs in DC2.4 cell lines

Figure 3 clearly displays that NPs internalization increases with time. With the increase in time, the NPs concentration increased both on the surface and the centre of the cells, which indicates the NPs were continuously internalized throughout the incubation time and not just during the initial hours of incubation. The images from the mid-section of the cells show the NPs concentration in the cytoplasm increases with the time, and the NPs were present around the nucleus and were not observed inside. The results obtained from these studies are identical to that of nanoparticle uptake by MoDCs.

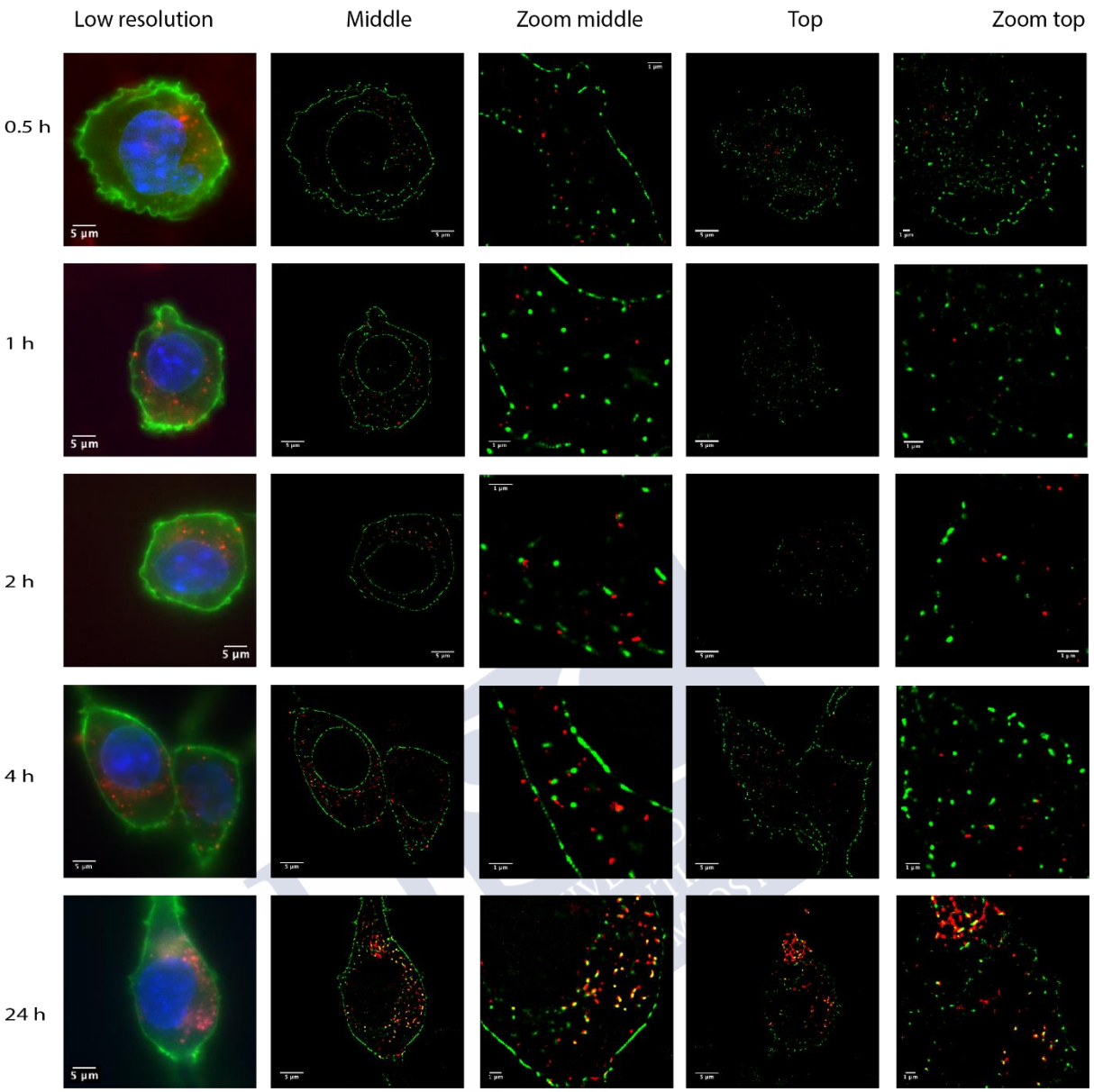

Figure 3- Internalization of the Cy5-GC-CNPs by DC2.4 cell lines at different time points (0.5, 1, 2, 4 and 24h), when incubated with NPs 0.5 µg/ 25,000 cells. The cell membrane is stained with wheat germ agglutinin-488 (WGA-488; green colour), the nucleus stained with DAPI (blue colour) and the nanoparticles are labelled with Cy5 (red colour).

In addition, the study was performed to analyse the fate of nanoparticles that are internalized during 1 h of incubation with DC2.4 cells. To understand the localization of nanoparticles in DC2.4 cells, the imaging was done in 2 planes of 0.5 µm thickness, at the middle and the top of the cells. **Figure 4** displays the change in NPs concentration with time, inside the cells. At the 1h of incubation, the NPs were mainly observed on the surface and very few were present in the cytoplasm. After 4h the NPs have mainly seen the cytoplasm and very few were present

on the surface. This shows the nanoparticles that were present on the cell surface were internalized completely. However, at 24h the NPs concentration inside the cells have considerably decreased, this suggests that the internalized NPs were processed after 24h. In this study, higher NPs concentration (2.5 µg instead of 0.5 µg; at 4h and 24h) was used to make sure that some fluorescence is seen after 24h (as we are only incubating the DCs with NPs for 1h). Overall, the study shows that the nanoparticles internalized by the cells were processed with time.

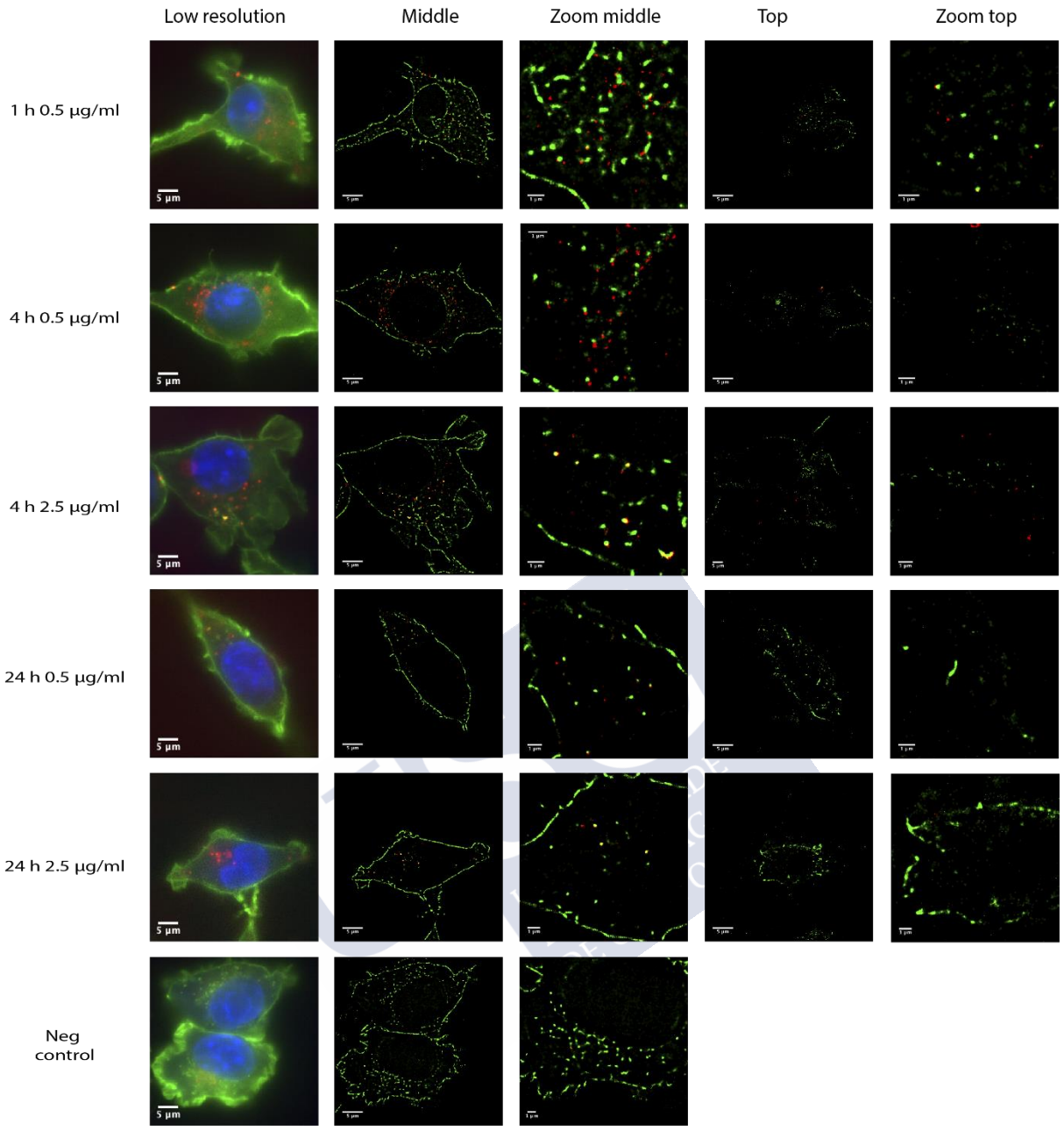

Figure 4: Internalization of Cy5-GC-CNPs by DC2.4 cell lines at different time points (1, 4 and 24h), when pulsed (incubated for 1h with NPs and then washed) with two different concentrations NPs (0.5 and 2.5 µg/ 25,000 cells). The cell membrane is stained with wheat germ agglutinin-488 (WGA-488; green colour), the nucleus stained with DAPI (blue colour) and the nanoparticles are labelled with Cy5 (red colour).

3.3. Endosomal uptake of GC-CNPs in DC2.4 cell lines at 4h.

To study the endosomal uptake of the nanoparticles, both the nanoparticles and the endosomes were labelled with different dyes. The nanoparticles were labelled with Cy5 (red), and the endosomes were labelled with Lamp2-488 (green). As observed in **Figure 5**, we clearly

see the internalization of nanoparticles in the DC2.4 cell line. However, it shows no endosomal uptake of the nanoparticles, as there is no co-localization of green and red fluorescence. In contrary, the literature shows that the nanoparticles coated with the chitosan were delivered to early or late endosomes, while the uncoated ones ended in the sub-cellular compartments of the DCs [9].

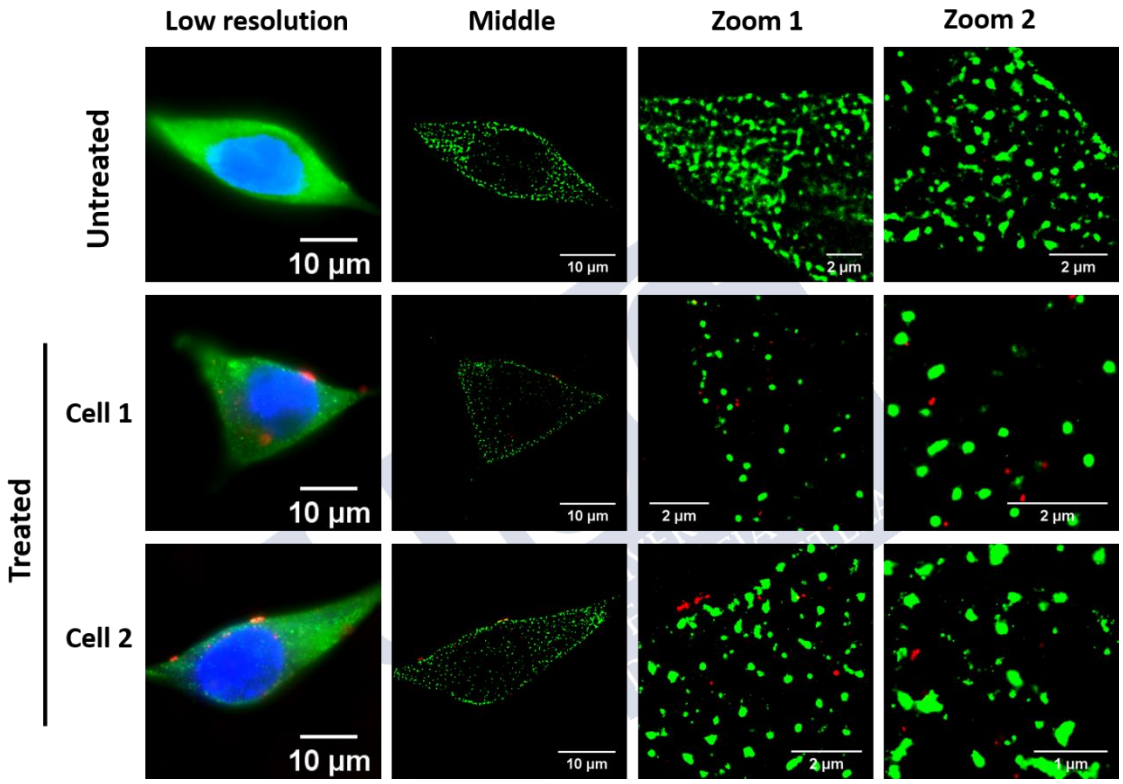

Figure 5- Study to determine the endosomal uptake of the Cy5-GC-CNPs by DC2.4 cell lines after 4h incubation at 37 °C. When pulsed (incubated for 1h with NPs and then washed) with GC-CNPs (2.5 µg/ 25,000 cells). The endosomes were stained with anti-Lamp2-488 (Lamp2-488; green colour), the nucleus stained with DAPI (blue colour) and the nanoparticles are labelled with Cy5 (red colour).

Also, the literature suggests that the chitosan derivatives are mainly internalized by the mannose receptor mediated endocytosis [10]. However, the results obtained for our study is supported by the theory of endosomal escape of the chitosan nanoparticles due to proton sponge effect. However, these studies were performed only once without any replicates and it is necessary to repeat the experiments in order to allow any conclusions on intracellular

processing of these particles. In addition, similar studies in the presence of different inhibitors should be performed to further confirm the pathways involved in the internalization of GC-CNPs.

Conclusions

Overall, the STORM analysis was successfully used to investigate the interaction of the nanoparticles with dendritic cells. The STORM images clearly show that the nanoparticles were internalized by the dendritic cells, and the uptake was increasing with the time. The nanoparticles internalized during 1h were being processed and a significant reduction in the nanoparticle concentration inside the cells was observed at 24h.

4. Acknowledgements

I would like to thank Maria Arista Romero for her help in performing the experiments with DC2.4 cell lines and imaging the cells using super-resolution microscope. The work was supervised by Silvia Pujals.

5. References

[1] J. Wright, Nanotechnology: Deliver on a promise, Nature. 509 (2014). doi:10.1038/509s58a.

[2] S. Nie, Understanding and overcoming major barriers in cancer nanomedicine, Nanomedicine. 5 (2010) 523–528. doi:10.2217/nnm.10.23.

[3] A. Ivask, A.J. Mitchell, A. Malysheva, N.H. Voelcker, E. Lombi, Methodologies and approaches for the analysis of cell-nanoparticle interactions, Wiley Interdiscip. Rev. Nanomedicine Nanobiotechnology. 10 (2018) e1486. doi:10.1002/wnan.1486.

[4] L. Möckl, D.C. Lamb, C. Bräuchle, Super-resolved Fluorescence Microscopy: Nobel Prize in Chemistry 2014 for Eric Betzig, Stefan Hell, and William E. Moerner, Angew. Chemie Int. Ed. 53 (2014) 13972–13977. doi:10.1002/anie.201410265.

[5] D. Kamiyama, B. Huang, Development in the STORM, Dev. Cell. 23 (2012) 1103–1110. doi:10.1016/j.devcel.2012.10.003.

[6] S.W. Hell, Nanoscopy with Focused Light (Nobel Lecture), Angew. Chemie Int. Ed. 54 (2015)

8054–8066. doi:10.1002/anie.201504181.

[7] M.G.L. Gustafsson, Nonlinear structured-illumination microscopy: Wide-field fluorescence imaging with theoretically unlimited resolution, Proc. Natl. Acad. Sci. U. S. A. 102 (2005) 13081–13086. doi:10.1073/pnas.0406877102.

[8] E. Betzig, Single Molecules, Cells, and Super-Resolution Optics (Nobel Lecture), Angew. Chemie Int. Ed. 54 (2015) 8034–8053. doi:10.1002/anie.201501003.

[9] V. Durán, H. Yasar, J. Becker, D. Thiyagarajan, B. Loretz, U. Kalinke, C.M. Lehr, Preferential uptake of chitosan-coated PLGA nanoparticles by primary human antigen presenting cells, Nanomedicine Nanotechnology, Biol. Med. 21 (2019). doi:10.1016/j.nano.2019.102073.

[10] Y. Han, L. Zhao, Z. Yu, J. Feng, Q. Yu, Role of mannose receptor in oligochitosan-mediated stimulation of macrophage function, Int. Immunopharmacol. 5 (2005) 1533–1542. doi:10.1016/j.intimp.2005.04.015.

Abbreviations

α-GalCer, α-galactosylceramide

AAD, Aminoactinomycin D

APCs, antigen-presenting cells

APC, Allophycocyanin

BSA, bovine serum albumin

CD, Cluster of Differentiation (CD4, CD8, CD25, CD28, CD80, CD83 and CD86)

CD, Circular dichroism

CLO, Chlorpromazine

CLSM, Confocal laser scanning microscopy

Cit-D, Cytochalasin-D

CNPs, Chitosan nanoparticles

CP, Capsular polysaccharides

CRM197, Cross-reacting material of diphtheria toxin with amino acid 197 substitution

CS, Chitosan

Cy5, Cyanine-5

DAPI, 4',6-diamidino-2-phenylindole

DCs, Dendritic cells

DHA, 5-(N, N-Dimethyl)amiloride hydrochloride

DMSO, Dimethyl sulfoxide

DT, Diphtheria toxoid

ELISA, Enzyme-linked immunosorbent assay

EM, Electron microscopy

EU, Endotoxin units

FACS, Fluorescence activated cell sorting

FBS, Fetal bovine serum

FCS, Fetal calf serum

FEG-SEM, Field emission gun Scanning electron microscopy

FITC, Fluorescein Isothiocyanate

GBSIII, Type III polysaccharide of group B Streptococcus

GC, Glycoconjugate

GC-CNPs, Glycoconjugate encapsulated chitosan nanoparticles

GM-CSF, Granulocyte-macrophage colony stimulating factor

HLA, Human leukocyte antigen

iDCs, Immature dendritic cells

IgA, Immunoglobulin A

IgG, Immunoglobulin G

IgM, Immunoglobulin M

IFN-γ, Interferon

IL, Interleukin

LAL, Limulus amebocyte lysate

LC 50, Lethal concentration 50

LPS, lipopolysaccharide

mDCs, Mature dendritic cells

MFI, Mean fluorescence intensity

MHCII, Major histocompatibility class II

MoDCs, Monocyte derived dendritic cells

MPLA, Monophosphoryl lipid A

MS, Mass spectrometry

MTS reagent, (3- (4,5-dimethylthiazol-2-yl) -5- (3-carboxymethoxyphenyl) -2- (4-sulfophenyl) -2H-tetrazolium)

NPs, Nanoparticles

OVA, Ovalbumin

PALM, Photoactivation localization microscopy

PBLs, Peripheral blood lymphocytes

PBMCs, Peripheral blood mononuclear cells

PCV, Pneumococcal conjugate vaccine, containing 7 serotypes (PCV7) or 13 serotypes (PCV13)

PE, Phycoerythrin

PFA, Paraformaldehyde

PGA, Poly glutamic acid

PLA, Poly lactic acid

PLGA, Poly (lactide-co-glycolic acid)

pDNA, Plasmid DNA

Pn14TS, Pneumococcal serotype 14 tetrasaccharide

PPA, Pneumococcal protein antigens

PPSV, Pneumococcal polysaccharide vaccine

PsaA, Pneumococcal surface adhesin A

PSG, Penicillin-Streptomycin-Glutamine

RPMI, Roswell Park Memorial Institute medium

R2, RPMI-1640 medium supplemented with FBS (2%) and PSG (1x)

R10, RPMI-1640 medium supplemented with FBS (10%) and PSG (1x)

RT, Room temperature

SD, Standard deviation

SEB, Staphylococcal enterotoxin B

SIM, Structured illumination microscopy

Spn, Streptococcus pneumoniae

STED, Stimulation emission depletion

STORM, Stochastic optical reconstruction microscopy

TNF, Tumor necrosis factor

TPP, Tripolyphosphate

TS, Tetrasaccharide

TT, Tetanus toxoid

WGA, Wheat germ agglutinin

USC
UNIVERSIDADE
DE SANTIAGO
DE COMPOSTELA

Ethical considerations and Permissions

I. Animal Studies:

1. Specific pathogen-free C57BL/6 mice (6 weeks-old, female) were purchased from Janvier (Le Genest-St-Isle, France).

2. All the animal experiments were performed at Lille Pasteur institute according to the ethical guidelines (agreement number AF 16/20090 and 00357.03).

II. Primary cell line, Human monocyte derived dendritic cells

1. Buffy-coats used to collect the dendritic cells were obtained from anonymous donors and were kindly donated by the Agency for the Donation of Organs and Blood (ADOS, Santiago de Compostela) with the approval of the Director of the Agency and the Clinical Research Ethics Committee of Galicia (2014/543).

2. For heparinized blood from the healthy volunteers, an informed consent was obtained from the volunteers in accordance with the guidelines of the Ethical Committee of Clinical Research of Galicia.

XUNTA DE GALICIA
CONSELLERÍA DE SANIDADE
Secretaría Xeral Técnica

Secretaria Técnica
Comité Autonómico de Ética da Investigación de Galicia
Secretaria Xeral. Consellería de Sanidade
Edificio Administrativo San Lázaro
15703 SANTIAGO DE COMPOSTELA
Tel: 881 546425; ceic@sergas.es

galicia

DITAME DO COMITÉ DE ÉTICA DA INVESTIGACIÓN DE SANTIAGO-LUGO

Juan Manuel Vázquez Lago, Secretario do Comité de Ética da Investigación de Santiago-Lugo

CERTIFICA:

Que este Comité avaliou na súa reunión do día 20/01/2015 o estudo:

Título: Diseño de nanovacunas terapéuticas basadas en péptidos: aplicación al tratamiento de enfermedades autoinmunes
Promotor: África González Fernández, María Josefa Alonso Fernández, Rubén Varela Calviño
Tipo de estudo: Outros
Versión:
Código do Promotor:
Código de Rexistro: 2014/543

E, tomando en consideración as seguintes cuestións:

- A pertinencia do estudo, tendo en conta o coñecemento dispoñible, así coma os requisitos legais aplicables, e en particular a Lei 14/2007, de investigación biomédica, o Real Decreto 1716/2011, de 18 de novembro, polo que se establecen os requisitos básicos de autorización e funcionamento dos biobancos con fins de investigación biomédica e do tratamento das mostras biolóxicas de orixe humana, e se regula o funcionamento e organización do Rexistro Nacional de Biobancos para investigación biomédica, a ORDE SAS/3470/2009, de 16 de decembro, pola que se publican as Directrices sobre estudos Posautorización de Tipo Observacional para medicamentos de uso humano, e a Circular nº 07/2004, investigacións clínicas con produtos sanitarios.
- A idoneidade do protocolo en relación cos obxectivos do estudo, xustificación dos riscos e molestias previsibles para o suxeito, así coma os beneficios esperados.
- Os principios éticos da Declaración de Helsinki vixente.
- Os Procedementos Normalizados de Traballo do Comité.

Emite un **INFORME FAVORABLE** para a realización do estudo **polo/a investigador/a do centro:**

Centros	Investigadores Principais
Universidade de Vigo	África González Fernández
Univerisdade de Santiago de Compostela	María Josefa Alonso Fernández
	Rubén Varela Calviño

En Santiago de Compostela, a 20 de xaneiro de 2015
O secretario

juan.manuel.vazquez.lago@sergas.es
Firmado digitalmente por juan.manuel.vazquez.lago@sergas.es
Nombre de reconocimiento (DN): cn=juan.manuel.vazquez.lago@sergas.es
Fecha: 2015.01.30 10:28:10 +01'00'

Juan M. Vázquez Lago

DE ASIS A COMPOSTELA · 1214 · 2014 ·

Attributions to the icons employed in the figures and graphical abstract

The drawings and schemes presented in this thesis are prepared by myself using powerpoint presentation or adobe illustrator CC 2017. The icons used in thesis for the construction of schemes and graphical abstract were designed by Freepick at www.flaticon.com.

Permission to re-use a published paper as Chapter 1

Original paper: M. Prasanna, D. Soulard, E. Camberlein, N. Ruffier, A. Lambert, F. Trottein, N. Csaba, C. Grandjean, Semisynthetic glycoconjugate based on dual role protein/PsaA as a pneumococcal vaccine, Eur. J. Pharm. Sci. 129 (2019) 31–41. doi:10.1016/J.EJPS.2018.12.013.